Th-Pos247

HARD AND SOFT SULFATE AND SULFONATE ANIONS IN PROTEIN PRECIPITATION-BIORECOGNITION. Rex Lovrien and Daumantas Matulis, Biochemistry Dept., Univ. Minnesota, St. Paul 55108

Proteins can be precipitated and coprecipitated out of solution by over a dozen different techniques. Selection of techniques determines cost, scaleability, unit process interfacing, feasibility of upstream vs. downstream operation. Molecular principles involved range from completely pushing methods (sulfate kosmotrope salting out) to completely pulling with matrix organic sulfonate ligands at the other extreme. Some methods are hybrids, both push and pull. In all cases how water is handled is an unseen but crucial factor in the overall equilibria. Sulfate salts and sulfate/sulfonate organic ligands exert themselves by mixtures of factors expressed by how hard vs. how soft they are in the Pearson sense. Water molecules, aliphatic hydrocarbons are hard, poorly polarizable. Aromatics are soft, and polarizable. Molecular volumes of large soft ligands get important when they displace water and lower average dielectric constants around ligands exerting electrostatic forces. The large (huge) differences in concentrations of compounds able to force precipitation indicate what several of the precipitation mechanisms rest on, vis a vis sulfate/sulfonate softness or hardness, their reliance on pushing vs. pulling mechanisms.

Th-Pos248

SELF-ASSOCIATION OF IL-8 AND ITS MUTANTS: EFFECTS OF IONIC STRENGTH AND PH((Jun Liu, Henry B. Lowman, Caroline A. Hébert and Steven J. Shire))Department of Pharm R&D, Protein Engineering and Immunology, Genentech, Inc., 460 Pt. San Bruno Blvd., South San Francisco, CA 94080.

IL-8 is a chemoattractant involved in many inflammation processes. The NMR and X-ray crystallography data show that it essentially exists as a non-covalent linked homodimer at high concentration (Clore, G. M. *et al.* (1990) *Biochemistry* **29**, 1689; Baldwin, E. T. *et al.*(1991) *Proc. Natl. Acad. Sci. USA* **88**, 502.). Although several in vitro studies suggest that IL-8 is exclusively monomeric at the nanomolar physiological concentrations at which it displays maximal chemotactic activity (Paolini, J. F. *et al.* (1994) *J. Immunol.* **153**, 2704.), it is still unclear whether the IL-8 is able to dimerize on the cell surface. In this study, the self-association of IL-8 and its mutants were examined in different buffer conditions by analytical ultracentrifugation. We show that IL-8 self-associates strongly to a dimer (Kd<10 nM) in 50 mM phosphate buffer at pH 5.3, whereas in 0.15 M PBS at pH 7.2, the self-association is considerably weaker with Kd on the order of μM. The effects of ionic strength and pH on thermodynamic properties of IL-8 dimerization and conformation changes were followed by analytical ultracentrifugation and CD. In addition, we have also generated several mutants with reduced hydrophobicity on the dimer interface. We show that these variants have much weaker association constants and appear to be independent on the change of buffer conditions.

SODIUM/CALCIUM EXCHANGER

Th-Pos249

CHARACTERIZATION OF THE Na/Ca EXCHANGER cDNA IN DROSOPHILA. ((C. Valdivia, P. Kofuji, W. J. Lederer and D. H. Schulze)) Departments of Physiology and Microbiology and Immunology, University of Maryland School of Medicine, Baltimore MD 21201.

Using classical approaches of homology screening we have cloned the full length cDNAs for the Na/Ca exchanger from Drosophila using a human cDNA as a probe. The Drosophila Na/Ca exchanger has many of the same characteristics of previously described mammalian exchanger, a series of N terminal and C terminal hydrophobic regions suggesting this protein to be a multipass membrane protein and a large intracellular loop between these transmembrane regions. The overall homology between the human and Drosophila is 44% identity and 60% including similar amino acid substitutions. The Drosophila cDNA is more similar to the Na/Ca exchanger found in most tissues (NCX1) than the recently described second Na/Ca exchanger (NCX2). Notable differences between the human and Drosophila sequences : the absence of an N-terminal glycosylation site in Drosophila, the Drosophila sequence is shorter than the human because of three sets of deletions in the intracellular loop region, one of these deletions (45AA) in the Drosophila sequence results in the loss of some of the region that contains the cassette type exons created by alternative splicing of exons in the mammalian gene. We have independent cDNA clones from Drosophila that display sequence variation at the equivalent position in the mammalian cDNAs where alternative splicing has been demonstrated, suggesting a further parallel between the Drosophila and mammalian Na/Ca exchanger cDNAs. We have also used the Drosophila cDNA to map the Na/Ca exchange gene to chromosome 3 (93A-B) using polytene chromosomes.

Th-Pos250

ANOMALOUS REGULATION OF THE Na^+-Ca^{2+} EXCHANGER FROM *DROSOPHILA*. ((L.V. Hryshko, D.A. Nicoll, S. Matsuoka, J.N. Weiss, E. Schwarz, S. Benzer, and K.D. Philipson)) UCLA Cardiovasc. Res. Labs, Los Angeles, CA 90024 and Div. Biology, CIT, Pasadena, CA 91825.

The Na^+-Ca^{2+} exchanger from *Drosophila* (Schwarz and Benzer, submitted) was expressed in *Xenopus* oocytes and characterized electrophysiologically using the giant excised patch technique. This protein shares 48% amino acid identity to the canine cardiac Na^+-Ca^{2+} exchanger, NCX1. The Na^+-Ca^{2+} exchanger from *Drosophila* exhibits similar properties to previously characterized Na^+-Ca^{2+} exchangers (NCX1 and NCX2) including Na_i affinities, IV relationships, and sensitivity to the peptide inhibitor, XIP. However, the Na^+-Ca^{2+} exchanger from *Drosophila* exhibits a completely opposite response to cytoplasmic Ca^{2+}. Both NCX1 and NCX2 are stimulated by cytoplasmic Ca^{2+} in the micromolar (0.1-10 μM) range. This stimulation of exchange current is mediated by occupancy of a regulatory Ca^{2+} binding site distinct from the Ca^{2+} transport site. In contrast, the Na^+-Ca^{2+} exchanger from *Drosophila* is inhibited by cytoplasmic Ca^{2+} over this same Ca^{2+} concentration range. The inhibition of exchange current is evident for both forward and reverse modes of transport. Pre-incubation of patches with micromolar cytoplasmic Ca^{2+} led to inhibition of subsequent currents whereas large initial currents were observed when patches were pre-incubated in zero Ca^{2+} containing solutions. Thus, occupancy of the putative regulatory Ca^{2+} binding site regulates exchange activity independent of Ca^{2+} at the transport site. These data should provide a rational basis for subsequent structure-function studies targeting the Ca_i regulatory mechanism.

Th-Pos251

IDENTIFICATION OF IMPORTANT AMINO ACID RESIDUES OF EXCHANGER INHIBITORY PEPTIDE XIP ((Z. He and K. D. Philipson)) Cardiovascular Research Laboratory, UCLA School of Medicine, Los Angeles, CA 90024. (Spon. by D. A. Nicoll)

The Na^+-Ca^{2+} exchanger plays an important role in cardiac contractility by extruding Ca^{2+} across the plasma membrane during excitation-contraction coupling. A 20 amino acid peptide, XIP, synthesized to mimic a region of the exchanger inhibits the activity of the exchanger (JBC 266:1014-1020). We are attempting to identify amino acids of the XIP peptide which are essential for inhibitory function. XIP peptides with various modifications were synthesized and Na^+-Ca^{2+} exchange activity was then assayed in the presence of these peptides as $^{45}Ca^{2+}$ uptake into Na^+-loaded cardiac sarcolemmal vesicles. Deletion of the first 5 residues at the N-terminus or the last 7 residues at the C-terminus, respectively, caused modest decreases in the inhibitory activity of XIP, whereas deletion of the first 8 residues at the N-terminus or the last 9 residues at the C-terminus completely eliminated inhibitory activity. In addition, replacement of tyrosines 6, 8, 10, and 13 with tryptophans did not change the inhibitory activity of XIP. However, XIP inhibitory activity was eliminated when all four tyrosine residues were replaced by alanine. Moreover, replacement of arginine 12 or 14 with alanine decreased inhibitory activity, while replacement of other positively-charged residues with alanine did not affect inhibitory activity. Our data suggest that positively-charged residues, arginines 12 and 14, and aromatic residues, tyrosines 6, 8, 10, and 13 play an important role in interactions with the exchanger.

Th-Pos252

TISSUE-SPECIFIC EXPRESSION OF THE SECOND ISOFORM OF THE Na/Ca EXCHANGER, NCX2 ((B.D. Quednau, N. Brecha, and K.D. Philipson)) Cardiovascular Research Laboratory, UCLA and V.A. Medical Center, Los Angeles, CA 90024

The Na/Ca exchanger NCX1 first cloned from heart is also present in several other tissues. Alternative splicing of NCX1 mRNA generates a wide variety of tissue-specific splicing isoforms. Recently, Li et al. (JBC 269: 17434, 1994) have cloned a second Na/Ca exchanger from rat brain, NCX2, which is most abundant in brain and skeletal muscle. In comparison to NCX1, the NCX2 mRNA lacks a stretch of 111 nts at a position where alternative splicing of NCX1 occurs. We have investigated the tissue-specific expression of NCX2 in rat by RT-PCR using primer pairs spanning the missing nucleotide sequence. We could detect NCX2-specific transcripts in almost all tissues without finding any alternatively spliced isoforms. Less sensitive Northern Blot analysis confirmed that NCX2-specific mRNA is abundant only in brain and skeletal muscle. To further investigate the expression of NCX2 in the brain we performed in situ hybridization and immunocytochemistry with rat brain sections. A NCX2-specific RNA-probe detected transcripts in the Purkinje cell and granular cell layers of the cerebellar cortex, the hippocampus, the midbrain, the cerebral cortex, and to a lesser extent in the olfactory bulb. Similar rat brain sections were analyzed by immunocytochemistry using a polyclonal antibody against a fusion protein which contained 302 aa of the loop region of NCX2. The staining shows a pattern of expressed protein that corresponds to the in situ hybridization data. The distinct distribution and high abundance of NCX2 in the brain suggests that the protein might play an important role in this tissue.

Th-Pos253

INTRACELLULAR AND EXTRACELLULAR PROTONS HAVE OPPOSING MODULATORY EFFECTS ON CARDIAC NA/CA EXCHANGE. ((Doering, A. E. and Eisner, D. A.)) Dept. of Vet. Preclin. Sciences, University of Liverpool, P.O. Box 147, Liverpool L69 3BX, UK.

In preparations of isolated sarcolemma, the cardiac Na/Ca exchanger is highly sensitive to changes in intracellular pH. We have measured Na/Ca exchange current under whole cell voltage clamp and recorded changes in intracellular or extracellular pH using the fluorescent pH indicator SNARF. In the intact rat ventricular myocyte, the Na/Ca exchanger is strongly inhibited by intracellular protons at physiological pH around 7.0. The current amplitude increases 300% with an alkalinization to about 7.5, and is 50% inhibited by acidification to about 6.7. When intracellular pH is buffered with 50 mM HEPES and extracellular pH is varied, Na/Ca exchange is 60% inhibited by alkalinization from 7.4 to 8.0 and 30% stimulated by acidification from 7.4 to 6.8. It is difficult to predict the net effect of a pH perturbation due to the complexity of proton interaction with the Na/Ca exchanger, but it is clear that changes in pH are an important modulator of Na/Ca exchange function. Extracellular pH may even change as a result of intracellular pH regulation involving transport of protons or acid equivalents across the cell membrane. In such a case, intracellular acidification would have a primary inhibitory and a secondary stimulatory effect on Na/Ca exchange.

Th-Pos254

THE TIME COURSE OF INWARD EXCHANGE CURRENT IN CARDIAC MYOCYTES IS CONTROLLED BY SUBCELLULAR CA RELEASE PATTERNS AND CELL GEOMETRY

((J. Hüser[1], R. Schwalm[1], P. Lipp[3], E. Niggli[3] & L. Pott[2])) [1]Dept. Cell Physiol., [2]Dept. Physiol., Ruhr-University Bochum, Germany; [3]Dept. Physiol., University of Bern, Switzerland (spon. by G. Boheim)

In cardiac myocytes intracellular Ca transients elicit inward currents (I_{EX}) reflecting Ca extrusion across the sarcolemma via electrogenic Na/Ca-exchange. In atrial myocytes combined measurements of Ca and membrane currents revealed a variable and complex time course of I_{EX} which was interpreted in terms of subcellular Ca gradients.

Here we present a simple mathematical model examining the possible effect of subcellular inhomogeneous Ca release and individual cell geometry on the time course of I_{EX}. In this model the cell was represented as a linear sequence of elements each of which was characterized by an individual cell-surface/volume ratio (s/v ratio). A Ca wave travelling through the cell was simulated by combining the one-dimensional diffusion equation and a simple differential equation accounting for the SR Ca release/uptake function. The whole-cell membrane current was calculated as the sum of the membrane currents of each element (product of the local Ca and the local s/v ratio). Profiles of s/v ratios derived from elongated cultured atrial myocytes (s/v ratio larger at both ends compared to central regions) gave rise to two components in the onset phase of I_{EX} when a Ca transient with wave-type characteristics was simulated. During these Ca waves the dependence of I_{EX} (reflecting I_{NaCa}) and Ca was not linear, similar to previous experimental observation in elongated cells. In contrast, I_{EX} simulated for s/v ratios of spherical cells exhibited a linear relation comparable to experimental data. The results of these simulations indicate that the cell geometry (i.e. the spatial distribution of the s/v ratio) and the subcellular Ca release patterns determine the time course of I_{EX} and most likely also other Ca dependent membrane currents.

Th-Pos255

THE AUTOINHIBITORY REGIONS OF THE CA PUMP (C28) AND THE NA/CA EXCHANGER (XIP) BIND TO HUMAN ERYTHROCYTE ANKYRIN AND BAND 3 ((W.-Y. Xu, C. C. Hale, M. A. Milanick)) Physiology, and Dalton Cardiovascular RC, Univ. of Missouri, Columbia, MO 65212

I-125XIP (RRLLFYKYVYKRYRAGKQRG) was crosslinked to membranes with either BS3 or EDC. With EDC, XIP associated with several membrane proteins with major labeling at approximately 215 and 80-105 kDa. In addition, BS3 crosslinked membranes were digested with Protease K. The water soluble proteolytic fragments were separated by HPLC. The amino acid sequence analysis showed that I-125XIP crosslinked to ankyrin and band 3. One labeled HPLC fraction had an N-terminal sequence corresponding to residues 935-942 of ankrin, in the 62 kDa spectrin-binding domain. Another labeled HPLC fraction had an N-terminal sequence corresponding to residues 336-345 of band 3; the first transmembrane spanning region is predicted to start at residue 376. In the presence of 40-fold excess of unlabeled XIP and VIP 10-28 (YTRLRKQMAVKKYLNSILN), C28R2 (LRRGQILWFRGLNRIQTQIRVVKAFRSS) and Bachem peptide # H9685 (QRRQRKSRRTI) crosslinking of I-125XIP to proteins was not observed. All of these peptides bind calmodulin. Pentalysine partially reduced the crosslinking of I-125XIP. Peptide ET-1 (FKLLAGRWPF) did not reduce the binding. Since the cardiac Na/Ca exchanger binds ankyrin (Li *et al.* 1993, J.B.C. 268:11489), it is possible that the Na/Ca exchanger associates with ankyrin via the XIP domain. The competition of the Ca pump peptide C28 with I125-XIP implies the possibility that the Ca pump also associates with cytoskeletal ankyrin and band 3. Supported by NIH DK37512 (MAM), a RCDA from NIH-DK (MAM), and AHA (CCH).

Th-Pos256

POSSIBLE COMPLICATIONS OF SUBMEMBRANE CALCIUM GRADIENTS AND CALCIUM BUFFER FUNCTION IN THE STUDY OF Na/Ca EXCHANGE CURRENT (I_{NaCa}) IN GIANT CARDIAC MEMBRANE PATCHES. ((Anatolii Kabakov and Donald W. Hilgemann)), Department of Physiology, UTSW Medical Center at Dallas, Dallas, TX, 75235-9040.

Evidence is presented that Ca^{2+} buffers modulate I_{NaCa} function in giant membrane patches from guinea pig myocytes by multiple mechanisms. For outward I_{NaCa} (Ca^{2+} influx mode; dependent on cytoplasmic Ca^{2+} binding at a regulatory site), reduction of EGTA from 10 to 0.2 mM with a fixed EGTA:Ca ratio of 1:0.7 has only little effect under control conditions. When outward I_{NaCa} is stimulated by ATP or phosphatidylserine (PS), however, the current is strongly enhanced on reduction of buffer capacity. In the absence of Ca in the cytoplasmic solution, I_{NaCa} decreases as EGTA is increased with a K_i of about 5 mM; 10 mM BAPTA is more effective than 40 mM EGTA in suppressing the current. To test whether significant submembrane Ca^{2+} changes might occur when other transmembrane Ca fluxes are activated, the Ca ionophore, A23187, was used to induce electroneutral Ca transport. After application of ATP or PS, A23187 (4 μM; 4 mM extracellular Ca^{2+}) strongly enhances outward I_{NaCa} in the absence cytoplasmic Ca^{2+} and in the presence of high Ca^{2+} buffer concentrations. For inward I_{NaCa}, reduction of EGTA from 10 to 1 to 0.1 mM with an EGTA:Ca ratio of 1:0.85 (pH 7; 1.8 μM calculated Ca^{2+}) decreases I_{NaCa} by about 2 and 3 fold, respectively. Current-voltage relations become flatter at low EGTA, as if an electroneutral process (e.g. Ca^{2+} diffusion to the membrane) becomes rate-limiting.

Th-Pos257

FAST CAPACITANCE MEASUREMENTS IN THE STUDY OF MEMBRANE TRANSPORTER ELECTROGENICITY IN GIANT MEMBRANE PATCHES. ((Chin-Chih Lu and Donald W. Hilgemann)), Department of Physiology, UTSW Medical Center at Dallas, Dallas, TX, 75235-9040.

The electrogenic, charge-moving reactions of ion transporters will constitute nonlinear, time-dependent components of total membrane capacitance. Conformational changes of transporters, ion concentration changes, and changes of membrane potential may all enable or disable charge-moving transporter reactions. Such changes should then appear as a change of membrane capacitance if capacitance is monitored at slow perturbation rates with respect to the kinetics of charge movements. With this background, we describe capacitive signals for the Na/K pump, for the cardiac Na/Ca exchanger, and for the GAT1 (GABA/Na/Cl) cotransporter. Capacitance of giant cardiac or oocyte patches was monitored via lock-in amplifiers using 0.5 to 3 mV sinusoidal perturbations applied at 1 to 50 kHz. Transporter-related capacitance changes are 0.1 to 0.3 pF in patches of 8 to 15 pF. Voltage-capacitance relations for native membrane are nearly linear, and transporter-related capacitance changes can be monitored at 1 kHz resolution during voltage step protocols. For the cardiac Na/K pump, an 'E_1' versus 'E_2' capacitance increase is demonstrated and associated with extracellular sodium binding. For the Na/Ca exchanger, expressed in oocyte membrane, capacitance changes are associated with sodium binding and translocation, but not (clearly) with calcium binding and translocation. For the GAT1 transporter, the method is being used to probe multiple possible sources of electrogenicity.

Th-Pos258

MODIFICATION OF THE NA-CA EXCHANGE-DEPENDENT CA COMPARTMENT BY DIBUCAINE IN CULTURED NEONATAL RAT CARDIOMYOCYTES ((S.Y. Wang & G.A. Langer)) Cardiovascular Research Labs, UCLA School of Medicine, Los Angeles, CA 90024-1760.

The present study examines the effect of modification of the sarcolemmal (SL) Ca binding by dibucaine on the Na-Ca exchange-dependent Ca compartment. An on-line isotopic technique was employed to measure total Ca in the compartment in intact cells. A "gas-dissection" technique was used to isolate SL membrane. Cell shortening and intracellular Ca transients were measured with video and fluorescent techniques respectively. Dibucaine reduces the Ca content in the compartment of intact cells in a dose-dependent manner. It also suppresses both non-specific and compartment-specific SL Ca binding. Ca content of sarcoplasmic reticulum remains unchanged in the presence of dibucaine and can be released by caffeine. The effect of dibucaine can be interpreted on the basis of its ability to interact with SL Ca binding sites resulting in displacement of Ca bound to the inner leaflet. This reduction of SL-bound Ca would decrease the local Ca concentration at the exchanger and thus greatly reduce Ca efflux via the exchanger. The present study supports the hypothesis that the discrete Na-Ca exchange-dependent Ca compartment is localized to the subsarcolemmal space and that SL-bound Ca is critical for the optimal function of Na-Ca exchange. (Supported by Laubisch and Castera Funds)

Th-Pos259

INTRACELLULAR FREE SODIUM IN COMPENSATED AND FAILING HYPERTROPHIED GUINEA PIG HEARTS. ((L.A. Jelicks and F.M. Siri)) Albert Einstein College of Medicine, Bronx NY 10461

Guinea pig hearts subjected to gradual left ventricular pressure overload following ascending aortic banding develop hypertrophy (LVH) and failure (LVF), accompanied by abnormalities in myocyte action potentials, free calcium transients, and slow inward calcium current density. To explore concomitant changes in free myoplasmic sodium ($[Na^+]_i$) which may also be involved in the pathophysiology of heart failure, normal (N: n=21), LVH (n=5) and LVF (n=9) Langendorff-perfused guinea pig hearts were examined using ^{23}Na nuclear magnetic resonance spectroscopy (NMR). Baseline $[Na^+]_i$ was significantly elevated in LVH (14.1 $\pm$ 2.5 mM, mean $\pm$ SD) versus N (5.1 $\pm$ 1.5 mM, $P < 0.01$) and versus LVF (7.8 $\pm$ 3.2 mM, $P < 0.01$). In subsets of N (n=5) and LVF (n=5), increasing the fluid volume of an intraventricular balloon from 100 to 300 μL caused significantly less increase in $[Na^+]_i$ in LVF (5.6 $\pm$ 2.5 %) than in N (14.7 $\pm$ 6.3 %, $P < 0.02$) when perfusion pressure was optimized for both groups. Thus, $[Na^+]_i$ appears to increase at an early stage of the disease process, then declines toward normal. The fact that this increase is not progressive suggests that homeostatic regulation of $[Na^+]_i$ is maintained, and that this transitory change may have some compensatory role, such as providing inotropic support via Na^+-Ca^{++} exchange.

Th-Pos260

THE ROLE OF $[CA^{2+}]_i$ AND NA^+:CA^{2+} EXCHANGE IN THE "SPIKE AND DOME" CONFIGURATION OF THE ACTION POTENTIAL IN CANINE VENTRICULAR MYOCARDIUM. ((B. Szabo, A. Kulcsar, P. Volders, R. Lazzara)) Univ. Okla. HSC/V.A. Med.Ctr., Oklahoma City, OK 73104.

The generation and function of the "dome" in the cardiac ventricular action potential (AP) of larger mammals has not yet been clarified. We hypothesized that during the dome a second I_{Ca} is activated by the sarcoplasmic reticulum (SR) Ca^{2+} release and stimulation of the depolarizing Na^+:Ca^{2+} exchange current (I_{ex}). We used isolated canine ventricular myocytes. The stimulation, the recording of the AP and buffering of $[Ca^{2+}]_i$ was performed by using cell attached patch electrodes. $[Ca^{2+}]_i$ was measured with fura-2/AM, and unloaded shortening with a video edge detector. For an inhibition of I_{Ca} or I_{ex} D600 or $NiCl_2$ was used, respectively. I_{ex} was also altered by varying sarcolemmal $[Na^+]$ and $[Ca^{2+}]$ gradients (Na^+ substituted by Li^+). The dome was changed by constant current pulses applied intracellularly with various intervals after the upstroke of the AP. We observed that high $[Ca^{2+}]_o$ (up to 5 mM) which increases I_{Ca} also increased the dome and contraction. However, if I_{ex} was inhibited both the dome and contraction were abolished and could not be restored by stimulating I_{Ca}. These observations suggest that a) the activity of I_{Ca} and the dome is elicited by the depolarizing effect of I_{ex} b) the activity of I_{Ca} during the dome is necessary for the replenishment of the SR with Ca^{2+} fur subsequent contractions c) that activation of I_{Ca} by I_{ex} that generates the dome is an important mechanism for regulation of the contraction.

Th-Pos261

DEVELOPMENTAL CHANGES IN THE Na^+-Ca^{2+} EXCHANGER IN RABBIT CARDIAC VENTRICULAR MYOCYTES. ((T.K. Chin and G.A. Christiansen)) University of Utah, Salt Lake City, UT 84113. (Spon. by K.W. Spitzer)

Previous developmental studies have shown structural and functional immaturity of the sarcoplasmic reticulum (SR), and a decreased Ca^{2+} channel density in neonates compared to adults. To study developmental changes in the Na^+-Ca^{2+} exchanger, we measured Na^+-Ca^{2+} exchange current (I_{NaCa}) in freshly isolated cardiac ventricular myocytes from neonatal (age 1-5 days) and adult (age 8-10 weeks) New Zealand White rabbits using whole cell disrupted patch clamp techniques. The pipette solution contained (in mM) Na^+ 10, Cs^+ 130 and EGTA 14 (pH=7.4, internal Ca^{2+} 100 nM). Cells were held at -40 mV, and perfused externally at 32° C. with a solution containing (in mM) Na^+ 144, K^+ 0 and Ca^{2+} 2.7 (pH=7.1). An outward current previously shown to represent reverse I_{NaCa} was elicited by decreasing Na^+_o from 144 to 0 mM, using a rapid external solution switcher with a $T_{½}$<3 msec. I_{NaCa} density (in pA/pF, mean$\pm$SEM), was 5.04$\pm$1.38 in 8 neonatal myocytes compared to 1.65$\pm$0.25 in 10 adult myocytes (significant, P<0.02). To determine whether Exchanger Inhibitory Peptide (XIP) inhibits I_{NaCa} in neonates, I_{NaCa} was measured with the protocol above, at 5 minute intervals for 20 minutes, and with 20 mM Na^+ in the pipette. In control cells (n=4), the amplitude of I_{NaCa} increased with time, presumably with the rise in Na^+_i. However, with 10 μM XIP in the pipette (n=3), the increase in I_{NaCa} was inhibited. In summary, I_{NaCa} density is increased in myocytes from neonatal rabbits compared to adults. An increase in Ca^{2+} influx through reverse Na^+-Ca^{2+} exchange may compensate in part for an immature SR. XIP inhibits I_{NaCa} in neonatal myocytes and may be useful in studying developmental changes in the contribution of Na^+-Ca^{2+} exchange to cardiac contraction.

Th-Pos262

REDOX MODULATION OF RAT BRAIN Na^+/Ca^{2+} EXCHANGER. ((R.A. Colvin, J. Schummers, and N. Davis)) Dept. Biological Sciences, Ohio University, College of Osteopathic Medicine, Athens, OH 45701.

The heart exchanger is known to be modulated by redox reactions. We examined redox modulation of the brain exchanger since molecular cloning has revealed unique isoforms in the brain. When plasma membrane vesicles were incubated with 1mM DTT at 37°C for 1 hr a 35% decrease in Na/Ca exchange activity was seen. There was no stimulation when vesicles were incubated with Fe/DTT. Addition of 10mM H_2O_2 reversed the effect of DTT. Sodium Nitroprusside (SNP) (0.1mM), which releases both NO and ferrocyanide, had no effect, but when added to DTT treated vesicles caused a further (25%) inhibition. The effect was dose dependent with a half maximal effect seen at 2μM. Ferrocyanide did not cause inhibition when added after DTT treatment. Initial velocity experiments were performed with various concentrations of Ca and Vmax and Km determined. DTT inhibition resulted from a decrease in Vmax with no effect on the Km for Ca. H_2O_2 was able to reverse the Km effect. There was no effect of DTT/SNP on either the Km or Vmax. There was no effect of DTT or DTT/SNP on membrane permeability to Ca. Western analysis showed a single band of MW 116 kDa in the presence of NEM. Incubation with DTT resulted in the appearance of a second protein of 19 kDa. In summary, redox modulation of the brain exchanger is quite different than the heart exchanger. The results indicate that plasma membrane preparations of brain exchanger contain important disulfide bridges that modulate Ca affinity. The large cytoplasmic loop may be clipped by proteases *in situ*, and a peptide fragment released when disulfide bridges are reduced by DTT. The mechanism of SNP inhibition appears to be due to NO production and is still under investigation.

Th-Pos263

ALTERNATIVE SPLICING MODIFIES THE C-TERMINAL TRANSMEMBRANE DOMAINS OF THE Na^+/Ca^{2+} EXCHANGER ((N. Gabellini*,T. Iwata+ and E. Carafoli*+)) *Dept. of Biol.Chem., University of Padova, 35121 Padova, Italy. +Inst. of Biochem. Swiss Federal Inst. of Technol.(ETH), 8092 Zürich (Switzerland).

The complete amino acid sequence of the exchanger was assumed to be encoded in the 5' proximal region (~3 kb) of the 7 kb mRNA. The deduced secondary structure of the Na^+/Ca^{2+} exchanger predicts 11 trans-membrane (TM) domains and a large intracellular loop between TM segments V and VI. Expression of a canine cDNA fragment comprising the largest portion of the 5' region (6 kb) of the 7 kb mRNA in human kidney 293 cells showed that this sequence contained an intron that could be alternatively spliced in four types of rearranged transcripts. Reverse transcribed PCR analysis and DNA sequencing of the amplified DNA fragments revealed that a short sequence at the 3' end of the 6 kb cDNA was alternatively connected to bases 3198, 2821, 2620 and 1844, respectively. In the first case the adjoining exon was located after the putative stop codon of the proposed sequence. In the second and third type of rearrangement a hydrophobic sequence encoded by the spliced-in exon was linked with the IV or the V extracellular loops, and could possibly replace TM segments IX or XI. In the fourth type of transcript the exon sequence introduced a stop codon in the large intracellular loop after only one additional amino acid. RNAse protection analysis revealed that these alternative splicings also occurred in heart and brain. The shortened transcripts were more abundant when naturally expressed in tissues than in 293 cells. Measurements of Ca^{2+} uptake in 293 cells expressing the modified exchanger protein indicated a higher exchanger activity in comparison with that of 293 cells expressing a 3.7 kb cDNA missing the 3' region.

Th-Pos264

GLUTAMATE REGULATION OF Na^+/Ca^{2+} EXCHANGER mRNA LEVELS IN NEURONAL CULTURES OF RAT CEREBRAL CORTEX. ((V.Janapati., L.Luckenbill-Edds. and R.A.Colvin)) Department of Biological Sciences, Program in Neurobiology, Ohio University, Athens, OH-45701.

The Na^+/Ca^{2+} exchanger is a major Ca^{2+} regulating transmembrane protein. In neurons it is thought to be responsible for the Ca^{2+} efflux after glutamate-induced Ca^{2+} influx. Reduced expression of the exchanger could lead to increased susceptibility to Ca^{2+} dyshomeostasis and glutamate induced excitotoxicity which are implicated in age associated neurological disorders. Previous results have shown decreased expression of the exchanger in aging rat cerebral cortex, hippocampus and cerebellum and alteration in the exchange activity in human brain tissue with Alzheimer's pathology. To understand how the exchanger expression and activity is regulated during elevated Ca^{2+}[i] we are studying the effect of glutamate on the expression/regulation of the Na^+/Ca^{2+} exchanger. Exposure of neuronal cultures to 10μM glutamate, but not 5μM concentration for up to 1hr caused a gradual decline in both 15kb and 7kb transcripts of the exchanger by 38% and 36% respectively. Ca^{2+}[i] levels were monitored in fura-2 loaded neuronal cultures at intervals from 0-2hrs after the addition of glutamate in Kreb's medium. Basal Ca^{2+}[i] was 48.7nM. Addition of 5μM and 10μM glutamate lead to an elevation of Ca^{2+}[i] to 192.8nM and 244.9nM, respectively. The Ca^{2+}[i] levels were elevated throughout the period of glutamate treatment. Consistent elevation of Ca^{2+}[i] levels above a threshold point may cause down regulation of mRNA levels of the exchanger.

Th-Pos265

SODIUM-CALCIUM EXCHANGE ACTIVITY RETARDS INTRACELLULAR STORE REFILLING AND STORE-DEPENDENT CALCIUM INFLUX IN TRANSFECTED CHO CELLS. ((Melissa Vazquez, Galina Chernaya and John P. Reeves)) Department of Physiology, UMDNJ-NJ Medical School, Newark, NJ 07103

$InsP_3$-sensitive intracellular Ca stores in CHO cells were depleted by treating the cells for 1 min with 10 μM ionomycin in a Ca-free medium. The cells were centrifuged and resuspended in a Ca-free medium containing 0.3% bovine serum albumin to scavenge the ionomycin. Subsequent addition of 1 mM $CaCl_2$ led to a rapid refilling of the $InsP_3$-sensitive stores, as assessed by the $[Ca]_i$ transient elicited by extracellular ATP in fura 2-loaded cells. In transfected CHO cells expressing the bovine cardiac Na/Ca exchanger (CK1.4 cells), the rate of store refilling was slower than in control cells transfected with the vector alone (C1 cells). When placed in a Na-free medium (Li-substitution), the rate of store refilling was greatly accelerated in the CK1.4 cells; Na-removal had no affect on the rate of store refilling in the C1 cells. Thapsigargin (Tg) treatment also depleted the $InsP_3$-sensitive stores, but subsequent store refilling was prevented due to blockade of the SERCA ATPase. The increase in $[Ca]_i$ produced by the addition of 1 mM $CaCl_2$ to Tg-treated CK1.4 cells was much smaller than that observed in C1 cells and was greatly enhanced by removal of extracellular Na. The results indicate that Na/Ca exchange activity sharply reduces the net entry of Ca in response to depletion of $InsP_3$-sensitive stores, probably by catalyzing Na_o-dependent Ca efflux.

Th-Pos266

SODIUM-CALCIUM EXCHANGE ACTIVITY IS REGULATED BY THE ACTIN CYTOSKELETON IN TRANSFECTED CHO CELLS. ((M. Condrescu, G. Chernaya, J.F. Aceto, C. Kroupis, J.P. Gardner and John P. Reeves)) Department of Physiology and Hypertension Research Center, UMDNJ-NJ Medical School, Newark, NJ 07103

Treatment of transfected CHO cells expressing the bovine cardiac Na/Ca exchanger with mitochondrial inhibitors in the absence of glucose depleted the cells of ATP and produced a rapid breakdown in the actin cytoskeleton, as revealed by FITC-phalloidin staining. These changes were associated with a reduction in ^{45}Ca uptake by ouabain-treated cells and a 2-fold decrease in the K_i for external Na as a competitive inhibitor of ^{45}Ca uptake. Treatment of the cells with 1 μM cytochalasin D for 30 min produced effects similar to those of ATP depletion on both the actin cytoskeleton and ^{45}Ca uptake. However, cytochalasin D did not inhibit Na_o-dependent Ca efflux by the exchanger, a process which was markedly inhibited by ATP depletion. The effects of both ATP depletion and cytochalasin D on exchange activity were absent or greatly reduced in cells expressing two different mutants: (a) a deletion mutant missing 450 out of 520 amino acids within the central hydrophilic domain, and (b) a mutant in which a string of acidic amino acids at the C-terminal end of the hydrophilic domain (723-EDDDDDECGEE) were changed to alanines. The results indicate that the kinetic properties of the Na/Ca exchanger in these cells are regulated by interactions with the actin cytoskeleton and that the central hydrophilic domain of the exchanger participates in these interactions.

Th-Pos267

VOLTAGE-DEPENDENCE OF Ca/Ca EXCHANGE MEDIATED BY THE REGULATED AND DEREGULATED Na/Ca EXCHANGER IN MUSCLE CELLS. ((J. Tie, R. Espinosa-Tanguma, J. DeSantiago and H. Rasgado-Flores)) FUHS/Chicago Medical School. North Chicago Il 60061.

In muscle cells, a mild treatment with α-chymotrypsin activates the Na/Ca exchanger by removing its dependece on intracellular Ca^{2+} (i.e. becomes deregulated). Internally perfused, voltage-clamped barnacle muscle cells were used to study the effect of α-chymotrypsin on the voltage-dependence of the extracellular Ca^{2+} (Ca_o)-dependent Ca^{2+} efflux (Ca/Ca exchange). The fluxes of Ca^{2+} were measured radiometrically from cells perfused with 10 μM Ca^{2+}. To reduce the membrane conductance the internal and external solutions were free of Cl^- and K^+. To remove Na/Ca and promote Ca/Ca exchange the main extracellular cation was Li^+. Both before and after α-chymotrypsin treatment, there was a linear relationship between the normalized (%) Ca_o-dependent Ca^{2+} efflux and membrane potential (from -60 to +20 mV). In the absence of the protease-treatment, Ca/Ca exchange decreased with depolarization and increased with hyperpolarization (slope= 21 $\pm$ 3 % per 25 mV). However, exposure to α-chymotrypsin induced reversal of the voltage dependence of the Ca/Ca exchange. Namely, Ca/Ca exchange increased with depolarization and decreased with hyperpolarization (slope= 22 $\pm$ 1.75 % per 25 mV). Since α-chymotrypsin did not affect the membrane conductance (~12 pS/cm^2) it is suggested that the enzyme alters the voltage-dependence of the rate-limiting translocation step.

Th-Pos268

EFFECT OF MEMBRANE POTENTIAL ON ACTIVITY OF RECONSTITUTED MITOCHONDRIAL Na^+/Ca^{2+} ANTIPORTER. ((M. Jaburek and K. D. Garlid)) Dept. of Chemistry, Biochemistry, and Molecular Biology, Oregon Graduate Institute of Science & Technology, Portland, OR 97291-1000.

The mitochondrial Na^+/Ca^{2+} antiporter plays a key role in the regulation of matrix Ca^{2+}. We have purified and reconstituted this antiporter from beef heart mitochondria and shown that it catalyzes electroneutral Na^+/Ca^{2+} exchange in the absence of $\Delta\Psi$ (membrane potential) [Li et al. (1992) J. Biol. Chem. *267*, 17983]. However, recent studies using intact mitochondria have suggested that Na^+-dependent Ca^{2+} efflux is affected by $\Delta\Psi$ [Baysal et al. (1994) Am. J. Physiol. *266*, C800]. We examined the effect of $\Delta\Psi$ on Na^+ and Ca^{2+} fluxes mediated by the purified Na^+/Ca^{2+} antiporter using fluorescent probe techniques. $\Delta\Psi$ was controlled by varying internal and external K^+ in the presence of valinomycin. We found that inside-positive $\Delta\Psi$ stimulated Na^+-dependent Ca^{2+} uptake and Ca^{2+}-dependent Na^+ efflux, whereas negative $\Delta\Psi$ reduced these fluxes. These effects were superimposed on significant electroneutral Na^+/Ca^{2+} exchange at $\Delta\Psi = 0$. These results confirm that $\Delta\Psi$ can modulate the activity of mitochondrial Na^+/Ca^{2+} exchange and suggest that the Na^+:Ca^{2+} stoichiometry may vary between 2:1 and 3:1. (Supported by NIH grant HL 36573)

Th-Pos269

BEPRIDIL AS A TOOL TO STUDY Na^+/Ca^{2+} ECHANGE SYSTEM IN GLUTAMATE-TREATED CULTURED NERVE CELLS. ((V.Pinelis*,B.Khodorov*, D.Fajuk*, T.Storozhevych*, N.Vinskaya*, O.Vergun*, L.Khaspekov+, A.Lyzhin+, I.Victorov+)) *Institute of Pediatrics, Institute of General Pathology and Pathophysiology, +Brain Research Institute, Moscow, Russia.

Blockade of $Na^+_o/Ca^{2+}{}_i$ exchange by bepridil (Bp) in fura-2 loaded resting cultured hippocampal neurons and cerebellar granule cells either did not change the basal $[Ca^{2+}]_i$ or caused its small increase. In contrast, application of Bp (50μM) during the action of 100 μM glutamate (GLU) induced a pronounced additional $[Ca^{2+}]_i$ elevation. After the termination of 15-30 min GLU challenge most of cells exhibited high $Ca^{2+}{}_i$ plateau. In these cells application of Bp in the post-glutamate period usually failed to cause a further increase in $[Ca^{2+}]_i$. In other cells with a partial or complete $[Ca^{2+}]_i$ recovery Bp elicited a new considerable raise of $[Ca^{2+}]_i$. Conclusion is drawn that Na^+/Ca^{2+}exchange-mediated Ca^{2+} extrusion does not contribute much to a maintenance of basal $[Ca^{2+}]_i$, is greatly accelerated during GLU application (especially in the begining of its action) but is suppressed in the period of post-glutamate $Ca^{2+}{}_i$ plateau. (Supported by ISF,MBA 000).

Th-Pos270

CARDIAC SARCOLEMMAL SODIUM-CALCIUM EXCHANGE IN ELDERLY RATS. ((Malcolm M. Bersohn)) Veterans Affairs Medical Center and University of California, Los Angeles, CA 90073

Abnormalities of ventricular relaxation are prevalent in the elderly and have been hypothesized to be related to alterations in calcium transport. To investigate the effect of aging on the cardiac sarcolemmal sodium-calcium exchanger, I purified sarcolemmal vesicles from hearts of 4, 12, and 27 month old Fischer 344 rats, with two hearts pooled for each preparation. Sarcolemmal purification was assessed by the ratio of K^+-*p*-nitrophenylphosphatase activity in the sarcolemma (SL) to that in the crude homogenate (H). I measured the initial velocity of sodium-calcium exchange as Na^+_i-dependent $^{45}Ca^{2+}$ uptake at Ca^{2+}_o from 5-40 μM and calculated the Km and Vmax for each experiment. Means $\pm$ SE:

Age (months)	4	12	27
Purity (SL/H)	21 $\pm$ 4	24 $\pm$ 1	19 $\pm$ 4
Km (μM Ca^{2+})	8.3 $\pm$ 0.8	9.0 $\pm$ 0.7	8.0 $\pm$ 0.6
Vmax (nmol $Ca^{2+}\cdot mg^{-1}\cdot s^{-1}$)	2.08 $\pm$ 0.13	2.12 $\pm$ 0.06	1.65 $\pm$ 0.12*

*P<0.05 vs both young and middle-aged

In elderly but not middle-aged rats, there is a reduction in maximal velocity for sodium-calcium exchange with no change in calcium affinity. Because sodium-calcium exchange is the major mechanism for sarcolemmal calcium efflux, a 20-25% reduction in Vmax could be a cause for the abnormalities in ventricular relaxation in the elderly.

Th-Pos271

Na-Ca EXCHANGE INFLUENCES Ca^{2+} SIGNALS AND CATECHOLAMINE RELEASE IN CHROMAFFIN CELLS ((Allan S. Schneider and Chung-Ren Jan)) Dept. Pharmacology & Toxicol, Albany Medical College, Albany, NY 12208

In an effort to understand the role of Na/Ca exchange in cytosolic Ca^{2+} signaling and neurohormone secretion, we have tested the effects of cellular Na^+ loading and depletion on $^{45}Ca^{2+}$ uptake, cytosolic Ca^{2+} levels and catecholamine release from cultured bovine adrenal chromaffin cells. Evidence was found for Na^+-dependent uptake of Ca^{2+} across the plasma membrane during a depolarizing stimulus. The effect of this Ca^{2+} uptake on catecholamine release was dependent on intracellular Na^+ levels. Evidence was also found for Na/Ca exchange across intracellular organelle membranes. In one set of experiments, a spontaneous rise and oscillation in cytosolic Ca^{2+} was observed following a period of cellular Na^+ loading in the absence of extracellular Ca^{2+}. There was an accompanying rise in basal catecholamine release. In other experiments Na^+-dependent $^{45}Ca^{2+}$ transport across the cell surface was found to be related to the amount of exocytotic chromaffin granule membrane inserted into the plasma membrane. The latter results are consistent with our earlier report (Jan and Schneider, J. Biol. Chem. 267, 9695-9700, 1992) of Na^+-dependent Ca^{2+} efflux across exocytotic secretory vesicle membranes contributing to the decay of the Ca^{2+} signal for catecholamine release. The combined results suggest that Na/Ca exchange across secretory vesicle and plasma membranes can influence the rise and decay of cytosolic Ca^{2+} signals for neurohormone release. Supported by: NIH-DK39220;Am.Heart Assoc.NYS Affil.90-049G

Th-Pos272

SODIUM/CALCIUM EXCHANGE IN SLOW SKELETAL MUSCLE FIBERS OF THE CHICKEN. ((J. Muñiz, M. Huerta, M. Diaz* and X. Trujillo)) Centro Universitario de Investigaciones Biomédicas, Universidad de Colima, Apdo. postal 199, Colima, Colima, 28000 México.

The Na/Ca exchange was investigated by contractile response to alteration of the extracellular sodium concentration in slow muscle fibers of the chicken. Isometric tension was recorded from slow bundles of anterior latissimus dorsi muscle of the chicken up to 3 weeks old. Normal solution was (mM): NaCl, 167; KCl, 5; $CaCl_2$, 5; $MgCl_2$, 2 and glucose 2g/l, pH was adjusted to 7.4 with imidazole-chloride. Na^+-free solutions were prepared by replacing NaCl with an osmotically equivalent amount of TEACl. When Ca^{2+} was omitted from the solution, it was replaced by 10 mM $MgCl_2$. Experiments were done at room temperature (20-22oC). Contractures were evoked in solutions where the extracellular sodium was reduced or withdrawn. The contractile responses were dependent upon sodium concentrations. When external calcium was omitted from the solution, the tension of the sodium withdrawal contracture was greatly reduced. These results suggest that Na/Ca exchange is present in the membrane of slow skeletal muscle fibers of the chicken.

* CONACyT Fellowship

Th-Pos273

HYPO-OSMOTIC STRESS REDUCES SODIUM-CALCIUM EXCHANGE CONDUCTANCE IN ISOLATED GUINEA-PIG VENTRICULAR MYOCYTES ((A.R. Wright, S.A. Rees, J.I. Vandenberg, V.W. Twist and T. Powell)) University Laboratory of Physiology, Parks Road, Oxford, UK

Hypo-osmotically induced cell swelling has been shown to affect many ion transport pathways, and the present study has found that hypo-osmotic stress reduces sodium-calcium exchange conductance in guinea-pig ventricular cells. Whole cell current recordings at 31 - 34 °C were made during a 20 mV to -110 mV ramp, repeated at four second intervals with a holding potential of -90 mV, using the whole cell voltage clamp technique. The pipette solution contained (mM): NaCl, 12.3; $CaCl_2$, 18.2; BAPTA, 30; $MgCl_2$, 1.8; HEPES, 5; Mg-ATP, 10; TEA-Cl, 5; Aspartic acid, 42; pH 7.4 with CsOH, giving a 300 mOsm solution with 300 nM free calcium. The isotonic superfusing solution contained (mM): NaCl, 70; $BaCl_2$, 2; $MgCl_2$, 2; $CaCl_2$, 2; sucrose, 140; HEPES, 5; and Ouabain, 20 µM; Nicardipine 2 µM; pH 7.4 with NaOH. The hypo-osmotic superfusate contained variable amounts of sucrose, total omission giving 150 mOsm. 2mM $NiCl_2$ was added briefly to block exchanger current (I_{NaCa}) before and after switching from isotonic to hypotonic solution. The slope conductance of I_{NaCa} was then calculated for 20 mV segments of the ramp and was found to decrease linearly with decreasing osmolality, with similar changes throughout the voltage range for each osmolality. Total omission of sucrose from the hypo-osmotic solution led to a 40 ± 6% decrease in I_{NaCa} with no significant change in reversal potential (n=9). When 25 µM Exchanger Inhibitory Peptide (XIP) was present in the pipette solution the remnant of exchanger current after 30 minutes perfusion (Typically 25% of initial I_{NaCa}) was reduced on sucrose removal by 46 ± 14% (n=3). In a further experiment, external $CaCl_2$ was replaced by the calcium chelator EGTA to abolish I_{NaCa} before switching osmolality, and no difference in whole cell conductance resulted from the osmolality change. These results suggest that I_{NaCa} is reduced by hypo-osmotic stress through mechanisms which seem not to depend upon membrane potential.

Th-Pos274

PHOSPHOARGININE STIMULATES Na-Ca EXCHANGE IN DIALYZED SQUID AXONS. Beaugé, L & *DiPolo, R., Instituto de Investigación Médica M. y M. Ferreira, Córdoba, Argentina, *Centro de Biofísica y Bioquímica, IVIC, Caracas, Venezuela, and Marine Biological Laboratory, Woods Hole, USA.

Dialyzing squid giant axons without ATP and with $[Ca^{2+}]_i$ around 1 µM we found that the basal levels of the Na_o-dependent Ca efflux were significantly higher in the presence of 5 mM N^{ω}-Phosphoarginine (Pa). In the following up work we confirmed the existence of a Pa-stimulation of the Na/Ca exchanger showing that: i) it occurs in the complete absence of ATP; ii) it is independent of, and additive to, the ATP-stimulated exchange; iii) it is largely, but not absolutely, dependent on Mg^{2+} ions; (iv) the onset rate increases together with the ionized calcium concentration; (v) it is fully and rapidly reversible and has a K_m for Pa around 7.7 mM. The ATP and ADP concentrations, estimated or measured in the axon, were negligible and could not account for the results observed with Pa. The addition of vanadate has the following effects: (1) stimulates Na-Ca exchange over the levels reached with Pa, and (2) maintains the Pa effect once the phosphagen has been withdrawn. On the other hand, phosphocreatine, a closely related compound, has no effect on the Na-Ca exchanger. This work demonstrates for the first time the presence, in squid axons, of a new form of metabolic regulation of the Na/Ca exchanger directly and solely related to Pa and different from that due to MgATP. This novel mechanism is likely to play a physiological role in Ca extrusion through the Na/Ca exchanger particularly at micromolar $[Ca^{2+}]_i$. It remains to be explored whether a comparable system exists in vertebrates in which phosphocreatine could replace phosphoarginine as the activating substrate. (Supported by Grants from NSF, USA (BNS9120177), CONICIT, Ve (S1-2651) and CONICET, Arg. (PID-BID 1053).

Th-Pos275

AN AXOPLASMIC FACTOR FROM SQUID GIANT AXONS INDUCES A MgATP STIMULATION OF Na-DEPENDENT ^{45}Ca UPTAKE IN MEMBRANE VESICLES FROM SQUID OPTIC NERVES. DiPolo, R.,*Berberián, G.,Delgado, D. Rojas, H, & *Beaugé, L. Centro de Biofísica y Bioquímica, IVIC, Caracas, *Instituto M. y M. Ferreira, Córdoba, Argentina, Venezuela and Marine Biological Laboratory, Woods Hole, USA.

Membrane vesicles from squid optical nerves do not show any MgATP effect on the Na/Ca exchanger. A possible explanation could be that an important regulatory factor has been lost during their preparation. We have explored whether a cytoplasmic factor may be required for that MgATP effect. Membrane vesicles were prepared by differential centrifugation and loaded with 300 mM NaCl, 0.1 mM EDTA and 30 mM MOPS-Tris pH 7.4. Axoplasm from fresh squid nerves was homogenized in 1:1 vol of 20 mM MOPS-Tris (pH 7.4, 20 oC), 1 mM DDT, 0.1 mM EDTA, 0.2 mM EGTA and an antiproteases cocktail (0.5 mM PMFS and 10 µg/ml of Aprotinine, Leupeptin and Peptatin A) in a ratio 1:1 (w/v). The homogenate was centrifuge at 10000 x g for 10 min and the supernatant used for transport assays. ^{45}Ca uptake was measured at 20° C in media with high (300 mM) or low (30 mM) Na. In addition, all media contained enough MOPS-Tris to maintain the osmolarity at 700 mOsmols, and 0.1 mM vanadate. When present, Mg^{2+} was 1.5 mM and ATP 1 mM. Na-gradient dependent Ca uptake (high Na - low Na) from a medium containing 0.6 µM Ca^{2+} was measured for 10 sec in 200 µl total volume containing 10 µl vesicles (50-60 µg protein) with or without axoplasm (10 µl; 150 µg protein). In the presence of Mg^{2+} and ATP, Ca_i/Na_i exchange was 0.594 ± 0.076 (n=19) and 0.184 ± 0.041 (n=13) nmole/mg Prot.10 sec with and without axoplasm respectively. Activation of Na-dependent Ca uptake by preincubation with axoplasm failed to appear (i) in the absence of ATP and or Mg^{2+} ions, and (ii) when the axoplasm was pre-heated at 70 °C for 20 min or digested with trypsin. Furthermore, no stimulation by ATP was observed when albumin (300 µg) was used instead of axoplasm. These experiments support the existence of an axoplasmic protein which induces a MgATP stimulation of the Na/Ca exchange in vesicles from squid optical nerve. (Supported by Grants from NSF, USA (BNS9120177), CONICIT, Ve (S1-2651) and CONICET, Arg. (PID-BID 1053).

Th-Pos276

CA^{2+} RELEASE IS THE RATE LIMITING STEP OF PHOTORECEPTOR NA^+:CA^{2+},K^+ EXCHANGER CYCLE. ((A. Navangione, G. Rispoli and V. Vellani)) Istituto di Fisiologia Generale, Via Borsari 46, Ferrara, Italy 44100.

The reaction cycle of photoreceptor Na^+:Ca^{2+},K^+ exchanger was studied in isolated rod outer segment (OS) recorded in whole cell voltage clamp and dialyzed with saturating $[Ca^{2+}]_i$ (> 1 mM) and $[K^+]_i$ (> 50 mM). The exchange current I_E (-48±1.9 pA, n=14; V_m= 0 mV) recorded in OS bathed in > 80 mM Na_o^+ (all 0 Ca^{2+} solutions contain 2 mM EGTA) was little affected by increasing $[Na^+]_i$ or $[K^+]_o$ by tens of mM, while it was rapidly (with the time course of the solution change, <50 ms) and strongly reduced (I_E = -6.4±0.3 pA) by switching to 5 mM Ca_o^{2+}. Reverse exchange current recorded with > 80 mM $[Na^+]_i$ and saturating $[Ca^{2+}]_o$ and $[K^+]_o$, was also little affected by increasing $[Na^+]_o$ or $[K^+]_i$ by tens of mM, while it was blocked by 5 µM $[Ca^{2+}]_i$. This suggests that Ca^{2+} release is a rate limiting step in the exchange cycle, while Na^+ and K^+ release are not. The exchange current decayed rapidly to zero (< 50 ms) upon switching to 166 mM Li_o^+ or 166 mM K_o^+ or 159 mM Li_o^+ + 5 mM Ca_o^{2+}. At this point, switching back to 166 mM Na_o^+, the current recovered I_E in two phases: a fast one, lasting few tens of ms and of amplitude I_F, followed by a slower one with an exponential time course (τ = 363±20 ms). The largest I_F (-57.5±2.7 pA) was recorded after 0 Ca_o^{2+} preapplication, while I_F was -37.5±1.4 pA after Ca_o^{2+} preapplication. It was necessary to perfuse in 0 Ca_o^{2+} for at least 3 s, after Ca_o^{2+} preapplication, to maximize I_F; however, as soon as Ca_o^{2+} was presented after the 0 Ca_o^{2+} perfusion, I_F was reduced. Thus the exchanger binds Ca_o^{2+} in less than 50 ms, while it releases Ca_o^{2+} in about 360 ms: Ca_o^{2+} release is then the rate limiting step in the exchange cycle, giving a turnover rate of about 3 Ca^{2+} ions/s extruded and a density of 10^4 mol/µm^2. This large density may be designed to prevent disuniform distribution of $[Ca^{2+}]_i$ that may dramatically affect the photoreceptor light response.

Th-Pos277

DYNAMIC CONFORMATIONAL CHANGE OF THE JUNCTIONAL FOOT PROTEIN (JFP) DURING E-C COUPLING IN TRIADS. ((M. Yano[1], R. El-Hayek[1], B. Antoniu[1], and N. Ikemoto[1,2])). 1, Boston Biomed. Res. Inst.; 2, Dept. Neurology, Harvard Med. Sch., Boston, MA.

The electro-mechanical coupling hypothesis originally proposed by Schneider and Chandler predicts mechanical changes, or , in biochemical terms, conformational changes in the JFP/Ca^{2+} release channel protein during e-c coupling. Here we present new evidence that T-tubule depolarization produces first a rapid conformational change in the JFP, and subsequently Ca^{2+} release from the SR. The JFP moiety of the triad was covalently labeled in a site-directed fashion with the fluorescent conformational probe MCA (Kang et al., 1992). After polarizing the T-tubule moiety and loading the SR with Ca^{2+}, the T-tubule was depolarized by the $K^+ \rightarrow Na^+$ replacement protocol (triads: Ikemoto et al., 1994; skinned fiber: Lamb and Stephenson, 1990). This induced a rapid increase of the fluorescence intensity of the JFP-bound probe (ΔF), which preceded SR Ca^{2+} release (monitored using fluo-3 as a Ca^{2+} probe). Both the amplitude of ΔF and the amount of SR Ca^{2+} release increased with the increased magnitude of T-tubule depolarization. Blockage of the T-tubule $\rightarrow$ SR communication by nimodipine or neomycin inhibited both ΔF and SR Ca^{2+} release. These results suggest that upon T-tubule depolarization the JFP undergoes a conformational change from one state (C1) to the other (C2), which is prerequisite to the channel activation and Ca^{2+} release (Ca): C1 $\rightarrow$ C2 $\rightarrow$ Ca. (Supported by grants from NIH and MDA)

Th-Pos278

CONFORMATIONAL CHANGE OF THE JUNCTIONAL FOOT PROTEIN (JFP) IS INVOLVED IN THE REGULATION OF POLYLYSINE-INDUCED Ca^{2+} RELEASE FROM THE SR. ((R. El-Hayek[1], M. Yano[1], B. Antoniu[1], and N. Ikemoto[1,2]). 1, Boston Biomed. Res. Inst.; 2, Dept. Neurology, Harvard Med. Sch., Boston, MA.

Nanomolar concentrations of polylysine bind specifically to the JFP and induce a rapid Ca^{2+} release from SR (Cifuentes *et al*, 1989). In an attempt to monitor the events occurring in the JFP upon direct stimulation by polylysine, the JFP moiety of the triad from rabbit skeletal muscle was labeled in a site-directed fashion with the fluorescent conformational probe MCA (Kang *et al*, 1992). The fluorescence intensity of the JFP-bound MCA showed essentially the same activation/inhibition pattern as that of SR Ca^{2+} release. Both MCA fluorescence and polylysine-induced Ca^{2+} release showed similar bell-shaped [Ca^{2+}]-dependence curves. Furthermore, increasing concentrations of polylysine used to induce Ca^{2+} release at 1 μM Ca^{2+}, produced similar changes in the MCA fluorescence. The consistent parallelism between MCA fluorescence and Ca^{2+} release activity suggests that activation of Ca^{2+} release is mediated by a conformational change of the JFP. The conformational change appears to be a prerequisite mechanism of Ca^{2+} release because 5 mM Mg^{2+} inhibited Ca^{2+} release without affecting the conformational change. Together with our finding that a similar mechanism operates in depolarization-induced Ca^{2+} release (cf neighboring abstract), this suggests that the activation of different types of Ca^{2+} release may be mediated by a common mechanism involving a conformational change in the JFP. (Supported by grants from NIH and MDA).

Th-Pos279

REGULATORY CONFORMATIONAL CHANGE OF THE JUNCTIONAL FOOT PROTEIN (JFP) IS ALTERED IN MALIGNANT HYPERTHERMIA-SUSCEPTIBLE PORCINE MUSCLE SR. ((R. El-Hayek[1], M. Yano[1], B. Antoniu[1], C. F. Louis[2], J. R. Mickelson[2], and N. Ikemoto[1,3])). 1, Boston Biomed. Res. Inst.; 2, Dept. Vet. Pathobiol., Univ. of Minnesota; 3, Dept. Neurol. Harvard Med. Sch., Boston, MA. (Spons by P. Graceffa)

Our previous study on polylysine-induced Ca^{2+} release in normal (N) and malignant hyperthermia-susceptible (MHS) porcine muscle SR (El-Hayek *et al*, 1994) has shown that Ca^{2+} release in MHS-SR is activated at much lower concentrations of polylysine than N-SR. Here we show that the altered ligand sensitivity of MHS-SR Ca^{2+} release may be due to an altered JFP conformational change. Specific MCA labeling of the JFP of N and MHS-SR was performed as done with the rabbit preparation (cf neighboring abstract). Contemporaneous measurements of (a) Ca^{2+} release from the SR and (b) the fluorescence intensity of the JFP-bound MCA probe were carried out at different concentrations of polylysine. In agreement with our previous study with unlabeled preparations, the concentration of polylysine for half-maximal activation (C_{50}) of Ca^{2+} release was much lower in MHS-SR than N-SR. The MCA fluorescence paralleled the polylysine-activation of Ca^{2+} release in both SR preparations; thus, the C_{50} of MCA fluorescence increase was significantly lower in MHS-SR than N-SR. These results are consistent with the notion that a conformational change in the JFP appears to be an essential step in the mechanism regulating channel activation. The region of the JFP that includes the site of the point mutation in MHS (a.a. 615) might be responsible for an altered MCA response. (Supported by grants from NIH and MDA).

Th-Pos280

CALCIUM TRANSPORT BY TRANSVERSE TUBULE IS DECREASED IN MALIGNANT HYPERTHERMIA SUSCEPTIBLE SKELETAL MUSCLE. ((M. Alfonzo[1,2], J.R. López[2,3])) [1]Escuela de Medicina José M. Vargas, UCV, [2] Instituto Venezolano de Investigaciones Científicas, Caracas, Venezuela.[3] Department of Anesthesiology, Brigham and Women's Hospital, Boston, MA

Malignant hyperthermia (MH) is characterized by an alteration in myoplasmic Ca^{2+} homeostasis. We measured Ca^{2+} transport by the transverse tubule (T-tubule) vesicles prepared from muscle biopsies removed from Yorkshire non-MH susceptible swine (NMHS), and Poland China MH susceptible swine (MHS). Skeletal muscle T-tubule vesicles from NMHS and MHS were prepared by the method of Hidalgo et al (*Biochim. Biophys. Acta* 854:279-86, 1986). Control experiments were conducted in the presence of oxalate, phosphate, and orthovanadate to characterize the microsomal preparation. In NMHS and MHS in the absence of ATP, negligible amounts of Ca^{2+} were accumulated. T-tubules vesicles prepared from NMHS and MHS displayed a difference in Ca^{2+} transport capacity. NMHS T-tubule vesicles accumulated 29±6 nmol Ca^{2+}/mg (n=15) at 2 min, 40±2 (n=17) at 5 min, 64±3 (n=16) at 10 min, and 115±4 (n=19) at 15 min. In MHS Ca^{2+} transport was reduced by 30% at 2 min ($p<0.001$), by 39% at 5 min ($p<0.001$), by 52% at 10 min ($p<0.0001$) and by 62% at 15 min ($p<0.0001$). Stimulation of Ca^{2+} uptake by calmodulin was similar in NMHS and MHS T-tubule vesicles. These results show that ATP-dependent calcium uptake by T-tubules vesicles in MHS is significantly decreased. This deficiency in T-tubule calcium transport could explain, in part, the abnormal intracellular Ca^{2+} concentration observed in MHS skeletal muscle. (Partially supported by grant from Laboratorio Elmor, Venezuela).

Th-Pos281

IMMORTALIZED CELL LINES FROM DYSGENIC SKELETAL MUSCLE: EVIDENCE FOR TRIAD FORMATION WITHOUT DIHYDROPYRIDINE RECEPTOR α SUBUNITS. ((J.A. Powell, L. Petherbridge and B.E. Flucher*)) Smith College, Northampton, MA 01063 and *NINDS, NIH, Bethesda MD 20892. (Spon. by S.P. Scordilis)

Muscular dysgenesis, a homozygous recessive (*mdg/mdg*) disorder in the mouse, has served as a model to study the function of the α_1 subunit of the dihydropyridine receptor (DHPR), and its role in triad formation because the α_1 of the DHPR is absent in this mutant muscle. We have generated companion cell lines derived from dysgenic and normal (+/+) muscle by transfection of dissociated myoblasts with a plasmid containing the BK virus Large T antigen. Cell lines of dysgenic (GLT) and normal (NLT) have been expanded at passage 7 and are capable of fusing and differentiating up to passage 12 for NLTs and 18 for GLTs. While the degree of differentiation is lower than that observed in primary cultures, both cell lines express muscle-specific proteins and begin organization of sarcomeres as demonstrated by immunocytochemistry. Similar to the situation in primary cultures, dysgenic (GLT) myoblasts show a higher incidence of cell fusion than do their normal counterparts (NLT). NLT myotubes develop spontaneous contractile activity; fluorescent calcium recordings show calcium release in response to depolarization. In contrast, GLTs show neither spontaneous nor depolarization-induced calcium transients, but they do respond to caffeine. The expression and organization of triad proteins, DHPR α_1 and α_2 subunits and RyR, are the same in the cell lines and primary cultures. GLT myotubes lack the α_1 subunit and the α_2 subunit is mistargeted to the plasma membrane despite the apparently normal formation of T-tubules. The RyR is expressed, and is either diffusely distributed or aggregated in clusters, which correspond to junctions with regularly spaced feet in electron microscopy. This finding provides evidence for the formation and partial differentiation of triad junctions without the DHPR α subunits. (Supported by grants from MDA and The Blakeslee Fund to J.A.P.)

Th-Pos282

DANTROLENE RECEPTOR FROM MALIGNANT HYPERTHERMIA SUSCEPTIBLE SKELETAL MUSCLE ((S.S. Palnitkar* and J. Parness)) Depts. Anesthesia*, Pediatrics and Pharmacology, UMDNJ-Robert Wood Johnson Medical School, New Brunswick, NJ 08903

Skeletal muscle contraction is normally effected by a process known as excitation-contraction couplung (ECC). Malignant hyperthermia (MH) is a genetic susceptibility to volatile anesthetics and depolarizing muscle relaxants causing skeletal muscle hypercontracture and hypermetabolism, due to a defect in ECC. Dantrolene, a hydantoin derivative, is the only specific therapy for this syndrome. It inhibits the release of Ca^{2+} from the sarcoplasmic reticulum (SR) seemingly by turning down the gain on ECC. However the site and mechanism of action of dantrolene are not known. Recently we have developed a specific assay for [^{3}H]dantrolene binding to heavy SR (single class of binding sites, Kd 277±25 nM and Bmax 13.1±1.5 pmol/mg protein). We have also shown that the dantrolene and ryanodine receptors are pharmacologically distinct. We have been successful in applying this binding assay to MH-susciptible porsine skeletal muscle SR membranes. Preliminary results indicate that the drug binds to a single class of binding sites with a Kd and Bmax of 428±79 nM and 18.5±5 pmol/mg protein, respectively. This is the first report of the identification of a dantrolene receptor in MH-susceptible skeletal muscle.

Th-Pos283

K^+ DEPOLARIZATION INDUCED CHANGES IN INTRACELLULAR CALCIUM IN MALIGNANT HYPERTHERMIA SUSCEPTIBLE MYOBALLS.

((J.R. López[1,2], E. Fermin[1], C. Pérez[1], P. Allen [2]))
[1]Instituto Venezolano de Investigaciones Cientfficas, Caracas Venezuela, [2]Department of Anesthesiology, Brigham and Women's Hospital, Harvard Medical School, Boston, MA.

Malignant hyperthermia (MH) is a myopathy associated to a dysfunction in intracellular Ca^{2+} homeostasis. We studied changes in intracellular Ca^{2+} concentration induced by membrane depolarization in single myoballs using the fluorescent indicator Fluo-3. Myoballs were prepared from neonatal (3-4 d) Yorkshire non-susceptible (NMHS), and Poland China swine MH susceptible (MHS). Resting membrane potential (Vm) was monitored with a conventional 3M KCl microelectrode. In the presence of physiological $[K^+]_o$ (5 mM) intracellular Ca^{2+} concentration ($[Ca^{2+}]_i$) in MHS was 2.2 fold higher than in NMHS (236±7 nM vs 107±2 nM, $p<0.001$). High $[K^+]_o$ induced similar depolarization in NMHS and MHS myoballs. This depolarization was associated to a transient rise in $[Ca^{2+}]_i$ that was always greater in the MHS. In NMHS $[Ca^{2+}]_i$ was enhanced by 1.9 and 3.2 fold while in MHS by 2.5 and 4.1 fold in the presence of 10 and 20 mM $[K^+]_o$, respectively. Incubation of NMHS and MHS myoballs in low Ca^{2+} solution (3 mM EGTA-no added Ca^{2+}) did not modify the effect of high $[K^+]_o$ on $[Ca^{2+}]_i$. Theses result show (i) there is a disturbance in the regulation of intracellular Ca^{2+} in MHS myoballs which is manifested by a higher $[Ca^{2+}]_i$; (ii) NMHS and MHS myoballs displayed similar depolarization response upon change of $[K^+]_o$. However, $[Ca^{2+}]_i$ change is always greater in MHS; (iii) the Ca^{2+} involved in K^+-depolarization appears to arise from intracellular store, because it is not modified by removal of $[Ca^{2+}]_o$.

Th-Pos284

THE KINETICS AND EFFECT OF CALCIUM LOADING ON DEPOLARIZATION-INDUCED CALCIUM RELEASE IN ISOLATED TRIADS.

((J.W. Kramer and A.M. Corbett)) Dept. of Physiology & Biophysics, Wright State University, Dayton, Ohio 45435.

Isolated triads from skeletal muscle were loaded with calcium and diluted into a solution which would provide approximately 58 mV depolarization using a variable ratio stopped flow device from SLM-Aminco (1:5 ratio used) and 10 μM fura-2 (pentapotassium salt) as a calcium indication. A 12 msec lag phase was observed during which there was no fluorescence change, followed by a biphasic release of calcium. A double exponential fit to the data yielding time constants of 7-13 msec for the fast phase of release and 0.3-100 sec for the slow phase of release. The time constants for depolarization-induced calcium release in this system is very similar to that observed by Delbono and Stefani (1992, J. Physiol. 463:689-707) for depolarization-induced calcium release from cut rat skeletal muscle fibers. In a separate line of experiments, we examined the effect of calcium loading on depolarization-induced calcium release. In these experiments, we varied loading from 126-503 nm/mg and used maximal depolarization to induce calcium release (1:20 dilution; 75 mV depolarization). We found that as loading of the vesicles was increased, the percent calcium release which was induced by depolarization dropped inversely, in a linear manner. Since there is a mixture of triads and isolated terminal cisterna in our "triadic" vesicle preparation, this study seems to indicate that triadic vesicles load calcium faster than isolated terminal cisternae. The mechanism responsible for this differential calcium loading rate for the two vesicle populations is not yet known. However, this data indicates it is possible to effectively increase the signal from isolated triads upon depolarization simply by reducing the total amount of calcium loaded.

Th-Pos285

USE OF HA1 TAGGED CALSEQUESTRIN (CS-*HA1*) AS A PROBE TO STUDY SARCOPLASMIC RETICULUM TARGETING.

((A. Nori, K.A. Nadalini, A. Martini, R. Rizzuto and P. Volpe)). Dipartimento di Scienze Biomediche Sperimentali, Università di Padova, Padova, Istituto di Patologia Generale, Università di Messina, Messina Italy.

Calsequestrin (CS) is the junctional Sarcoplasmic Reticulum (jSR) component responsible for intralumenal Ca^{2+} storage. We have recently proposed that concentration of CS is involved in SR differentiation (see Villa et al. Exp. Cell Res. 209: 140-148, 1993). Since the CS targeting mechanisms to SR are still debated, our interest is to identify CS domains involved in the process. The whole cDNA of rabbit skeletal muscle CS and part of the 3' untranslated region were introduced in the expression vector pCDNA; a seven-amino acid epitope of the influenza virus haemagglutinin (referred to as HA1) was added in frame at the N-terminal of the CS by PCR cloning in the same vector. The complete construct was transfected in muscle and non muscle cell systems (HeLa, C2, L8, myotubes). Highly specific anti-HA1 antibodies were used to distinguish CS-*HA1* from endogenous CS. The immunofluorescence pattern showed retention of CS-*HA1* into intracellular compartments, ie, ER and small round-shaped structures in the cell lines. In trasfected myotubes, CS-*HA1* was localized in fluorescent strands running parallel to the longitudinal axis of the myotubes (where developing ER/SR is supposed to be localized). These results seem to confirm that CS-*HA1* is correctly sorted in ER and SR compartments in muscle and non-muscle systems The CS-*HA1* is, thus, a powerful tool for the identification of targeting sequences of CS by site-directed mutagenesis. (Work supported by funds of Italian Telethon and MURST, 60%).

Th-Pos286

DISULFIDE BONDS, GLYCOSIDATION SITES AND MEMBRANE TOPOLOGY OF SKELETAL MUSCLE TRIADIN.

((H. Fan, N.R. Brandt and A.H. Caswell)) Dept Pharmacology, University of Miami, Miami, FL 33136

Native triadin is a disulfide linked homopolymer of variable subunit number. Triadin in intact triads is largely unaffected by trypsin, while triads whose membrane has been disrupted by hypotonicity or mild detergent treatment release both soluble and membrane bound fragments. Soluble fragments appear in order during the course of proteolysis of M_r 18, 13, 11 and 7K. The binding epitopes of triadin monoclonal antibodies, GE4.90 and AE8.91, are located at C-terminal 34 amino acids and between amino acids 110-163 respectively. Two dimensional gel electrophoresis immunoblots with mAb GE4.90 of the soluble fragments using non-reducing and reducing conditions in each dimension reveals the presence of dimers formed between identical domains of two triadin molecules at cysteine residue 670. Glycosidase, Endo F, reduced the M_r of these fragments indicating the *in vivo* glycosidation of asparagine residue 625. Immunoblots of the insoluble fragments using AE8.91 indicate the presence of a dimer formed between identical domains of two triadin molecules at cysteine 271. These observations demonstrate that triadin forms a disulfide-linked polymer through mirror image intermolecular disulfide bonds of both cysteines. The cytoplasmic location of the mAbs requires that each disulfide reside in a separate segment of a membrane spanning β sheet. Three β sheet segments and one α helix account for the membrane spanning domains of triadin giving rise to extensive cytoplasmic and luminal regions. Supported by Am. Ht Assoc.

Th-Pos287

BINDING SITES OF TRIADIN MONOCLONAL ANTIBODIES AND THE DIHYDROPYRIDINE RECEPTOR (DHPr) II - III LOOP ON SKELETAL MUSCLE TRIADIN FUSION PEPTIDES.

((H. Fan, N.R. Brandt, *M. Peng, *A. Schwartz and A.H. Caswell)) Dept of Molec & Cellular Pharmacology, University of Miami, Miami, FL 33136, and *Institute of Molec Pharm & Biophys, University of Cincinnati, Cincinnati, OH 45267-0828

Triadin, an intrinsic SR protein, binds to the DHPr and junctional foot protein in skeletal muscle. In order to localize the interacting domains within triadic proteins, fusion peptides were synthesized using an expression system which includes a phosphorylation site. Expressed peptides (numbers in brackets correspond to the amino acid sequence) are α_1 $DHPr_{664-799}$ (664-799), triadin 1 (1-49), triadin 2 (68-389), triadin 2' (110-389), triadin 2a (68-278), triadin 2a1 (67-163), triadin 2a2 (165-240), triadin 2b (242-389), triadin 2b1 (242-299), triadin 3 (370-706), triadin 3a (370-562), triadin 3b (551-706), triadin 3b1 (551-672) and triadin 3b2 (673-706). Two triadin mAb, GE4.90 and AE8.91, have cytoplasmic epitopes through their binding to intact vesicles in conformity with other evidence. AE8.91 binds to triadin 2 , 2', 2a and 2a1 indicating an epitope between residues 110 and 163. GE4.90 binds to triadin 3, 3b and 3b2 indicating an epitope at the C terminus. Phosphorylated $DHPr_{664-799}$ binds to triadin in intact vesicles. It binds to triadin fusion peptides, triadin 2, 2a, 3, 3b and 3b1 but not 1 or 3b2. Phosphorylated triadin 2, but not triadin 1 or 3b2, binds to $DHPr_{664-799}$. These observations require an extensive cytoplasmic domain of triadin which includes the binding site to a portion of the DHPr which is critical for signal transmission. Supported by AHA and NIH.

Th-Pos288

EFFECTS OF DIFFERENT LIGANDS ON THE INTERACTION OF THE JUNCTIONAL FOOT PROTEIN OF SKELETAL MUSCLE WITH TRIADIN AND DETERMINATION OF TRIADIN BINDING REGIONS.

((H.K.Motolke, H. Fan and A.H. Caswell)) Dept of Pharmacology, University of Miami, Miami, FL 33136

Triadin binds reversibly to the junctional foot protein (JFP) of skeletal muscle. The Ca^{2+} release channel activity of the JFP is modulated by various physiological and pharmacological ligands. The influence of these reagents on the strength of binding between the JFP and triadin was investigated using purified labelled JFP and triadin immobolized on nirtocellulose. Ca^{2+} at 10 mM concentration inhibited binding by 70% whereas Mg^{2+} produced a dose dependent increase in binding. ATP (10 mM) caused a 60% decrease in binding between the two proteins. AMP-PNP and ADP also inhibited binding suggesting that the inhibition occurs through binding to an effector site rather than covalent modification of the channel protein by phosphorylation. The polycationic dye, ruthenium red (10 μM) also inhibited binding by 74%. These data indicate that the potency of binding between triadin and the JFP is controlled in a complex manner by activators or inhibitors of channel opening.

The binding of JFP to expressed triadin peptides was investigated in a similar protocol. JFP bound strongly to the putative cytoplasmic loop of triadin between amino acids 100 and 270 and more weakly in the putative luminal region between amino acids 270 and 685. No significant binding was detected to the N or C terminal 40 amino acids. Supported by Am. Ht Assoc.

Th-Pos289

SUBCELLULAR EC-COUPLING IS CONTROLLED BY THE T-TUBULES IN VENTRICULAR MYOCYTES

((P.Lipp[1], J.Hüser[1,2], L.Pott[2] and E.Niggli[1])) Departments of Physiology, [1]University of Bern, Switzerland and [2]University of Bochum, Germany.

In cardiac muscle a subcellularly homogeneous Ca transient is governed by Ca release from the sarcoplasmic reticulum (SR) triggered by voltage-dependent Ca entry during the action potential. In contrast to ventricular cells, atrial myocytes which lack T-tubules are known to exhibit spatially complex Ca release patterns when dialyzed with a high concentration of citrate. We used voltage-clamped guinea-pig ventricular myocytes and ratiometric confocal microscopy (mixture of Fluo-3 and Fura-Red) to investigate the role of the T-tubules during ec-coupling. Freshly isolated myocytes were compared to cells kept in short-term culture (1-2 d). After 1 day the ventricular myocytes lost a functional T-system as revealed by visualizing the cell membranes with Di-8-ANEPPS and by measuring the cell capacitance (123.4±17.7 pF, n=9 vs. 46.9±3.5 pF, n=15; mean±S.E.). The myocytes were dialyzed with a high concentration of citrate to partially uncouple Ca influx from SR-Ca release. In freshly isolated cells trains of I_{Ca} resulted in an alternation between Ca release and Ca influx signals that were spatially uniform (i.e. only temporal uncoupling). After 1 day in culture trains of I_{Ca} triggered subcellular Ca release events with complex spatial properties: (i) homogeneous Ca release, (ii) Ca waves propagating through the entire cell and (iii) spatially restricted Ca release. These observations suggest that in ventricular myocytes lacking the T-tubules Ca signaling was uncoupled temporally and spatially similar to atrial cells. We conclude that the T-system in ventricular myocytes ensures a subcellularly homogeneous Ca transient by increasing the reliability of ec-coupling. These results also support the notion that the cellular microarchitecture controls subcellular Ca signaling in general.

Th-Pos290

INHIBITION OF CARDIAC NA-CA EXCHANGE BY ANTISENSE OLIGONUCLEOTIDES

((E. Niggli[1], B. Schwaller[2] and P. Lipp[1])) [1]Dept. of Physiology, University of Bern, [2]Dept. of Histology, University of Fribourg, Switzerland.

Ca extrusion during relaxation is the established role for the Na-Ca exchange in cardiac myocytes, but it may also contribute to more rapid events of excitation-contraction coupling. However, it has been difficult to investigate the cellular and molecular function of this transporter because no specific pharmacological blocker is available. We have chosen an alternative approach to selectively inhibit the Na-Ca exchange activity in neonatal rat cardiac myocytes. Cell cultures were incubated with 1 µM of a phosphorothioate antisense oligonucleotide (19 bases) directed against the 3' nontranslated region of the Na-Ca exchanger mRNA. After 24 and 48 hours in culture myocytes were dialyzed with a mixture of the Ca indicators Fluo-3 and Fura-Red under whole-cell voltage-clamp conditions. Ca transients were elicited by superfusing the cells with zero Na while the fluorescence ratio was simultaneously recorded at high temporal resolution with a laser scanning confocal microscope in the line-scan mode. Na-Ca exchange activity was estimated by following the decay of the Ca signals (in the presence of 10 µM ryanodine to minimize interference from intracellular Ca stores). After 24 h the $t_{1/2}$ for the decay was 1.2±0.04 s (mean ± S.E., n=5 cells) in control cells. In cells exposed to the oligonucleotide $t_{1/2}$ was prolonged up to 3.5 s (mean 2.6±0.3 s, n=4 cells). After 48 h in the same culture medium, $t_{1/2}$ was still prolonged up to 2.9-fold. This finding suggests that the Na-Ca exchange was significantly reduced within 24 h. Antisense oligonucleotides therefore represent a useful tool to investigate the cellular and molecular function of the Na-Ca exchanger.

Th-Pos291

FLASH PHOTOLYSIS OF DM-NITROPHEN AND DIAZO-2 IN CARDIAC MYOCYTES CHARACTERIZED BY CONFOCAL MICROSCOPY

((P.Lipp, C.Lüscher and E.Niggli)) Department of Physiology, University of Bern, Switzerland.

Submicroscopic concentration gradients during Ca influx are believed to be important for Ca release from the sarcoplasmic reticulum (SR) in cardiac myocytes. Photorelease of Ca or Ca-buffer from "caged" compounds may be a useful tool to manipulate intracellular Ca (Ca_i) in a spatially homogeneous way. Voltage-clamped guinea-pig ventricular myocytes were dialyzed with DM-nitrophen or diazo-2 (2 mM). Simultaneously, spatial properties of Ca_i jumps were resolved by ratiometrically measuring Ca_i on a confocal microscope with a mixture of 33 µM Fluo-3 and 66 µM Fura-Red. The ratios were converted into Ca_i values with an *in-vivo* calibration (operational k_D = 2.08 µM, R_{min}=0.08, R_{max}=2.15). Molecular interactions between caged compounds and the indicators were not detectable. Photolysis of diazo-2 during a Ca transient decreased Ca_i rapidly and in a spatially homogeneous way. Photorelease of Ca from DM-nitrophen caused a rapid increase in Ca_i that slowly declined to resting values. The amplitude of the photolytically triggered Ca transients was smoothly graded with the flash energy. Analysis of confocal image sequences and rapid line-scans (500 Hz) revealed spatially uniform Ca transients indicating homogeneous Ca release from the SR. Intranuclear Ca signals usually lagged behind cytoplasmic transients, probably due to diffusion of Ca through pores in the nuclear envelope. However, Ca transients generated by photolysis did not exhibit this kinetic difference indicating that photolysis of DM-nitrophen resulted in a spatially uniform increase of Ca_i. The combination of flash photolysis with ratiometric confocal microscopy may therefore facilitate the analysis of spatial aspects of Ca signal transduction.

Th-Pos292

KINETICS OF CONTRACTIONS INITIATED BY PHOTOLYSIS OF CAGED CALCIUM AND CAGED ATP IN SMOOTH MUSCLE

((B. Zimmermann, G.C.R. Ellis-Davies*, J.H. Kaplan*, A.V. Somlyo, A.P. Somlyo)) Dept. of Molecular Physiology and Biological Physics, University of Virginia, Charlottesville, VA 22908, *Dept. of Biochemistry and Molecular Biology, Oregon Health Sciences University, Portland, OR 97201

A long (1-2sec at room temp.) delay between activation of a receptor and contraction is a characteristic property of smooth muscle (1). The purpose of the present study was to investigate, through photolysis of a new caged Ca^{2+} - NP-EGTA (2) - and caged ATP, the contributions to the delay by, respectively, myosin light chain phosphorylation by myosin light chain kinase (MLCK) and the reactions that follow the increase in cytoplasmic $[Ca^{2+}]$ and precede phosphorylation. In rabbit portal veins permeabilized with β-escin, Ca^{2+} jumps from pCa 7.0 to 5.5, induced by photolysis of NP-EGTA, resulted in contraction with a delay that ranged between 470±32msec (mean±S.E.M.) with no added calmodulin (CaM) and 198±43msec in the presence of 100µM CaM, with an EC_{50} of 12µM. The delay following photolysis of caged ATP (from low tension rigor at pCa5.5) was 45±3msec, and was not affected by exogenous CaM (0-40µM tested). Increasing $[Ca^{2+}]$ further to pCa4.5 increased the delay to 76±5msec. Surprisingly, following simultaneous photolysis of NP-EGTA and caged ATP (from low tension rigor, 40µM CaM) the delay was only 110±16msec. The longer delay preceding activation by photolysis of NP-EGTA than caged ATP is consistent with a significant contribution to the activation delay by prephosphorylation reactions, possibly the isomerization of the CaM-MLCK complex (3). However, the shortening of this delay by simultaneous photolysis of caged ATP and NP-EGTA (from rigor) remains to be explained, and could result from the elimination of inhibitory phosphorylation of MLCK due to the absence of ATP, in these experiments, prior to photolysis. *Supported by DFG Zi467/1-1 and NIH 5PO1 HL19242.*
(1) Somlyo AP, Somlyo AV (1990) *Ann.Rev.Physiol.* 52:857-874; (2) Ellis-Davies GCR., Kaplan JH (1994) *Proc.Natl.Acad.Sci.* 85:6571-6575; (3) Török K, Trentham DR (in press) *Biochemistry*

Th-Pos293

RATE OF Ca^{2+} RELEASE FOLLOWING LASER PHOTOLYSIS OF Ca^{2+} COMPLEXES OF NITROPHENYL-EGTA AND DM-NITROPHEN

((G.C.R. Ellis-Davies, J.H. Kaplan, and *R.J. Barsotti)) Dept. of Biochemistry and Molecular Biology, OHSU, Portland, OR and *Bockus Research Institue, Graduate Hospital, Philadelphia, PA.

Laser flash photolysis techniques have been used to obtain estimates of the rate of photorelease of Ca^{2+} from two Ca^{2+} cages: nitrophenyl-EGTA (*PNAS* **1994**,*91*,187) and DM-nitrophen (*PNAS* **1988**,*85*,6751). Laser photolysis at 347 nm (180 mJ) of NP-EGTA (2.1 mM) saturated with Ca^{2+} (2.2 mM) at pH 7.2 and 100 mM KCl, with Ca-orange-5N (50 µM) as the Ca indicator [excitation:488 nm; detection:570 nm], gave an increase in fluorescence with a half-time of 22 µs at 24°C (A, signals were obtained under non-saturating conditions for the dye). Irradiation of DM-nitrophen produced similar time-dependent fluorescent signals. Photolysis of NP-EGTA (2 mM) with Ca^{2+} (1.5 mM) produced pulses of Ca^{2+} (B). The free $[Ca^{2+}]$ stabilised to 3 µM in 2 ms, from an initial value of 100 nM. Laser flash photolysis of NP-EGTA:Ca^{2+} elicited a biexponential aci-nitro transient with decay half-times (monitored at 458 nm) of 1.5 and 7.3 µs (C). These results suggest that both Ca^{2+} cages photorelease Ca^{2+} extremely rapidly and can be used to initiate most Ca^{2+}-dependent physiological processes with adequate kinetic resolution.
Supported by HL30315 & GM39500 to JHK and HL40953 to RJB

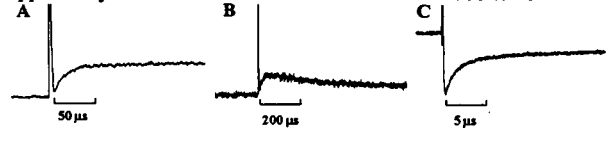

Th-Pos294

INTRACELLULAR CALIBRATION OF INDO-1 IN ISOLATED SKELETAL MUSCLE FIBERS OF XENOPUS.

((D.G. Allen and H. Westerblad)) University of Sydney, NSW 2006, Australia; Karolinska Institute, S-171 77 Stockholm, Sweden.

In recent years fluorescent Ca^{2+} indicators have become increasingly popular. While these indicators are good at reporting changes of the free cytoplasmic $[Ca^{2+}]$ ($[Ca^{2+}]_i$), it is more difficult to obtain the absolute $[Ca^{2+}]_i$. This is because properties of the indicators change in the intracellular environment, which means that *in vitro* calibrations performed in simple salt solutions will not be valid. We have measured $[Ca^{2+}]_i$ with indo-1 in intact, single muscle fibers of *Xenopus* bathed in a a standard Ringer solution (22 °C). Indo-1 was microinjected into fibers and we used a complete intracellular calibration method to convert fluorescence ratios (400 nm/505 nm) to $[Ca^{2+}]_i$. This calibration method can be used in all cells accessible to microelectrode penetration and involves microinjection of either 500 mM EGTA or 1 M $CaCl_2$ to get the minimum and maximum fluorescence ratio, respectively. To obtain a ratio at intermediate $[Ca^{2+}]_i$, we injected a solution with a ratio of [EGTA] to [Ca^{2+}-EGTA] of 2 (pH 7.0) which sets $[Ca^{2+}]$ to 200 nM. This method gave an intracellular dissociation constant of indo-1 of 261 ± 18 nM (S.E.M; n = 4), which is somewhat higher than the value we obtained *in vitro* (~230 nM). With this calibration we get a resting $[Ca^{2+}]_i$ of 42.8 ± 6.1 nM (n = 9). We also studied kinetics of indo-1 by measuring the rate of $[Ca^{2+}]_i$ decline in twitches. This analysis gave an intracellular Ca^{2+} off rate of indo-1 of about 80 s^{-1}, which compares to about 130 s^{-1} *in vitro*. Thus, both the dissociation constant and the Ca^{2+} off rate of indo-1 were altered by the intracellular environment.

Th-Pos295

A NOVEL METHOD FOR CALIBRATION OF INDO-1 IN INTACT RABBIT CARDIAC MYOCYTES ((J.W.M. Bassani, R.A. Bassani and D.M. Bers)) Loyola Univ Chicago, Maywood, IL 60153.

Fluorescent Ca indicators have been extremely valuable in understanding $[Ca]_i$ regulation in many cell types. The calibration of these indicators in the intracellular environment has, however, been a continuous challenge. We performed *in vivo* calibrations of indo-1 in isolated rabbit ventricular myocytes loaded with the acetoxymethylester form of indo-1 and used the perforated patch variation of whole cell voltage clamp. Voltage, [Na] and [K] gradients were eliminated to approach equilibrium. We also took advantage of the powerful Na/Ca exchange in cardiac myocytes so that $[Ca]_i$ would be equilibrated with $[Ca]_o$ (as there was no [Na] or E_m gradient). The equilibration of [Na] and [Ca] across the membrane was tested by measuring the reversal potential of Na current and poking the cell to test for changes in $[Ca]_i$-dependent fluorescence ratio. The apparent dissociation constant, K_d for indo-1 in the cellular environment was 844 nM, which is ~2-3 times higher than that in aqueous solutions. A related null point approach was also used to determine the $[Ca]_i$ in intact cells at rest for very long periods (82 ± 6 nM). This is lower than that measured 15 s after a train of steady state twitches ($[Ca]_i$ = 294 ± 53 nM). These experiments also allowed the direct assessment of the shortening *vs* $[Ca]_i$ relationship in intact cells.

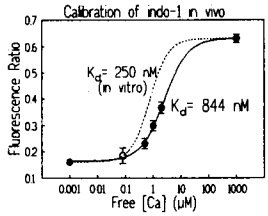

Th-Pos296

KINETIC PROPERTIES OF CALCIUM INDICATORS IN RESPONSE TO CALCIUM SPIKES ((A.L. Escobar, P. Velez, F. Cifuentes, M. Fill and J. L. Vergara*)) Department of Physiology, UCLA Sch. of Med., Los Angeles, CA 90024 and Dept. of Physiology, UTMB, Galveston, TX 77555

A confocal spot detection optical setup was used to record fluorescence signals in response to calcium pulses, elicited by flash photolysis of DM-nitrophen (DM-n), with the calcium indicators CaGreen-2, CaGreen-5N, CaOrange-5N, Fluo-3 and Rhod-2. 10 μl samples of solutions containing 100 mM KCl, 10 mM MOPS (pH 7), 2-10 mM DM-n, 10-100 μM of the calcium dyes were put in a chamber placed on the stage of the spot detection microscope. The pCa of the solutions was carefully adjusted to different values and monitored with a Ca^{2+} electrode. An Argon laser was used as a source of light for excitation; fluorescence was detected with a PIN photodiode connected to an integrated head stage of a patch clamp amplifier. A quartz fiber optic (200μm in diameter) was used to deliver 50 ns UV flashes of variable energy. Temperature, 18 °C. Our results yield the following conclusions: (a) DM-n $[Ca^{2+}]$ changes are almost perfect spikes (half-width < 30 μs) at pCa 9 and broader transients followed by a step at pCa 7. (b) The Ca^{2+} spikes were used to measure the dissociation rate constant (k_{off}) of the Ca dyes. Typical values are 5500 s^{-1} for CaOrange-5N and 175 s^{-1} for Fluo-3. (c) The association rate constant (k_{on}) for these dyes, calculated from measured K_d and k_{off}, are $1x10^8$ $M^{-1}s^{-1}$ and $2.7x10^8$ $M^{-1}s^{-1}$, respectively. (d) Experiments at pCa 7 were used to verify the kinetic rate constants of the dyes and to obtain those of DM-n (k_{on}= $7.5x10^7$ $M^{-1}s^{-1}$; k_{off}= $3.8x10^{-1}$ s^{-1}. (e) CaOrange-5N was the only indicator tested that reported transient changes in Ca^{2+} concentration with a first-order kinetic limitation. All the other dyes introduced severe distortions which impeded a quantitative deconvolution of the fluorescence transients into changes in the free $[Ca^{2+}]$. Supported by NIH AR25201

Th-Pos297

KINETIC RESPONSES OF LOWER-AFFINITY, VISIBLE-WAVELENGTH FLUORESCENT Ca^{2+} INDICATORS IN SINGLE FROG TWITCH FIBERS. ((S. M. Baylor, Mingdi Zhao, S. Hollingworth, and M. Konishi)) Department of Physiology, University of Pennsylvania, Philadelphia, PA 19104.

In physiological studies of many cells, it is often desirable to record the spatially-averaged change in cytoplasmic free Ca^{2+} ($\Delta[Ca^{2+}]$) with kinetic fidelity. In frog fibers activated by an action potential, the time course of the fluorescence change (ΔF) of many higher-affinity indicators (including quin-2, indo-1, fura-2, rhod-2, fluo-3, fura-red, calcium-green, calcium-green 2 and calcium orange) substantially lags that of $\Delta[Ca^{2+}]$. In contrast, ΔF from furaptra, a lower-affinity indicator (Raju et al., 1989), tracks $\Delta[Ca^{2+}]$ without significant delay (Konishi et al., 1991). A disadvantage of furaptra is that its absorbance bands peak at wavelengths λ < 400 nm. We have therefore examined ΔF of three lower-affinity indicators (Molecular Probes Inc.) that have major absorbance bands at visible λ. Indicators were injected into single fibers, either alone or in combination with furaptra. ΔF's from Ca-green-5N and Ca-orange-5N lagged ΔF of furaptra by several ms. Surprisingly, ΔF from mag-fura-red was biphasic (with 480 nm excitation). The earlier component was as fast as $\Delta[Ca^{2+}]$ whereas the later component slightly preceded the fiber's tension response. The later component appears to be a consequence of $\Delta[Ca^{2+}]$ (since it's amplitude is greatly reduced in the presence of BAPTA) and to reflect activity of an oriented structure accessible to myoplasm -- for example, the myofilaments or the SR calcium pump. Supported by NIH NS-17620.

Th-Pos298

AM LOADING OF CALCIUM INDICATORS INTO FROG SKELETAL MUSCLE FIBERS. ((Mingdi Zhao, S. Hollingworth and S. M. Baylor)) Department of Physiology, University of Pennsylvania, Philadelphia, PA 19104.

The ability of intact fibers to load with the AM form of four tetracarboxylate indicators (fura-2, rhod-2, fluo-3 and fura-red) and two tricarboxylate indicators (furaptra and mag-fura-red) was studied at 16°C. An AM form (Molecular Probes Inc) was dissolved in 100% DMSO (sometimes with Pluronic added), then diluted into normal Ringer's to final concentrations of 8-20 μM indicator and 0.1-0.5% DMSO. Loading was detected as a time-dependent increase in a fiber's resting fluorescence (F); in fibers with substantial loading, intracellular indicator concentration ([D]) could be estimated from associated absorbance measurements. Rates of loading varied greatly with different indicators. With the tricarboxylates, large [D]'s were found after 1-hour: 250-500 μM with furaptra (N=3); 100-150 μM with mag-fura-red (N=5). With the tetracarboxylates, loading was so much slower (by 10-100 fold) that [D]'s were difficult to estimate. (However, BAPTA, a non-fluorescent tetracarboxylate buffer, loaded well, with intracellular concentrations after 1-hour indirectly estimated to be near mmolar.) Changes in F due to action potential stimulation (ΔF) were also measured. In general, ΔF waveforms observed following AM loading were very similar to those observed following micro-injection of the free acid forms. Normalized signal amplitudes (ΔF/F), however, can be smaller with AM loading, since F does not always arise entirely from hydrolysed indicator within the myoplasm. Supported by NIH 17620.

Th-Pos299

MEASUREMENTS OF CALCIUM TRANSIENTS IN CHICK HEART USING LOW AND HIGH LEVELS OF FURA-2. ((M.A.P. Brotto, T. M. Nosek, R. E. Godt and T. L. Creazzo)) Medical College of Georgia, Augusta GA 30912-2000.

We have studied Ca^{2+} transients using the fluorescent dye fura-2/AM in isolated chick embryonic (days 11 and 15) myocytes and trabeculae. Ca^{2+} transients were stimulated in isolated ventricular myocytes by field stimulation. Using a microspectrofluorometer (SPEX) attached to an inverted microscope, we found that varying the cytoplasmic fura-2 concentration ([fura-2]) from 16 to 60 μM did not produce noticeable effects on the size and shape of Ca^{2+} transients. This suggested no significant Ca^{2+} buffering by fura-2. However, increasing [fura-2] above 70 μM reduced the peak magnitude of transients as well as increased the duration. Calcium transients were not detectable above background noise at [fura-2] > 90 μM. We found that loading the cells at 37 ° C in a rotating bath for 8-10 min. with 1-2 μM fura-2/AM, washing, and allowing 45 min. for the deesterification of the dye at room temperature provided a reproducible [fura-2] in the range of 20-30 μM. In a separate series of experiments, free running trabeculae were dissected and placed on the stage of a inverted microscope that was attached to a microspectrofluorometer (PTI), mounted between a force transducer and a moveable arm, and electrically stimulated until force was stable. Trabeculae were exposed to 5-10 μM fura-2 /AM until the fluorescence signal was 1.5-2.5 times background; this level of loading was achieved at room temperature after 70±30 min. and at 37 °C after 30±20 min. Under these conditions we did not observe a decrease in twitch force. However, loading for longer periods or in the presence of higher [fura-2], significantly depressed twitch force and Ca^{2+} transients. We conclude that it is possible to accurately measure Ca^{2+} transients in fura-2 loaded embryonic chick isolated myocytes as well as force and Ca^{2+} transients in multicellular preparations provided that [fura-2] is held to relatively low levels. This work was supported by NIH grant HL36059.

Th-Pos300

AUTOFLUORESCENCE CHANGES CAUSED BY HALOTHANE CAN LEAD TO ERRONEOUS INTERPRETATION OF FURA-2 SIGNALS IN CARDIAC MUSCLE. ((DG Stephenson*, P Garzella, DE Wingrove, DR Claflin , FJ Julian)) Dept. of Anesthesia, Brigham & Women's Hospital, Boston, MA02115; * Zoology, LaTrobe University, Victoria, Australia.

Cardiac cells are known to fluoresce intensely when excited by UV light. This autofluorescence is associated to a large extent with the mitochondrial NADH pool. Here we report that halothane (1% v/v; 0.95 MAC @ 37° C) reversibly increased the intensity of the autofluorescence signal of rat myocardium by about 20% at 25°C when emission was recorded at 510 nm. In the Figure below are shown the autofluorescence excitation spectra from a papillary muscle before exposure to and after removal of halothane (CONTROLS) and after equilibration in the presence of 1% v/v halothane. The Figure also shows the difference between the spectra in the presence of halothane and in the control solutions (DIFF) and the excitation spectrum of an NADH solution that has been scaled to the peak of the DIFF response. Note the similarity between the DIFF and the NADH spectra, suggesting that halothane causes an increase in intracellular [NADH]. When papillary muscles were loaded with Fura-2AM (15 μM for 60 mins at 25°C), the maximum intensity of the fluorescence signal doubled in magnitude. If the change in autofluorescence caused by halothane is disregarded, the 340/380nm intensity ratio increases by about 20%. This would normally be interpreted as higher intracellular $[Ca^{2+}]$. The results suggest that halothane exerts a reversible potentiating action on the cellular [NADH], possibly by inhibiting the electron transport chain in the mitochondria, and indicate that work with fluorescent probes loaded in cardiac preparations must consider changes in autofluorescence resulting from various interventions. Supported by NIH GM48078 and ARC (DGS).

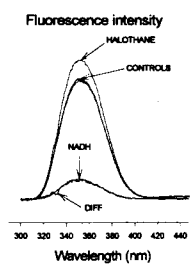

Th-Poe301

FURA-RED: A SUPERIOR INDICATOR FOR RECORDING $[Ca^{++}]_i$ TRANSIENTS IN PERFUSED HEARTS.

Y.M. Wu and W.T. Clusin, Stanford Medical Center, Stanford CA

To determine the feasibility of recording Ca transients in vivo we studied the properties of the long wave length indicator fura-red. Epicardial regions of saline perfused rabbit hearts were loaded by infusion of fura-red AM (10 μM) into the extracellular space using a small needle and syringe pump. Hearts were illuminated at 490nm and emissions recorded at > 630 nm. Ratiometric signals could be obtained as the F>630/F550 ratio, 550 nm being an isobestic point for fura-red, hemoglobin and myoglobin. Fura-red loaded hearts gave large $[Ca^{++}]_i$ transients at >630 nm (up to 20% of total signal), which were barely affected when the perfusate was switched to blood. Fluorescence was unaffected by bradykinin--which acts on endothelial cells. Transients were abolished and fluorescence was reduced 60 ± 3% by 0.1 mM Mn^{++} (over 45 min) which quenches cytosolic fura-red. An additional 12 ± 2% reduction occurred with high Mn^{++} (30 mM + ionomycin, 1.5 μM). This fluorescence is inferred to arise from nuclei and mitochondria. Remaining fluorescence(29 ±4%) is ascribed to autofluorescence and to partly deesterified fura-red. $[Ca^{++}]_i$ transients were calibrated by infusion of ionomycin(1.5 μM), high Ca (100 mM) and EGTA (30 mM) through the needle that was used to infuse the fura-red AM. Mean systolic $[Ca^{++}]_i$ was 2.9 ± 0.2 x Kd. Mean diastolic $[Ca^{++}]_i$ was 1.4 ± 0.3 x Kd. The systolic/diastolic $[Ca^{++}]_i$ ratio was 1.9, which is identical to the ratio obtained with indo-1. The above techniques would be directly applicable to open chest in vivo preparations. Fura-red is superior to five other calcium indicators for this purpose.

Th-Poe302

CALCIUM ORANGE-5N: A LOW AFFINITY INDICATOR ABLE TO TRACK THE FAST RELEASE OF CALCIUM IN SKELETAL MUSCLE FIBERS.

((F. Cifuentes, A.L. Escobar, and J. L. Vergara)) Department of Physiology, UCLA School of Medicine, Los Angeles, CA 90024. (Sponsored by C. Kasper).

Calcium transients, elicited by action potential stimulation, were recorded in frog single skeletal muscle fibers using global and confocal spot detection techniques and the fluorescent indicator CaOrange-5N. The Ca-binding properties of this dye were characterized in cuvette at 0.1 M ionic strength (17 °C), yielding a K_d of 53 μM, a max./min. fluorescence ratio of 4, and a frequency response of about 1 KHz. Global fluorescence transients, measured with 300-500 μM intracellular dye in the presence of 50 μM EGTA, showed an initial delay of 1-2 ms, peak values of 5-20 μM, 4-6 ms time to peak, and 20-30 ms decay time constants. Adding 6 mM DM-nitrophen or 5-50 mM EGTA intracellularly, reduced the amplitude of these transients by 50-80%, increased their rate of decay by 2 to five-fold, and only slightly reduced the time to peak. Under these conditions, localized transients detected on Z-lines at the border of the muscle fiber showed initial delays of less than 1 ms, peaked in about 2 ms and showed decay time constants of about 5 ms. In contrast, localized Z-line transients recorded at the center of the fiber showed a slightly broader time course but distinct additional initial delays of 1.5 - 3.5 ms, dependent on the fiber diameter. In conclusion: a) CaOrange-5N is a Ca^{2+} indicator able to monitor fast changes in $[Ca^{2+}]$ in skeletal muscle fibers under different buffering and detection conditions, without introducing severe distortions due to its own dynamic limitations. b) In response to an action potential, the localized release of Ca^{2+} occurs, after a brief latency, during a period lasting about 1-2 ms. c) Global detection of Ca^{2+}-transients show a significant spread in the rising phase, probably due to propagation in the t-tubules. Supported by NIH AR25201 and Fondecyt, Chile 92-0060 (FC).

Th-Poe303

FOCAL INCREASES IN INTRACELLULAR $[Ca^{2+}]$ DETECTED BY AEQUORIN BUT NOT BY FURA 2 IN HISTAMINE AND CAFFEINE STIMULATED SWINE CAROTID ARTERY.

((Christopher M. Rembold, Dee A. Van Riper & Xiao-Liang Chen)) Cardiovascular Division, University of Virginia, Charlottesville, VA 22908 USA

We hypothesized that the homogeneity of intracellular $[Ca^{2+}]$ ($[Ca^{2+}]_i$) varies and is regulated in arterial smooth muscle. We evaluated this hypothesis by exploiting the different characteristics of several $[Ca^{2+}]_i$ indicators: 1) aequorin that can measure focal increases in $[Ca^{2+}]_i$, 2) Fura 2 that is predominantly a measure of mean cytoplasmic $[Ca^{2+}]_i$, and 3) myosin light chain phosphorylation and force that reflect increases in $[Ca^{2+}]_i$ near the contractile apparatus. From the differences in the observed aequorin and Fura 2 signals, we developed an index of the relative degree of $[Ca^{2+}]_i$ homogeneity as the ratio of the aequorin signal and Fura 2 signal. Stimulation with 1-10 μM histamine or 20-40 mM $[K^+]_o$ did not alter the aequorin/Fura 2 ratio. Stimulation with 100 μM histamine or removal of extracellular Ca^{2+} decreased the aequorin/Fura 2 ratio indicating increased $[Ca^{2+}]_i$ homogeneity. After removal of extracellular Ca^{2+}, stimulation with 100 μM histamine or restoration of extracellular Ca^{2+} transiently increased the aequorin/Fura 2 ratio. Although both of these experiments demonstrated a transient decrease in $[Ca^{2+}]_i$ homogeneity, only histamine stimulation led to increased myosin phosphorylation and force, suggesting that these two focal increases in $[Ca^{2+}]_i$ occurred in different cellular regions. Addition of caffeine (20 mM) induced a transient contraction and a sustained increase in the aequorin/Fura 2 ratio, suggesting that caffeine inhibits sustained smooth muscle contraction by localizing increases in $[Ca^{2+}]_i$ to a region distant from the contractile apparatus. Phosphorylation of myosin light chain kinase did not appear to underlie caffeine's inhibition of contraction. These data suggest that there can be transient and sustained focal increases in $[Ca^{2+}]_i$. Aequorin detected focal increases in $[Ca^{2+}]_i$ during release and refilling the intracellular Ca^{2+} store and with caffeine stimulation.

Th-Poe304

MEASUREMENT OF SR FREE Ca^{2+} AND Mg^{2+} IN PERMEABILIZED CULTURED SMOOTH MUSCLE CELLS USING FURAPTRA.

((T. Sugiyama and W.F. Goldman)) Dept. Physiol., Univ. Maryland Med. Sch. and GRECC, Baltimore V.A.M.C., Baltimore, MD 21201

The concentrations of intra-sarcoplasmic reticulum (SR) free Ca^{2+} ($[Ca^{2+}]_{SR}$) and Mg^{2+} ($[Mg^{2+}]_{SR}$) were measured in furaptra-loaded, saponin-permeabilized, A7r5 cells. After cell permeabilization, cytosolic furaptra was washed away from continuously superfused preparations and only furaptra trapped within membrane delimited organelles remained. Under these conditions, Ca^{2+}-independent fluorescence emitted from trapped furaptra excited at 346 nm (isosbestic point) decreased with a $T_{1/2}$ = 30 min. Thapsigargin-induced SR Ca^{2+}-ATPase inhibition caused near total depletion of Ca^{2+} and the mitochondrial uncoupler, FCCP, had no additional effect, confirming that Ca^{2+} measurements were from SR. Calibration curves relating ratios of intra-SR furaptra fluorescence excited at 370 nm and 346 nm to $[Ca^{2+}]$ and to $[Mg^{2+}]$ were calculated *in situ*; K_d values for Ca^{2+} and Mg^{2+} binding were 49 μM and 6.8 mM, respectively. Resting $[Ca^{2+}]_{SR}$ ranged from 75-130 μM with a mean of 97.2 ± 2.2 μM (n = 376), while $[Mg^{2+}]_{SR}$, estimated in the absence of Ca^{2+}, was ~1.0 mM. Stimulation with inositol 1,4,5-trisphosphate ($InsP_3$) resulted in partially-reversible, time-dependent declines in $[Ca^{2+}]_{SR}$ but at a slower rate than expected (k = 9.2 x 10^{-3} sec^{-1}). Pretreatment with GTP caused a 4-fold increase in the rate of $InsP_3$-evoked SR Ca^{2+} release (k = 36.0 x 10^{-3} sec^{-1}), although GTP had no effect by itself. These observations indicate that furaptra will be a valuable tool with which to directly study $[Ca^{2+}]_{SR}$ and may provide important hints as to the nature intra-SR Ca^{2+} binding and other aspects of SR function.

Th-Poe305

IMAGING $[Ca^{2+}]$ IN INTRACELLULAR STORES OF INTACT FROG NEURONS.

((A.I. Bustamante, Z. Cseresnyes, M.G. Klein, M.F. Schneider)) Dept. of Biol. Chem., Univ. of MD., Baltimore, MD 21201

Neurons were enzymatically dissociated from frog (R. pipiens) sympathetic ganglia, maintained 2-6 days in culture and heavily loaded with fura-2 (2 μM AM; 50 min). Fluorescence images at 510 nm were recorded at successive 2 μm planes with 380, 358 or 350 nm excitation and nearest neighbor deblurred. Images due to indicator trapped in spaces (= stores) not continuous with cytosolic water were extracted from total images (= store + cytosol) by subtraction of cytosolic from total images. The cytosolic image was based on Mn^{2+} quench images of cytosolic indicator or microinjected rhodamine images of cytosolic space and was calculated assuming indicator fluorescence to be proportional within the nucleus and cytoplasm. The method was verified using microinjected fura-2 free acid. Fura-2 ratio images (both 380/358 and 350/358) calculated from the store fluorescence images showed near saturation of fura-2 by calcium, both before and after calcium release by caffeine, indicating that $[Ca^{2+}]$ within the store remained high relative to the fura-2 calcium affinity. However, depletion of store calcium by 2 hr exposure to 8 μM thapsigargin in calcium-free Ringers resulted in store images showing low saturation of fura-2. We are exploring the use of lower affinity indicators to monitor images of store $[Ca^{2+}]$ at physiological levels before and after calcium release. Supp. by NIH.

Th-Pos306

A PRACTICAL APPROACH TO DETERMINE QUALITY INTERPROTON DISTANCE BOUNDS FROM 2D-NOE INTENSITIES: CONSIDERATIONS OF EXPERIMENTAL RANDOM NOISE AND PEAK INTEGRATION ERRORS [[H. Liu, H. P. Spielmann, D. E. Wemmer, and T. L. James]] UCSF, San Francisco, CA. 94143-0446 and UC Berkeley, Berkeley 94720.

Large distances (~5A) which correspond to weak NOE intensities are generally more important than short distances for structure determinations. But weak intensities suffer seriously from experimental random noise and peak integration errors. To reflect this effect in a realistic way, a method, i.e. random noise MARDIGRAS, is introduced to generate quality distance bounds from 2D-NOE intensities. The basic MARDIGRAS algorithm, using a complete relaxation matrix approach, has been previously described (B. A. Borgias and T. L. James. JMR 87, 475(1990)) and shown to provide reasonably good distances, but experimental error can compromise the quality of the resulting restraints. In our new approach, random noise errors are added to the NOE intensities N times in a random way (typically N=30). Relative integration errors may also be added. MARDIGRAS calculations are carried out for the N sets of intensities, and average distances are generated. The lower and upper bounds of the distances are calculated from the standard deviations of the distances of the N MARDIGRAS runs. The method has been applied to an interstrand cross-link DNA-drug complex (XL). The fact that all the fixed (known) distances, especially those large ones in the drug, can be well reproduced shows that random noise MARDIGRAS is a reasonable approach to generate distance constraints from NOE intensities. It will be shown that correct structures can be determined using these constraints. On the other hand, distance constraints derived from the isolated 2-spin approximation method give an incorrectly bent structure.

Th-Pos307

PARTIAL ASSIGNMENT OF BACKBONE NMR RESONANCES IN GLUTAMINE-BINDING PROTEIN OF *ESCHERICHIA.COLI* ((J. Yu, N. Tjandra, V. Simplaceanu, P. F. Cottam, J. Lukin, and C. Ho)) Department of Biological Sciences, Carnegie Mellon University, Pittsburgh, PA 15213

Heteronuclear multi-dimensional NMR experiments such as HNCA, HN(CA)HA, HNCO, HN(CO)CA, HCACO, HCA(CO)N, CBCA(CO)NH have been carried out to establish backbone resonance assignment of glutamine-binding protein (GlnBP) of *E.coli,* a periplasmic protein of 226 amino acid residues. The high degree of degeneracy of the NMR spectra encountered with a protein of this size provides a challenging problem in the design of NMR experiments, as well as of the isotopic labeling. We have previously assigned His, Trp, and Met residues using site-specific isotopic labeling. In order to resolve the degeneracy to the point of a complete backbone assignment, several different combinations of labeling the GlnBP are currently being investigated. Two such samples presently used in our experiments are: [^{13}C'-Tyr, ^{15}N-U], and [^{13}C'-Phe, ^{15}N-U] labeled GlnBP complexed with glutamine. The chemical shift information obtained from HNCO experiments on these samples provides markers and check points. In combination with the amino acid type information given by the CB chemical shifts from the CBCA(CO)NH experiment and the chemical shift information from the 3D data and the previously assigned His, Trp, Met residues, type-specific labeling enables us to make progress in the assignment of backbone resonances of GlnBP [Supported by a grant from NSF(DMB-8816384)].

Th-Pos308

SOLUTION STRUCTURE OF A 44 RESIDUE CONSENSUS PEPTIDE OF APOLIPOPROTEINS BY NMR. ((Fengli Zhang, George Poulos, James A. Hamilton and David Atkinson)) Dept. of Biophysics, Boston University School of Medicine, 80 E. Concord Street, Boston, MA 02118.

The exchangable apolipoproteins that function to stabilize lipoprotein particles, transport lipid and activate enzymes of lipid metabolism share a common primary sequence motif of 22 amino acids repeated tandemly throughout the sequence (R. Nolte and D. Atkinson, 1992, Biophys. J. 63, 1221-39). The solution structure of a 44 residue apoprotein consensus peptide $(PLAEELRARLRAQLEELRERLG)_2$ was studied by 2-D NMR. CD shows this peptide to have 87% α-helix conformation in solution, which increases to 97% in the presence of lipid or TFE. The peptide forms nascent HDL disc-like structures with DMPC similar to apoA-I. TOCSY, COSY and NOESY spectra of the peptide in 33% TFE + 67% H_2O were recorded on Bruker 500MHz DMX NMR spectrometer at 40°C. The 2-D NMR data was processed by using NMRI software. The TOCSY and COSY spectra were used to identify individual spin system types. NOESY spectra, especially the amide region, were used for sequential assignments. Molecular dynamics and simulated annealing carried out with the XPLOR computer programs were used to calculate the peptide conformation based on the NOE constraints obtained by 2-D NMR. Our NMR results, together with computational studies suggest that the peptide adopts a two antiparallel α-helical bundle structure. This structure may represent a fundamental structural domain within the apolipoproteins.

Th-Pos309

ASSIGNMENT OF BACKBONE ^{1}H, ^{13}C, AND ^{15}N RESONANCES OF GLUTAMINE-BINDING PROTEIN BY A NOVEL PROBABILISTIC METHOD. ((J. A. Lukin*, N. Tjandra*, A. P. Gove†, S. N. Talukdar†, J. Yu*, P. F. Cottam*, V. Simplaceanu*, and C. Ho*)) *Department of Biological Sciences and †Department of Electrical and Computer Engineering, Carnegie Mellon University, Pittsburgh, PA 15213.

The polypeptide backbone and β-carbon resonances of uniformly ^{13}C- and ^{15}N-labeled glutamine-binding protein (GlnBP) have been detected by several heteronuclear 3D-NMR experiments. Constant-time HNCA, HN(CA)HA, HNCO, HN(CO)CA, HCACO, HCA(CO)N, and CBCA(CO)NH experiments provide overlapping sets of chemical shifts, which ideally would be sufficient to extend a known assignment in both directions along the protein backbone. However, this method cannot be readily performed manually because of the extensive chemical shift degeneracy seen in a protein as large as GlnBP (25 kDa). We have developed an automated, probabilistic approach for assigning 3D-NMR cross peaks of a protein of known primary sequence. Given a tentative assignment, the algorithm calculates an overall score based on the probability of matching the chemical shifts of each peak with (i) overlapping peaks from different 3D experiments; and (ii) chemical shift distributions of the underlying amino-acid type. This joint probability is maximized by shuffling peak assignments using a simulated annealing strategy. The Monte-Carlo moves recognize assignment constraints provided by experiments performed on specifically-labeled GlnBP samples. Published data on previously assigned proteins are used to test the program. Using this method, we are progressing towards the complete backbone resonance assignment of GlnBP, a necessary step in the determination of this protein's solution structure.

Th-Pos310

DETECTION OF CL⁻ BINDING TO BAND 3 BY DOUBLE-QUANTUM-FILTERED ^{35}CL NMR. ((D. Liu)) Dept. of Biophysics, Univ. of Rochester, Rochester, NY 14642.

Double-quantum-filtered (DQF) NMR of ^{23}Na has been used to study its multiexponential relaxation in many biological systems. We recently applied DQF NMR of ^{35}Cl to study binding of Cl^- to external sites on intact red blood cells, including the outward-facing anion transport sites of band 3, an integral membrane protein. The DQF ^{35}Cl NMR signal was observed in cell suspensions containing 150 mM KCl, but no DQF signal was observed in cell-free medium. The DQF signal remained after the cells were treated with eosin-5-maleimide (EM), a noncompetitive inhibitor. In contrast, the DQF signal can be totally eliminated by adding 500 μM 4,4'-dinitrostilbene-2,2'-disulfonate (DNDS), a competitive inhibitor of band 3. Therefore, it seems that only the binding of Cl^- to transport sites of band 3 can give rise to a DQF signal for ^{35}Cl. In accordance with this concept, analysis of single quantum free induction decay (FID) signals revealed that buffer and DNDS-treated cells fitted a single exponential function, whereas the FID signals of untreated control cells and EM-treated cells were biexponential. A modified DQF experiment shows that a portion of DQF signal comes from motion-restricted Cl^-. (Supported by NIDDK grant DK27495.)

Th-Pos311

INFLUENCE OF GRAMICIDIN ON THE DYNAMICS OF PHOSPHOLIPID MODEL MEMBRANES. STUDY OF LIPID BILAYERS AND INDUCED-H_{II} PHASES BY SOLID-STATE ^{13}C NMR SPECTROSCOPY. ((Christine Le Guernevé, Mario Bouchard and Michèle Auger)), Département de chimie, CERSIM, Université Laval, Québec, Canada, G1K 7P4.

Natural abundance ^{13}C solid-state NMR spectroscopy was used to investigate the effect of the incorporation of gramicidin on the dynamics of phosphatidylcholine bilayers. The combined used of ramped-amplitude cross-polarization (RAMP-CP) and magic-angle-spinning have already been shown to allow the obtention of highly resolved spectra. In order to examine both the fast and slow motions of lipid molecules, ^{1}H spin-lattice relaxation times as well as proton and carbon spin-lattice relaxation times in the rotating frame were calculated for each resolved resonances in the spectra. The effect of gramicidin was studied in two model membrane systems : dimyristoylphosphatidylcholine (DMPC) and dioleylphosphatidylcholine (DOPC). The dynamics of the polar head group, the glycerol backbone and the fatty acyl chains have been determined in the pure DMPC and DOPC bilayers as well as in the presence of gramicidin. Furthermore, the DOPC H_{II} phase induced by gramicidin in excess water was also investigated. The results show the reliability of these techniques in the study of lipid dynamics in both bilayers and H_{II} phase organizations.

Th-Pos312

MAGNETIC ORIENTATION OF MEMBRANE PROTEINS FOR NMR STRUCTURAL STUDIES. ((Charles R. Sanders, Olga Vinogradova, Lech Czerski, and Geoffrey C. Landis)) Dept. of Physiology and Biophysics, Case Western Reserve University, Cleveland, Ohio 44106.

Work is described which was designed to test the scope of using magnetically orientable model bilayer systems as a tool for structural studies of membrane proteins by NMR. Specifically:

i. Using both CHAPSO and short chained-PC as orientation-promoting agents, phosphatidylcholine bilayers were semi-systematically tested for their orientability as a function of acyl chain lengths and unsaturation, the presence of negatively charged lipids, the presence of cholesterol, and temperature. Several new systems were characterized which may be more optimal for certain studies than previously described DMPC-based systems.

ii. The effect of reconstituting transmembrane peptides and proteins upon the orientational behavior of normally magnetically orientable systems was tested. A variety of results were obtained ranging from complete disruption of orientation to no perturbation.

iii. The NMR spectroscopic properties of selectively labeled transmembrane peptides which could be successfully reconstituted were assessed.

iv. The effect of reconstitution upon the functional properties of an integral membrane enzyme diacylglycerol kinase was assessed.

v. It was observed that a number of surface-associating peptides not only failed to disrupt sample magnetic orientation, but yielded oriented sample NMR spectra of extremely high quality. A method for assigning oriented-sample resonances was also established.

Th-Pos313

STUDY OF MOLECULAR MOTION OF ATP IN VISCOUS SOLUTIONS VIA ^{2}H, ^{13}C AND ^{31}P NMR LINE SHAPES ((Yan Lin and B. D. Nageswara Rao)) Dept. of Physics, Indiana Univ. Purdue Univ. Indianapolis, 402 N. Blackford St., Indianapolis, IN 46202 (Supported in part by NIH GM 43966 and IUPUI)

An isolated adenosine triphosphate (ATP) molecule has three categories of internal mobilities: the glycosidic reorientation of the adenine base with respect to the ribose, the motion of the phosphate chain, and the ribose pucker. The first two motions are of large amplitude, and the third is of low amplitude. It is reasonable to surmise that when MgATP is bound to enzymes for which it is a substrate, the large amplitude motions will be arrested due to the topology of the binding site. In order to gain some insight into these motions, ^{13}C, ^{31}P and ^{2}H line shape measurements have been carried out on ATP, MgATP and AMP as a function of viscosity using glycerol and sucrose solutions. ^{13}C measurements were made on [2-^{13}C]ATP(or AMP) and ^{2}H measurements on [8-^{2}H]ATP(or AMP). ^{13}C results have been analyzed by considering the relaxation mechanism of ^{13}C-^{1}H dipolar interaction and ^{13}C chemical shift anisotropy(CSA), along with their interference effects. ^{2}H results were analyzed on the basis of the quadrupole relaxation of ^{2}H. All the interaction parameters, viz. the ^{13}C CSA tensor elements and the ^{2}H quadrupole coupling constant have been independently determined by solid-state experiments. The results are clearly indicative of the presence of the large amplitude internal motions superposed on an overall motion. The overall motion is assumed to be isotropic with a linear dependence on viscosity. In comparison, the internal mobilities display a more complex viscosity dependence suggesting that the internal mobilities are weakly attenuated by solvent packing at high viscosities.

Th-Pos314

COMPLETE RELAXATION AND CONFORMATIONAL EXCHANGE MATRIX (CORCEMA) ANALYSIS OF NOESY SPECTRA: APPLICATIONS TO TRANSFERRED NOESY AND PROTEIN FOLDING STUDIES **((Hunter N. B. Moseley, Ernest V. Curto, and N. Rama Krishna)) Department of Biochemistry and Molecular Genetics, University of Alabama at Birmingham (UAB), Birmingham, AL, 35294**

The single conformation assumption, often used in Distance Geometry or back-calculation analysis of NOESY spectra, produces inherently flawed results, because macromolecules undergo complex dynamics involving multiple conformations. Including conformational dynamics in spectral analysis may yield better molecular structures with both structure and dynamic components (dynamic structure). We have developed a very general program called CORCEMA, an extension of earlier work from this laboratory. It incorporates the multistate conformational exchange formulation and calculates resonance intensities for NOESY/ROESY experiments for an individual molecule or set of interacting molecules based upon a dynamic structure model. CORCEMA allows the study of multiple conformations (states), correlation times, and internal motions like ring flipping and methyl rotation as well. Here we present two examples of CORCEMA application: (i) a three-state model of the folding pathway of penta-L-alanine (α-helix $\rightleftarrows$ β-III-turn (3-10 helix) $\rightleftarrows$ β-II-turn), and (ii) a three-state model of a transferred NOESY experiment depicting hinge-bending motion of a thermolysin-inhibitor complex. Analysis predicted systematic changes in NOESY intensities due to exchange kinetics which may be tested by experiment.

Th-Pos315

^{13}C- AND ^{15}N-NMR RELAXATION STUDIES OF PEPTIDE MOTIONAL DYNAMICS IN PRE-FOLDED STATES. ((K.H. Mayo, V.A. Daragan, E. Ilyina)) University of Minnesota, UMHC, Box 609, Minneapolis, MN 55455.

In aqueous solution, platelet factor-4 (PF4) folding-core peptide: TAQLIAT-LKNGRKISLDL, forms a relatively well defined native-like turn at LKNGR which may be stabilized by hydrophobic interactions from "sticky ends." In the present study, backbone and side-chain motional dynamics of this 20mer have been studied by ^{13}C- and ^{15}N-NMR relaxation. Specific amino acids have been isotopically enriched for greater sensitivity and resolution of side-chain methylene and methyl groups. Multiple dipolar auto- and cross-correlation times have been determined as a function of temperature. Various motional models were used to fit experimental and molecular dynamics data. Rotational jump models which allow for diffusive-like fluctuations within potential minima best explain the experimental data. Short control peptides of four to six residues each were studied to assess motional restrictions in the absence of "folded" populations. Relative to control peptides, backbone and side-chain motions were considerably more conformationally restricted in the PF4 folding-core peptide. Hydrophobic residues, which showed the greatest effects, were more motionally restricted at higher temperatures consistent with the hydrophobic effect modulating folding. Results are discussed in terms of protein folding models.
This project has been supported by an NSF/NAS Research Grant.

Th-Pos316

OFF-RESONANCE ROTATING FRAME NUCLEAR OVERHAUSER EFFECT SPECTROSCOPY. ((K. Kuwata, P. Ladam, D. Brooks and T. Schleich)) Dept. of Chemistry and Biochemistry, University of California, Santa Cruz, CA 95064.

A modified ROESY experiment designated O-ROESY was developed. The salient difference between the ROESY and the O-ROESY experiments is that the usual on-resonance spin-lock was replaced by an off-resonance spin-lock applied at a frequency off-resonance from the resonance(s) of interest. The resulting cross-peak intensities obtained at the different off-resonance spin lock frequencies define a cross-peak intensity dispersion curve, which contains a continuously increasing NOESY contribution at the expense of ROESY, as the off-resonance spin lock frequency is increased. A theoretical formalism was developed for the analysis of the cross peak intensity dispersion curves which permitted the evaluation of the internal motional correlation time of the internuclear vector defined by the 2 "communicating" protons (τ_i), its order parameter (S), the correlation time for overall rotational motion ($\tau_{o,eff}$), as well as the proton internuclear distance (r_{kl}). Analysis of O-ROESY cross-peak intensity dispersion behavior for several C_α proton pairs (spins k and l) in the stable β-strand region of lysozyme yielded the following: Arg-45/Thr-51, τ_i = 1.0 ± 0.2 ns, S = 0.86 ± 0.02, $\tau_{o,eff}$ = 6.4 ± 0.3 ns; Val-2/Asn-39, τ_i = 1.2 ± 0.6 ns, S = 0.82 ± 0.09, $\tau_{o,eff}$ = 6.3 ± 0.2 ns. Similar experiments were performed on BPTI, an RNA oligonucleotide fragment, and a DNA dodecamer. (Supported by NIH grant EY 04033)

Th-Pos317

K^+-RIBOSOME INTERACTIONS DETERMINE THE LARGE ENHANCEMENTS OF ^{39}K NMR TRANSVERSE RELAXATION RATES IN VIABLE CELLS ((M. Li†, H.J. Guttman*, S. Cayley†, C.F. Anderson*, and M.T. Record, Jr.*†))Departments of Chemistry* and Biochemistry†, University of Wisconsin-Madison, Madison, WI 53706 U.S.A.

As a probe of physical chemical properties of the intracellular environment of viable cells, we measured ^{39}K NMR transverse relaxation rates in concentrated cell slurries of *Escherichia coli* K-12 grown in minimal medium with osmolarities from 0.1 OsM to 1.0 OsM and in plasmolyzed cell slurries. We find that the ^{39}K transverse relaxation at a resonance frequency of ~18.67 MHz is bi-exponential, and 100% of the expected signal intensity is detected under all conditions. Not only the absolute magnitude of both fast and slow components of the ^{39}K NMR transverse relaxation are very fast, also the separation between these two is larger compared to previous measurements on ^{23}Na and ^{39}K in protein, tRNA and DNA solutions *in vitro*. The homogeneous nature and the 100% visibility of the ^{39}K signal we observed indicate the existence of fast exchange among all the multiple, magnetically distinguishable populations of ^{39}K which probably present in the cytoplasm.

To understand the origins of the striking NMR relaxation behavior of ^{39}K in viable cells, we have investigated NMR transverse relaxation rates of ^{39}K (also ^{23}Na and ^{35}Cl) in ribosome solutions and in concentrated DNA solutions *in vitro*. At concentrations of the ions and of ribosome that to the extent possible mimic those of the cytoplasm of *E. coli*, ^{39}K, ^{23}Na and ^{35}Cl transverse relaxation rates all exhibit bi-exponential behavior, and all exhibit the large magnitudes and the large separation between the slow and the fast relaxation rates observed in viable cells. Ribosome solutions are the only *in vitro* model system discovered to date that could give rise to ^{39}K transverse relaxation rates comparable to those in viable cells (including *E. coli*). We propose that K^+-ribosome interactions are the dominant source of both the NMR and thermodynamic properties of K^+ in *E. coli*. Also, we find that the NMR properties of quadrupolar ions in solutions of ribosomes are qualitatively different from those in analogous solutions of DNA.

Th-Pos318

MULTIDIMENSIONAL NMR IN LIPID SYSTEMS: COHERENCE TRANSFER THROUGH J COUPLINGS UNDER MAS.

((J.D. Gross*, P.R. Costa*, J.-P. Dubacq‡, D.E.Warschawski#, P.-N. Lirsact, P.F. Devaux#, and R.G. Griffin*)) *FBNML and Dept. of Chemistry, MIT, Cambridge MA, 02139; ‡LPDMV, C.N.R.S., U.R.A. 1810, Ecolé Normale Supérieure, 75230 Paris, France; †CEA, DIEP, CE Saclay, 91191 Gif sur Yvette Cedex, France; #LBC URA 526, Université Denis Diderot, 75251 Paris Cedex 05, France.

The combination of Magic Angle Spinning (MAS) with multidimensional chemical shift correlation techniques routinely employed in solution NMR provides high resolution spectra of lipid/water systems in the L_α and H_{II} phases. We report here the use of J couplings for coherence transfer in a glycolipid/water system under MAS. Techniques such as HSQC and TOCSY may be employed without modification provided that the rate of sample rotation is greater that the motionally averaged CSA and dipolar couplings. The connectivity information provided by these experiments permits the identification of individual membrane components.

Th-Pos319

Magnetic Resonance Spectroscopic Monitoring of Transitions in Dehydrated and Hydrated Mammalian Stratum Corneum as a Function of Temperature. S.J. Rehfeld, U. Simonis, W.Z. Plachy, Dept. of Chem. & Biochem. SF State Univ. 94132.

Stratum Corneum is a multi-component & multi-phasic system composed primarily of polygonal corneocytes, containing keratin and a small amount of bound fatty acids, with a cell wall of covalently bound "ceramides". The corneocytes are embedded in a lamellar bilayer structure composed primarily of hydroxy and nonhydroxyceramides, cholesterol and free fatty acids in ≈mole ratio of 1:1:1. This unique structure is responsible for serving as a water barrier, and it controls the permeability of drugs through the skin. Existence of many components and phases possessing solid-solid, solid-liquid, liquid-liquid and protein-lipid mixtures requires different experimental approaches for resolving origins of transitions. In the physiologic temperature range both ESR (spin probe technique) and proton NMR spectra results show a broad transition mediated by hydration. In both cases hydration and temperature increased the "fluidity of the lipids". Variation of either temperature or hydration results in a redistribution of lipids in subphases and/or domains altering both composition and molecular order of these phases. Significant differences are found between species of mammalian SC, probably due to differences in keratin structure. We will discuss how these spectral studies compare with physical measurements on different time scales.

Th-Pos320

A NOVEL NMR-COMPATIBLE BIOREACTOR FOR MRI AND MULTINUCLEAR NMR SPECTROSCOPY OF PERFUSED CELLS: APPLICATION TO ISOLATED RAT HEPATOCYTES.

((J. M. Macdonald, M.P. Grillo, D. T. Tajiri, O. Schmidlin, J. Kurhanewizc, L.-H. Chang, and T. L. James)) Department of Pharmaceutical Chemistry, University of California, San Francisco, CA.

We have developed a NMR-compatible bioreactor for non-invasive monitoring of ^{31}P and ^{13}C metabolites and near microscopic (64 μm resolution) magnetic resonance images (MRI). The bioreactor design is ideal for perfusion of hepatocytes because of (1) its similarity to liver ascinus architecture, (2) uniform perfusion of cells, (3) rapid and easy extrication of cell mass without destruction of bioreactor, (4) rapidity of preparation, (5) ability to use high resolution MRI's to check fiber integrity and cell distribution, and (6) its small volume which permits use of only one animal per study. We demonstrate the ability to monitor bioenergetics by ^{31}P NMR of hepatocytes with 30 min timepoints and maintain viability in the bioreactor for at least 4 hrs using Krebs-Heinseleit (K-H) buffer. ^{31}P spectra obtained from hepatocytes perfused in the bioreactor were similar to those obtained from liver of intact rat. Hepatocyte extracts, obtained after 4 hrs of perfusion with K-H buffer revealed an ATP/ ADP ratio of 3.1, indicative of normal energy charge. Staining with trypan blue revealed 80% viability of cells after 4 hrs of perfusion. Non-phosphate K-H buffer was also tested in order to obtain pH information, but hepatocytes did not remain viable. The MRI's revealed diverse information including (1) cell distribution, (2) flow dynamics, (3) fiber integrity, (4) magnetic susceptibility, (5) air bubbles and, (6) coil inhomogeneity. Various inoculation methods were used to increase cell packing, and thus increase temporal resolution. We demonstrate that ^{13}C studies are feasible by using solutions contained in the cell space, and customized pulse-sequences.
This is an ideal model for non-invasive *in vivo* cell studies with the ability to monitor endogenous or xenobiotic kinetics.

EPR/ODMR/ESR

(See also Th-Pos444)

Th-Pos321

EVIDENCE FOR ENERGY TRANSFER IN COMPLEXES OF ECO-RI METHYL TRANSFERASE WITH 2-THIOURACIL-CONTAINING OLIGODEOXYNUCLEOTIDES USING OPTICALLY DETECTED MAGNETIC RESONANCE. ((Prieto Sheaffer, M. C., A. H. Maki, R. Kuimelis, K. Nambiar))-Chemistry Dept, UC Davis, Davis, CA, 95616

The objective of this research was to use modified oligodeoxynucleotides as photosensitizing probes in nucleic acid to protein energy transfer studies. Specifically, we sought evidence for triplet-triplet energy transfer from 2-thiouracil (^{S2}U) replacing T in oligodeoxynucleotides to intrinsic tryptophan (trp). The protein was *Eco*-RI methyl transferase (MTase), which requires S-adenosylmethionine (AdoMet) as a cofactor. An inactive cofactor analog (sinefungin), and a 14 base-pair modified DNA containing the methylation site (GAATTC) were used in our study to create a stable ternary complex [Reich et al., (1991) *Biochemistry* 30, 2940]. By evaluating the energy transfer from ^{S2}U positioned at different sites within the binding site of MTase, we hoped to learn about the structure, distances, and interactions of DNA and MTase in the ternary complex. Microwave-induced delayed phosphorescence experiments conducted on ternary complexes were compared with experimental controls that consisted of a mixture of the oligodeoxynucleotide and MTase in the absence of sinefungin. The ^{S2}U in DNA was excited exclusively and the phosphorescence of trp sensitized by triplet-triplet energy transfer was monitored. We present evidence that the triplet state of trp is sensitized by energy transfer from ^{S2}U when in a ternary complex and not in the experimental controls lacking the ternary complex. Two of the trp sublevels in the ternary complex decay with rates that are 3 to 6 times faster than that of normal trp. However, the third sublevel decays with a constant of ~2-9 s^{-1}, over an order of magnitude faster than normal trp. We believe this unusually rapid decay results from the reverse transfer of energy from trp back to ^{S2}U.

Th-Pos322

PROPERTIES OF THE TRYPTOPHAN BINDING SITE OF E. COLI TRP HOLO-REPRESSOR CHARACTERIZED BY PHOSPHORESCENCE AND OPTICAL DETECTION OF MAGNETIC RESONANCE OF THE TRYPTOPHAN-FREE MUTANT.

((Z. Li[1], A.H. Maki[1], M.R. Eftink[2], C.J. Mann[3], and C.R. Matthews[3]))
[1]Department of Chemistry, University of California, Davis, CA 95616;
[2]Department of Chemistry, University of Mississippi, University, MS 38677;
[3]Department of Chemistry, Pennsylvania State University, University Park, PA 16802

Both tryptophan residues of wild-type *E. coli* trp repressor protein, which binds L-Trp as corepressor and regulates the expression of *trp* operon, were replaced by phenylalanines using site-directed mutagenesis. With the tryptophan-free repressor mutant, W19/99F, we were able to characterize properties of the L-Trp corepressor binding site that were not readily accessible with wild-type and single-Trp mutants in previous phosphorescence and ODMR studies. Binding of L-Trp to mutant W19/99F shifted its 0-0 phosphorescence band at 77 K from 407 nm to 409 nm. The ODMR transition frequencies of both D-E and 2E transitions at 1.2 K were found to be independent of the monitored phosphorescence wavelength. In addition, the bandwidths of both D-E and 2E transitions were considerably reduced. These results indicate that the local environment of the Trp-binding site is hydrophobic and more homogeneous than that of solvated L-Trp. Significant changes of zero field parameters, particularly E, and triplet state sublevel decay constants, were also observed. Formation of a ternary mutant repressor complex with L-Trp and a synthetic oligonucleotide operator sequence gave rise to changes of the triplet sublevel decay constants, that indicated that local conformational change of the repressor protein at the Trp binding-site may occur in the presence of the oligonucleotide.

Th-Pos323

MEMBRANE INTERACTIONS OF THE ISOLATED TRANSMEMBRANE DOMAIN OF DIPHTHERIA TOXIN: A SITE-DIRECTED SPIN-LABELING STUDY. ((Kyoung Joon Oh[1], Hangjun Zhan[2], Yeon-Kyun Shin[1], Wayne L. Hubbell[1], and R. John Collier[2])) [1]Jules Stein Eye Institute and Department of Chemistry & Biochemistry, University of California, Los Angeles, CA 90024; [2]Department of Microbiology and Molecular Genetics, Shipley Institute of Medicine, Harvard Medical School, Boston, MA 02115

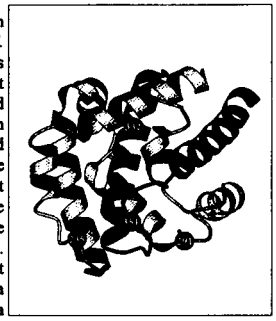

The transmembrane (T) domain of diphtheria toxin (residues 202-378, see figure), was expressed in *E. coli*. Like the holotoxin, the isolated T domain was stable and monomeric at neutral pH, but underwent a conformational change and inserted into lipid bilayers at acidic pH. Single cysteine substitution mutants were prepared at sites 235, 291, 332 and 351 and modified with a sulfhydryl-specific nitroxide reagent, and the EPR spectra and solvent accessibilities of the attached nitroxides were analyzed. In solution, the data are consistent with the crystal structure of the T domain in the holotoxin. Upon membrane binding at low pH: (i) a nitroxide at 332, located in hydrophobic helix 8, moves from a site buried in the protein to a lipid-exposed site at a depth of about 15Å in the bilayer; (ii) a nitroxide at 351 moves from the solvent-exposed 8-9 interhelical loop to a site buried within the new structure; (iii) 235 and 291 move from solvent-exposed loops to an interfacial site. These results are consistent with a large-scale tertiary rearrangement in which the hydrophobic helical hairpin is inserted into the bilayer.

Th-Pos324

DISTANCE DETERMINATION IN PROTEINS USING DESIGNED METAL ION BINDING SITES AND SITE-DIRECTED SPIN LABELING ((John Voss[1,2], Wayne L. Hubbell[2] and H.Ronald Kaback[1])) [1]Howard Hughes Medical Institute and [2]Jules Stein Eye Institute and Department of Chemistry and Biochemistry, UCLA, Los Angeles, CA 90024

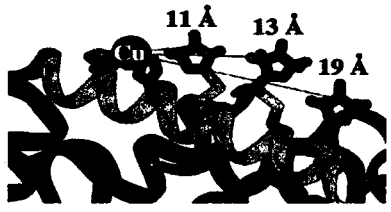

For most membrane proteins, structural information must be obtained by non-crystallographic means, and spectroscopic methods for determination of intramolecular distances are extremely useful in this regard. The magnetic dipolar interaction between a nitroxide spin label and a paramagnetic metal ion has been previously exploited to measure distances in natural metalloproteins. To generalize this powerful method, molecular genetic techniques can be used to introduce both a metal ion binding site and a nitroxide side chain at selected positions. To evaluate the strategy, a His-X_3-His metal ion binding site was introduced in the long inter-domain helix of T4 lysozyme (K65H, Q69H) in combination with a nitroxide side-chain at position 71, 76 or 80, corresponding to 11, 13, and 19 Å from the metal ion site (see figure). Addition of stoichiometric amounts of Cu^{+2} produced changes in the nitroxide EPR spectrum quantitatively related to the interspin distance deduced from the known lysozyme structure. Initial application to a protein of unknown structure, lactose permease, will be presented.

Th-Pos325

HYDROGEN-BONDING INTERACTION OF THE [2FE-2S] CLUSTER OF REDUCED FERREDOXIN - INVESTIGATION BY ESEEM SPECTROSCOPY. ((A. Rompel, O. Burghaus, H. Cheng[§], B. Xia[§], J.L. Markley[§], V.K. Yachandra, K. Sauer, M.P. Klein)) Structural Biology Division, LBL, & Dept. of Chem., UCB, CA 94720; [§] Dept. of Biochem., Univ. of Wisconsin-Madison, Madison-Wi 53706.

Iron-sulfur clusters are ubiquitous components of electron transfer proteins involved in photosynthesis, nitrogen fixation, and oxidative phosphorylation. Plant-type ferredoxins display redox potentials between -305 and -455 mV. The mechanism by which the redox potential is modulated is still not well understood, but hydrogen bonding is thought to be an important affector.

The [2Fe-2S] ferredoxin isolated from *Anabaena* 7120 contains two iron atoms tetrahedrally coordinated by two inorganic sulfides and by thiolate sulfurs of cysteinyl residues. The N-atoms of Cys^{46} and Arg^{42} are within hydrogen-bonding distance of the inorganic sulfur atoms. To study their putative interaction we performed pulsed EPR experiments on ferredoxins in which ^{15}N was selectively incorporated into the arginine or cysteines, and the C_α- or C_β-protons of the four Cys-residues were deuterated.

The Fourier-transform spectra of the wild type and all the isotopic labeled samples contain different frequencies. Four or more lines are observed between 0 and 5 MHz. These peaks probably arise from deuterium and nitrogen nuclei. Comparisons indicate that nitrogen of Cys^{46} influence the [2Fe-2S] site, whereas ^{15}N Arg^{42} gives nearly the same spectrum as the wild type. Similarily the α-protons interact less with the paramagnetic cluster than do the β-protons. (Supported by Deutsche Forschungsgemeinschaft and Department of Energy (DOE) DE-AC03-76SF00098.)

Th-Pos326

STRUCTURAL DYNAMICS OF THE FERRIC ENTEROBACTIN RECEPTOR, FepA, AS STUDIED BY SITE-DIRECTED SPIN LABELING. ((Phillip E. Klebba, Jun Liu, C. K. Murphy, and Jimmy B. Feix)) Departments of Chemistry and Biochemistry, Univ. of Oklahoma, Norman, OK 73019 and Biophysics Research Institute, Medical College of Wisconsin, Milwaukee, WI 53226. (Spon. by J. S. Hyde)

FepA is an 81 kDa outer membrane protein that is responsible for iron uptake *via* the siderophore, ferric enterobactin, in a large number of enteric bacteria. Our previous studies have shown that structurally FepA is a ligand-gated porin, with an extracellular domain containing the binding site for ferric enterobactin and a large transmembrane channel that will allow diffusion of hydrophilic solutes up to 1500 Da (Rutz *et al.*, Science **258**, 471-5, 1992; Liu *et al.*, PNAS **90**, 10653-7, 1993). We have utilized electron spin resonance site-directed spin labeling (SDSL) and non-denaturing polyacrylamide gel electrophoresis to examine cation-induced changes in FepA structure. Site-specific mutants were generated introducing cysteine residues into FepA surface peptides. These cysteines were labeled with a series of sulfhydryl-specific spin labels, and their locations in the protein tertiary structure characterized by accessibility to paramagnetic relaxation agents. Changes in spin label motion and accessibility were observed corresponding to formation of different conformational states of FepA. SDSL is a valuable approach for examining dynamic changes in defined regions of protein structure. Supported by USPHS grants GM51339 and RR01008 and NSF grant #MCB9212070.

Th-Pos327

EPR POWER STUDIES OF THE MIXED VALENCE SITE IN N_2OR — AN UNDERLYING SIGNAL ((W.E. Antholine, S. Pfenninger, J.S. Hyde, P.M.H. Kroneck, and W.G. Zumft) National Biomedical ESR Center, Milwaukee, WI 53226 USA and Univ. Konstanz and Karlsruhe, Germany)

Nitrous oxide reductase, N_2OR, from the bacterium *Pseudomonas stutzeri* is the terminal electron acceptor in a respiratory chain converting N_2O to N_2:$N_2O+2H^++2e^- \rightleftharpoons N_2+H_2O$. N_2OR has two identical subunits, each carrying four Cu atoms (1). Two Cu atoms in each subunit form a mixed valence $[Cu_A(1.5)...Cu_A(1.5)]$, $S=1/2$ center as first determined by EPR (2,3). The active site in N_2OR presumably involves the two remaining Cu atoms, referred to as the $[Cu_Z...Cu_Z]$ center. A mutant form of N_2OR has the $[Cu_A(1.5)...Cu_A(1.5)]$ center but not the $[Cu_Z...Cu_Z]$ center. In this study, a second wave in the signal versus power curve for the wild type enzyme at 4.2 K confirms the presence of a second species with a smaller T_1. Fractions of the low power signal were subtracted until the negative peaks vanished. The striking feature of the residual is the resolved fine structure in the $g_\parallel$ region. By comparison of the EPR detectable signals in both wild type N_2OR and mutant N_2OR, a likely explanation for the underlying signal is a signal from a second binuclear copper center. Pros and cons for assigning the signal to an altered form of $[Cu_A...Cu_A]$ or to the catalytic center $[Cu_Z...Cu_Z]$ are discussed. This work supported by NSF grant DMB 9105519.

1. W.G. Zumft *et al. Eur. J. Biochem.* 208:31-41, 1992
2. P.M.H. Kroneck *et al.*, *FEBS Lett.* 268:274-276, 1990.
3. W.E. Antholine *et al. Eur. J. Biochem.* 209:875-881, 1992.

Th-Pos328

SELECTIVE LABELING OF MEMBRANE PROTEIN SULFHYDRYL GROUPS WITH METHANETHIOSULFONATE SPIN LABEL. ((Chafia Hejase de Trad[a], William James[b] and D.A. Butterfield [b,c])), [a]Department of Physics, American University of Beirut, Beirut, Lebanon, [b]Department of Chemistry and [c]Center of Membrane Sciences, University of Kentucky, Lexington, KY 40506-0055.

Electron paramagnetic resonance was used to characterize the first use of a thiol-specific spin label in membranes. Procedures for use of the spin-label, 1-oxyl-2,5,5, tetramethyl- Δ^3 - Pyrroline-3-methyl(methanethiosulfonate;MTS) covalently attached to membrane proteins in human erythrocyte membranes are reported. The major findings are:(1) MTS was found to be thiol specific in membranes as it is for soluble proteins; (2) MTS labels ghost proteins in as few as 30 minutes at room temperature, providing a distinct advantage when sensitive or fragile membranes are to be used; (3) the distribution of the spin label suggests that the major cytoskeletal protein, spectrin, and the major transmembrane protein, Band 3, incorporate the highest percentage of spin label. This procedure expands the tools with which the researcher can investigate the physical state of membrane proteins and its alteration upon interaction of membrane perturbants or in pathological conditions. Supported in part by grants from NSF (EHR-9108764) and NIH(AG-10836 to D.A.B.).

Th-Pos329

ESR STUDY OF DISAGGREGATION OF PROTEINS IN LIPID MEMBRANES, ((M.T. Ge, D.E. Budil, and J.H. Freed)), Baker Lab of Chemistry, Cornell University, Ithaca, NY 14853

ESR studies have been performed on the disaggregation of an integral membrane protein, bacteriorhodopsin (BR) and a peptide, gramicidin A' (GA) in both well-aligned multilayers and dispersions of DPPC. The isopotential spin-dry ultra-centrifugation (ISDU) method was used to align the lipid membranes. For the ISDU-aligned DPPC membranes containing both GA and BR, ESR spectra of spin labeled cholestane (CSL) obtained slightly below the main phase transition (T_c) of DPPC reveals a new component with increased ordering of the lipids associated with a broad endothermic peak in the DSC, suggesting a disaggregation of both GA and BR prior to the T_c of the lipid. For lipid dispersions containing various amounts of GA at temperatures below and near the T_c of the lipid, a sudden increase in the ordering of ESR spectra from a spin labeled lipid, 16-PC, was also observed. This increase is in proportion to the amount of GA incorporated. If the lipid dispersions containing GA are preheated to 75° C annealed at this temperature for 30 minutes, and then cooled down to 0° C, no increase in the ordering of 16-PC is observed at temperatures below and near the T_c of the lipid. Instead, the ordering of 16-PC decreases steadily with temperature through the temperature range studied. These observations also suggest that GA molecules aggregate below the T_c of the lipid, and it has a dramatic effect on the packing of the lipid molecules.

Th-Pos330

IMPROVED EPR LINEWIDTH ANALYSIS FOR MEASUREMENT OF OXYGEN CONCENTRATION AND CORRELATION TIME ((A. W. Reese, C. Mailer and B. H. Robinson)) Department of Chemistry Bagley Hall BG-10 University of Washington Seattle WA 98195 . Supported by NIH GM 32681

The interaction of oxygen with nitroxide spin probes makes them particularly sensitive monitors of [O_2] for use in finding the structure of transmembrane proteins or monitoring physiological processes. Many different schemes have been developed from the NO - O_2 interaction with EPR linewidth (T_{2e}) measurements being the most common. In the past analysis has required simulations with large main frame computers. Recently Bales made desktop computing possible by modelling the experimental lineshape as the sum of a Gaussian and a Lorentzian line. Halpern *et al.* used this model with specially synthesized mono-protonated probes to obtain accurate Lorenztian linewidths as a function of dissolved [O_2]. We have obtained extremely accurate Lorentzian linewidths from experimental spectra by convolution of the theoretical EPR lineshape for a single line (or set of lines) with a Gaussian(either continuous or discrete). The effects of Zeeman frequency, (over)modulation amplitude and phase and microwave phase and power can be included. Data analysis is done with a commercial software package (MATLAB The Mathworks Cambridge MA) on a desk top computer. The oxygen concentration can be easily and directly obtained from the broadening of a single EPR line of a fully perdeuterated ^{14}N or ^{15}N nitroxide. Rotational correlation times faster than a few nanoseconds can also be accurately measured from the linewidths.

Th-Pos331

A Neural Network For the Fast Computation of ESR Slow Motional Spectral Parameters: Utility for Biological Macromolecules ((Gary V. Martínez, Glenn L. Millhauser)) Department of Chemistry and Biochemistry, University of California, Santa Cruz, CA 95064

The problem we are attacking may be stated as follows: given an ESR spectrum, what is the correlation time τ_c and the motional anisotropy N? For spectra in the motional narrowing regime, this is not difficult; however, for spectra in the slow motion regime, there is no simple mapping that relates the spectrum to τ_c and N because one cannot obtain these parameters directly from the ESR spectrum. It is thus necessary to obtain these parameters by simulation of the ESR spectrum (L. J. Berliner and J. Reuben. *Spin Labeling: Theory and Applications; Biological Magnetic Resonance,* Chapter 2, Plenum Press, New York, 1989). In order to determine these values quickly, we have employed the use of Feed Forward Neural Networks. We have used a training set that varies both in τ_c and N. Thus, once trained, the Neural Network can quickly output the above values given the experimental spectrum. The use of these networks facilitates the application of spin labels for systems with correlation times greater than 2 ns as is the case for many large biomolecules.

Th-Pos332

Can we "Toac" Peptides? The incorporation and characterization of a new Fmoc nitroxide spin label into peptides. ((Paul Hanson, Gary Martinez, Glenn Millhauser, Fernando Formaggio‡, Claudio Toniolo‡)) Department of BioChemistry and Chemistry, University of Santa Cruz, Santa Cruz, Ca. 95064; ‡ Department of Organic Chemistry, Universita Degli Studi, Via Marzolo, 1, 35131, Padova, Italy

A series of doubly labeled peptides analogous to peptides previously studied in this lab(1, 2) have been built using the Fmoc-Toac nitroxide label. In these new peptides, the spin label(3) is rigidly attached to the backbone of the peptide. Several exciting results have come about via the ESR and circular dichroism experiments. Analysis of the ESR spectrum indicates that two signals are present: at low temperatures a broad dipolar component has been assigned to the α-helical conformation and arises as a result of the orientation of the two labels with respect to each other. The onset of broadening and a five line spectrum at higher temperatures due to scalar j-coupling is indicative of a transition from a predominantly α-helical conformation to a conformation with both 3_{10} and α-helical contributions. Such spectral information may offer the first opportunity to perhaps quantify the relative amounts of the α- and 3_{10} populations in the peptides. CD results indicate that these new labels are highly helix promoting and alter the structure from their parent analogs. Analysis of the shape of the CD curves provides useful and complimentary information for interpreting and supporting the ESR data. 1. W. R. Fiori Lundberg K.M., Millhauser, G.L., *Nature Structural Biology* 1, 374-377 (1994) 2. S. M. Miick, G. V. Martinez, W. R. Fiori, A. P. Todd, G. L. Millhauser, *Nature* 359, 653-655 (1992). 3. R. Marchetto, S. Schreier, C. R. Nakaie, *Journal of American Chemical Society* 115, 11042-11043 (1993).

BILAYERS, NMR

Th-Pos333

MOLECULAR STIRRER FOR NONFREEZABLE WATER OF PHOSPHATIDYL CHOLINE LIPID BILAYER BETWEEN -40C and -110C((C-H Hsieh and W. Wu)) Institute of Life Sciences, National Tsing Hua University, Hsinchu, Taiwan 30043

The packing and dynamics of lipid bilayers at the phosphocholine headgroup region have been investigated by solid state NMR measurements of H_2O/choline-D_{13} DMPC at subzero temperatures. Three overlapping signals with ^2H NMR quadrupolar splittings ($\Delta\nu_Q$) of 115.2, 36.1 and 9.3 KHz were detected for sample with hydration state of 2 ± 1 water per lipid. The signal with largest $\Delta\nu_Q$ of 115.2 KHz was assigned to be from the $-CD_2$ of choline C_α and C_β methylene segment and the other two signals with smaller $\Delta\nu_Q$ of 36.1 and 9.3 KHz from the $-CD_3$ of choline C_γ methyl group. The low $\Delta\nu_Q$ of two coexisting $-CD_3$ signals are due to fast rotational motions of $-CD_3$ and $-N(CD_3)_3$ group, respectively, with three-fold symmetry. Thus, extensive motions at the $-N(CD_3)_3$ group of PC are still present at temperatures as low as -100 C. In addition, two different headgroup bilayer structures, which can be distinguished by the mobility of $-N(CD_3)_3$ group, coexist between -40C and -110C. The free energy difference between the two structures is found to be 27 KJ/mol for hydration state higher than 8 water per lipid and 9 KJ/mol for hydration state of 2 water per lipid. The results suggest a simple molecular mechanism to explain non-freezable water of PC lipid bilayers (Wu et al., 1991, J. Biol. Chem. 266, 13602-13606) and shed new light on the headgroup structures of the polymorphic gel-state bilayers. SUPPORTED BY NSC, TAIWAN

Th-Pos334

A DEUTERIUM NMR STUDY OF THE EFFECT OF CHOLESTEROL ON 16:0-18:2 PC ((M.R. Morrow[1], P.J. Davis[2], B. B. Bonev[1] and K.M.W. Keough[2])) Depts. of Physics[1] and Biochemistry[2], Memorial University of Newfoundland, St. John's, Newfoundland, Canada A1B 3X7.

The effect of cholesterol on the phase transition of heteroacid phosphatidylcholines with one unsaturated PC depends on the nature of the unsaturated chain. By DSC, the phospholipid 16:0-18:2 PC is found to have a broad, weak transition at about -18°C which is completely eliminated by less than 15 mole % cholesterol (Keough et al. 1989. *Biochim. Biophys. Acta 989*:51-55; Hernandez-Borrell & Keough 1993 *Biochim. Biophys. Acta 1153*:277-282). We have used ^2H NMR to examine the behavior of 16:0-18:2 PC-d_{31} from 4°C to -24°C in the presence of 0, 7, and 15 mole % cholesterol. In the absence of cholesterol, the change from axially symmetric liquid crystal powder pattern to the gel phase spectrum is gradual. Addition of cholesterol increases saturated-chain quadrupole splittings in the liquid crystal spectra and reduces the sensitivity of the splittings to temperature. There is no evidence of phase separation over the range of temperature and cholesterol content studied. Cholesterol is also found to decrease the sensitivity of the mean transverse relaxation rate to temperature. (Supported by NSERC and MRC Canada.)

Th-Pos335

CONFORMATIONS OF PHOSPHATIDYLINOSITOLS AND A 2-*O*-METHYL-INOSITOL ANALOG: RELEVANCE TO PHOSPHOLIPASE C ((C. Zhou and M. F. Roberts)) Boston College, Chestnut Hill MA 02167.

The solution conformation of chiral diheptanoylphosphatidylinositol (D- and L-inositol isomers) has been probed by NMR spectroscopy. A key feature is an NOE between the inositol C2 proton and an *sn*-3 glycerol CH_2 proton in the diC_7P(D-)I but not in the diC_7P(L-)I isomer. The observed positive NOEs and dihedral angles derived from coupling constants were used with QUANTA to construct a model of each chiral species. The inositol ring is nearly parallel to the chain packing direction, hence perpendicular to the membrane surface, leaving the phosphate ester accessible to attack by phospholipase C enzymes. Chemical shifts and ^{13}C T_1s (obtained by ^1H detection of ^{13}C because of severe overlap in the ^{13}C spectrum) were also used to assess conformation and lipid dynamics in monomer and micelle states. The inositol 2-OH group is assumed a necessary structural requirement since D-*myo*-1,2-cyclic inositol monophosphate is the initial product generated by PI-PLC. To test this, we have synthesized a 2-*O*-methylinositol derivative. The introduction of the methyl group lowers the CMC of $diC_7P(2\text{-}OCH_3)I$ compared to diC_7PI. An NOE (negative because of the presence of large micelles) between an *sn*-3 glycerol proton and the inositol C-2 proton constrains the orientation of the inositol ring with respect to the glycerol backbone in a conformation similar to diC_7P(D-)I. Modeling $diC_7P(2\text{-}OCH_3)I$ suggests that the methyl group blocks one side of the phosphate. PI-PLC cannot hydrolyze $diC_7P(2\text{-}OCH_3)I$, consistent with mechanistic expectations. However, non-specific PLC enzymes which are able to hydrolyze PI, albeit poorly, are also unable to hydrolyze this derivative. The latter result is consistent with the modified PI conformation where the methyl group at C2 shields one side of the phosphate from attack.

Th-Pos336

PROBE LOCATION MODELS IN 1,2-DIMYRISTOYL-sn-GLYCERO-3-PHOSPHOCHOLINE (DMPC) VESICLES BY NMR SPECTROSCOPY *[J. C. Smith, D. J. Gill, and S. Chandrasekaran], Department of Chemistry, Georgia State University, Atlanta, GA, 30303* NOESY and truncated NOE spectroscopy have been used to ascertain the location(s) of the potential-sensitive molecular probes tetraphenyl borate (TPB) and oxonol V (OX-V) in 10 mM suspensions of small unilamellar vesicles prepared by sonication of DMPC. NOESY spectra were obtained as a function of mixing time (τ_{mix}) from vesicles containing either TPB at 20 or 6-8 or OX-V at 20, 8, or 4 mol percent. In TPB studies at a τ_{mix} of 50 ms, cross peaks between the acyl chain terminal methyl, (CH_3), and the unresolved methylene, $(CH_2)_n$, protons (^1H) and the *ortho* ^1H of TPB present at 6-8 mol percent are observable. Cross peaks between the *meta* and *para* ^1H and the preceding acyl ^1H are detectable at τ_{mix}'s of 100, 150, and 200 ms as are cross peaks to the choline $N(CH_3)_3$ and methylene ^1H plus those of two acyl methylenes near the DMPC ester linkage. When the TPB content is raised to 20 mol percent, the relative intensity of the cross peaks to the head group ^1H increases relative to that from the hydrocarbon region. TPB NOE measurements yielded maximum values of 45, 45, and 20 percent when the $(CH_2)_n$, CH_3 and $N(CH_3)_3$ resonances were saturated. Development of cross peak intensity as a function of τ_{mix} is in qualitative agreement with buildup rates observed in the time-dependent NOE measurements. NOESY spectra from vesicles containing OX-V at 4 or 8 mol percent exhibited cross peaks between OX-V phenyl ^1H and those of the $(CH_2)_n$ and CH_3 at a 150 ms τ_{mix}. At a 200 ms τ_{mix}, cross peaks to the $N(CH_3)_3$, the choline methylenes and to methylenes near the ester linkage are observed. The intensity of OX-V cross peaks to the choline region increases relative to that of those to the hydrocarbon region when the OX-V mol percent is increased from 4 to 8. Cross peaks between the vinyl and the vicinal ^1H in vesicles containing a double bond at the 9,10 position in both chains and the phenyl ^1H of both TPB and OX-V are observable at a 150 ms τ_{mix}. These observations suggest a location model in which TPB and OX-V have populations in both the DMPC bilayer head group/interface region as well as the hydrocarbon region. Volume integration of the cross peaks from these regions indicates that the major probe population is in the acyl methylene section of the bilayer.

Th-Pos337

A MULTINUCLEAR SOLID STATE NMR STUDY OF THE MOLECULAR INTERACTIONS IN THE DPPC-CHOLESTEROL BINARY SYSTEM. ((Wen Guo and James A. Hamilton)) Department of Biophysics, Boston University School of Medicine, 80 E. Concord Street, Boston, MA 02118.

We performed a systematic study of the dipalmitoylphosphatidylcholine (DPPC)-cholesterol (C) binary system with X_c = 0-0.65 by solid-state NMR with magic angle sample spinning (MASNMR). Above the main transition temperature of fully hydrated DPPC (T_m), C increases the acyl chain rigidity as shown by the increase of the ^1H chemical shift anisotropy and the downfield shifts of ^{13}C acyl chain resonances with increasing X_c. Interactions between C and DPPC were manifested through the chemical shifts of the DPPC carbonyl carbons. The ^{13}C=0 (sn1) chemical shift first decreased and then increased as a function of X_c with a minimum at X_c~0.25, and the ^{13}C=0 (sn2) increased only slightly when X_c <0.25, then increased significantly. These results suggest substantial changes in the ester group conformations caused by interactions between the steroid ring and the acyl chains. Below T_m, the ^{13}C and ^{31}P MASNMR lineshapes clearly showed the coexistence of gel-like and liquid crystalline phases in the range of X_c = 0.1-0.35. With X_c<0.1, the DPPC gel phase is only slightly disordered by C, and with X_c >0.35, the gel phase is abolished. When X_c >0.5, crystalline C monohydrate was detected as a separate phase coexisting with the DPPC-C bilayer structure. The ^{31}P powder pattern also became asymmetric with increased signal intensity in the downfield region, showing that super-saturation of C not only reduced the motions of the chain and glycerol backbone, but also changed the headgroup conformation.

Th-Pos338

A CUBIC PHASE WITH REVERSED MICELLES STUDIED BY X-RAY DIFFRACTION AND PULSED FIELD GRADIENT ^1H NMR. ((G. Orädd and G. Lindblom)) Department of Physical Chemistry, University of Umeå, S-901 87 Umeå, Sweden.

The partial phase equilibria of two systems containing phosphatidylcholine, diacylglycerol and water has been investigated using a combination of classical methods together with x-ray diffraction and NMR techniques. In particular the extension of the phase regions of the lamellar, the reversed hexagonal and the cubic phases have been determined. By pulsed field gradient ^1H NMR the diffusion coefficients have been measured of all three components in a cubic phase composed of either soybean phosphatidylcholine, diacylglycerol and heavy water or of the synthetic components 1,2-dioleoyl-*sn*-glycerol-3-phosphocholine (DOPC), 1,2-dioleoylglycerol (DOG) and heavy water. The extension of the phase region of the cubic phase did not seem to change appreciably for the two ternary systems studied. The translation diffusion coefficient of DOPC is more than an order of magnitude smaller ($3\cdot10^{-13}$ m^2s^{-1}. 59 °C) than the lateral diffusion coefficient of DOPC in a macroscopically oriented lipid bilayer ($5\cdot10^{-12}$ m^2s^{-1}, 35°C; Lindblom et al. *Biochemistry* 1981, 20: 2204-2207), while the diffusion coefficients of water and DOG were found to be about two orders of magnitude larger at 59 °C. From these NMR diffusion data it is concluded that the cubic phase is built up of closed reversed micelles.

Th-Pos339

A CUBIC PHASE WITH REVERSED MICELLES STUDIED BY X-RAY DIFFRACTION AND PULSED FIELD GRADIENT ^1H NMR. ((G. Orädd and G. Lindblom)) Department of Physical Chemistry, University of Umeå, S-901 87 Umeå, Sweden.

The partial phase equilibria of two systems containing phosphatidylcholine, diacylglycerol and water has been investigated using a combination of classical methods together with x-ray diffraction and NMR techniques. In particular the extension of the phase regions of the lamellar, the reversed hexagonal and the cubic phases have been determined. By pulsed field gradient ^1H NMR the diffusion coefficients have been measured of all three components in a cubic phase composed of either soybean phosphatidylcholine, diacylglycerol and heavy water or of the synthetic components 1,2-dioleoyl-*sn*-glycerol-3-phosphocholine (DOPC), 1,2-dioleoylglycerol (DOG) and heavy water. The extension of the phase region of the cubic phase did not seem to change appreciably for the two ternary systems studied. The translation diffusion coefficient of DOPC is more than an order of magnitude smaller ($3\cdot10^{-13}$ m^2s^{-1}, 59 °C) than the lateral diffusion coefficient of DOPC in a macroscopically oriented lipid bilayer ($5\cdot10^{-12}$ m^2s^{-1}, 35 °C; Lindblom et al. *Biochemistry* 1981, 20: 2204-2207), while the diffusion coefficients of water and DOG were found to be about two orders of magnitude larger at 59 °C. From these NMR diffusion data it is concluded that the cubic phase is built up of closed reversed micelles.

Th-Pos340

^2H NMR STUDIES OF MONOUNSATURATED LIPID BILAYERS. ((Stephen R. Wassall, M. Alan McCabe, Cynthia W. Browning, Stephen P. Schuh and Sherrel D. Harris)) Department of Physics, Indiana University-Purdue University Indianapolis, Indianapolis, IN 46202-3273.

The tremendous impact that the position of double bonds has upon the properties of membranes is the focus of our recent research by solid state ^2H NMR. We compared [$^2H_{31}$]16:0-18:1PC (1-[$^2H_{31}$]palmitoyl-2-*cis*-octadecenoylphosphatidylcholine) bilayers in which the double bond is at the Δ6, Δ9, Δ12 or Δ15 position. Moments reveal that the temperature of the gel to liquid crystalline phase transition T_C varies by more than 40°C, exhibiting a minimum when the double bond is in the middle of the chain. Energy minimized structures obtained with the CHARMm force field for isomers of 16:0-18:1DG (1-palmitoyl-2-*cis*-octadecenoylglycerol) qualitatively correlate with this behaviour. They indicate that introduction of unsaturation at the Δ9 or Δ12 position causes greater disruption to acyl chain conformation than at the Δ6 or Δ15 position. Moment analysis also demonstrates that average order in the liquid crystalline state of [$^2H_{31}$]16:0-18:1PC changes by over 35%. At equal temperature the dependence resembles that seen for T_C, while the variation is inverted and the Δ12 isomer is most ordered at equal reduced temperature. Order parameter profiles generated from depaked spectra, which all possess the same shape, indicate that moving the unsaturation down the 18:1 *sn*-2 chain lengthens the characteristic plateau region of approximately constant order in the upper portion of the [$^2H_{31}$]16:0 *sn*-1 chain.

Determination of the orientation of the double bond in potassium [9,10-$^2H_2$]oleate bilayers is the goal of current work, which will serve as a model for similar studies planned for phospholipids. (Supported by ACS, PRF.)

Th-Pos341

^{1}H MAS NMR SPECTROSCOPIC STUDIES ON N-METHYL-DOPE LIPID DISPERSIONS.

((Zhen-jia Chen*, Richard M. Epand#, Ruth E. Stark* and Leon C.M. Van Gorkom*)) *College of Staten Island / CUNY, Department of Chemistry, 2800 Victory Blvd, Staten Island, NY 10314, USA. # McMaster University, Department of Biochemistry, 1200 Main St. West, Hamilton, Ontario, L8N 3Z5, CANADA

N-Methyl-DOPE (1,2-dioleoyl-*sn*-glycero-3-N-methylphosphoethanolamine) lipid dispersions form a lamellar (L_α) phase which converts to an inverted hexagonal (H_{II}) phase at temperatures above 65 °C. This phase transition is not reversible upon cooling, and instead an isotropic phase with cubic symmetry is formed. In the lamellar phase of N-Methyl-DOPE we observed two distinct water resonances, where the downfield shifted peak with the shorter T_1 relaxation time was ascribed to hydrogen-bonded water in slow exchange with other water molecules. The upfield peak with a long T_1 relaxation time was ascribed to an exchange-averaged resonance arising from water molecules in the bulk and at the lipid solvation sites. The hydrogen-bonded water also showed intense cross-peaks in 2D-NOESY experiments with the γ-CH_3 and β-CH_2 of the lipid headgroup. Upon heating through the phase transition, the water is expelled from the hydrogen-bonded bridge between the NH of one lipid and the PO_4^- of its neighboring lipid molecule. In the hexagonal phase the NH and PO_4^- of neighboring lipids are now close enough in space to hydrogen bond directly. Comparative studies on lamellar DOPC (1,2-dioleoyl-*sn*-glycero-3-phosphocholine) dispersions did not indicate the presence of strongly hydrogen bonded water between lipid molecules.

Th-Pos342

EFFECTS OF CHOLESTEROL, GANGLIOSIDES, & SPHINGOMYELIN ON ETHANOL-BILAYER INTERACTIONS.

((Judith A. Barry & Klaus Gawrisch)) NIAAA, NIH, Rockville, MD 20852

^{2}H NMR was used to monitor the ways in which cholesterol, gangliosides, and sphingomyelins modify the effects of ethanol on saturated phosphatidylcholine (PC) bilayers. It was found that ethanol affects bilayers of varying lipid composition differently, modifying lipid packing profiles down the chains. In general, ethanol binding disordered the lipid mixtures much more beyond the "plateau" region closest to the interface, and the disordering increased progressively down the chain. Exceptions were PC bilayers containing 30 to 67 mol% cholesterol, which were disordered by ethanol uniformly along the chain, and to only a very small degree. In contrast, low amounts of cholesterol enhanced the effect of ethanol, correlating to the relationship between cholesterol content and water permeability. With 10 mol% gangliosides, however, even low cholesterol concentrations attenuated the disordering effect of ethanol. Sphingomyelin mixed with PC rendered the lowest quarter of the PC chains more disordered by ethanol. These results demonstrate the influence of lipid composition on the changes induced in the bilayer interior by ethanol binding in the lipid-water interface.

Th-Pos343

HOW ACYL CHAIN UNSATURATION MAY AFFECT THE SHAPE AND PACKING OF A PHOSPHOLIPID MOLECULE.

((L.L.HOLTE AND K.GAWRISCH)) NIAAA, NIH, BETHESDA, MD 20892

We have used ^{2}H NMR to measure the effects of increasing sn-2 unsaturation on the order parameter profiles of stearic acid sn-1 chains in phosphatidylcholine at 37°C. Increasing unsaturation results in a maximum decrease of 0.7Å in the sn-1 chain length. Most of this decrease has occurred by the addition of the third double bond to sn-2 and no further reductions were observed with addition of 4, 5, or 6 double bonds. Using the assumption that both chains were of equal length, the hydrophobic cross-sectional area of the entire molecule was calculated and ranges from 65Å^2 (18:010:1PC) to 70Å^2 (18:022:6PC). Unsaturation of the sn-2 chain results in a non-uniform change of area along the sn-1 hydrocarbon chain. The area increase around carbon atom 14 is 3-4 times greater than the increase for the top part of the chain. This asymmetric area increase that is largest towards the end of the chain suggests a non-cylindrical shape for the sn-1 chain. Such a shape may indicate special packing requirements for lipids with polyunsaturated sn-2 chains and/or deeper penetration of solvent molecules into bilayers rich in polyunsaturated acyl chains.

Th-Pos344

INFLUENCE OF UNSATURATION AND HEADGROUP SIZE ON CHAIN PACKING IN LIPID BILAYERS.

((F. Separovic, L.L. Holte and K. Gawrisch)) NIAAA, NIH, Bldg 31 Rm 1B-58, Bethesda MD 20892-2088.

Solid-state ^{2}H and ^{31}P NMR spectroscopy was used to study hydrated mixtures of dioleoylphosphatidylethanolamine (DOPE) and phosphatidylcholine (PC) with perdeuterated stearic acid ($18{:}0_{d35}$) in position sn-1, and 18:0, 18:1ω9, 18:2ω6, 18:3ω3, 20:4ω6, 20:5ω3 or 22:6ω3 in position sn-2. For DOPE/PC (5/1) dispersions, the lipids formed lamellar phases at lower temperatures and, above 308±5K, non-bilayer structures were formed as indicated by NMR spectra representative of hexagonal and isotropic/cubic phases. The order parameter profile of the PC sn-1 chains for DOPE/PC mixtures were of higher order than for pure PC systems corresponding to the same fatty acid combination. Increased order in the upper part, or plateau region, of the chain was found for all fatty acids. However, with 2-6 double bonds, the biggest change occurred in the region of carbon positions 11-13. This higher order corresponds to an increase in the perdeuterated hydrocarbon chain lenth of 0.12±0.04nm in the liquid crystalline lamellar phase relative to a pure PC bilayer. There was little effect on membrane thickness attributed to increasing the degree of sn-2 unsaturation after the first double bond. The smaller PE headgroup results in higher order or a more extended configuration of the sn-1 chain of the PC, and the DOPE matrix moderates the effect of increasing unsaturation on the bilayer.

IR/RAMAN

Th-Pos345

A METHODOLOGY FOR OVERCOMING EXPERIMENTAL DIFFICULTIES IN THE DETERMINATION OF GLOBAL 2° STRUCTURE OF PROTEINS IN H_2O BY FTIR.

((J.J. Unruh and T.F. Kumosinski)) ERRC, USDA, Philadelphia, PA 19118

Much controversy exists concerning the influence of experimental artifacts on the number of component FTIR vibrational bands attributed to the amide I and II envelopes of proteins in water. Whether these bands represent unique populations of vibrating protein groups in a particular global 2° structure or whether the bands are due to instrumental and environmental fluctuations, needs to be addressed from an experimental view. We present here a detailed experimental methodology with all the modifications required to eliminate potential environmental, instrumental, or sample fluctuations. Actual vapor and instrument residual spectra are presented, and compared with the component bands obtained from the nonlinear regression analysis of lysozyme and alpha-lactalbumin. Lysozyme and alpha-lactalbumin were successfully analyzed repetitively at a variety of sample temperatures (20-60°C) without detectable influences from the environment, the instrument or the cell assembly. This method for obtaining FTIR spectra yields repetitive results comparable with values derived from X-ray crystallographic data.

Th-Pos346

USING FAR-INFRARED SYNCHROTRON RADIATION TO STUDY COLLECTIVE MOTIONS OF PROTEINS.

((A. Xie, L. M. Miller, E. M. Scheuring, B. Sclavi, M. R. Chance)). Department of Physiology & Biophysics, Albert Einstein College of Medicine, Bronx, NY 10461.

Recently, a number of theoretical and experimental interests have been focused onto how proteins use collective motions to carry out their biological functions, including electron tunneling in energy transduction, and proton transfers in enzyme reactions. To establish correlations between collective motions of proteins and their reactivities, we have studied far-infrared (FIR) absorption spectra of dried, hydrated, and deuterated purple membrane (pm) and met myoglobin (Mb) films, and a number of amino acid (aa) monomers and polymers. FIR spectra of dried pm and Mb are very different, while those of hydrated pm and Mb exhibit two similar bands at 164 and 230 cm^{-1}, related to water absorption. The number of bands in an aa polymer is much less than those in the corresponding monomer. Furthermore, no common bands were found between L-Leu and poly-L-Leu, and between L-Ala and poly-L-Ala from 50 to 400 cm^{-1}, indicating negligible contributions of side chain absorption to the observed FIR bands of these polymers. Also the observed bands from poly-L-Ala and poly-L-Leu are different, suggesting none of them arising from localized motions of polypeptide backbone, but associated to collective motions of polymers. These studies will provide insights into the nature of collective motions and their roles in protein reactivities.

This work is supported by NIH grants HL-45892 and RR-01633.

Th-Pos347

INFRARED STUDY OF SECONDARY-STRUCTURE CHANGES IN CAPRINE WHOLE CASEINS; EFFECTS OF CALCIUM AND TEMPERATURE. ((A. Mora-Gutierrez[1], T.F. Kumosinski[2], D.M.Curley[2] and H.M. Farrell[2], Jr.)) [1]Prairie View A&M University, CARC, Prairie View, TX 77446 and [2]USDA, ERRC, Philadelphia, PA 19118.

Fourier transform infrared (FTIR) spectra of two caprine whole caseins, selected for their α_{s1}-casein content, have been obtained at 2 cm^{-1} resolution from 1350 to 1800 cm^{-1} under submicellar (Ca^{2+} removed) and micellar (Ca^{2+} re-added) conditions. Detailed analysis of the amide I band was made, using second derivative and deconvolution procedures. A comparison of the spectra of caprine casein micelles characterized by low content of α_{s1}-casein with that of caprine casein micelles high in α_{s1}-content shows that both proteins exhibit similar, though not identical, changes in secondary structural elements. Upon binding of Ca^{2+} ions to carboxylate and serine phosphate groups, the caprine caseins adopt a highly flexible and hydrated conformation at 15°C and 37°C. The main components of the caprine micellar structure are β-sheets and turns. Self-association of caprine caseins into submicelles results in a significant increase in turn structure at 37°C, due to the enhancement of hydrophobic interactions.

Th-Pos348

AN INFRARED-DETECTABLE GROUP SENSES CHANGES IN CHARGE DENSITY ON THE NICKEL CENTER IN HYDROGENASE. ((K. A. Bagley, E. C. Duin, W. Roseboom, S. P. J. Albracht, and W. H. Woodruff)). Department of Chemistry, SUNY College at Buffalo, Buffalo, NY 14222; MST-14, Los Alamos National Laboratory, Los Alamos, NM 87545; and The E.C. Slater Institute for Biochemical Research, University of Amsterdam, Amsterdam, The Netherlands.

Infrared studies of nickel hydrogenase from *Chromatium vinosum* reveal the presence of a set of three absorption bands in the 2100-1900 cm^{-1} spectral region. These bands have line widths and intensities rivaling that of a band arising from the carbon monoxide stretching frequency (ν(CO)) in the Ni(II).CO species of this enzyme, but do not themselves arise from carbon monoxide. The frequencies of these bands are unaffected by either exchanging the enzyme into D_2O or reducing the enzyme with D_2 indicating that these infrared features do not arise from an exchangeable hydrogen species. Taken together, these observations indicate that these bands arise from a chemical species that is unusual in a protein. To further explore the nature of the chemical species that gives rise to these IR bands, eight different states of the nickel center have been produced depending on the redox state and/or the activity state of the enzyme and the presence of carbon monoxide. In seven of these states, the set of three IR absorption bands have unique frequency positions. Additionally, the position of each of these three infrared absorption bands respond in a consistent way to changes in the formal redox state of the nickel center and to photodissociation of hydrogen bound to the nickel. We conclude that the set of three infrared bands arise from an intrinsic, non-protein group in the enzyme which is very near the nickel, perhaps a ligand to the Ni, and that this group senses changes in charge density at the Ni site.

Th-Pos349

ERYTHROCYTE PEROXIDATION: QUANTITATIVE FT-IR SPECTROSCOPY STUDIES OF EXTRACTED LIPIDS, ISOLATED MEMBRANES, AND INTACT CELLS
((David J. Moore[1,2], Richard H. Sills[2], and Richard Mendelsohn[1])) [1]Department of Chemistry, Rutgers University, Newark, New Jersey 07102 and [2]Department of Pediatrics, University of Medicine and Dentistry of New Jersey and the Children's Hospital of New Jersey, Newark, New Jersey 07107

FT-IR spectroscopy has been used to quantitatively monitor peroxidative damage to human erythrocyte membranes. The integrated intensity of the olefinic =C-H stretch at ~3012 cm^{-1} was monitored in model phospholipids, extracted erythrocyte lipids, and isolated membranes. A precise linear correlation ($r^2 = 0.99$) between the number of C=C bonds per molecule and the intensity of the 3012 cm^{-1} band was determined for model phospholipids. Using the intensity of the 3012 cm^{-1} band, a decrease in the number of C=C bonds in the cell membrane was quantitatively monitored in lipids from peroxidized erythrocytes. Furthermore, in erythrocyte lipids and model phospholipids, a new feature was observed at 1260 cm^{-1} in peroxidized samples which is most likely due to a C-O stretch or an O-H bending mode. Control and peroxidized erythrocytes, and membranes isolated therefrom, were suspended in a mixed D_2O/H_2O buffer system. This buffer system created a spectral window in the C-H stretching region which permitted direct measurement of the 3012 cm^{-1} band in membrane spectra. In peroxidized samples a significant loss in C=C bonds was quantitated directly from the membrane spectra. To examine the effect of peroxidation upon membrane conformational order, the second derivative spectra of intact cells and isolated membranes were obtained. The frequency of the conformationally sensitive symmetric CH_2 stretching mode was monitored in the second derivative spectra, both as a function of temperature and peroxidation. As expected, increasing temperature resulted in increasing membrane acyl chain conformational disorder, however, peroxidation did not induce any detectable change in conformational order.

Th-Pos350

FT-IR SPECTROSCOPY INVESTIGATIONS OF MIXED-CHAIN PHOSPHOLIPID MONOLAYERS AT THE AIR/WATER INTERFACE: THE INFLUENCE OF THE POSITION OF THE UNSATURATED FATTY ACID ACYL CHAIN ON THE CONFORMATIONAL ORDER
((Arne Gericke[1], Joseph W. Brauner[1], Ravi K. Erukulla[2], Robert Bittman[2] and Richard Mendelsohn[1]))
[1]Department of Chemistry, Rutgers University, Newark College of Arts and Science, 73 Warren St., Newark, New Jersey 07102 and [2]Department of Chemistry and Biochemistry, Queens College, City University of New York, Flushing, New York 11367

In general, naturally occuring mixed-chain phospholipids have the fatty acid acyl chain with the higher melting point at the *sn*-1 position, while at the *sn*-2 position the fatty acids with lower chain-lengths or unsaturation are found. These studies address the question whether the position (*sn*-1 or *sn*-2) of an unsaturated fatty acid acyl chain in a mixed-chain saturated/unsaturated phospholipid influences the molecular structure of a model biomembrane at the air/water interface. Palmitoyl-d31-oleyl-phosphatidylcholine monolayers, with the perdeuterated saturated fatty acid acyl chain either at the *sn*-1 or *sn*-2 position, are investigated at the air/water interface *in situ* by External Infrared Reflection-Absorption Spectroscopy. The frequencies of the methylene C-H and C-D stretching vibrations, which are known to be conformationally sensitive, are monitored for different temperatures and states of compression and compared for the different fatty acyl chain positions. In addition, it is possible to study separately the conformational order of the saturated and unsaturated fatty acid acyl chain and, therefore, to analyze the influence of the unsaturation in both chains.

Th-Pos351

SPATIAL MAPS OF OPTICAL COEFFICIENTS OF TISSUE LIKE PHANTOMS IN TURBID MEDIA USING NEAR INFRARED LIGHT. ((S.A. Walker, M.A. Franceschini, S. Fantini, J. Maier, and E. Gratton)) Lab for Fluorescence Dynamics, Department of Physics, Univ. of Illinois at U-C

Optical tomography in tissue is a possible alternative to current methods for locating tumors in the human body (i.e. Magnetic Resonance Imaging, X-ray techniques). It has the advantages of safety, portability, and relatively low cost. Near infrared light is used because of its deep penetration into human tissue (typically several centimeters). In this wavelength region, human tissue is highly scattering, causing light to propagate in a diffusive manner. In turbid media, a high frequency (about 100 MHz) intensity modulated light source produces a "photon density wave". By measuring the phase and amplitude of this wave, one can recover the scattering and absorption coefficients (m_s' and m_a respectively) of a macroscopically homogeneous, highly scattering medium. In imaging applications, when macroscopic inhomogeneities are present, we use a precalibrated measurement protocol to recover the optical coefficients. This protocol consists of a single distance, single modulation frequency measurement in a macroscopically homogeneous medium of known m_s' and m_a (the calibration sample), followed by a measurement at the same distance and frequency in the investigated medium.

We performed an experiment in which we simultaneously scanned a single source and single detector, facing each other, in a grid pattern across the sampled volume. We worked in the infinite geometry employing 2% low fat milk as the strongly scattering medium. Absorbing and scattering macroscopic inhomogeneities were embedded in the host medium, with optical coefficients ranging from 2 to 12 times those of the background. The optical maps we obtained could localize the inhomogeneities and correctly estimate their optical nature. Supported by National Institutes of Health grant RR03155.

Th-Pos352

EFFECTS OF CURVED BOUNDARIES ON THE MEASURED LINEAR TRANSPORT COEFFICIENTS OF TISSUE-LIKE PHANTOMS IN THE NEAR INFRARED. (A. Cerussi, W.M. Yu, S. Fantini, M.A. Franceschini, E. Gratton) LFD, University of Illinois at Urbana-Champaign, Urbana, IL 61801)

We are studying the effects of curved boundaries on photon density waves (PDW) in strongly scattering tissue-like phantoms. PDW are generated in highly scattering media by intensity modulated light sources, which are employed in the frequency domain experimental approach. These PDW are spherical waves in an infinite, homogeneous medium where scattering dominates over absorption. The measured frequency domain parameters, such as relative phase shift and intensity, can be translated into linear absorption (μ_a) and reduced scattering (μ_s') coefficients in both infinite and semi-infinite media. A commonly used assumption is that the angular photon density is nearly isotropic; it is composed of an isotropic term plus a smaller angular contribution. This diffusion approximation of the Boltzmann transport equation, however, is not valid in the presence of finite boundaries. Near a boundary, the space is not isotropic and the diffusion approximation is no longer valid. Although there has been success in recovering the linear coefficients for the semi-infinite case, the curvature of a boundary further thwarts efforts to measure accurately μ_a and μ_s'. The overall goal of our work is the interpretation of frequency domain data using near-infrared light for *in vivo* studies of human tissue. Of practical importance are studies done on the head, which should be more affected by the curvature of the skull. The correct determination of the transport coefficients is essential for optical tomography and brain oxygenation measurements.
Supported by National Institutes of Health CA57032 and UIUC.

Th-Pos353

TISSUE REDUCED SCATTERING AS A NEAR-INFRARED SPECTROSCOPY TOOL: CORRELATION BETWEEN IN-VIVO BLOOD GLUCOSE AND REDUCED SCATTERING ((John S. Maier, Scott A. Walker, Sergio Fantini, Maria Angela Franceschini, Enrico Gratton)) Laboratory for Fluorescence Dynamics, Dept. of Physics, Univ. of Illinois at Urbana Champaign, 1110 West Green street, Urbana IL 61801-3080

Most of the emphasis in near-infrared tissue spectroscopy is placed on the use of absorption characteristics of tissues and how they relate to underlying physiology or pathology. In order to accurately determine the absorption coefficient of bulk tissue at a near-infrared wavelength one must separate the effect of tissue scattering from absorption, thereby determining the reduced scattering coefficient of the tissue. Development of physical models which connect changes in reduced scattering coefficient with changes in physiology will allow use of reduced scattering in answering physiological questions. One such model is the relationship between index of refraction mismatch and scattering. The effectiveness of an inhomogeneity as a scatterer is related to the difference between its refractive index and the refractive index of the surrounding medium. As the indices approach one another, the scattering caused by the inhomoganeity decreases. We consider changes in refractive index of the intracellular and extracellular fluid caused by changes in glucose concentration and the effect this has on the reduced scattering coefficient of the tissue as a whole.

We have designed and constructed a frequency-domain near-infrared tissue spectrometer capable of measuring the reduced scattering coefficient of tissue with enough precision to detect changes in glucose levels in the physiological and pathological range. We will present in vitro experimental results along with results of an in vivo experiment on a human subject. This work was supported by National Institutes of Health grant RR0315 and the University of Illinois at Urbana-Champaign

Th-Pos354

SCALED QUANTUM MECHANICAL FORCE FIELDS FOR PEPTIDES IN SOLUTION: FTIR AND RAMAN OF ALA_n

Alan F. Weir†, Alfred H. Lowrey‡, and Robert W. Williams†. †Department of Biochemistry, Uniformed Services University of the Health Sciences, 4301 Jones Bridge Rd, Bethesda, MD 20814-4799. ‡Laboratory for the Structure of Matter, Naval Research Laboratory, Washington, D.C., 20375-5000.

To provide more reliable structural interpretations of amide frequencies in peptides and proteins, we are developing a Scaled Quantum Mechanical Force Field for peptides in solution. Scale factors have been built up from *ab initio* calculations and Raman and FTIR spectra of over 40 isotopic species of 5 different molecules at a variety of pH values representing the chemical groups in peptides. Here we report our final results for alanine-alanine. A single set of scale factors has yielded good agreements between experiment and calculation for AA at pH 1, 7, and 13. Our HF/4-31G scale factors for the amide COs, CNs, and NHib are 0.83, 0.85, and 0.74, respectively. Corresponding force constants vary (9.46 to 10.1 for the COs).

We have adopted a novel approach to the supermolecule calculations: To avoid redundant internal coordinates and artifacts from the vibrational coupling of statically hydrogen bounded water molecules, we delete cartesian coordinates and cartesian coordinate force constants for water molecules prior to transformation into internal symmetry coordinates. This operation preserves the effect of hydrogen bonding from water on the electronic structure of the peptide.

Th-Pos355

STUDY OF THE RIBONUCLEASE S-PEPTIDE IN SOLUTION AND WITHIN THE RIBONUCLEASE S COMPLEX BY MEANS OF THE DIFFERENTIAL RAMAN SPECTROSCOPY. ((R. Gilmanshin, J. Van Beek, R. H. Callender)) Department of Physics, City College of New York, New York, NY 10031. (Spon. by M. Gunner)

Bovine pancreatic ribonuclease (RNase) A can be enzymatically cleaved between the 20 and 21 amino acid residues resulting in RNase S, which is capable of maintaining both tertiary structure and enzymatic activity similar to that of native protein. Under some conditions, the isolated S-peptide (1-20 fragment of the RNase) forms helix in solution and when combined with S-protein (a RNase S without the S-peptide). To compare the solvated helical forms of the S-peptide with its structure when complexed with the S-protein, we measured the Raman spectra of these forms by means of differential spectroscopy. The spectrum of the S-peptide within the RNase S complex is characterized by much sharper vibrational bands than the spectra of the S-peptide in water solution. The amide I components of the disordered parts are at different positions for solvated (1672 cm^{-1}) and protein bound (1658 cm^{-1}) forms of the S-peptide while the "helical" component is at the same wavenumber (1642-1644 cm^{-1}) for the both S-peptide forms. Other spectral differences are also found.

Th-Pos356

FINGERPRINTING KERATIN FIBERS WITH FT-RAMAN SPECTROSCOPY. ((C. Pande)) *Clairol Inc. Stamford, CT. 06922.*

Human hair is primarily composed of keratin proteins. Cystine is the most abundant amino acid in hair and constitutes ~10% of the fiber weight. The mechanical and, to some degree, the optical properties of these fibers are dependent on the integrity of the constituent proteins. Natural weathering and cosmetic chemical treatments cause undesirable fiber damage.

We are developing *in situ* spectroscopic probes to fingerprint functional groups in hair to better characterize hair damage. This, we feel, is the essential first step in reducing damage. We have previously shown the potential of FT-Raman technique in this regard[1]. Using this method, we have now identified the mercaptan (-SH) group as one of the products of hair photodamage. Also, peptide bonds are affected as a result of photodamage. Under ambient conditions, hair fibers are hydrated and bind ~10 % water by weight. The accessibility of the hair proteins to D_2O (exchange with H_2O) is being used as an indicator of hair damage. Analysis of these data will provide significant insight into hair structure and changes in it resulting from cosmetic chemical treatments and weathering.

[1] Pande, C. *Biophys J.* 64, 2, A276, 1993

BILAYERS, OPTICAL PROBES

Th-Pos357

DETERMINATION OF MICRODOMAIN STRUCTURE IN BINARY LIPID MIXTURES BY IR SPECTROSCOPY AND AFM IMAGING. ((S. Widayati and R.A. Dluhy)) Department of Chemistry, University of Georgia, Athens, GA 30602

Current research in this laboratory involves using a combined spectrscopic/imaging strategy which uses IR spectroscopy to obtain conformation information and scanning probe microscopy to obtain complementary morphological information about biomembrane models. These methods have been applied to the quantitative determination of microdomain segregation in binary mixtures of of fatty acids. ATR-IR spectroscopy was used to study normal, protiated fatty acids of different chain lengths [i.e. $CH_3(CH_2)_nCOOH$, where n=18-22] which were combined in binary mixtures with perdeuterated stearic acid [i.e. $CD_3(CD_2)_{16}COOH$]. The influence of the chain length difference on the segregation of the protiated and deuterated components into microphase domains within the thin film was determined by the factor-group splitting of the CH_2 and CD_3 scissoring modes at 1460 and 1088 cm^{-1}, respectively. In addition, microdomain segregation at the molecular level has also been observed in these systems using atomic force microscopy. Clear regions of hexagonal and orthorhombic structure, as well as macroscale lateral separation between the two components, are observed in the same binary mixtures which were studied by IR. The results from both the IR and AFM provide, for the first time, a new means of quantifying phase separation in two-dimensional membrane models.

Th-Pos358

INFRARED SPECTROSCOPY OF THE ASYMMETRIC PO_2 STRETCH REPORTS THE PHASE TRANSITIONS OF MODEL MEMBRANES AND CELLS. ((L.M. Crowe, S.B. Leslie, and J.H. Crowe)) Univ. of Calif., Section o Molec. and Cell. Biol., Davis, CA 95616.

We have reported previously that the asymmetric PO_2 stretch, determined by FTIR, can be used to follow phase transitions in model lipid bilayers and in whole cells (Biophys.J, 61: A241, 1992). The present word represents an expansion of the previous data and several examples are given. The CH_2 symmetric and asymmetric stretches have been widely used for following membrane transitions in the past. FTIR is sensitive and reveals membrane transitions which cannot be detected by differential scanning calorimetry. However, some samples, especially dry ones, scatter infrared light so that the CH_2 stretches which detect the phase transition become too noisy to use. Dry cells in the presence of solute (which may become concentrated by the drying) may also show significant contributions from the solute in this region. Further, many cells (e.g. yeast, pollen) contain droplets of neutral lipid or lipid bodies which contribute strongly to the CH_2 signal and mask membrane transitions. We have found, using model membranes of phospholipids, isolated membrane preparations,and whole cells that the asymmetric PO_2 stretch accurately reports membrane phase transitions and can be used to follow transitions in difficult samples where the CH_2 stretch is not useable. (Supported by NSF IBN 93-08581, NIH 5RO1-AI-20900-8, and ONR USN N00014-94-1).

Th-Pos359

FTIR STUDY OF THE INTERACTION OF PUROINDOLINES WITH PHOSPHOLIPID MEMBRANES. ((T. Le Bihan, J.-E. Blochet and M. Pézolet)) CERSIM, Département de chimie, Université Laval, Québec, Canada and ((D. Marion)) Laboratoire de Biochimie et Technologie des protéines, INRA, Nantes, France.

Puroindolines are water soluble basic proteins that have been isolated from wheat grain. Although their physiological function is yet unknown, puroindolines display a strong effect on membrane lipids thus suggesting a supposed role for these proteins in the defense mechanism of plants. FTIR has been used in order to investigate the interaction of these proteins with phospholipids at the molecular level. The conformation and orientation of both the phospholipid and the protein in the complexes have been studied by polarized attenuated total internal reflectance. Spectra have been collected in both H_2O and D_2O using various phospholipids (different acyl chains length and headgroups). Preliminary results suggest that puroindolines, despite the fact that they are water soluble, can penetrate the hydrophobic core of the membrane. The membrane insertion mechanism of one of these puroindolines most likely involves a molten globule state. Puroindolines have also a preferential affinity for anionic lipids with short acyl chains.

Th-Pos360

STUDY OF SOLUBILIZED WATER IN INVERTED MICELLES BY MEANS OF IR AND UV-VISIBLE SPECTROSCOPY. ((S. Alex and A. Berthod) Institut de Chimie, Montréal, Qué, Canada and UA CNRS 435, Laboratoire des sciences analytiques, Lyon, France)

A mixture of diethyl-hexyl phosphoric acid (HDEHP) and its sodium salt (NaDEHP) reversed micelles provides a good model to mimic hydrophilic pockets in apolar media. The reversed micelles were obtained by mixing HDEHP (or NaDEHP) at various concentrations with heptane in presence of water. The concentrations selected were 1.5 M HDEHP, 0.75 M HDEHP and 0.5 M HDEHP. Similar solutions were made with NaHDEHP. Mixtures of HDEHP/NaDEHP at a 1/1 molar ratio were also tested. The structure of solubilized water and the interactions between the solvent and the surfactant were investigated by means of IR spectroscopy. The shape and the intensity of the OH stretching band and of the OH bending vibration mode are affected by the concentration of H_2O and the nature of the interactions between the surfactant and the solvent. The restricted field of the inverted micelle's core induces OH vibration changes, proving that embedded water state differs from that of ordinary water. For instance, large water concentrations do not promote surfactant aggregates and reduce stress on water, leading to a more flexible structure. UV-Visible measurements on cosolubilized colored metal ions such as Co(II) and Fe(III) were used to complete the study. These cations were useful probes as they show marked solvatochromic effects depending on their coordination states to either water and/or $POOH/POO^-$ moieties. Elimination and addition of water molecules from and to metal ions cosolubilized in the inverted micelles are a function of the nature of these tight spaces. The data from both the IR and UV-Visible spectra demonstrate that the amount of water directly affects the flexibility-rigidity and hardness-softness of the core.

Th-Pos361

IMPORTANCE OF PHOSPHATIDYLETHANOLAMINE AS A MEMBRANE MATRIX. ((M. B. Bazzi and G. L. Nelsestuen)) Dept. Biochemistry, University of Minnesota, St. Paul, MN 55108.

Previously, we reported that the annexins exhibited strong preferences membranes containing phosphatidylserine dispersed in phosphatidyl-ethanolamine (PE) over those dispersed in phosphatidylcholine (PC)(Bazzi et al.1992, Biochemistry 31, 1125). This study extended these findings by examining a variety of acidic phospholipids and membrane-binding proteins. Annexin VI and V displayed preferences for certain acidic phospholipids in the membranes. Substituting PE for PC as membrane matrix did not change the order of preferences, but reduced the calcium requirement of binding by about 8-fold for all acidic phospholipids tested. Calcium requirements of binding were not influenced by the presence of ethylene glycol (changes in the hydration properties of phospholipids) or cholesterol (melting properties). Maximum binding of annexin VI or V, at constant calcium,was consistent with 3-4 fold more accessible PS in PE membranes than corresponding PC membranes. Binding of cytochrome C, which interacts with membranes electrostatically, displayed similar properties; maximum binding of cytochrome C also suggested higher accessibility of PS in PE membranes. PE may function by virtue of its smaller hydration shell or by special arrangement of phospholipids in PE matrix. (Supported in part by Grant 38819 from NIH).

Th-Pos362

INTERACTION OF SIALIC ACID WITH DPPC MULTILAMELLAR LIPOSOMES IN THE GEL STATE AS MEASURED WITH RAMAN SPECTROSCOPY ((Centeno, S., Romero, E. Della Vedova C. O., Alonso-Romanowski, S.)) Quinor, U. N. Q., R. Saenz Peña 180, 1876 Bernal, Argentina (Spon. by Juan Pablo Rossi)

Raman spectroscopy was used to study the effects of the dehydration (D) in presence of sialic acids and subsecuents rehydration (R), on the vibrational spectra of multilamellar liposomes of DPPC in the gel phase. The Raman spectra indicated that the D/R process by itself lowers the number of gauche conformers of fatty acids, leading to a greater packing of the acyl chains. The phosphate heads groups signals of the sialic acid modified membrane are different when compared to those observed for other sugars such as galactose and trehalose, pointing that there is a close relationship between the chemical structure of the carbohydrate and its interaction with DPPC membranes.

Th-Pos363

FTIR ANALYSIS OF ACYL CHAIN CONFORMATION AND ITS ROLE IN THE FREE ENERGY OF BINDING OF NATIVE AND MUTANT CYTOCHROME B5 TO LIPID VESICLES.
((Robert W. Doebler, A. W. Steggles*, and Peter W. Holloway)) Dept. of Biochemistry, Univ. of Virginia Sch. Med., Charlottesville, VA. *Dept. of Biochemistry, Northeastern Ohio Univ. Coll. Med., Rootstown, OH.

Cytochrome b_5 binds spontaneously to lipid vesicles via a 43 amino acid nonpolar domain. A mutant form of cytochrome b_5, where Trp 108 and 112 in this domain are replaced by Leu, has a self-association constant 4 times less than that of the native, presumably due to the differences in hydrophobicity of the membrane-binding domains. However, the relative membrane-affinities of the two forms, measured by fluorescence inter-vesicle exchange, are not the same as the relative self-association constants. Hence, membrane-binding is not due entirely to the hydrophobic difference between the two domains. FTIR analysis of the CH_2-wagging bands between 1400-1300 cm^{-1} show that the number of gauche conformers in the lipid acyl chains depend upon both the protein and lipid component and thus will contribute to the difference in the overall change in enthalpy of binding ($\delta\Delta H_b$). Native cytochrome b_5 lowers the number of gauche bonds in DMPC LUVs and increases the number in POPC LUVs. The mutant has a similar effect, but not as pronounced. We attribute this to a difference in bulk between the replaced residues, as well as a difference of protein topology within the two types of lipid. The difference in enthalpy change due to lipid perturbation ($\delta\Delta H_{lp}$) from FTIR allows the calculation of the $T\delta\Delta S_{lp}$ term, which correlates empirically with the shift in the 2850 cm^{-1} CH_2-stretching band. Supported by a Grant-in-Aid from the American Heart Association, Virginia Affiliate, Inc.

Th-Pos364

CALORIMETRIC AND SPECTROSCOPIC STUDIES OF THE THERMOTROPIC PHASE BEHAVIOR OF AQUEOUS DISPERSIONS OF THE 1,2-DIESTER, 1,2-DIETHER, 1-ACYL 2-ALKYL AND 1-ALKYL 2-ACYL DERIVATIVES OF DIPALMITOYL PHOSPHATIDYLCHOLINE. ((R.N.A.H. Lewis & R.N. McElhaney)) Department of Biochemistry, University of Alberta, Edmonton, Alberta Canada; ((W. Pohle)) Institut für Molekularbiologie, Friedrich-Schiller Universität, D-07708, Jena, Germany.

The phase behavior of dipalmitoylphosphatidylcholine and its 1,2-diether, 1-acyl 2-alkyl and 1-alkyl 2-acyl derivatives were studied by differential scanning calorimetry and FTIR spectroscopy. Substitution of the acyl chains of DPPC with appropriate ether-linked chains results in relatively small increases in the chain-melting transition temperature (<4°C). However, the same structural change alters the gel-phase packing of the lipid hydrocarbon chains and causes an increase in the polarity of the environments of the polar headgroup and polar/apolar interface. The latter observations are surprising because substitution of an ester-linked chain of a diacyl glycerolipid with the ether-linked analogue should decrease the polarity of that region of the lipid molecule. These results cannot be rationalized without considering the possibility that the conformation of the glycerol backbone of DPPC and differs from that of its ether-linked counterpart. The latter suggestion brings into the question the issue of whether mono- and di-ether glycerolipids are good models of the diacylglycerolipids.

(Supported by Medical Research Council of Canada, the Alberta Heritage Foundation for Medical Research and the Deutsche Forschun gsgemeinschaft)

Th-Pos365

MIXED-CHAIN PHOSPHATIDYLCHOLINES: CALORIMETRIC AND SPECTROSCOPIC STUDIES OF THE EFFECT OF HYDROCARBON CHAIN LENGTH AND ASYMMETRY ON GEL-STATE PACKING. ((R.N.A.H. Lewis & R.N. McElhaney)) Department of Biochemistry, University of Alberta, Edmonton, Alberta Canada

The thermotropic phase behavior of the 42 mixed-chain phosphatidylcholines with even-numbered, n-saturated fatty acyl chains whose length ranges from 10 to 22 carbon atoms was studied by differential scanning calorimetry and by Fourier-transform spectroscopy. Our studies have identified six spectroscopically distinct types of gel phases, the formation of which was governed by a combination of both hydrocarbon chain length and hydrocarbon chain chain-length asymmetry. Our calorimetric studies have also identified several distinct patterns of thermotropic phase behavior, some of which can be correlated with the formation of the gel phases that have been characterized spectroscopically. These observations can be rationalized on the basis of differing requirements for the optimization of both hydrocarbon chain packing interactions in the hydrophobic domain and for polar interactions in the headgroup and polar/apolar interfacial domains of the lipid bilayer.

(Supported by Medical Research Council of Canada and the Alberta Heritage Foundation for Medical Research)

Th-Pos366

APPEARANCE OF A SHIFTED GEL-TO-LIQUID CRYSTALLINE PHASE TRANSITION TEMPERATURE FOR SATURATED PC SYSTEMS WITH WIDE INTERBILAYER SPACINGS.

((W.R. Perkins, P.L. Ahl,, P.A. Harmon, J.L. Slater, S.R. Minchey, and A.S. Janoff.))
The Liposome Company, Inc., Princeton, NJ 08540.

The thermodynamic properties of phospholipid bilayer membranes have been characterized in great detail over the past three decades. Of the thermal events examined none have been more scrutinized than the gel to liquid-crystalline 'main' phase transition temperature (T_m). For most investigations, the systems studied were multilamellar vesicle (MLV) dispersions in distilled water. Here we examined MLV, freeze-thaw MLV (FATMLV), and interdigitation-fusion vesicle (IFV) systems with and without solute for the symmetric saturated chain phosphatidylcholine series di-16:0 through di-20:0. Systems made in the presence of 150 mM NaCl exhibited two main phase transition temperatures! We believe that this second peak corresponds to a shift of the T_m in the presence of salt for vesicle systems with wide interbilayer spacings (FATMLVs and IFVs). We believe that the 'expected' T_m persists in these systems due to the presence of multilamellar structures where solute exclusion between bilayers occurs. Although the ratio of the two enthalpies varied from preparation to preparation the positions of the transition temperatures remained fixed. Consequently, the separation between the two peaks was a constant value (ΔT_m) for each lipid system and a plot of ΔT_m versus chain length revealed a linear relationship for the series di-17:0 through di-20:0 (ΔT_m = 1.4°C to 0.6°C, respectively).

Th-Pos367

THERMOTROPIC PROPERTIES OF PHOSPHOLIPID MIXTURES CONTAINING PHOSPHATIDYLETHANOL ((Olga P. Bondar and Elizabeth S. Rowe.)) Department of Biochemistry and Molecular Biology, University of Kansas Medical School, and VA Medical Center, Kansas City, MO 64128.

One of the byproducts of ethanol metabolism is the unique phospholipid phosphatidylethanol (PETH), which can reach as high as 2 mole% of membrane lipids in animal models of alcoholism. In order to elucidate the effect of this ethanol metabolite on the properties of the membranes, and its possible role in membrane adaptation to ethanol, we have investigated the physical properties of dipalmitoylphsophatidylethanol (DPPETH) as a pure lipid, as well as in mixtures of other phospholipids. Differential Scanning Calorimetry (DSC) has been used to examine the binary phase diagrams of DPPETH with several phosphatidylcholines and phosphatidylethanolamines. It was found that mixtures of phosphatidylethanol with these lipids are unstable even at relatively low mole % PETH. In many cases, the initial scans show miscibility; however, repeat DSC scans show the appearance of lateral phase separations which is dependent on the number of scans. These results are discussed in terms of their significance for the ethanol adaptation of membranes. (Supported by the Department of Veterans Affairs.)

Th-Pos368

ADIABATIC COMPRESSIBILITY OF PROTEIN FREE AND PROTEIN FILLED REVERSE MICELLES. (A. Amarene, M. Gindre, B. E. Basham,* P. C. Kahn,* C. Nicot, W. Urbach, and M. Waks) Laboratoire d'Imagerie Parametrique, URA 1458 CNRS, Université Paris 6, France, and *Rutgers University, New Brunswick, NJ 08903, USA

Reverse micelles are microdroplets of water stabilized in apolar solvents by a surfactant monolayer. Often called water-in-oil microemulsions, these self-assembled thermodynamically stable, spheroidal droplets selectively solubilize enzymes or membrane proteins and thus constitute a good membrane mimetic system (C. Nicot and M. Waks in *Structure and Reactivity in Reverse Micelles*, ed. M. Pileni, Elsevier, 1989, pp 342-360). We report measurements of the sound propagation velocity in reverse micellar solutions at increasing water to surfactant molar ratios (W_o). For measurements of sound velocity (u) a small volume differential acoustic velocimeter was developed. High precision density (ρ) and sound velocity measurements allow determination of the adiabatic compressibility, $\beta = 1/\rho u^2$. At low water to surfactant mole ratios the adiabatic compressibility increases sharply with increasing amounts of water present in the system up to a W_o value of about 8 and then levels off, reflecting probably the variation of the specific volume of the encapsulated water as reported by Etchells and Kahn (Biophys. J. 64: 2-2 A291, 1993). We also present adiabatic compressibilities of the reverse micellar system after insertion of membrane proteins or after solubilization of water soluble proteins therein.

Th-Pos369

EFFECT OF ETHANOL ON THE BILAYER PROPERTIES OF THE *N*-METHYLATED SERIES OF 1,2-DIPALMITOYL-*SN*-GLYCERO-3-PHOSPHOETHANOLAMINE. ((M. M. Batenjany, C. Parrett, T.J. O'Leary, and J.T. Mason)) Department of Cellular Pathology, Armed Forces Institute of Pathology, Washington, DC 20306-6000.

Differential scanning calorimetry was employed to investigate the effect of ethanol (0-300mg/mL) on the thermotropic behavior of the *N*-methylated series of 1,2-dipalmitoyl-*sn*-glycero-3-phosphoethanolamine (DPPE). As demonstrated previously ethanol was found to induce a fully interdigitated bilayer phase in the trimethyl derivative (DPPC) at ethanol concentrations above 50mg/mL, whereas ethanol did not induce interdigitation in DPPE bilayers at concentrations up to 300mg/mL. Ethanol was found to induce a fully interdigitated bilayer phase in the dimethyl derivative (dmDPPE) at ethanol concentrations above 90mg/mL, but no interdigitated bilayer phase was detected in the monomethyl derivative (mDPPE) at ethanol concentrations up to 300mg/mL. Ethanol was found to induce the formation of a crystalline bilayer phase in mDPPE and DPPE at alcohol concentrations above 160mg/mL when the ethanol was added to preformed multilamellar vesicles (MLVs). In contrast, if ethanol was included in the buffer used to hydrate the phospholipids this crystalline phase was not formed. It is proposed that the intermolecular hydrogen bonding in mDPPE and DPPE bilayers is sufficiently strong to inhibit the partitioning of ethanol into the bilayer interface. This prevents the formation of an interdigitated bilayer phase and reduces the permeability of the bilayer to ethanol. The latter effect causes an osmotically driven dehydration of the interstitial water layers of the MLVs, thus promoting the formation of a crystalline bilayer phase.

Th-Pos370

AN APPROXIMATION FOR THE HYDROPHOBIC ATTRACTION IN MOLECULAR DYNAMICS OF SURFACTANTS AND PROTEINS. ((James F. Rusling and T.F. Kumosinski)) U. of Connecticut, Storrs, CT 06269-3060. (Spon. by Harold M. Farrell, Jr.)

The measured long-range force between hydrophobic surfaces coated with surfactants is several orders of magnitude larger than the expected van der Waals attraction. Hydrophobic attractions, of magnitude similar to that found by experiment, were applied to molecular dynamics simulations of surfactant micelles, monolayers and bilayers, as well as amino acids, amino acid side chains, and proteins. The hydrophobic attractive force was approximated by multiplying the default value in the Tripos force field for van der Waals attraction between hydrocarbon chains of surfactants, and hydrophobic side chains of amino acids with a scaling factor of up to 75 X. Results were compared to simulations without this hydrophobic attraction. Inclusion of the hydrophobic attractive force provided dynamic structures for all simulations which more closely resembled models supported by experimental solution and X-ray crystallographic data. Scaling of the hydrophobic attractive force was used to provide simulations of gel and liquid crystal phases of the surfactant bilayers. For peptides, scaling of the hydrophobic attractive force was utilized for mimicking experimental solution hydrophobicity scales.

Th-Pos371

INCORPORATION OF THE SURFACE TENSION INTO SIMULATION OF A FLUID PHASE LIPID BILAYER MEMBRANE ((Chiu, S.-W.[1], Clark, M.[2], Balaji, V.[1], Subramaniam, S.[1,3,4,5], Scott, H. L.[2], and E. Jakobsson[1,3,4,5])) [1]Nat'l Center for Supercomputing Appl., Univ. of Ill., Urbana, IL 61801, USA, [2]Dep't of Physics, Okla. St. Univ., Stillwater, OK 74078-0444 [3]Dep't of Physiol., [4]Biophys. P'g'm., [5]Beckman Inst. for Advanced Sci. and Tech., Univ. of Ill., Urbana, IL 61801 [Supported by NSF]

We have incorporated surface tension into periodic boundary conditions in a molecular dynamics computation of a DMPC bilayer. This has enabled us to produce a hydrated fluid phase membrane starting from an initial configuration of the x-ray crystal structure. Formally the surface tension is introduced as a negative pressure in the direction of the membrane plane. The magnitude of the negative pressure is derived from experiments correlating surface tension, temperature, and molecular density in PC monolayers at air-water interfaces. For our system of 100 DMPC molecules and 2130 waters, the negative pressure is calculated to be about -100 atmospheres. The fluid phase bilayer membrane computed with this boundary condition agrees well with PC bilayer experimental results with respect to hydrocarbon order parameters, orientation of phospholipid headgroups, roughness of the membrane surface, and number of waters associated with each phospholipid molecule. The emergence of a realistic fluid phase from independently derived parameters, initial conditions, and boundary conditions gives us confidence in the essential correctness of the physical description of the membrane embodied in the simulations. Because the boundary conditions were derived from monolayer experiments our results support the concept that the properties of monolayers, when considered at the appropriate temperature and surface pressure, correspond closely to the properties of half a bilayer (MacDonald and Simon, 1987).

Th-Pos372

PROBING THE ASSEMBLY MECHANISM OF THE CRITICAL UNILAMELLAR STATE; ACCELERATING THE TRANSFORMATION FROM MLV'S TO ULV'S AT T*. **((N.L. Gershfeld and L. Ginsberg)) NIAMS, NIH, Bethesda, MD 20892, and Royal Free Hospital School of Medicine, London, UK.**

We have previously established from Cp-T measurements that the rate at which multilamellar liposomes of DMPC spontaneously transform to large unilamellar vesicles at T*, the critical temperature for the formation of the unilamellar state, is extremely slow with a $t_{1/2}$ of the order of 50-100 hrs (Biophys. J. 65:1174-1179, 1993). A method has been developed for identifying T* that is several orders of magnitude faster than the Cp-T measurement, and that also provides some insights into the mechanism of the MLV-ULV transformation. We reasoned that this transformation necessarily involves opening of bilayers to permit the release of interior lamellae, and that a fluorescent dye in the interlamellar aqueous space would provide a sensitive probe of the process. We have examined the transformation with two lipids: DMPC (T* = 28.96°C) and egg PC (T* = 25°C), using liposomes containing 5,6 carboxyfluorescein at fluorescence self-quenching concentrations. For both lipid preparations significant dye leakage begins 1-2 degrees below T*, reaching a maximum at T*. At temperatures above T* dye leakage virtually ceases. Details of the method will be presented. Leakage of dye confined to the temperature range of the MLV-ULV transformation is consistent with the thermodynamic prediction of a spontaneous change in the topology of MLV's towards ULV's at T*.

Th-Pos373

NONIDEAL MIXING OF PHOSPHATIDYLSERINE AND PHSPHATIDYLCHOLINE: UN-SYMMETRICAL INTERACTIONS CAUSE A SHIFT OF THE 2-PHASE REGION. ((J. Huang, A. Hinderliter, and G. W. Feigenson)) Section of Biochemistry, Molecular and Cell Biology, Cornell University, Ithaca, NY 14853.

(12:1,12:1)PC/(16:0,18:1)PS and (14:1,14:1)PC/(16:0,18:1)PS lipid mixtures at pH 7 in 800 mM KCl buffer show lamellar fluid-fluid phase separation at $0.50 \leq \chi_{PS} \leq 0.80$ and $0.6 \leq \chi_{PS} \leq 0.84$, respectively. The increased width of the 2-phase region implies that increasing the acyl chain length difference of PS and PC increases the nonideal interaction between PS and PC. The fact that the centers of the 2-phase regions are located at $\chi_{PS} > 0.5$, suggests that interaction between PS and PC is un-symmetrical. We investigated whether the size difference of PS and PC headgroups would give such a shift, using a mean-field Flory-Huggins theory modified for a hard-disk lattice model. We found that the shift could have a contribution from, but could not be totally caused by the estimated size difference of PS/PC headgroups. The origin of the un-symmetrical interaction is still unknown, but it can be expressed phenomenologically by a composition-dependent interaction energy term.

Th-Pos374

FLUCTUATIONS AND MEMBRANE HETEROGENEITY. ((J.R. Abney[1,2] and B.A. Scalettar[1])) [1]Dept. of Physics and [2]Northwestern School of Law, Lewis & Clark College, Portland, OR 97219.

Biological membranes contain many specialized domains, ranging from tens of nanometers to several microns in size and characterized by different concentrations and compositions of protein. Because these domains influence membrane function, considerable attention has focused on understanding their origin. Here we analyze the relationship between number fluctuations and domain formation. Number fluctuations were analyzed by modeling the membrane as a two-dimensional fluid containing interacting protein solutes. The characteristic size and lifetime of a domain in which one would expect to observe a fluctuation of specified magnitude was calculated. Domain size was found to depend on the nature of the interprotein force (e.g., attractive or repulsive) and on the average protein concentration. Domain size was largest at low protein concentrations and in the presence of attractive interprotein forces and was smallest at high protein concentrations and in the presence of repulsive interprotein forces. Domain lifetime was found to depend on domain size and on the diffusion coefficient of the proteins. In a "typical" membrane containing 5-nm proteins with diffusion coefficient 10^{-10} cm^2/s at a density of 1,000/μm^2, a 30% fluctuation will yield domains characterized by a twofold difference in local concentration; these domains persist over a distance of about 100 nm and have a lifetime of about 0.25 s. Number fluctuations can account for much of the microheterogeneity commonly observed in electron micrographs.

Th-Pos375

THE TEMPERATURE - COMPOSITION PHASE DIAGRAM OF THE MONOERUCIN/WATER SYSTEM DOES INCLUDE THE INVERTED HEXAGONAL (H_{II}) PHASE ((H. Qiu and M. Caffrey)) Chemistry Dept., The Ohio State University, Columbus OH 43210

The original phase diagram for the monoerucin/water system constructed by Lutton in 1965 (*J. Am. Oil Chem. Soc.* 42:1068) on the basis of "consistency" and light microscopy includes the lamellar and fluid isotropic phases. Indeed, Lutton was careful to remark on the absence of the H_{II} phase in this system, despite the fact that the H_{II} phase was expected based on erucic acid being a long chain, unsaturated fatty acid. In a separate study involving use of a lyotrope gradient in combination with time - resolved x-ray diffraction the H_{II} phase was shown to dominate the phase diagram, especially in the high temperature region (Caffrey, M. *Biophys. J.* 55:47, 1989.). Since the lyotrope gradient is a non-conventional method for phase diagram determination, we have resorted to the more traditional isoplethal - diffraction method for constructing the equilibrium phase diagram for monoerucin in water. This study confirms the presence of the H_{II} phase that extends from *ca.* 10 to 20 %(w/w) water and from *ca.* 40 °C to 130 °C. Coexistence with an excess water phase is observed above *ca.* 20 %(w/w) water in the same temperature range. The low temperature region of the diagram is dominated by the lamellar crystalline phase. Full structure characterization of these and other phases in the system will be reported.

Th-Pos376

HYDROSTATIC PRESSURE-INDUCED HEADGROUP TILT IN PHOSPHATIDYLCHOLINES, A ^{2}H-NMR STUDY. ((B.B. Bonev and M.R. Morrow)) Dept. of Physics, Memorial University of Newfoundland, St. John's, Newfoundland, Canada A1B 3X7.

The effects of pressure and temperature on the DPPC headgroup conformation were investigated by ^{2}H-NMR. Isothermal compression is found to produce a decrease in choline α- and an increase in β- and γ-deuteron splittings. A similar counterdirectional change is seen in the presence of positive surface charges and has been attributed to tilting of the headgroup away from the bilayer surface in response to the torque exerted on the phosphocholine dipole by the positive surface charges (Seelig et al. 1987. *Biochemistry 26*:7535–7541). The direction of this effect is consistent with the ordering of the acyl chains, observed under the same conditions. It is also found that at elevated pressure the α-splitting increases with temperature, while β- and γ-splittings decrease. This temperature dependence is stronger than at ambient pressure and suggests that the headgroup conformation may be temperature dependent at elevated pressure. (Supported by NSERC Canada.)

Th-Pos377

MEMBRANE FLUIDITY RESPONSE TO β-IONONE AND MENTHONE.

((M. Bouchard, N. Boudreau and M. Auger)) CERSIM, Département de chimie, Université Laval, Québec, Canada, G1K 7P4.

We have examined the interaction between two odorants, menthone and β-ionone, with DMPC membranes in order to investigate the characteristics of olfactory receptors. Our results indicate that odorants with different odors incorporate in the membrane at different depths and therefore have different effects on the membrane fluidity. The infrared results suggest that the incorporation of both β-ionone and menthone in the membrane decreases the phase transition temperature of the lipid but that β-ionone has a greater effect on the order of the lipid acyl chains. In addition, the ATR spectroscopy results suggest a reorientation of the polar head group of the lipids due to the incorporation of the odorants. We have also studied the effects of the odorants on the polar head group and the acyl chains of the lipids by ^{2}H solid-state NMR spectroscopy. These results indicate that the site of incoporation of the two odorants is near the interfacial region.

LIPID INTERACTIONS

Th-Pos378 ***(Presented at W-AM-F9)***

POLYION/MONOLAYER INTERACTIONS: THE EFFECT OF OLIGONUCLEOTIDES ON PHOSPHOLIPID PHASE BEHAVIOR.

((Jie Liu and David G. Rhodes)) Pharmaceutics Division, College of Pharmacy, The University of Texas at Austin, Austin, TX 78712-1074

Clinical application of antisense oligonucleotides will require that the molecules be nuclease resistant and able to cross cell membranes. As oligonucleotides are polyanions, it is unlikely that these molecules directly penetrate the bilayer. Nevertheless, it has been observed that "naked" DNA can cross membranes. In order to determine a mechanism for this function, we have used phospholipid monolayers as model systems to investigate the microscopic phase behavior in the presence of monovalent and divalent small ions, oligonucleotides and other polyions. Compression isotherms of anionic (DPPG) monolayers on buffered subphase have relatively high compressibility up to the collapse point, with an ill-defined coexistence region at $\pi \approx 20$ mN/m. Low concentrations (μM) of Ca^{++}, result in a well defined transition at ~10 mN/m leading to an incompressible solid phase, and isotherms at moderate Ca^{++} concentrations (mM) indicate a single, relatively incompressible phase. The effect was not due simply to ionic strength. Addition of low concentrations of polylysine also condensed monolayers, resulting in a well defined transition at surface pressures which decreased with increasing concentration. Oligonucleotides at relatively low concentrations exhibited a Ca^{++}-mediated condensation effect, but the effect in the presence of Mg^{++} appears to be weaker. These results suggest that interaction of oligonucleotides with DPPG and other anion-containing bilayers may be mediated by calcium or other divalent cations.

Th-Pos379

EFFECT OF LIPID COMPOSITION AND LIPID-DNA CHARGE RATIOS ON PHYSICAL PROPERTIES AND TRANSFECTION ACTIVITY OF CATIONIC LIPID-DNA COMPLEXES (Yuhong Xu[#*], Sek-Wen Hui[*], Francis C. Szoka, Jr.[#]) * Membrane Biophysics Lab, Roswell Park Cancer Institute, Buffalo, NY14263 # School of Pharmacy, University of California, San Francisco, CA94143

Cationic lipids complexed to plasmid DNA can mediate transfection of mammalian cells *in vitro* and *in vivo*. The physical properties of one complex, DOTMA,(N-[1-[2,3-Bis(oleyloxy]propyl]N,N,N-trimethylammonium chloride)-DOPE-DNA, has been described (Gershon et al., Biochemistry 32: 7143, 1993) and we have studied DNA complexes formed from DOTAP,(1,2-dioleoyl-3-trimethylammonium-propane). We examined the influence of lipid/DNA charge ratio and lipid composition of DOTAP, DOTAP/monooleoylglyceride, DOTAP/DOPE, DOTAP/DOPC), on morphology of the complex in freeze fracture EM, complex diameter by dynamic light scattering, electrophoretic mobility, protection of DNA from degradation be DNAse I and correlated these findings with *in vitro* transfection activity. Around a charge ratio(+/-) 2/1 - 4/1, the complexes have maximum diameters ranging from 100 to 1000 nm depending upon reaction concentration, positive zeta-potentials around 20mV, protection of most DNA molecules against DNAse degradation for up to 2hr. Transfection activity was most active at this range. Among the cationic liposomes high activity correlates with the appearance in freeze fracture EM of high radius curvature structures on the membrane, such as tubes with DOTAP/DOPE, pits with DOTAP/MOG, short strands with DOTAP, revealed by freeze fracture electron microscopy. Complexes with relative smooth membranes such as DOTAP/DOPC have very little transfection activity. Supported by GM30969 (SWH) and DK46052(FCS).

Th-Pos380

EFFECTS OF HISTONE III-S AND DIOLEIN ON THE STRUCTURE OF LIPID BILAYERS. ((E.M. Goldberg[1], D.S. Lester[2], D.B. Borchardt[3], and R. Zidovetzki[1])) Departments of [1]Biology and [3]Chemistry, University of California, Riverside, CA 92521, and [2]FDA/CDER/DRT, Laurel, MD 20708.

The combined effects of protein kinase C (PKC) activator diolein and commonly used PKC substrate histone III-S on the structure of lipid bilayers composed of bovine liver phosphatidylcholine (PC) and dipalmitoylphosphatidylserine (DPPS) were studied using ^{2}H-NMR. Addition of either chain-perdeuterated dipalmitoylPC or DPPS allowed separate observation of the effects of diolein and histone III-S on either the PC or PS lipid component. In the absence of diolein, the addition of histone III-S at 1:5 (wt/wt) to PC/DPPS (4:1 mole/mole) bilayers resulted in an increase of the order parameters of the acyl side chains of the DPPS, but not the PC, lipid component. The addition of diolein alone (25 mole%) to the phospholipids resulted in the increased ordering of the acyl side chains of both PC and DPPS. The effects of histone III-S and diolein on the order parameters of PC and PS acyl chains were additive: significantly larger order parameter increase was observed with the PS component in the presence of both compounds. In addition nonbilayer lipid phases were observed when both diolein and histone III-S were present. Histone III-S is a commonly used substrate for in vitro PKC assays, and as the physical properties of bilayers have been shown to strongly affect PKC activity, the presence of large amounts of histone III-S in PKC activity assays may itself greatly affect the results of these assays.

Th-Pos381

THE DISSOCIATION RATES OF VERY LONG CHAIN FATTY ACIDS (VLCFA) FROM, AND FLIP-FLOP ACROSS, PHOSPHOLIPID BILAYERS ((Fengli Zhang and James A. Hamilton)) Department of Biophysics, Boston University School of Medicine, 80 East Concord Street, Boston, MA 02118.

The movements of fatty acids across membranes and between different membranes play important roles in biological functions. The dissociation and flip-flop rates of C20:0, C22:0 and C24:0 fatty acids in small unilamellar phosphatidylcholine vesicles (SUVs) were studied by a fluorescence method that measures pH changes inside the vesicles (Kamp and Hamilton, Proc. Natl. Acad. Sci. 1992, 89, 11367-11370). The flip-flop rates for all these VLCFA are very fast ($t_{1/2} < 1$ sec). The $t_{1/2}$ for dissociation of these VLCFA from SUVs were 20, 300 and 2300 seconds for C20:0, C22:0 and C24:0 respectively. The dissociation rate constants were not dependent on the concentration or nature (SUVs or bovine serum albumin) of the acceptor. These rate constants, together with those measured by other methods [C14:0, C16:0 and C18:0 by a stop-flow method (Daniels et. al. Biochemistry 1985, 24, 3286-3292) and C26:0 by an NMR method (Ho and Hamilton, unpublished)], showed a strong log linear relation with the chain length of the fatty acid. The dissociation rate constants for VLCFA are much lower than those for normal dietary fatty acids. For example, the rate constant for C24:0 is 10^4 smaller than that for C16:0. In peroxisomal disorders of VLCFA metabolism such as adrenoleukodystrophy, the accumulation of VLCFA in membranes could affect membrane structure and cell functions.

Th-Poe382

INDUCTION OF NON-BILAYER STRUCTURES IN DIACYLPHOSPHATIDYLCHOLINE MODEL MEMBRANES BY TRANSMEMBRANE α-HELICES. IMPORTANCE OF MISMATCH AND PROPOSED ROLE OF TRYPTOPHANS. ((J. A. Killian[a*], I. Salemink[a], D.V. Greathouse[b], R.E. Koeppe II[b])) [a]Dept. of Biochemistry of Membranes, University of Utrecht, Padualaan 8, 3584 CH Utrecht, The Netherlands and [b]Dept. of Chemistry and Biochemistry, University of Arkansas, Fayetteville, Arkansas 72701.

We have investigated the effect of different hydrophobic polypeptides on the phase behaviour of diacylphosphatidylcholines with varying length. The polypeptides are uncharged and consist of a sequence of alternating leucine and alanine, with variable length, and flanked on both sides by tryptophans. Circular dichroism measurements demonstrated that these peptides adopt an α-helical conformation with a transmembrane orientation. ^{31}P NMR measurements showed that incorporation of the peptides affects lipid phase organization depending on the difference in hydrophobic length between the peptide and the bilayer. When a 17 amino acid residue long peptide (WALP17) was incorporated, a bilayer was maintained in lipids containing acyl chains of 12 and 14 C-atoms, an isotropic phase was formed at 16 C-atoms, and an inverted hexagonal (H_{II}) phase at 18 and 20 C-atoms. For a 19 amino acid residue long peptide (WALP19) similar changes in lipid phase behaviour were observed, but at acyl chain lengths appr. 2 C-atoms longer. It is proposed that the tryptophans at both interfaces of the peptides are important for inducing the formation of non-bilayer structures by keeping the peptide from aggregating on a macroscopic scale upon increasing the mismatch.

Th-Poe383

EFFECT OF HELICES 1 AND 2 OF *BACILLUS THURINGIENSIS ISRAELENSIS* TOXIN ON THE ORGANIZATION OF PHOSPHOLIPID MEMBRANES ((R.M.Epand, R.F.Epand, E.Gazit, and Y.Shai)). McMaster University, Hamilton, ON L8N 3Z5 Canada, and Weizmann Institute of Science, Rehovot, 76100, Israel. (Spon. by P.K. Rangachari)

The *Bacillus thuringiensis var. israelensis* (Bti) pore forming cytolytic toxin contains four putative α-helical hydrophobic segments, two of which bind strongly to phospholipid membranes and can fold into an α-helical structure within the membrane [Gazit & Shai (1993) Biochemistry 32, 12363-12371]. These have been termed helix-1, which is slightly amphipathic and comprised of residues 50-71, and helix-2 which is highly amphipathic and corresponding to residues 110-131 [Ward, Ellar and Chilcott (1988) J. Mol. Biol. 202, 527-535]. Although the toxin is cytolytic, helix-2 is a class A and not a class L amphipathic helix known to characterize cytolytic polypeptides. To gain insight into the mode of action of the toxin we determined how each of these peptides affected the bilayer to hexagonal phase transition temperature (T_H), and how this property is related to its structure and organization in its membrane-bound state. This parameter has been shown to be useful in predicting how peptides will affect membrane stability. We found that while helix-2 slightly raises T_H, helix-1 is a strong promoter of the H_{II} phase and lowers T_H by 3,360 degrees/mol fraction of peptide. Interestingly, rearranging the sequence of helix-1 to an ideal amphipathic α-helix did not change its helicity (measured by CD) nor its mode of interaction with membranes. However, this rearrangement causes about a two-fold increase in the effectiveness of the peptide in lowering T_H.

Th-Poe384

AMPHIPATHIC PEPTIDE EFFECTS ON THE LATERAL DOMAIN ORGANIZATION OF LIPID BILAYERS. ((I.V.Polozov, [1]A.I.Polozova, [2]Yu.G.Molotkovsky, [3]G.M.Anantharamaiah, [3]J.P.Segrest and [1]R.M.Epand)) [1]Department of Biochemistry, McMaster University, 1200 Main St. W., Hamilton, ON, L8N 3Z5, [2]M.M. Shemyakin Institute of Bioorganic Chemistry, Russian Academy of Sciences, Moscow 117871, Russia, and [3]Depts. of Medicine and Biochemistry and the Atherosclerosis Research Unit, University of Alabama Medical Center, Birmingham, Alabama 35294

Lateral domain organization of biological membranes is thought to be of biological importance; however, the factors inducing such an organization are not yet completely understood. Using lipid-specific fluorescent probes we studied the effects of membrane active peptides on the lateral lipid segregation in model binary systems. Amphipathic peptides 18L and 18A feature the archetype sequences of the L- and A-type amphipathic α-helix according to a recent classification (Segrest et al., Proteins (1990) 8, 103-117). Because of their effect on the L_α-H_{II} phase transition, 18A and 18L have been designated as bilayer stabilizer and destabilizer respectively, and this property is attributed to difference in the ratio of the hydrophillic to hydrophobic volumes in the membrane active α-helical conformation. 18L posess a narrow positively charged hydrophillic region and a bulk hydrophobic volume, contrary to 18A with a narrower hydrophobic region and a wide surface of positively and negatively charged amino acid residues. We examined the possibility of the induction of lateral segregation of lipids due to a shape complementarity mechanism in DOPC:DOPE membranes. We found that shape compensation by itself is unable to induce lateral segregation. Thus effects of A and L type peptides in zwitterionic membranes are produced via the modulation of the properties of the membrane as a whole. A different situation was found in the case of acidic-zwitterionic lipid mixtures (PC:PG). 18L is cationic and 18A has positive charges at peptide-lipid interface, although overall it is zwitterionic. Both peptides were able to induce lipid segregation by preferential association with acidic lipids in fluid as well as in gel state membranes. Preferential association of peptides with acidic lipids was capable of modulating a pre-existing lateral organization of the membrane, i.e., in the course of the gel-liquid crystalline phase transition both peptides stabilized or destabilized the gel phase, depending on whether acidic lipids (PG) were the low or the high melting component. Contrary to what was found in acidic lipid-containing membranes, in the zwitterionic binary systems (PC:PE) both peptides associated with the fluid phase. Both peptides were actually unable to penetrate into the lipid membrane in the gel state, while binding with the high affinity to the fluid membranes. If trapped kinetically by cooling from the fluid phase, peptides dissociated from the gel membrane on the timescale of hours. Similar effect of both peptides with opposing biological activities on membrane lateral organization implies that these effects may take place with a number of other membrane active peptides.

Th-Poe385

CONFORMATION AND ORIENTATION OF ANTIMICROBIAL PEPTIDES IN LIPID BILAYERS. ((Amy Bankert, Janet Hammer and Jack Blazyk)) Chemistry Department, College of Osteopathic Medicine, Ohio University, Athens, Ohio 45701.

The molecular mechanism of magainins, a class of amphipathic cationic peptides with broad antimicrobial properties, remains unclear. Since these peptides selectively permeabilize the plasma membrane of target microorganisms at concentrations which have no effect on mammalian plasma membranes, their promise as clinically useful antibiotics is tangible. We are using FT-IR spectroscopy to determine how model amphipathic cationic peptides interact with lipid bilayers containing PC and/or PG in the presence or absence of cholesterol. Peptide A, $(KIAGKIA)_3$-NH_2, possesses much greater bactericidal potency than naturally-occurring magainins, yet remains nonhemolytic. Peptide B, identical to Peptide A except that alanine at position 7 is replaced by 3-fluoroalanine, is similar in antimicrobial activity. The more cationic Peptide C, $(KIAKKIA)_3$-NH_2, is an even better bactericidal agent. The effects of peptide binding on lipid fluidity are revealed by monitoring the position and width of the symmetric methylene C–H stretching band of the lipid acyl chains as a function of temperature. These peptides increase the phase transition temperature in the cholesterol-free lipid bilayers and cause phase separations in the cholesterol-containing lipid systems. Peptide conformation is evaluated by comparing the amide I' band of the peptides in different lipid environments. Using resolution enhancement, the broad amide I' band is resolved into a major component near 1650 cm^{-1} (associated with α-helical secondary structure) with a shoulder at ~1635 cm^{-1}. Conformational differences due to lipid composition and fluidity are noted among the three peptides. In addition, polarized attenuated total reflectance FT-IR experiments of the peptides in planar lipid multilayers attempt to compare the orientation of the α-helical axis with respect to the bilayer. These data provide some insight into the factors which determine the basis of selectivity between prokaryotic and eukaryotic plasma membranes.

Th-Poe386

COMPARATIVE STUDIES ON THE INTERACTIONS OF TRANSMENBRANE PEPTIDE ANALOGUES, $K_2L_{24}K_2$-AMIDE & $K_2LA)_{12}K_2$-AMIDE, WITH PHOSPHATIDYLETHANOLAMINE BILAYERS. ((Y-P Zhang, R.N.A.H. Lewis, R.S. Hodges & R.N. McElhaney)) Department of Biochemistry, University of Alberta, Edmonton, Alberta, Canada.

The interactions of two transmembrane peptide analogues, $K_2L_{24}K_2$-Amide (P_{24}) & $K_2(LA)_{12}K_2$-Amide [$(LA)_{12}$], with n-saturated phosphatidylethanolamines (PEs) (n=11-20) were studied by high sensitivity DSC and FTIR. Our FTIR results suggest that P_{24} forms predominantly α-helix under all conditions, whilst the conformation of $(LA)_{12}$ is more sensitive to lipid phase changes. In lipid fluid phaseS the amide I band of $(LA)_{12}$ is typical of predominant α-helix, but in the lipid gel phase the amide I band of $(LA)_{12}$ is significantly altered, due to either a strong distortion to the peptide α-helix or a major conformation change. DSC studies also indicate that both peptides broaden the gel/fluid phase transitions of all PEs and decrease the transition temperatures. However $(LA)_{12}$ is more perturbing of the thermodynamic properties of the host lipids than is P_{24}. We believe that such differences can be attributed to differences between the surfaces architectures of the peptides and to the fact that the conformation of $(LA)_{12}$ is more sensitive to the disposition of the lipids. These results, and our previous studies of these two peptides with PC bilayers, indicate that the interaction of even simple hydrophobic transmembrane peptides with lipid bilayers can span a broad spectrum of possibilities.

(Supported by the Medical Research Council of Canada and by the Alberta Heritage Foundation for Medical Research)

Th-Poe387

LOCALIZING MELANOTROPIC PEPTIDES IN PHOSPHOLIPID BILAYERS: SPIN LABEL AND FLUORESCENCE STUDIES. ((K.A. Riske, Z.S. Macêdo, M.H. Biaggi, T.A. Furquim, A.S. Ito and M.T. Lamy-Freund)) Inst. Física, Universidade de São Paulo, CP 20516, CEP 01452-990, SP, Brasil.

The present work studies the penetration depth of peptides in lipid membrane bilayers. Structural perturbations on the lipid phase caused by the linear tridecapeptide α-MSH (α-melanocyte-stimulating hormone), and the biologically more active peptide, the analog [Nle^4, $DPhe^7$]-α-MSH, were monitored by spin labels placed at the lipids head group and at different positions of the hydrocarbon chain. Correlation times and apparent order parameters were calculated from the spin labels ESR spectra. A comparison of the variations caused by the peptides on the above parameters of the different probes used, with those caused by other molecules, like cholesterol, carotenoids, integral and surface proteins, suggests that both peptides do penetrate the bilayer, and not just lie at its surface. Those results were corroborate by measurements of the peptides membrane penetration depth with the parallax fluorescence quenching method, using the single tryptophan residue present at position 9, and the same spin labels mentioned above as fluorescent quenchers. (Financial support: FAPESP, FINEP and CNPq.).

Th-Pos388

STRENGTH AND STABILITY OF MEMBRANE ANCHORAGE OF DIPRENYLATED AND S-ACYLATED PEPTIDES. ((Serge Shahinian and John R. Silvius)) Department of Biochemistry, McGill University, Montréal, Québec, Canada H3G 1Y6.

Various intracellular regulatory proteins of the rab, src, ras and other families can be modified with two acyl or isoprenyl chains, which appear to be required to target the modified proteins to specific cellular membrane compartments. A simple but untested model to explain this requirement postulates that a dual lipid modification serves to suppress spontaneous intermembrane exchange of the 'anchored' protein, allowing the protein to be retained for long times in a given membrane compartment once initially targeted there by the appropriate cellular machinery. To assess this possibility, we have examined the rates of spontaneous interbilayer transfer of various doubly lipid-modified peptides, with sequences and modifications reflecting those of naturally occurring proteins such as p21$^{H\text{-}ras}$, pp56^{lck} and rab3A. Our results indicate that the common 'dual-anchor' motifs myristoyl-GC(palmitoyl)X-, -C(palmitoyl)XC(farnesyl)-OMe and -C(geranylgeranyl)XC-(geranylgeranyl)-OMe could all serve to anchor modified proteins to a given membrane very tenaciously (halftime for spontaneous interbilayer exchange = tens of hours), consistent with the above model. However, our results suggest that another 'dual anchor' that may be found in certain rab and rab-homologous proteins, a terminal -C(geranylgeranyl)C(geranylgeranyl)-OH motif, may be more marginally well-suited to support protein targeting by the above mechanism. In a complementary study we have shown that a cysteine-linked palmitoyl (or related acyl) group constitutes the most lipophilic single modification of intracellular proteins yet identified, a finding consistent with the 'tenacious' membrane binding observed for dual-anchor motifs incorporating a long-chain S-acyl residue. (Supported by the MRC of Canada and les Fonds FCAR du Québec).

Th-Pos389

MUTUAL INTERACTION AMONG ANNEXIN VI, CALCIUM AND MEMBRANE STUDIED BY STOPPED-FLOW FAST KINETICS: EFFECT OF PHOSPHATIDYLETHANOLAMINE. ((Y.LU, M.D. Bazzi and G.L. Nelsestuen)), Department of Biochemistry, University of Minnesota, St.Paul, MN 55108.

Previous studies have shown that membranes containing the neutral phospholipid, phosphatidylethanolamine (PE) instead of phosphatidylcholine (PC) are much more effective in binding several proteins, including annexins to phospholipid bilayer surfaces that contain acidic phospholipids. Stopped-flow technique was used to examine the affects of PE vs. PC on the kinetics of annexin-membrane association, EGTA-induced protein dissociation, as well as quenching and dequenching of fluorescent-labeled acidic phospholipid, NBD-PA. In the presence of 1 mM calcium and at relatively low protein/phospholipid ratios, the binding of annexin VI to membranes was fast and appeared to be collision-limited. EGTA-induced protein dissociation was very rapid but dependent on the membrane composition. The presence of PE in membranes decreased the EGTA-induced protein dissociation rate. This rate may reflect the dissociation of calcium ions from the protein-calcium-membrane complexes. This slower dissociation rate for complexed calcium ions may be the underlying basis for earlier observations that PE in the membrane decreased the calcium required to support protein-membrane association. PE also slowed down both the fluorescence quenching and dequenching of NBD-PA as annexins bound or dissociated from the membrane. PE's effect on the fluorescence dequenching rate increased with PE content in the membrane continuously from 0% to 80%. These results suggested that PE might alter some aspect of phospholipid "microdiffusibility" in membranes. The mechanisms of the PE effects are unclear, but may be related to the formation of inter-phospholipid hydrogen-bonds. (Supported in part by grant GM38819 from the NIH).

CELL MEMBRANES II

Th-Pos390

PROBING THE CONFORMATION OF LACTOSE PERMEASE IN NATIVE MEMBRANES. S. Frillingos and H.R. Kaback, HHMI/UCLA, Los Angeles, CA 90024.

Lactose permease of *E. coli* has 12 transmembrane-domains and catalyzes H^+/β-gal symport. Recently, a model was presented describing the packing of helices in the C-terminal half of the permease [Jung, K. et al. (1993) *Biochemistry 32*, 12273], and evidence for ligand-induced conformational changes was documented [Jung, K. et al. (1994) *Biochemistry 33*, 3980; Jung, H. et al. (1994) *Protein Science 3*, 1052; Wu, J., & Kaback, H.R. (1994) *Biochemistry*, in press]. These studies utilize purified permeases containing one or two Cys residues and site-directed fluorescence spectroscopy. We now describe a novel assay that probes the reactivity of single-Cys permeases in the native membrane. Single-Cys permease containing a biotin acceptor domain is expressed, and membranes are prepared. The membranes are treated with [^{14}C]N-ethylmaleimide in the absence or presence of a high-affinity ligand, solubilized with dodecylmaltoside, and the permease is purified by avidin affinity chromatography. Labeling is then quantitated after SDS/PAGE by phosphorimaging. Control experiments demonstrate that ligand blocks Cys148 (helix V) and enhances the reactivity of V315C (helix X) permease in agreement with transport data and fluorescence measurements. The reactivity of P31C (helix I) is greatly enhanced in the presence of ligand. A similar but less striking effect is observed for P28C, which lies on the same face of the helix, while reactivity of P29C or P30C, on the opposite face, is marginal and unaffected by ligand. Using oriented membrane vesicles, it should be possible to determine the accessibility of any site-directed Cys residue from either side of the membrane.

Th-Pos391

DESIGN OF MACROMOLECULES TO CROSS BIOLOGICAL MEMBRANES. STEP 1: BINDING INTO MEMBRANE LIPID. ((G. Krishnan, R. D. MacGregor, S. B. Shohet, and C. A. Hunt)) School of Pharmacy, University of California, San Francisco, CA 94143.

Can macromolecules be delivered directly through the plasma membrane into the cytoplasm? Apocytochrome c (Apo c) binds to specific sites on mitochondria and equilibrates across the outer mitochondrial membrane. To determine whether this observation might be applicable to other macromolecule-membrane systems, we characterized the binding of Apo c to a different biological membrane system, red blood cells (RBC), and also characterized the binding of other macromolecules to RBC. We demonstrate that our data is consistent with the hypotheses that macromolecules can bind into membrane lipid, and that the number of lipid binding sites are determined both by the geometry of the membrane skeleton and by the aggregation properties of the macromolecule being bound. The similarity in Apo c binding to different biological membranes, and the similarity in binding of different macromolecules to RBC, suggests that characteristics can be included in the design of macromolecules which will facilitate their passage through cell membranes. Supported by ONR grant N00014-91-J-1455.

Th-Pos392

SELECTIVE AND ASYMMETRIC MOLECULAR TRANSPORT ACROSS ELECTROPORATED CELL MEMBRANES. ((Ephrem Tekle, R. D. Astumian, and P. B. Chock)) NHLBI, NIH, Bethesda, MD. 20892 and University of Chicago, Chicago, IL 60637.

Transport of a divalent cation (Ca^{+2}) and three DNA indicators (Ethidium Bromide (EB), Propidium Iodide (PI), and Ethidium Homodimer (EthD-1)) across electroporated membranes of several mammalian cell lines was found to be selective and asymmetrical. In low salt medium, Ca^{+2} and EB preferentially transported across the anode facing cell membrane while PI and EthD-1 predominately entered at the site facing the cathode. In high salt medium, the entry site for Ca^{+2} and EB was reversed to the cathode facing hemisphere while it remained unchanged for PI and EthD-1. In all these experiments, the observed transport patterns remained unaffected whether the dyes (or ion) were present during or added after the electroporating pulse. The data suggest asymmetric pores are created on both sides of the membrane facing the electrodes with smaller pore size (but higher in number) on the anode side and larger pores (with lower population) on the cathode side. Furthermore, the rate of resealing of the membrane pores is significantly enhanced in high ionic strength medium, thus, affecting the entry site. The observed asymmetric transport pattern is neither caused by electrophoresis induced by the externally applied electric field nor is it due to one-sided membrane breakdown as previously believed.

Th-Pos393

CELL FISSION AND FORMATION OF MINI CELLS BY ALTERNATING ELECTRIC FIELD. ((P. Marszalek[1] and T.Y. Tsong[2])) [1]Dept of Biochem, Univ of Minnesota, and [2]Dept of Biochem, Hong Kong Univ of Sci & Technol, Clear Water Bay, Kowloon, Hong Kong (Spon. by N.T. Yu).

High frequency alternating electric fields can produce many biochemical and morphological changes of cells in suspension. One of these effects is the transient shape deformation due to the strong shear stress experienced by a cell. We have used this effect of electric fields to induce budding of membrane vesicles and cell fission in sea urchin eggs. Several mini-cell bodies can be prepared from a single egg by carefully manipulating the frequency and the amplitude of the AC field, and the ratio between the inter-electrode spacing and the cell diameter, α. In a typical experiment, a sea urchin egg (diameter 75μm), suspended in a low ionic medium (conductance < 2mS/m), was located under the microscope between two platinum wire electrodes, separated by a distance of 200 μm. A medium AC field (2 MHz) was applied to attract the egg to one of the two electrodes via dielectrophoresis. The voltage was then slowly increased to approximately 1 kV/cm. The cell began to elongate and separated into two fragments, the larger one containing the nucleus. When the field was turned off, the mother cell and the daughter vesicle retracted to form spherical mini-cell bodies, which appeared to be stable - there was no colloidal osmotic swelling. This procedure could be repeated a few times to make several mini-cell bodies from a single egg. With practice, several mini-cell bodies can be made in a single fission. These procedures may be used to prepare mini-membrane vesicles for voltage clamp experiments, or to perform micro-surgical manipulation of cells, embryos, or chromosomes.

Th-Pos394

RECONSTITUTION OF SARCOLEMMAL INTEGRITY AND OF CONTRACTILITY FOLLOWING MECHANICAL INJURY IN STRIATED MUSCLE CELLS ((Monika Rozycka and Hugo Gonzalez-Serratos)) Department of Biophysics, University of Maryland, School of Medicine, Baltimore, Maryland 21201

The lipids of the sarcolemma are composed of 48% phospholipids, the main component of which is phosphatidylcholine, or lecithin. Since striated muscles deteriorate quickly after the sarcolemma brakes following mechanical damage, we are investigating whether such injuries can be reversed and repaired by providing the cells with phosphatidylcholine. The experiments were performed in single muscle cells isolated from the tibialis anterior or semitendinosus muscles of the frog, Rana pipiens. The membrane was damaged by either braking it by sucking through a 30 μm diameter pipet, pulling connective tissue attached to it, or touching it with a platinum electrode and passing electric current with 40 V pulses. Following mechanical injury, which was accompanied by a contracture and braking of the membrane, the cells were either left in the same solution or were bathed with a 35 mM lecithin Ringer solution. The recovery of either shortening or tension development during electric stimulation, and the integrity of the sarcolemma at the light microscopic level, were studied. In the presence of lecithin, the cells first responded with local twitches, while the membrane remained broken. Within 0.5 h, contractility and membrane damage started to recover; within 3 hours, tension development and integrity of the membrane were back to control levels. When this cells were placed again in normal Ringer, they remained viable and active for several hours. If the damaged cells remained in Ringer without lecithin, they stopped contracting and were completely destroyed within one hour. Our results suggest that lecithin can protect muscle fibers from the effects of sarcolemmal damage. Supported by NIH grant NS17048.

Th-Pos395

ALTERATION OF A_7r_5 AORTIC SMOOTH MUSCLE SARCOLEMMAL FLUIDITY DEPRESSES $^{45}Ca^{2+}$ INFLUX. ((M.R. Samardzija, R.C. Aloia, R.G. Hall, Jr. and R.R. Gonzalez, Jr.)) Department of Physiology and Pharmacology, School of Medicine, Loma Linda University, Loma Linda, CA 92350 and Anesthesiology Service, J.L. Pettis Memorial V.A. Hospital, Loma Linda, CA 92357. (Spon. by J.M. Tosk)

We observed that pentobarbital sodium (PB) attenuates the tonic but not the phasic component of contraction in vascular smooth muscle (VSM), implying that PB interferes with extracellular influx and not intracellular release of Ca^{2+}. Since PB is thought to increase artificial monolayer and nerve membrane fluidity, we examined $^{45}Ca^{2+}$ influx as a function of altered membrane fluidity in A_7r_5 (embryonic rat aortic) VSM cells. Fluidity was increased by treatment with docosahexaenoic acid (22:6), a polyunsaturated fatty acid (PUFA), as a comparison to the effect of PB incubation (30 μM, 20 min). PUFA and/or PB treatment had no effect on transient $^{45}Ca^{2+}$ influx in resting cells over a range of temperatures (32, 34.5, 37, 39.5, 41°C). However, PUFA treatment, in cells depolarized with 55 mM KCl in HEPES buffered (pH 7.4) physiologic saline solution, decreased $^{45}Ca^{2+}$ influx by 50% over the same temperature range. Incubation with PB, also decreased $^{45}Ca^{2+}$ influx in a similar fashion. When PUFA treated cells were incubated with PB, we observed an additive inhibitory effect. PUFA and PB treatment decreased $^{45}Ca^{2+}$ influx in VSM cells in a comparable manner, suggesting that PB may increase membrane fluidity.

Th-Pos396

AMINOGLYCOSIDE NEPHROTOXICITY AND PHOSPHOLIPIDOSIS. ((D. Carrier*, P. Eid*, N. Chartrand*, M.G. Bergeron# and D. Beauchamp#)) *University of Ottawa, Ottawa, Canada K1H 8M5 and #Centre Hospitalier de l'Université Laval, Quebec City, Canada G1V 4G2. (Spon. by H.C. Jarrell)

Aminoglycosides are clinically used, very potent antibiotics that may also lead to acute renal failure. Efforts are devoted to unravel the exact mechanism of this complication. Our infrared spectroscopic data indicate that the binding of these oligocationic drugs to negatively charged phospholipids, which are believed to be their receptors on kidney cell membranes, results in a decrease of the fluidity of the hydrophobic core. The degree of order of the bilayers can be restored by some inhibitors of the nephrotoxicity, like the lipopeptide daptomycin. Our hypothesis is that aminoglycosides interfere with the action of phospholipases in the lysosomes of kidney proximal tubules, inducing the formation of myeloid bodies. The effect of various aminoglycosides on phospholipase A2 activity is presented and correlated with their nephrotoxic potential. The action of nephrotoxicity inhibitors is also discussed.

Th-Pos397

CELL DIELECTRIC PHENOTYPE DETERMINED FROM ELECTROKINETIC STUDIES. ((P.R.C. Gascoyne, Y. Huang, X-B. Wang and F. F. Becker)) Box 89, UT M.D. Anderson Cancer Center, 1515 Holcombe Blvd., Houston TX 77030.

Cells subjected to an AC electric field exhibit various kinetic behaviors that depend on the nature of the field. Non-uniform fields induce cell dielectrophoretic translation (which include conventional dielectrophoresis in a spatially inhomogenous field and travelling wave dielectrophoresis in a temporally inhomogenous field); rotating fields cause cell electrorotation. The frequency dependency of these electrokinetic phenomena reflects the dielectric properties of the particular cell under investigation. These properties are determined by the cell structure and composition, and these, in turn, are closely associated with the cell type and its physiological state. We introduce here the concept that the frequency dependency of the electrokinetic properties constitutes a *dielectric phenotype* for the cell. Experimental data and a theoretical analysis are presented to support this concept. We illustrate characteristic electrorotation spectra for a variety of cell types (e.g. erythrocytes, lymphocytes, erythroleukemia and human breast cancer cells) and demonstrate the roles that membrane morphology, cytoplasmic organelles and nuclear properties play in defining the dielectric phenotype. We show that the specific capacitance of the plasma membrane can range from 8 to at least 100 mF/m^2, that the dielectric phenotype of hepatocytes includes a major contribution from internal organeles, and that the ratio of nuclear to cytoplasmic volume determines the nuclear dielectric contribution. Effects of cell physiological changes caused by cellular differentiation, mitotic stimulation, and cell activation and environmental stress on the dielectric phenotype are also illustrated.

Th-Pos398

ARE BIOPHYSICAL PROPERTIES OF TROUT SPERMATOZOAN PLASMA MEMBRANE INVOLVED IN SPERM ABILITY TO WITHSTAND TEMPERATURE STRESS. ((C.Labbe[1], G.Maisse[1], K.Muller[2], A.Zachowski[2], J.H.Crowe[3])). [1]INRA, Rennes, France;[2]IBPC, Paris, France; [3]Section Mol. Cell. Biol., UCDavis, USA (spon. by M.Wilson)

The effect of a 2 year period of adaptation to 8°C or 18°C was analyzed on rainbow trout sperm. As assessed by EPR at a given temperature and using spin labelled phospholipids, we did not observe any difference in plasma membrane (PM) fluidity regardless of the rearing temperature of the fish. Phospholipid fatty acids of the PM were only slightly modified by the adaptation temperature. This lead us to propose that trout spermatozoan PM may not display any homeoviscous adaptation. In another experiment, *in vitro* incubation temperature of spermatozoa was shown to greatly modify PM fluidity. However, it does not seem to have any influence neither on sperm function as displayed by the unmodified motility of this sperm nor on its ability to withstand freeze-thawing. FTIR studies were conducted on purified PMs and on liposomes made with the PM phospholipids. In both cases, the phase transition of the lipids was observed along a broad range of temperature. No plateau in CH_2 frequency was reached above the freezing point of the medium (-10°C). We conclude that the absence of an abrupt phase transition of the PM lipids might explain why trout spermatozoan PM does not exhibit homeoviscous adaptation in response to change in environmental temperature and why this cell is so unaffected by the surrounding temperature *in vitro*. (Supported by the Institut National de la Recherche Agronomique, France and by grants IBN 93-08581 from NSF and NOOO 14-94-1 from ONR)

Th-Pos399

THE MEMBRANE DYNAMICS OF *Escherichia coli* CELLS IS DEPENDENT ON THEIR PHYSIOLOGICAL STATE. ((I. Fishov, Z. Binenbaum, A.H. Parola and A. Zaritsky)) Ben-Gurion University of the Negev, P.O. Box 653, Be'er-Sheva 84105, Israel.

Temperature dependence of enzyme activities and parameters of paramagnetic membrane probes suggest that physically separate lipid domains of different fluidity and composition exist in a bacterial membrane. Specific lipid domains, formed by DNA-membrane interactions, were proposed to be involved in regulation of DNA replication and segregation and cell division. Here, polarisation of 1,3-diphenyl-1,3,5-hexatriene (DPH) fluorescence was used as a measure of membrane viscosity in bacteria *Escherichia coli* when their steady-state growth rate was modulated by different carbon sources or by changing the availability of a single carbon source. α-Methylglucoside (α-MG) was employed for competitive inhibition of glucose uptake. Membrane viscosity appeared to be independent on the α-MG-modulated growth rate, in contrast with the different carbon source case. A transient fall in polarisation was observed during the nutritional shift down achieved by addition of α-MG to the steady-state glucose growing culture. These polarisation changes are correlated in time with cell shape rearrangement during the same transition. The interrelation of the bacterial cell shape and its membrane viscosity at a constant growth rate was tested by low concentrations of penicillin-G (long cells) or mecillinam (spherical cells) treatments. The large difference in membrane viscosity between two extreme situations - fully initiated DNA (in presence of nalidixic acid) and condensed, terminated DNA without replication forks (chloramphenicol treatment) - indicates that DNA-membrane interaction leads to formation of highly ordered membrane domains. It is clear from these data that the membrane dynamics is reflecting structural as well as functional changes of bacterial cells.

Th-Pos400

THE MOSAIC STRUCTURE OF CELL MEMBRANES REVEALED BY TRANSIENT CONFINEMENT OF GPI-LINKED NCAM-125. ((R.Simson*, B.Yang*, P.Doherty†, S.Moore†, F.Walsh†, K.Jacobson*)). * Dept.,Cell Biol. and Anat., UNC-CH, N.C. 27599. † Dept.,Exp. Path., UMDS, Guy's Hosp., London SE1 9RT, UK.

Single particle tracking (SPT) provides a unique opportunity to monitor movements of single membrane proteins. Deviations in the protein motion from random behaviour may reveal interactions with other membrane components. We examined different isoforms of neural cell adhesion molecules (NCAM) in both 3T3 fibroblasts and C2C12 muscle cells, using colloidal gold to mark single proteins. Software was developed to separate random behaviour from motion that arises from interactions in the plasma membrane. About 28% of the population of a GPI linked NCAM isoform in muscle cells showed a mixture of confined and random diffusion, where the temporary confinement, in zones of approximately 300nm in diameter, lasted on average for 6 sec. before escape. The remaining unconfined NCAM were separated into a fast and an exteremly slow diffusing class. In a comparison with random behaviour the same software detected periods of confined diffusion in only 0.8% of simulated trajectories. Analysis of the NCAM diffusion mode indicates anomalous diffusion within confinement zones and for the observed slow proteins, suggesting areas of the membrane with a high concentration of immobile obstacles. Diffusion outside of confinement zones and for the unconfined proteins was normal, indicating regions with a low obstacle concentration. A mosaic structure of the membrane, consisting of randomly distributed regions with high and low obstacle concentrations could account for all observed diffusion modes. Supported by NIH GM 41402.

Th-Pos401

EARLY AFTERDEPOLARIZATIONS INDUCED BY E-4031 IN SINGLE RABBIT VENTRICULAR MYOCYTES ((Z. Zhou, C. Studenik and C. T. January)) Dept. of Medicine. University of Chicago, Chicago, IL 60637.

The experimental antiarrhythmic drug, E-4031, which blocks delayed rectifier potassium channels, has been reported to induce the polymorphic ventricular arrhythmia torsades de pointes in rabbits, and in cardiac muscle it increases action potential duration and induces early afterdepolarizations (EADs). We studied properties of E-4031 induced EADs in single rabbit ventricular myocytes. We used the amphotericin perforated patch method to record action potentials and cell shortening was monitored using an edge detector. E-4031 (10-200 nM) prolonged action potential duration and induced EADs in 16 of 17 myocytes. EADs were abolished by washout of E-4031 and could be reproduced by repeated application of E-4031. E-4031 induced plateau-type EADs with take-off potentials between -5 and -25 mV, and amplitudes up to 35 mV. A steep inverse relationship existed between EAD peak voltage and its take-off potential, and with large amplitude EADs small aftercontractions were observed. To study the role of intracellular Ca^{2+} in E-4031 induced EADs, cell contraction was abolished by BAPTA-AM (100 μM, n = 3) or thapsigargin (5 μM, n = 2). Under these conditions, E-4031 induced EADs were not blocked. In contrast, nifedipine (1 μM, n = 3) inhibited E-4031 induced EADs and shortened action potential duration. We conclude that, 1) the amphotericin perforated patch technique permits stable recordings of action potentials, EADs and cell contraction in isolated myocytes, 2) E-4031 induces characteristic plateau-type EADs, and 3) changes in intracellular Ca^{2+} are not essential in E-4031 induced EADs. Our results may suggest a central role for L-type Ca^{2+} channels in E-4031 induced EADs.

DIVERSE TRANSPORTERS AND EXCHANGERS

Th-Pos402

ELECTROSTATIC INTERACTIONS IN THE Na^+/GLUCOSE COTRANSPORTER SGLT1 ((Mariana Panayotova-Heiermann, Donald D F Loo, and Ernest M Wright)) UCLA School of Medicine, Department of Physiology, Los Angeles CA 90024-1751 (Spon. by Earl Homsher)

Electrostatic interactions are thought to play an important role in determining protein folding in transmembrane proteins. In the rabbit Na^+/glucose cotransporter SGLT1 we mutated the four conserved charged residues in putative transmembrane domains, ie Glu255 on M5, Asp273 on M6, Lys321 on M7 and Arg427 on M9; these were each replaced with Ala. The mutants were expressed in *Xenopus* oocytes and the two-electrode voltage-clamp was used to measure functional expression. Mutant E225A showed no changes in expression and steady-state kinetics. There was no detectable expression of mutants K321A and R427A. D273A showed a dramatic decrease in the ability to transport sugar, with $K_{0.5}^{\alpha MG} > 40$ mM. We conclude that the residues D273, K321 and R427, but not E255, are each situated within the membrane. The decrease in functional expression was due to a reduction of electrostatic interaction within the hydrophobic core. We are currently identifying the residues involved in electrostatic interaction by complementation analysis. Supported by NIH grant DK44602.

Th-Pos403

KINETICS OF Na^+/GLUCOSE COTRANSPORT MEDIATED BY SGLT2 ((Bryan Mackenzie, Donald D F Loo, Mariana Panayotova-Heiermann, and Ernest M Wright)) UCLA School of Medicine, Department of Physiology, Los Angeles CA 90024-1751 (Spon. by J McD Tormey)

Renal glucose re-absorption is mediated by two Na^+-dependent transporters with discrete substrate affinities and loci in the proximal tubule. We investigated the characteristics of SGLT2 (*J Biol Chem* **269**, 22488), a low affinity glucose transporter cloned from pig kidney, using two-microelectrode voltage-clamp in cRNA-injected *Xenopus* oocytes. We determined α-methyl-D-glucopyranoside (αMG) and Na^+ kinetic parameters as a function of external Na^+ and αMG concentrations. At all voltages (V_m) from −50 to −150 mV the affinity for αMG was reduced with diminishing external [Na^+]: eg, at −70 mV, $K_{0.5}^{\alpha MG}$ was 3 ± 0.5 mM at 100 mM Na^+, rising steeply below 10 mM Na^+, to 32 ± 7 mM at 1 mM Na^+. We observed a similar relationship for $K_{0.5}^{Na}$ as a function of $[\alpha MG]_o$. The maximal αMG-evoked current ($I_{max}^{\alpha MG}$) was independent of $[Na^+]_o$ whereas, at each V_m tested, I_{max}^{Na} fell by 70-80% as $[\alpha MG]_o$ was reduced from 50 to 1 mM. These data are consistent with an ordered, simultaneous transport model in which Na^+ binds first. Li^+ and H^+ can substitute for Na^+, more effectively at V_m −110 to −150 mV. In the absence of αMG, we observed Na^+-dependent pre-steady-state charge movements which were abolished by phlorizin. Thus SGLT2 and SGLT1 operate by a similar mechanism despite divergent sugar and Na^+ affinities and apparent Na^+/glucose stoichiometries. Supported by NIH grant DK19567; BM is a Research Fellow of the Human Frontier Science Program.

Th-Pos404

STOICHIOMETRY OF THE Na^+/Cl^-/TAURINE COTRANSPORTER (Donald D F Loo, Kathryn Boorer, Hemanta K Sarkar, and Ernest M Wright)) Dept of Physiology, UCLA School of Medicine, Los Angeles, CA 90024-1751 and Dept of Molecular Physiology and Biophysics, Baylor College of Medicine, Houston, Tx, 77030

Taurine is the major free amino acid in many tissues and has been hypothesized to serve as a neurotransmitter and osmolyte. Taurine is transported into cells using the Na^+ and Cl^- -dependent taurine transporter. To directly determine the stoichiometry of electrogenic taurine transport we have measured the uptake of [^{3}H]taurine under voltage clamp conditions in Xenopus oocytes expressing the Na^+/Cl^-/taurine cotransporter cloned from mouse retina (Sarkar et al, Invest. Opth. Vis. Sci 35:1491). With the membrane held at -70 mV, addition of 14 μM [^{3}H]taurine to the bath solution (100 mM NaCl buffer) generated an inward current (≈ 60 nA). The integral of the current over a 10 min period was compared to [^{3}H]taurine uptake. The ratio of the total charge transferred to the [^{3}H]taurine influx was ca. 10. In contrast, the Hill coefficient for Na^+ activation of taurine transport from electrophysiological analysis was approximately 2. Thus there is a discrepancy between flux and electrophysiological determinations of stoichiometry. This discrepancy indicates that besides Na^+, there is another ionic component, possibly Cl^-, in the current generated by taurine.
Supported by NIH grant NS2554.

Th-Pos405

AN OXONOL DYE IS A MORE POTENT INHIBITOR OF RED CELL BAND 3-MEDIATED ANION EXCHANGE THAN DIDS. ((P.A. Knauf, F.-Y. Law, and K. Hahn*)) Dept. of Biophysics, Univ. of Rochester Sch. of Med., Rochester, NY 14642 and *Div. of Virology, Dept. of Neuropharmacology, Scripps Research Inst., LaJolla, CA 92037

When cells are acutely exposed to the oxonol dye diBA (bis(1,3-dibutylbarbituric acid)pentamethine oxonol) at 0°C in a 150 mM Cl^- medium, the IC_{50} (concentration that gives half-inhibition of Cl^- exchange) is 146 ± 14 nM (n = 11), but inhibition increases with time. If cells are first pretreated with diBA for 10 min at 0°C and if diBA is also added to the flux medium, the IC_{50} is only 1.1 ± 0.2 nM. diBA is thus a more potent inhibitor than DIDS (4,4'-diisothiocyano-2,2'-stilbene disulfonate), for which the reported IC_{50} under similar conditions is 31 ± 6 nM (Janas et al., Am.J.Physiol. 257:C601, 1989). DiBA binds in 2 steps to band 3: an initial rapid binding is followed by a slow conformational change which increases the affinity. At 0°C, this second step is very slowly reversible, with $t_{1/2}$ > 50 h. In contrast to DIDS, the inhibitory effect of diBA does not decrease with increasing Cl^- concentration, indicating that diBA is a noncompetitive inhibitor. Analogues of diBA also strongly inhibit anion exchange. Thus, at least some of the oxonol dyes, which are commonly used to determine membrane potential, may have dramatic effects on anion transport. This may affect their ability to measure membrane potential reliably, but it suggests that they may be very useful probes for anion transport systems. (Supp. by NIH grants DK-27495, *AI-34929, *AI-09484 and *NS-12428)

Th-Pos406

LIGAND-GATED CHLORIDE CONDUCTANCE ASSOCIATED WITH A HUMAN GLUTAMATE TRANSPORTER

((J.I. Wadiche, R.J. Vandenberg, J.L. Arriza, S.G. Amara, and M.P. Kavanaugh)) Vollum Institute, Oregon Health Sciences University Portland, OR 97201. (Spon. by E.W. McCleskey)

Multiple clones encoding glutamate transporters have been isolated from a human brain cDNA library and expressed in *Xenopus* oocytes (Arriza et al. *J. Neuroscience* 14:5559 1994). All of the transporters mediate uptake of radiolabeled glutamate. In addition, they mediate strongly rectifying inward currents under voltage clamp in response to application of glutamate and analogs including D-aspartate and L-*trans*-pyrrolidine-2,4-dicarboxylic acid. The isoforms exhibited differences in the degree of rectification, however. Currents recorded during voltage pulses before and during application of glutamate showed that EAAT1, a cerebellum-specific isoform, mediated significant glutamate-dependent outward current at depolarized potentials. This outward current was not likely to be due to reverse transport of accumulated glutamate because it was also observed in response to the first application of substrate when the membrane was clamped at depolarized potentials (>0 mV). In addition, the reversal potential of the current was shifted 54±2 mV per 10-fold change in $[Cl^-]_o$, strongly suggesting that EAAT1 mediates a ligand-gated chloride conductance increase in addition to its transport function. The outward current induced by application of 1mM D-aspartate was not reduced by coapplication of 1 mM SITS, a concentration which strongly inhibits endogenous chloride channels. These results suggest the possibility that a glutamate transporter can serve a dual role as an intrinsic ligand-gated chloride channel.

Th-Pos407

A CONSERVED GLUTAMATE PLAYS A KEY ROLE IN ION SELECTIVITY AND TRANSPORT OF THE ANION EXCHANGERS AE1 AND AE2

I. Sekler, R.S. Lo and R.R. Kopito)) Department of Biological Sciences, Stanford University, Stanford, California 94305-5020, U.S.A.

The anion exchanger AE1 (band 3) serves as an important model for structure function studies of ion transporters. However, little is known about the role of specific residues participating in the anion transport mechanism or selectivity. Glutamate 699(E699) in AE1, is accessible and reactive with the membrane impermeable carboxyl-reagent, Woodward's reagent K applied, from the extracellular side, and is absolutely conserved among all anion exchangers sequenced so far. Thus this glutamate has been suggested to be a part of or near the pearmeation pore of the exchanger. We replaced E 699 of AE1 and the corresoponding glutamate (E1007) of the closely related anion exchanger AE2 with non polar or basic amino acid residues. Divalent (sulfate) and monovalent (chloride and bicarbonate) anion transport mediated by the wild type or mutant anion exchanger were examined in reconstituted proteoliposomes or whole cells. The rate of sulfate transport in wild type AE1 and AE2 or the mutants measured in proteoliposomes derived by freeze-thaw reconstitution was indistinguishable. Monovalent Cl^-/Cl^- or Cl^-/HCO_3 exchange was undetectabled in cells expressing AE2 (R or A 1007) mutants. The steep pH dependance for sulfate/sulfate exchange attributed to the proton co-transport process and characteristic at AE1 and AE2 proteoliposomes was largely abolished by the apolar or positively charged mutations. These data suggest that this glutamate residue plays a dual role in determining anion selectivity, and in proton coupling to sulfate transport.

Th-Pos408

MOLECULAR MODELING OF BAND 3, THE ERYTHROCYTE ANION EXCHANGER.

((Reinhart A.F. Reithmeier and Shek Ling Chan)) MRC Group in Membrane Biology, Department of Medicine and Department of Biochemistry, University of Toronto, Toronto, Ontario, Canada, M5S 1A8.

Band 3 is a member of a multi-gene family responsible for the exchange of anions across biological membranes. The membrane domain of the protein contains 14 potential transmembrane segments which come together to form a transmembrane channel. The available pool of exchanger amino acid sequences were analyzed for the following features: hydrophobic segments sufficiently long (21 residues) to span a lipid bilayer, tetra-peptide sequences containing a high reverse turn probability, sequence conservation and amphipathic helices. Potential helix N-cap and C-cap residues and helix initiation motifs were identified. Well-defined transmembrane segments were modeled as classical α-helices (ϕ, ψ = -57°, -47°) using CHARMm 22 and individual segments were energy minimized. The interaction between successive pairs of transmembrane helices were then modeled generating an ensemble of dimeric models. The contact of DIDS covalently attached to lysine 539 with helix 5 was also characterized. An improved folding model is presented. (Supported by the Medical Research Council of Canada).

Th-Pos409

DIFFERENTIAL ALLOSTERIC MODULATION OF HUMAN GLUTAMATE TRANSPORTER ISOFORMS BY ARACHIDONIC ACID

((N. Zerangue, S.G. Amara, and M.P. Kavanaugh))
Vollum Institute, Oregon Health Sciences University, Portland, Or 97201

Arachidonic acid is released during glutamatergic synaptic transmission by activation of postsynaptic glutamate receptors. Three glutamate transporters (EAAT1-3; Arriza et al. *J. Neuroscience* 14:5559 1994) cloned from a human motor cortex library were expressed in *Xenopus* oocytes and HEK-293 cells and the effect of arachidonate on transport kinetics was investigated. Arachidonate inhibited both uptake of [^{3}H]L-glutamate and transport currents mediated by EAAT1, a presumed glial transporter isoform. This inhibition occured by a 20-25% reduction in the transport V_{max}. In contrast, arachidonate increased glutamate transport mediated by EAAT2, another glial isoform, up to 2.5-fold by reducing its apparent affinity constant for glutamate. Arachidonate caused slight increases in transport mediated by EAAT3, a presumed neuronal isoform. The effects of arachidonate on the transport currents occured rapidly, were dose-dependent and saturable (EC_{50} 16-71 μM), and appeared to be mediated directly rather than by metabolites of arachidonate. This is the first report of arachidonate-mediated activation of glutamate uptake. Heterogeneity in the response of different transporter isoforms to arachidonate suggests the possibility for complex regulation of glutamatergic synaptic transmission via positive- or negative-feedback according to the transporter isoform(s) present in a particular synapse.

Th-Pos410

STUDY OF A RENAL AMINO ACID EXCHANGER USING INTERNALLY PERFUSED OOCYTES.

((X.Z. Chen, M.J. Coady and J.-Y. Lapointe)) Université de Montréal, Montréal, Canada, H3C 3J7. (Spon. by R. Laprade)

The mechanism for cystine reabsorption by renal proximal tubules and its interaction with other amino acids are not well understood. rBAT, a single transmembrane domain protein present in brush border membranes of proximal straight tubules, is inactive in patients suffering cystinurea. Normal rBAT expressed in *Xenopus laevis* oocytes increases the uptake of cystine and several neutral and positively charged amino acids in a Na-, K- and Cl-independent manner. Our rBAT clone, isolated from a rabbit renal cDNA library, generated an outward current upon external addition of alanine (the limited solubility of cystine prevents its use in electrophysiological experiments) which suggests that rBAT can mediate the exchange of a neutral for a charged amino acid. In direct support of this hypothesis, using the cut-open oocyte technique (Taglialatela et al 1992 Biophys J.61:78), external addition of 5 mM alanine generates a voltage-dependent outward current (31.7 ± 7.4 nA at 0 mV) only if a positively charged amino acid (.5mM arginine) is present in the cytosolic compartment. Conversely, external addition of .5 mM arginine generates a voltage dependent inward current (17.2 ± 2.5 nA at -60 mV) only in the presence of an intracellular neutral amino acid (5mM alanine). Comparison of arginine dependent currents with ^{14}C arginine uptakes in intact oocytes indicates that only 14% of the arginine entering the cell generates the uptake of a net positive charge (charged for neutral amino acid exchange) while the major portion of the arginine uptake is in exchange for another charged amino acid. The property of rBAT to function as an amino acid exchanger with a wide selectivity of substrates sheds some light on the problem of understanding the details of renal cystine reabsorption.

Th-Pos411

OVEREXPRESSION AND FUNCTIONAL RECONSTITUTION OF THE TRICARBOXYLATE TRANSPORT PROTEIN FROM RAT LIVER MITOCHONDRIA.

((Y. Xu, J.A. Mayor, D.A. Gremse, and R.S. Kaplan)) Dept. of Pharmacology, Univ. of South Alabama Coll. of Med., Mobile, AL 36688.

The cDNA encoding the mature form of the rat liver mitochondrial tricarboxylate transport protein (i.e., citrate transport protein (CTP)) has been amplified by PCR and subcloned into both the pET-21a(+) and the pET-28a(+) plasmids. These plasmids direct expression of CTP containing either 1 additional amino terminal methionine (pET-21a(+)) or a 21 residue amino terminal leader sequence that contains a histidine tag. Following transformation of E. coli BL21(DE3) cells with either plasmid, IPTG induced the expression of abundant quantities of CTP which accumulated within inclusion bodies. The inclusion body fraction was then isolated and the expressed CTP solubilized with sarkosyl. Employing the pET-21a(+) plasmid, we obtained approx. 7 mg of expressed CTP at a purity of 64% per liter of E. coli culture, while with the pET-28a(+) plasmid we obtained approx. 90 mg of CTP at a purity of greater than 95%. Upon functional reconstitution in a liposomal system, the expressed CTP catalyzed a 1,2,3-benzenetricarboxylate-sensitive citrate/citrate exchange. Data on the kinetics and the substrate specificity of the reconstituted CTP will be presented. In conclusion, the ability to express and purify large quantities of functional CTP paves the way for exploration of residues critical to the translocation mechanism by site-directed mutagenesis. Supported by NSF grant MCB-9219387 and NIH grant DK44993 to R.S.K.

Th-Pos412

KINETICS AND MECHANISM OF FE(III) RELEASE FROM HUMAN SERUM TRANSFERRIN. ((Sandra L. Mecklenburg,* Robert J. Donohoe* and Joseph Abra Watkins†)) Los Alamos National Laboratory,* CST-4, MS C345, Los Alamos, NM 87545; Department of Medicine, LSUMC-S,† Shreveport, LA 71130. (Sponsored by Jill Trewhella)

Human serum transferrin (HSTF) is the protein which serves in the body as a shuttle for iron between plasma and cells, which require iron for normal function. HSTF avidly binds two atoms of Fe(III) at neutral pH (≥ 7). Diferric HSTF is then preferentially bound by its receptor, which conveys the protein into the cell inside an endocytic vesicle. A proton-pumping cycle lowers the pH of the vesicle to ~5.6, which triggers the release of iron from HSTF. The apo protein is then released from the cell. It has been demonstrated previously that iron is bound more tightly by HSTF when complexed by its receptor at high pH but is released more easily at low pH, relative to free HSTF. The release of iron can be triggered *in vitro* by a similar decrease in the pH. Spectroscopic techniques including Raman, resonance Raman, FTIR, and UV-visible absorption have been used to examine the release of Fe(III) from HSTF as a function of pH in the presence and absence of the transferrin receptor. Raman and resonance Raman spectroscopy have permitted vibrational modes which are related to the active site to be distinguished. Stopped-flow kinetic studies have been conducted to determine the rate of iron release under these conditions.

Th-Pos413

TRANSPORT ACTIVITY OF THE BACTERIALLY EXPRESSED YEAST MITOCHONDRIAL PHOSPHATE TRANSPORT PROTEIN (PTP). SITE-DIRECTED MUTATIONS AT ASP, GLU AND HIS. ((A. Phelps, C. Briggs and H. Wohlrab)) Boston Biomedical Research Institute and Harvard Medical School, Boston, MA 02114.

PTP has been expressed as wild type and site-directed mutants in *E. coli* as inclusion bodies. The protein was solubilized with sarkosyl and reconstituted (Wohlrab, H., and Briggs, C. (1994) *Biochem. 33*, 9371). We have now replaced three of the six Asp with Asn or Glu, seven of the ten Glu with Gln or Asp, and one of the two His with Arg, Gln, Ala, Asn, or Lys. The phosphate uptake characteristics [net (zero trans) pHi=8.0, pHe=6.8] of these reconstituted mutants are: All those with detectable transport activities have the same Km as the wild type (1.3mM). Two mutants show somewhat higher Km's: Glu126Asp (3.22mM) and Asp39Glu (2.77mM). The Vmax's of all mutants are lower than the wild type (606μmol/min mg PTP). Those with a Vmax of less than 5% of the wild type, i.e. not able to grow on glycerol, are all the His32 mutants, Glu126Gln and Glu137Gln, Asp39Glu and Asp39Asn, and Asp236Glu and Asp236Asn. From these results we like to conlude that the PTP does possess a bacteriorhodopsin-like proton transport pathway via Glu126, His32, Glu137. The two residues Asp39 and Asp236 are just as critical and may provide a proton sink on the matrix side of the membrane. These two Asp do not tolerate a Glu substitution, while Glu126 and Glu137 do tolerate Asp substitutions. This difference could most likely be due to steric problems, i.e. the extra carbon of the R group of Glu. These results had been implicated from results with yeast mutants and their inability to grow on glycerol (Wohlrab, H. and Phelps, A. (1993) *FASEB J. 7*, 320). [Supported by NIH GM33357]

Th-Pos414

ANION DEPENDENCE OF BUMETANIDE BINDING AND ION TRANSPORT BY THE RABBIT PAROTID Na^+-K^+-2Cl^- COTRANSPORTER. **((Marilyn L. Moore and R. James Turner)) CIPCB, NIDR, NIH, Bethesda MD 20892, USA.**

The anion dependence of [^{3}H]-bumetanide binding and ^{22}Na transport by the rabbit parotid Na^+-K^+-2Cl^- cotransporter was studied in acinar basolateral membrane vesicles (BLMV). There are two Cl sites associated with the bumetanide binding event, a high-affinity stimulatory site and a lower-affinity inhibitory site (J. Membr. Biol. 102:71, 1988). We demonstate that formate shares only the stimulatory site and SO_4 only the inhibitory site. The initial rate of [^{3}H]-bumetanide binding was stimulated by formate or low [Cl] and inhibited by SO_4 or high [Cl]. In contrast, [^{3}H]-bumetanide dissociation was independent of the ionic composition of the dissociation medium. However, when [^{3}H]-bumetanide was bound to membranes in the presence of formate its rate of dissociation was >4-times faster than when binding took place in the presence of Cl. These observations indicate that the binding of bumetanide and the stimulatory anion are ordered such that the anion must necessarily bind first and subsequently cannot dissociate until after bumetanide dissociates. In zero trans flux experiments, extravesicular SO_4 and formate had no effect on ^{22}Na transport via the cotransporter. Thus neither of the anion sites associated with bumetanide binding is a Cl transport site. However, we show here that SO_4 inhibits transport when present in the intravesicular space. Since the BLMV preparation is predominantly oriented cytosolic-side-in, this observation indicates the presence of an inhibitory cytosolic anion modifier site. The existence of such a site has been hypothesized in several tissues to explain the apparent down-regulation of Na^+-K^+-2Cl^- cotransport activity at high intracellular Cl levels. Our data confirm the existence of this site and suggest that it is, in fact, the inhibitory anion site previously shown to be associated with bumetanide binding.

Th-Pos415

KINETICS OF ELECTROGENIC CATIONIC AMINO ACID TRANSPORTERS ((E.M. Klamo and M.P. Kavanaugh)) Vollum Institute, Oregon Health Sciences University, Portland, OR 97201 (Spon. by M. Forte)

Cloned cationic amino acid transporters were expressed in *Xenopus* oocytes and studied by measuring radiolabel uptake and transport currents under voltage clamp. Uptake of [^{3}H]L-arginine into oocytes mediated by the high-affinity transporter CAT1 is increased by the presence of intracellular unlabeled arginine, providing strong evidence for a two-state alternating access model in which unidirectional flux is accelerated in an exchange mode which bypasses a slow unliganded state transition. Kinetic modeling of zero-trans steady-state arginine currents suggests that this rate-limiting unliganded state transition is voltage dependent (*Biochemistry* 32 5781 1993). In agreemement with this hypothesis, a sodium-independent non-linear capacitive current is seen following voltage jumps in the absence of arginine using a p/4 protocol or by blocking the charge movement with N-ethylmaleimide or saturating arginine concentrations. Hyperpolarizing pulses from a holding potential of -30 mV in the presence of arginine result in an instananeous increase in the transport current followed by a slower relaxation to a new steady-state level in 250-300 ms. The ratio I_{inst}/I_{ss} was a saturable function of the concentration of arginine, in agreement with predictions of the model. A highly homologous clone, CAT2, is subject to alternative RNA splicing which results in two structural isoforms: a low apparent affinity form (CAT2α; K_m = 4 mM) and a high apparent affinity form (CAT2β; K_m = 180 μM). The decrease in apparent affinity exhibited by CAT2α is likely to be due at least in part to an increase in the rate constant governing the conformational transition of the unliganded transporter; in this isoform the time constants of the both the transition current and the steady-state relaxations were faster than the resolution of the amplifier. In further agreement with this model, uptake of [^{3}H]L-arginine was trans-stimulated in CAT2β but not CAT2α.

Th-Pos416

TRANSPORT MECHANISM OF A NOVEL HIGH-AFFINITY K^+ UPTAKE TRANSPORTER HKT1 FROM HIGHER PLANTS
((W. Gassmann, F. Rubio, D. P. Schachtman and J.I. Schroeder)) Department of Biology and Center for Molecular Genetics, University of California, San Diego, La Jolla, CA 92093-0116

Potassium serves as a major cationic mineral nutrient essential for plant growth. The high-affinity K^+ transporter provides the primary pathway for K^+ uptake from soils into roots when the soil K^+ concentration is low. However, the biophysical mechanism and the molecular structure of high-affinity K^+ uptake transporters in plants have remained unknown. Recently, a root-specific cDNA (HKT1) from wheat was isolated by expression cloning (1). Functional expression studies of HKT1 in *Xenopus* oocytes and yeast and in situ hybridizations have demonstrated that the K^+ uptake properties as well as the expression pattern in specialized root cells all strongly support the hypothesis that HKT1 encodes a first high-affinity K^+ uptake transporter from plants (1). HKT1 represents a novel class of K^+ uptake transporters, and recent results from functional expression studies in *Xenopus* oocytes and yeast aimed at understanding the biophysical mechanism of K^+ translocation by HKT1 will be presented. In addition, research aimed at identifying structural sites that may alter HKT1 activity will be discussed.

1) Schachtman DP, Schroeder JI (1994) Structure and transport mechanism of a high-affinity potassium uptake transporter from higher plants. Nature 370: 655-658

Th-Pos417

PHOTOINCORPORATION OF ^{125}I INTO POLYPEPTIDES FROM IODIDE TRANSPORTING CELLS. ((Orlie Levy, Stephen M. Kaminsky and Nancy Carrasco)) Department of Molecular Pharmacology, Albert Einstein College of Medicine, Bronx, NY, 10461.

The accumulation of I^- in the thyroid is mediated by the Na^+/I^- symporter, an intrinsic plasma membrane protein that remains to be fully characterized. I^- transport into the thyroid is the first step in the biosynthesis of thyroid hormones T_3 and T_4. In an effort to identify the symporter a ^{125}I photolabeling method has been developed to label thyroid polypeptides with high affinity for I^-. Membrane vesicles prepared from thyroid and other cells were incubated in the presence of ^{125}I and irradiated with a mercury arc lamp. Polypeptides were then electrophoresed and visualized by autoradiography. Significantly, only polypeptides from I^--transporting cells were labeled, suggesting a strong link between polypeptide labeling and the ability of cells to transport I^-. The mechanism of the photolabeling reaction is thought to involve a charge transfer complex between the imidazolium ion from a histidine side chain and iodide. Absorption of light by the charge transfer complex produces the equivalent of a radical pair. The iodine atom can then diffuse locally and react with nearby side chains. NH_2-terminal sequencing information has recently been obtained for a 90 kDa polypeptide, which was identified to be the chaperone phosphoprotein calnexin. Furthermore, the expression of calnexin was found to be regulated by TSH.

Th-Pos418

A MICROSCALE METHOD TO DETERMINE MEMBRANE PROTEIN OLIGOMERIC STATE AND STOKES RADIUS.

((J.R. Casey and R.R. Kopito)) Department of Biological Sciences, Stanford University, Stanford, California 94305-5020, U.S.A.

Most membrane proteins are oligomeric and oligomeric state has been implicated in the function of many proteins. The self-association of membrane proteins into dimers, tetamers or higher oligomers has been studied by chemical crosslinking, radiation inactivation, sucrose gradient ultracentrifugation and several spectroscopic methods. One rapid, high resolution method to determine membrane protein oligomeric state is size exclusion high performance liquid chromatography, (SEC). Previously this methodology has required purified proteins so that low abundance proteins could not be analyzed by SEC. We have therefore combined the resolution power of SEC to immunological detection of the eluted protein, to allow the SEC analysis of very small amounts (0.2 µg) of membrane proteins expressed in mammalian cells. In this system, membrane proteins were expressed by transient transfection of HEK cells. Isolated membranes were solubilized in the nonionic detergent n-dodecyloctaethyleneglycol monoether ($C_{12}E_8$). Solubilized protein was applied to a TSK4000SW column, eluted with 0.1 M sodium chloride, 0.1% $C_{12}E_8$, 5 mM sodium phosphate, pH 7.0. Protein elution was monitored by collecting fractions of eluent, dot-blotting onto nitrocellulose and probing the nitrocellulose with an appropriate antibody, developed with chemiluminescent reagent and quantified by densitiometry. The column was calibrated with proteins of known Stokes radius and with purified erythrocyte AE1 protein. Erythrocyte AE1 protein eluted as a mixture of dimers and tetramers (Rs = 75 Å and 101 Å respectively). Both human AE1 and mouse kidney AE1 expressed in HEK293 cells eluted as a single peak with Rs = 72 Å, which indicates that these proteins are purely dimeric. The formation of tetramers may require the presence of ankyrin, which is not found in HEK293 cells. This system was also used to examine the oligomeric structure of cystic fibrosis transmembrane regulator.

Th-Pos419

THE DISSOCIATION KINETICS OF THE NI(II) COMPLEX OF IONOMYCIN IN 80% METHANOL-WATER.

((N. Khanna[1], D.R. Pfeiffer[2], R.W. Taylor[1])) [1]Department of Chemistry, University of Oklahoma, Norman, OK 73019 and [2]The Ohio State University, Columbus, Ohio 43210

Ionomycin, H_2I, is a unique example of a polyether ionophore which contains two ionizable moieties, a carboxylic acid and a β-diketone. Thus, ionomycin is able to form 1:1 charge-neutral complexes with divalent cations. Using the stopped-flow technique, we have studied the kinetics of the acid-induced dissociation of the 1:1 NiI complex under pseudo-first-order conditions at 25.0 °C and I=0.05M (Et_4NClO_4) in 80% methanol-water solutions. For comparison, similar studies were conducted with the model compound 2,6-dimethyl-3,5-heptanedione (DMHD). For both DMHD and ionomycin, the observed rate constants increase linearly with the hydrogen ion concentration and are affected very little by the metal ion concentration. A mechanism postulated to account for the kinetic data for the NiI and NiDMHD complexes is represented as: $H^+ + NiL \rightleftharpoons HL(E) + Ni^{2+} \rightleftharpoons HL(K) + Ni^{2+}$, where HL(E) and HL(K) represent the protonated enol and keto tautomers of the ligand, respectively. The value of the rate constant for the dissociation of the NiI is calculated to be 52±1 $M^{-1}s^{-1}$. The value of the rate constant for the dissociation of NiDMHD is calculated to be 480±7 $M^{-1}s^{-1}$.

In acidic solutions, formation of the NiI complex exhibits biphasic behavior although only one process is observed for the reaction of Ni(II) with DMHD. In neutral or mildly acidic solutions, the kinetics of the formation reactions of NiDMHD exhibit behavior indicative of general acid/base catalysis for buffers such as acetate, cacodylate and 2-[N-morpholino]ethanesulfonate.

Th-Pos420

KINETIC CONSTRAINTS OF CATION ACTIVATION OF THE Na/GLUCOSE COTRANSPORTER.

((B.A. Hirayama, D.D.F. Loo and E.M. Wright)) Department of Physiology, UCLA School of Medicine, Los Angeles, CA 90024-1751.

Ion-dependent transport proteins use electrochemical potential gradients to drive uptake of substrates into cells. We have compared the kinetics of sugar transport via SGLT1 energized by Na^+, Li^+ and H^+. Rabbit SGLT1 was expressed in Xenopus oocytes and sugar-induced steady-state currents were measured using the two-electrode voltage-clamp. The Table summarizes kinetics for V_m=-150mV.

Cation	$K_{0.5}$ (cation) mM	$K_{0.5}$ (sugar) mM	I_{max} (% I_{max} Na)
Na^+	30	0.2	100
Li^+	5	1.9	73
H^+	0.007	5.1	153

These results show that each parameter has a different cation selectivity: 1) sugar affinity in the order $Na^+ > Li^+ > H^+$; 2) maximal transport rate, with $H^+ > Na^+ > Li^+$; and 3) the affinity for cations is $H^+ > Li^+ > Na^+$. According to our kinetic model, trans-release of the cation is rate-limiting for I_{max}, under saturating substrate conditions, suggesting that Li^+ forms a more stable complex than Na^+ and H^+. Further consideration of the model will allow us to determine the steps involved in cation and sugar affinities.

Supported by NIH grants DK44602 and DK41301.

Th-Pos421

EFFECTORS OF GLYCINE EFFLUX IN BARNACLE MUSCLE CELLS.

((K. McGruder, C. Peña-Rasgado, and H. Rasgado-Flores)) Dept. Physiology & Biophysics. FUHS/The Chicago Medical School. N. Chicago, IL 60064

In barnacle muscle cells, exposure to hypoosmotic conditions induce cell swelling followed by an extracellular Ca^{2+} (Ca_o)-dependent loss of osmolytes (e.g. glycine, gly) and obligated water leading to regulatory volume decrease (RVD). Since verapamil and the specific antagonist of cAMP, Rp-cAMPS, inhibit the Ca_o-dependent RVD, we postulate that swelling activates Ca^{2+} influx and that the subsequent increase in the intracellular Ca^{2+} concentration ($[Ca^{2+}]_i$) induces the synthesis of cAMP which produces in turn osmolyte loss. To test this hypothesis we assessed the role of the likely effectors of RVD on cell volume and the efflux of ^{14}C-gly in internally perfused barnacle muscle cells. A reduction in extracellular osmolality from 1000 to 550 mOsm/kg H_2O induced cell swelling of 30%. If Ca_o was present, and the perfusate contained a relatively low Ca^{2+}-buffering capacity (i.e. 2 mM EGTA as opposed to the normal 8 mM), the swelling was followed by volume recovery of 60% and an increase in gly efflux of 1000 pmoles/cm^2 sec which were blocked by presence of 1 mM Rp-cAMPS. An isosmotic increase in $[Ca^{2+}]_i$ from 0.01 to 20 µM produced a volume loss of 25% and an increase in gly efflux of 653 pmoles/cm^2 sec which were blocked by RpcAMPS. Under isosmotic conditions, in the absence of Ca_o, addition of 1 mM cAMP induced volume loss of 12% and an increase in gly efflux of 146 pmoles/cm^2 sec. This indicates that the critical factor in the chain of events responsible for producing RVD is the synthesis of cAMP.

Th-Pos422

EFFECTS OF UREA ON VOLUME-SENSITIVE K-Cl COTRANSPORT IN SHEEP RED CELLS - EVIDENCE FOR TWO DIFFERENT SIGNALS OF SWELLING.

((P.B. Dunham)) Syracuse Univ., Syracuse, NY 13244

K-Cl cotransport in sheep red blood cells is activated by urea at non-denaturing concentrations up to 0.5 M. Pre-steady state kinetics of activation were measured and interpreted in terms of a three-state process for swelling-activation of K-Cl cotransport (Dunham et al. 1993 *J. Gen. Physiol.* 101: 733-765). Activation proceeded with a delay, like activation by swelling. In contrast, swelling activated K uptake further in cells in urea , but with no delay. With cotransport partially activated by reducing $[Mg]_c$, urea did not activate cotransport further. However swelling activated cotransport in these cells, and with no delay. Therefore urea activates the first conversion in the three-state process, A --> B, not the second, B --> C. Inactivation of cotransport following removal of urea proceeded without delay, indicating that urea promotes A --> B by inhibiting the reverse reaction, a protein kinase reaction, just as reducing $[Mg]_c$ does. Stimulation of cotransport by urea is nearly completely reversed by shrinkage, whereas activation by reducing $[Mg]_c$ is only partially reversed. Therefore urea inhibits the kinase indirectly, presumably as swelling does, reducing macromolecular crowding of cytoplasmic proteins (Minton et al. 1992 *Proc. Natl. Acad. Sci.* 89: 10504-10506). Swelling activates cotransport in two ways, one mimicked by urea and one not. Therefore there are two signals of swelling. The signal mimicked by urea is a reduction of macromolecular crowding (promoting A --> B). Since inside-out vesicles from sheep red cells, with no cytoplasmic protein, have swelling-activated K-Cl cotransport (Kracke & Dunham 1990 *Proc. Natl. Acad. Sci.* 87: 8575-8579), the other signal of swelling must be a mechanical change in the membrane (promoting B --> C). (Supported by NIH grant DK-33640.)

Th-Pos423

ELECTROPHYSIOLOGICAL STUDIES OF A PLANT H^+/AMINO ACID TRANSPORTER.

((K.J. Boorer, D.D.F. Loo, D. Bush, W.B. Frommer and E.M. Wright)). Department of Physiology, UCLA School of Medicine, Los Angeles, Ca 90024. (Spon. by J. Valentine).

Amino acids are transported into plant cells via H^+-dependent cotransporters. The H^+/amino acid transporter from *Arabidopsis thaliana* (NAT2/AAP1) has been cloned. This has enabled us to investigate its mechanism of transport by expression in *Xenopus* oocytes. Transport kinetics were measured using the 2-electrode voltage-clamp method where steady-state substrate-dependent currents were recorded as a function of $[amino\ acid]_o$ and $[H^+]_o$. The transporter exhibits a broad substrate-specificity with inward currents induced by neutral, basic and acidic amino acids. The apparent coupling coefficient n of the transporter for H^+ and L-alanine was determined by fitting the current/concentration data to the Hill equation. For H^+ n = 2 and for L-alanine n is between 1 and 2. The stoichiometry of H^+/L-alanine transport was determined directly by simultaneously recording the L-alanine-induced inward current and uptake of [^{3}H]-L-alanine whilst clamping the oocyte membrane potential at -70 mV. Using this method the stoichiometry is 1 H^+:1 alanine. In summary, NAT2/AAP1 is electrogenic, has a broad substrate-specificity and transports 2H^+:2 alanine per transport cycle.

Th-Pos424

MOLECULAR CLONING AND FUNCTIONAL EXPRESSION OF A CREATINE TRANSPORTER FROM HUMAN HEART. ((W. Dai, D.L. Kunze and H.K. Sarkar)) Baylor College of Medicine, Houston, TX 77030.

A high affinity creatine transporter present in the plasma membrane of the muscle cells maintains the creatine homeostasis in the muscle. We have cloned a creatine transporter cDNA from a human heart cDNA library by homology screening with a taurine transporter cDNA fragment. The encoded peptide revealed ~98% amino acid sequence homology to those of the creatine transporters from rat brain, rabbit brain, and muscle. For functional expression, *in vitro* transcribed RNA prepared from this clone was microinjected into *Xenopus* oocytes and the creatine uptake activity in injected oocytes was measured using [^{14}C]-creatine as a substrate. The induced creatine uptake activity in microinjected oocytes was found to be both Na^+- and Cl^--dependent, with an apparent K_m of 20 μM for creatine. While the rate of creatine uptake showed a sigmoidal dependence on the external concentration of Na^+, the rate was a single saturable process with respected to the external Cl^- concentration. β-Guanidinopropionic acid and γ-guanidinobutyric acid, two close analogs of creatine and known creatine transporter inhibitors, inhibited the induced uptake by ~85% and ~42% at 100 μM, respectively. In contrast, L-α-amino-β-guanidinopropionic acid was less effective and inhibited the induced uptake by ~30% only at 500 μM. [Supported by AHA Grant-in-Aid 91012730 and Texas ATP Grant 004949057 to HKS, by HL36840 to DLK.]

Th-Pos425

STEADY-STATE AND TRANSIENT CURRENTS IN NOREPINEPHRINE TRANSPORTERS. ((A. Galli, L. J. DeFelice, R. D. Blakely)) Anatomy & Cell Biology, Emory University School of Medicine, Atlanta GA 30322.

Norepinephrine (NE) transporters remove NE from noradrenergic synapses. Na gradients provide energy for uptake, and antidepressants and cocaine inhibit uptake. To study voltage regulation, we transfected 293 cells with cloned human NE transporters (hNET). Western blots verify expression of hNETs. Radiolabeled flux assays show that stably-transfected cells take up NE and the false transmitter, guanethidine (GU). In physiological solutions under whole-cell voltage clamp at 37 °C, NE and GU generate inward currents at negative voltages. Desipramine (DS) and cocaine inhibit this current. In 130 mM Na at -120 mV, K_m for NE- or GU-induced inward current is 0.6 or 1.1 uM, respectively. In 15 uM NE, K_m for Na is 15 mM. K_i for DS or cocaine is 0.05 or 1.7 uM, respectively. Neither Ni nor ouabain affect the induced currents. Mock-transfected and parental cells show no DS-sensitive currents. Induced current consists of steady-state and transient currents. DS or cocaine reveal a leak current in the absence of substrate. We define transients by subtracting the current in 2 uM DS. The transient charge (Q) in GU+DS or in DS alone ranged from 1-7 pC. Q(V) is independent of NE or GU. The maximum steady-state NE-induced current is -50 pA at -120 mV. GU-induced currents average -120 pA. 293 cells stably transfected with cloned transporters provide a useful model to study the voltage regulation of catecholamine uptake mechanisms in a mammalian expression system.

Th-Pos426

NMR STUDIES OF MERT, A MERCURY TRANSPORT PROTEIN ((D. M. Brabazon and S. J. Opella)) Department of Chemistry, University of Pennsylvania, Philadelphia, PA 19104, ((N. V. Hamlett)) Department of Biology, Harvey Mudd College, Claremont, CA 91711.

MerT is an integral inner membrane protein which participates in the Hg(II) transport process of a system which confers resistance to toxic mercuric compounds in bacteria. Structurally and mechanistically there is little known about merT, although hydropathy plots suggest that merT has three transmembrane helices. The 116 residue merT is fused to malE using the Maltose-Binding Fusion vector, pMal-c2. Factor Xa cleaves merT from malE, and size exclusion chromatography is used to separate the two proteins. Both multidimensional solution NMR spectroscopy of merT in micelles and high resolution solid state NMR spectroscopy of merT in phospholipid bilayers are being used to determine the structure and dynamics of merT.

Th-Pos427

PALMITOYL-CoA IS AN ALLOSTERIC INHIBITOR OF PROTON TRANSPORT THROUGH MITOCHONDRIAL UNCOUPLING PROTEIN. ((M. Modriansky, S. Vassanelli, and K. D. Garlid)). Dept. of Chemistry, Biochemistry, and Molecular Biology, Oregon Graduate Institute of Science & Technology, Portland, OR 97291-1000.

Mitochondrial uncoupling protein (UCP) catalyzes regulated proton backflux across the inner membrane to produce heat. UCP-mediated H^+ transport is activated by fatty acids and inhibited by purine nucleotides. We have recently shown this inhibition to be purely allosteric [Jezek et al. (1994) J. Biol. Chem., in press], raising the question of how UCP can be activated in the presence of high cytosolic ATP. Nedergaard and Cannon [(1994) New Comp. Biochem. *23*, 385] proposed that palmitoyl-CoA may act as a partial agonist by displacing nucleotides without completely inhibiting H^+ transport. We examined this suggestion using purified, reconstituted UCP. Palmitoyl-CoA (i) does not induce UCP-mediated H^+ transport, (ii) inhibits UCP-mediated H^+ transport regardless of GDP presence, and (iii) lowers V_{max} of laurate-induced, UCP-mediated H^+ transport without affecting the K_m for laurate. Thus, palmitoyl-CoA is a purely allosteric inhibitor of purified UCP and cannot be a partial agonist. (Supported by NIH grant GM 31086.)

Th-Pos428

COUPLING OF DRUG EFFLUX TO ELECTRODIFFUSIONAL ATP MOVEMENT THROUGH P-GLYCOPROTEIN. ((H. F. Cantiello and G. R. Jackson Jr.)) Renal Unit, Mass. Gen. Hosp. East and Dept. of Medicine, Harvard Med. Sch., Massachusetts.

The P-glycoproteins (Pgp) are responsible for the multidrug resistance phenotype. The molecular mechanism linking Pgp function to net drug efflux is, heretofore, unknown. We recently demonstrated that Pgp is a novel ATP-permeable ion channel (PNAS, 90:312, 1993). Whole-cell clamp and fluorescence imaging techniques were used in P-glycoprotein over-expressing (EX4N) cells to correlate the Pgp-mediated ATP currents with the ability of Pgp to move fluorescein, whose moiety is a substrate model for drug efflux through Pgp. Cells were dialyzed through the patch pipette with MgATP (100 mM) and either rhodamine 123 (10 μM) or fluorescein free acid (30 μM). Intracellular fluorescence reached an equilibrium concentration (22.5 ± 0.7 μM, n=4) in approximately 8 min. Under resting conditions, intracellular fluorescence remained constant for at least ten min. A depolarizing (constant) voltage of -100 mV was then applied for up to 5 min to activate Pgp. Whole-cell currents increased 639% and 1181% in positive and negative holding potentials, respectively, to elicit outward ATP movement. Fluorescent images taken over a 5 min period showed a decrease in intracellular fluorescence by 71.6% (17.1 vs. 4.8 μM, n=8, p<0.001). In the presence of verapamil (10 μM), currents were inhibited by 64.6% and 81.4% for positive and negative holding potentials (n=5). No decrease in fluorescence was observed in the presence of verapamil. No changes in equilibrium fluorescence were observed with intracellular Cl (140 mM) in both iso- and hypo-osmotic conditions. The data indicate that electrodiffusional ATP movement through Pgp is coupled to drug efflux, thus entailing a novel cotransport mechanism, which may be associated with the multidrug resistance phenotype.

Th-Pos429

REVERSIBLE AND PHOTOAFFINITY LABELING OF THE P-GLYCOPROTEIN DIHYDROPYRIDINE BINDING DOMAIN WITH THE NOVEL DRUG TRANSPORT INHIBITOR BZDC-DHP **((C. Borchers*, M. Dichtl, R. Boer+, J. F. Marecek§, G.D. Prestwich§, H. Glossmann and J. Striessnig)).** *Institut für Biochemische Pharmakologie, Universität Innsbruck; * Fakultät für Chemie, Universität Konstanz; + Byk Gulden Lomberg GmbH, Konstanz; § Department of Chemistry, State University of New York.*

The tritiated calcium antagonist [^{3}H]BZDC-DHP, (±)-2,6,dimethyl-4-(2-trifluoromethyl-phenyl)-1,4,dihydropyridine-3,5-dicarboxylic acid {2-[3-(4-benzoyl-phenyl)-propionylamino]-ethyl}ester ethyl ester}, was synthesized as a specific probe for dihydropyridine (DHP) binding domains on voltage-dependent L-type calcium channels (LTCCs) and p-glycoprotein (pgp), which mediates multidrug-resistance. BZDC-DHP is structurally related to azidopine but carries a photoreactive benzoyldihydrocinnamic acid substituent instead of a phenylazide ring. BZDC-DHP and azidopine possess similar affinity for the LTCC DHP receptor. In contrast, BZDC-DHP displays an order of magnitude higher affinity for the pgp. We exploited its high affinity to develop a binding assay for reversible pgp labeling. [^{3}H]BZDC-DHP (100 dpm/fmol) binds to pgp in membranes prepared from multidrug-resistant cells (ADR-5000 cells) with a Kd of 16 nM (B_{max}=49 pmol/mg of protein). Reversible binding is concentration-dependently inhibited by other DHPs (azidopine, nicardipine, dexniguldipine), multidrug-resistance reversal agents (ciclosporin A, verapamil, quinidine) and cytotoxics (vinblastine, vincristine). Ciclosporin A was the most potent inhibitor (IC_{50} = 5 nM), azidopine about ten-fold less potent (IC_{50}=100 nM) than BZDC-DHP. Saturable binding was absent in the respective sensitive cell line (CCRF-CEM). The potency of binding-inhibition correlated (n=8, r> 0.80) with the inhibition of energy-dependent drug-transport (measured by rhodamine 123 accumulation). IC_{50} values for the inhibition of BZDC-DHP strictly correlated with the inhibition of reversible [^{3}H]vinblastine binding (n=10, r>0.90). Some DHPs, like niguldipine, were stimulatory indicating binding to a different or overlapping site. Therefore at least two DHP molecules can simultaneously bind to the pgp. Specific [^{3}H]BZDC-DHP photolabeling occurred with high yield (about 50% of reversibly bound ligand were covalently incorporated) into a 170 kDa polypeptide that was specifically immunoprecipitated with pgp-specific sequence directed antibodies. Nonspecific labeling was lower than observed for [^{3}H]azidopine.

Taken together [^{3}H]BZDC-DHP is a drug-transport inhibitor of pgp with properties superior to [^{3}H]azidopine. Reversible binding assays employing this ligand should be useful to study the molecular pharmacology of the drug binding domains on pgp. It also provides a simple screening assay for drugs with high affinity for pgp that could serve as chemosensitizers.

This work was supported by grants from the Fonds zur Förderung der Wissenschaftlichen Forschung, Austria (S6601, S6602) and is part of the thesis of M.D.

Th-Pos430

INFLUENCE OF STEROIDS ON THE ATPase ACTIVITY OF P-GLYCOPROTEIN. ((S. Orlowski and M. Garrigos)) SBPM, DBCM, CEA, CE Saclay, F-91191 Gif/Yvette, France. (Spon. by J. Bourguet).

Overexpression of P-glycoprotein (P-gp) in tumor cells is associated with multidrug resistance. P-gp is also found in various normal tissues where steroids have been proposed as physiological substrates. Independent experiments have shown that P-gp displays an ATPase activity and transports dexamethasone (DXM) but not progesterone (PRG). To test the possibility of a coupling between the hydrolysis of MgATP and steroid transport we have studied the influence on the P-gp ATPase activity of four steroids: PRG, DXM, desoxycorticosterone (DCS) and corticosterone (CST). For this purpose, P-gp containing vesicles of purified total membranes from Chinese Hamster lung fibroblasts (DC-3F/ADX) were used. Despite close chemical structures for CST, DCS and PRG they differently influence P-gp ATPase activity. Indeed, CST is unable to stimulate the hydrolysis of MgATP by P-gp, whereas DCS and DXM induce a similar maximal stimulation of 1.3-fold at respectively 150 μM and 450 μM, and PRG displays a maximal stimulation of 2-folds at 100 μM. In contrast, verapamil, which is transported by P-gp and does not share any structural homology with steroids, induces a 1.6-fold activation of P-gp ATPase activity and compets with PRG for this activation. Thus correlation between stimulation of P-gp ATPase activity and substrate transport does not clearly appear.

Th-Pos431

THERMODYNAMICS OF SMALL PEPTIDE TRANSFER TO LIPID BILAYERS

((Marek Romanowski, Xiaoyun Zhu, Victor J. Hruby and David F. O'Brien))
Department of Chemistry, University of Arizona, Tucson, AZ 85721

Peptide transfer from water to a lipid membrane is a crucial step in the transmembrane passage of these solutes. Understanding of this process is a foundation of efficient drug delivery methods. Small peptides usually do not possess single conformation in water, rather they are characterized by a distribution of conformers. Based on thermodynamic analysis it appears that among all conformers present in water those compact structures that minimize the number of external hydrogen bonds (with water) and are potentially stable in the membrane interior, transfer into the membrane more efficiently. We propose that the water-to-membrane transfer follows the scheme:

extended folding in water $\rightleftharpoons$ compact folding in water $\rightleftharpoons$ compact folding in a membrane

Overall water-to-membrane transfer is affected by the extended-compact folding equilibrium in water, and can be controlled by those elements of the peptide design that enhance formation of a compact folding, e.g., β-turn. Membrane incorporation of peptides having different propensities for a compact structure formation will be discussed. Proposed contributions to the free energy of transfer are compared with experimental determinations by isothermal calorimetry. Coefficients of permeability across a model bilayer are determined to test validity of the proposed mechanism of peptide transfer. (Supported by NIDA Grant POI DA 06284)

Th-Pos432

TIME-RESOLVED STUDIES OF ANION BINDING TO PHARAONIS HALORHODOPSIN. ((I.Chizhov, M.Geeves, B.Scharf, B.Hess and M.Engelhard)) Max-Planck-Institut für Molekulare Physiologie, 44139 Dortmund, Germany

The removal of anions from pharaonis halorhodopsin (phR) results in a shift of the absorption maximum from 580 nm to 600 nm (phR^{blue}). The purple colour can be regained by the addition of various anions. This process was analysed using stop-flow techniques. In the case of Cl^- and Br^-, the absorbance changes follow a monoexponential reaction with half-lifes in the millisecond range. The observed kinetics and their dependence on the type of anion, their concentration and the temperature can be fitted assuming a two-step, one binding site model. The first step is diffusion-controlled and apparently does not change the absorption spectra of the chromophore. In the second step with the time constants between 1 ms and 100 ms the transition from blue to purple occurs. Using this model, the intrinsic rate constants of the reversible binding of anions could be calculated (see table) and the apparent activation energy was determined. The observed data supports single anion binding site in pharaonis halorhodopsin.

	K_d (mM)	K_1 (mM^{-1})	K_2	k_{+2} (s^{-1})	k_{-2} (s^{-1})
Br^-	1.0	0.020	49	320	6.5
Cl^-	2.3	0.032	14	200	14.0

Th-Pos433

VISUALIZATION OF THE REACTION LAYER IN THE IMMEDIATE MEMBRANE VICINITY ((Yuri N. Antonenko* and P. Pohl#))

*Moscow State University, Belozersky Institute of Physico-Chemical Biology, 119899 Moscow, Russia; #Martin-Luther-University, Department of Medical Physics and Biophysics, 06097 Halle, Germany

If transmembrane diffusion is followed by chemical reactions proceeding in the immediate membrane vicinity equilibrium is reached at a certain distance from the membrane. The purpose of the study was to determine the size of the reaction layer, i. e. the equilibrium distance. Therefore pH profiles of the unstirred layer near a planar bilayer lipid membrane were measured with the help of microelectrodes. The oxidation of acetaldehyde catalyzed by alkoholdehydrogenase in the presence of NADH induced pH shifts near the membrane. Enzyme/coenzyme and substrate were added to opposite sides of the membrane. The shape of the pH profiles obtained under these conditions was switched from an exponential to a bell like one if the proton permeability of the membrane had been enhanced due to the addition of acetate. With increasing reaction rates the position of the maximum was shifted toward the membrane. A theoretical analysis of the reaction and diffusion kinetics enabled us to conclude that the position of the maximum coincided with the border of the reaction layer at high enzyme concentrations.

Supported by the Deutsche Forschungsgemeinschaft Ro 1057/2-1

Th-Pos434

OSMOLYTES RESPONSIBLE FOR VOLUME LOSS IN RESPONSE TO ISOSMOTIC Ca^{2+} REMOVAL OR TO HYPOTONICITY IN MUSCLE CELLS.

((C.Peña-Rasgado, S.K. Pierce[a], and H. Rasgado-Flores)) Dept. Physiology & Biophysics. FUHS/The Chicago Medical School. N. Chicago, IL 60064 and [a]Dept. Zoology. Univ. Maryland. College Park, MD 20742.

Numerous experimental manipulations which increase the intracellular free Ca^{2+} concentration induce cell volume loss. This may occur under isosmotic conditions, e.g., when external Ca^{2+} (Ca_o) is replaced by Mg^{2+} (Amer. J. Physiol. 267:C768-C775, 1994) or under hypoosmotic conditions, e.g., during a Ca_o-dependent, regulatory volume decrease (RVD). We determined the osmolytes responsible for volume loss under both osmotic conditions in barnacle muscle cells. Organic osmolytes (i.e. free amino acids, FAA and methylamines) and inorganic ions accounted for ~78% and ~22% of the intracellular isosmotic activity, respectively. Isosmotic Ca_o removal-induced volume loss was accompanied by a net loss of ions (1K:1Cl) and FAA (mainly glycine and taurine). This process was not accompanied by a change in extracellular pH. During RVD, KCl and FAA were also lost but in this case the stoichiometry was 2K:1Cl and there was an extracellular alkalinization. The 2K:1Cl loss may be explained by the simultaneous loss of K^+ accompanied by Cl^- and in exchange with H^+ (i.e *via* a K^+/H^+ exchanger) or co-transported with OH^-. The lack of RVD observed in the absence of Ca_o cannot be due to the loss of intracellular osmolytes during isosmotic Ca_o removal because addition of Ca_o during cell swelling promoted RVD.

Th-Pos435

HORMONALLY INDUCED CHANGES IN SERUM Mg^{2+} IN ANESTHETIZED RATS

((D. KEENAN, A.ROMANI and A. SCARPA)) Dept. Physiol. & Biophys., CWRU., Cleveland, OH, 44106-4970, USA [Spon. G. Dubyak].

β-adrenergic agonists induce a marked Mg^{2+} efflux from isolated rat hearts or livers and from isolated cardiac or liver cells. In the present study we investigated whether the in vivo infusion of β-adrenergic agonists would result in an increase of serum Mg^{2+}. Urethane anesthetized rats were catheterized for infusion of adrenergic agonists (femoral vein), blood pressure monitoring (femoral artery) or blood sampling (tail artery) and allowed to equilibrate for 30 min to minimize the effects of endogenous catecholamines. Blood samples were withdrawn, centrifuged and deproteinized by HNO_3. The serum Mg^{2+} content was measured by atomic absorbance. Two pre-infusion samples were taken to monitor Mg^{2+} baseline. Animals were then infused with isoproterenol (ISO) doses ranging between 0.01-100 μg/kg/min for 10 min and sampled at 10 min. intervals thereafter. Control animals were infused with the vehicle (0.9% normal saline, (NS)). Other animals were infused with selective β_1 or β_2 agonists, sodium nitroprusside (NIP) to mimic the hypotensive effect of ISO, or pre-treated with β-adrenergic blockers. No difference in hematocrit between control and treated animals was observed. Infusion of ISO resulted in a dose dependent increase in serum Mg^{2+}, which was maximal 20 min after the infusion. The maximal change was a 22.8% increase, and occurred at the dose of 1 μg/kg/min. This represented a net increase of 6.9 μmol Mg^{2+}/300 g bw. The calculated EC_{50} was 116 ng/kg/min. Qualitatively similar results were observed in animals treated with the β_2 agonist salbutamol, but not with the β_1 agonist prenalterol. Infusion with NIP resulted in a modest and transient elevation (7%) of serum Mg^{2+}. The pre-treatment with β_1/β_2-blocker propranolol, but not β_1-blocker atenolol, inhibited the Mg^{2+} increase by 75%. These data indicate: i) that ISO induces a dose dependent increase in serum Mg^{2+}, and ii) that this effect is mediated through β_2-adrenergic receptors. Supported by N.I.H. HL 18708.

Th-Pos436

NADH-LINKED REDOX REACTION INDUCES A TRANSPORT OF CD^{2+} IN PLANT ROOT PLASMA MEMBRANE VESICLES. ((Shu-I Tu, Deidre Patterson, David Brauer, and An-Fei Hsu)) USDA, ARS, NAA, Eastern Regional Research Center, 600 E. Mermaid Lane, Philadelphia, PA 19118

Plant root plasma membrane contains a NADH-linked redox system. The redox activity, using either cytochrome c or ferricyanide as e^- acceptors, is not significantly affected by the presence of Ca and Cd cations. However, unlike Ca^{2+}, Cd^{2+} induced a redox-dependent light scattering increase of the vesicles. The extent of the increase was proportional to the concentration of added Cd^{2+}. This change in light scattering suggested a volume increase of the vesicles resulting from either membrane fusion or uptake of solutes. Accompanying the volume increase, a decrease of Cd^{2+} concentration in the extra vesicular space was observed by the use of divalent cation specific metallochromophore. This observation indicated an uptake of Cd^{2+} by the vesicles. Under a given redox condition, a similar percentage of decrease over a wide range of initial Cd^{2+} concentration was detected. This result suggests that the redox reaction may develop a similar trans-membrane Cd^{2+} potential. Since the membrane assumes an inside-out orientation in isolated vesicles, the study suggests a possible mechanism of plant cells to export toxic metal ions.

Th-Pos437

RED BLOOD CELL MEMBRANE PERMEABILITY ASSESSMENT OF PARAMAGNETIC MRI CONTRAST AGENTS

Y. Li and T. E. Conturo
Mallinckrodt Institute of Radiology .
Washington University School of Medicine, St. Louis, Missouri, U.S.A. 63110

Electrically neutral gadolinium (Gd) chelates have been used clinically as magnetic resonance imaging (MRI) contrast agents (e.g., Prohance™ and Omniscan™). To evaluate the use of these agents as plasma perfusion tracers, an NMR spectroscopic assay has been developed to determine the contrast agent permeability to cell membranes. T_1 relaxation enhancement of intracellular phosphate (Pi) is detected as evidence of intracellular agent. Unlike assays involving radioactivity, there is no need to separate cells from extracellular fluid and no contamination from extracellular Gd, and equilibration of Gd into RBCs can be studied.

Packed red blood cells were washed and buffered in citrate-phosphate-dextrose buffers with inhibition of anion transport to establish a high RBC Pi concentration and a stable transmembrane 0.9 unit pH gradient. ^{31}P NMR spectra were recorded at 7.05T and 28°C. The intracellular and extracellular Pi resonances were well resolved by 1.02 ppm due to the pH gradient. T_1 relaxation times were measured before and after addition of 1mM Gd(DTPA-BMEA) (Optimark,™ Mallinckrodt Medical, Inc.). Extracellular Pi T_1 was shortened from 11.9 sec to 0.295 sec upon addition of Gd, in agreement with the Gd relaxivity and the extracellular volume. Intracellular Pi T_1 was progressively shortened over time from 5.05 sec precontrast to 2.79 sec at 9 hr 40 min. The intracellular Gd concentration was calculated to be 15 μM 50 min after addition of the agent, and reached 106.5 μM after 9 hr 40 min. From these data, the first order rate constant for permeability through the RBC membrane was 0.0651 $day,^{-1}$ or over 300 times as slow as renal excretion. Similar results are expected for the other neutral contrast agents. Although the studied agent does possess some RBC membrane permeability, these data suggest that these neutral agents can be treated as plasma markers.

Th-Pos438

A Na^+-INDEPENDENT-K^+-DEPENDENT ACID LOAD RECOVERY MECHANISM IN LYMPHOCYTES. Portales, Diana[1]., González-Amaro, Roberto[1]. and Sánchez-Armáss, Sergio[2]. Inmunology [1] and Neuronal Physiology[2] Laboratories, Facultad de Medicina A.P. 1521-B San Luis Potosí, S.L.P. México. In the search of intracellular pH (pH_i) regulatory mechanisms in lymphocytes, we found that high K^+_o induced a fast recovery from an acid load. Normal human peripheral blood lymphocytes were stimulated by 24 h with phytohemagglutinin. The pH_i was assesed with BCECF, and the acid load was induced by the ammonium pre-pulse technique. The Na^+-free solution with high-K^+ content induced a recovery (initial rate $=v_i=0.024 \pm 0.0028$ min^{-1}, recovery 92%) similar to that obtained with Ringer solutions (RS, $v_i= 0.028 \pm 0.005$ min^{-1}, recovery 95%). In Na^+-free-5mM K^+ solution there was only a neglegible recovery. Neither the initial recovery rate nor the total recovery were significantly modified in Ca^{2+}-free-high K^+ solution. Thapsigargin preincubation (0.5 μM) prior to the acid load did not prevent the recovery seen in high-K^+ solution. The transfer of lymphocytes from RS to high-K^+ solution did not induce a cytosolic alkalinization. These results suggest that stimulated lymphocytes display a K^+/H^+ exchanger that is activated by acidification of the cytosol. Partially supported by CONACyT 1173-N9202 to RGA and 3699-N to SSA and FAI-UASLP C9-11.72 to DP.

Th-Pos439

LIGAND-INDUCED CONFORMATION CHANGES IN THE LACTOSE PERMEASE OF *ESCHERICHIA COLI*: EVIDENCE FOR TWO BINDING SITES. J. Wu, S. Frillingos, J. Voss and H. R. Kaback, HHMI/UCLA, Los Angeles, CA 90024

By using a lactose permease mutant containing a single Cys residue in place of Val331 (helix X), conformational changes induced by ligand binding were studied. Val331→Cys permease was purified and studied in dodecyl maltoside by site-directed fluorescence spectroscopy. The reactivity of Val331→Cys permease with MIANS is not changed over a low range of TDG concentrations (<0.8 mM), but the fluorescence of the MIANS-labeled protein is quenched in a saturable manner (K_d=0.12 mM) without a change in emission maximum. Over a higher range of TDG concentrations (1-10 mM), the reactivity of Val331→Cys permease with MIANS is enhanced and the emission maximum of MIANS-labeled permease is blue-shifted by 3-7 nm. The fluorescence of MIANS-labeled Val331→Cys permease is quenched by both acrylamide and iodide, but the former is considerably more effective. 0.2 mM TDG does not alter quenching by either compound, while 10 mM TDG decreases the quenching constant for iodide by about 50% and for acrylamide by about 20%. Finally, the EPR spectrum of nitroxide spin-labeled Val331→Cys permease exhibits two components with different mobilities, and TDG causes the immobilized component to increase. The results indicate that lac permease has more than a single binding site. TDG binding to a higher affinity site quenches the fluorescence of MIANS-labeled Val331→Cys permease, and occupation of a second lower affinity site causes position 331 to become more accessible from a hydrophobic environment.

Th-Pos440 ***(Presented at W-AM-A9)***

CALCIUM PERMEABILITY OF LIPID VESICLES AND FROG SKIN: THE INFLUENCE OF ACIDITY AND MEMBRANE PROTEINS. ((Todd P. Silverstein, Tracy M. Warwick, and Yi Zhang))
Chemistry Department, Willamette University, Salem, OR 97301

Acidity alters the rate of Ca^{2+} leakage across both frog skin and lipid vesicles. Ca^{2+} permeation across both membranes was biphasic, with a fast phase that was complete before the first measurement. The extent of Ca^{2+} release from sonicated phosphatidyl choline bilayer vesicles was pH-dependent during the fast phase, increasing abruptly between pH 6 and 5.5, from 35 ± 6 % to 54 ± 1 % of releasable Ca^{2+}. The slow phase of Ca^{2+} release was linear with time, and the rate was only mildly pH-dependent, decreasing from 0.135 ± 0.012 %/min at pH 7.1 to 0.072 ± 0.005 %/min at pH 3.5. Adding the membrane protein glycophorin significantly enhanced both the fast and the slow phase of Ca^{2+} release at pH 7.5, by 1.5x and 2.5x, respectively.

Calcium permeation across isolated frog skin increased exponentially with time and was fitted to a second order polynomial. Both the fast phase (complete before the first measurement) and the slow phase were pH-dependent. The initial Ca^{2+} concentration rose from 0.0 ± 0.5 μM (pH 7.5 to 5.5) to 90 ± 35 μM at pH 3.5. Furthermore, the acceleration rate of Ca^{2+} leakage across the membrane rose nearly 10-fold, from 0.002 ± 0.002 $\mu M/min^2$ (pH 7.5 to 5.5) to 0.019 ± 0.011 $\mu M/min^2$ at pH 3.5. In both membrane systems (frog skin and lipid vesicle), calcium permeability exhibited a break point around pH 5.5: Increased acidity below this range caused a breakdown in the Ca^{2+} permeability barrier of the membrane.

Th-Pos441

^{59}Fe-Transferrin(Tf) Serves as an Fe Donor for Transport by the Mitochondrial ATPase.((C-Y.Li, J.A.Watkins, and J.Glass)). Department of Medicine and Center for Excellence in Cancer Research, LSU Medical Center, Shreveport, LA. 71130.

The bovine heart mitochondrial ATPase was reconstituted into soybean phospholipid liposomes with 34 μM ^{59}Fe-NTA trapped in the liposomes in the presence or absence of ascorbate. The proteoliposomes showed 59Fe transport activity which was dependent on the presence of the ATPase. The iron transport after 2.5 hours from proteoliposomes was 51.0± 0.8% for $^{59}Fe^{+3}$ and 44.0 ±1.8% for $^{59}Fe^{+2}$ of the trapped iron. This transport corresponds to 0.013 μmole of Fe^{+3} and 0.011 μmole of Fe^{+2} transported per mg ATPase. Passive transport (i.e. in the absence of ATPase) of iron from liposomes was 5.6±2.0% for Fe^{+3} nd 4.5±1.0% for Fe^{+2} at 2.5 hrs. The transport was directly related to the concentration of reconstituted ATPase and decreased 2.5-3.7 fold if the ATPase was heat-treated at 60C°for 10 min before reconstitution. The transport appeared specific for Fe as trapped ^{14}C-dextran (M.W.5000) was transported 7.7 ± 1.7% and ^{14}C-sucrose trapped in proteoliposomes composed of PS :PE: PC (1:2:9)was only 7.1±1.7% at 2.5 hrs.If ^{59}Fe,^{125}I-labeled Tf was trapped ir soybean liposomes reconstituted with the ATPase, 59Fe transport out of the liposomes w:s observed with 56.9± 1.6% of the trapped ^{59}Fe and only 11.2 ± 0.5% of the ^{125}I transported i 2.5 hours. Passive transport of ^{59}Fe and ^{125}I from liposomes was 11.1 ± 2.3% and 2.1± 0.2% respectively. ^{59}Fe transport was partially dependent on the presence of ATP in the reaction medium as transport decreased to 29.0± 1.2% in the absence of ATP. Transport was also dependent on the ionic composition of the liposomes decreasing to 22% when the trapped KCl concentration was changed from 100 mM to 50 mM.FCCPand DCCD had little effect on ^{59}Fe transport from Tf. These results are compatible with the mitochondrial ATPase acting not only as a general iron transporter but also as being able to modulate release and transport of iron from a specific iron carrier.(support by NIH DK-37866)

Th-Pos442

EFFECTS OF CHARGE AND CONFORMATION ON MACROMOLECULE UPTAKE BY TUMORS. ((E.E.Uzgiris)) GE Research and Development Center, Schenectady, NY 12309

Much interest has been focused on the issue of drug delivery to tumors[1]. Transport of molecules from the blood circulation to tumors has been largely studied by the techniques of nuclear medicine or fluorescence. We use MR imaging to follow the uptake of macromolecules in a rat tumor model system[2]. We are thus probing the transport, not of trace amounts of material, but of significant quantities, as is required to effect the proton relaxation properties of tissue. The retention of macromolecules in the tumor interior is strongly dependent on macromolecular charge and conformation. The uptake proceeds through the capillary endothelium layer of tumors which is leaky compared to normal endothelium and thus one sees the uptake of both small molecules such as Gd-DTPA and large polymeric molecules of 400 kD, [2] a process largely driven by pressure gradients. A prolonged retention or trapping in the tumor interior is seen only for one type of molecular construct: a highly negatively charged polymeric molecule that is also likely in an extended, open conformation. An open extended conformation is deduced from nmr relaxivity measurements. Light scattering measurements are being undertaken to confirm this interpretation.

1) R.K.Jain, Scientific American,270,58,(1994).
2)L.R.Opsahl, E.E.Uzgiris, and D.R. Vera, Proc. SMR,2,909(1994)

Th-Pos443

A NOVEL METHOD FOR MODELING STEADY-STATE ENZYME SYSTEMS. ((J. Wagg & P.H. Sellers)) Rockefeller University, N.Y., N.Y., 10021.

Steady-state enzyme kinetics is based in part on the King-Altman method [1]. Lam & Priest developed an algorithm for computer based implementation of this method [2]. We have developed an alternative algorithm based on application of combinatorics and linear algebra. It is based on the methods of Happel & Sellers [3] and has a number of advantages over the method of Lam & Priest [2]. For example, unlike the method of Lam & Priest [2], the new algorithm can be used with another algorithm specifically designed to facilitate solution of isotope-exchange equations [4]. In addition, the underlying linear algebra and combinatorics of our new method can be implemented using matrix theory and since most programming languages are designed to work with matrices the method is readily amenable to computer based implementation. The new algorithm is being incorporated into an existing software package (SCoP; distributed by Simulation Resources of Berrien Springs, MI, USA) to facilitate kinetic analysis of sets of linked biochemical reactions, e.g., proposed mechanisms for multireactant/multiproduct osmoenzymes such as the Na,K-ATPase.

[1] King, E.L. & Altman, C.. J. Phys. Chem. 60:1375-1378, 1956.
[2] Lam, C.F. & Priest, D.G.. Biophysical J. 12:248-258, 1972.
[3] Happel, J. & Sellers, P.H.. J. Phys. Chem. 96:2593-2597, 1992.
[4] Wagg, J. J. theor. Biol. 128:375-385, 1987.
Supported by HHMI and NIH HL-36783.

Th-Pos444 *(See EPR/ODMR/ESR posters)*

OPTICAL AND EPR SPECTROSCOPIC STUDIES OF THE SEMIQUINONE FORM OF D-LACTATE DEHYDROGENASE OF ESCHERICHIA COLI. ((Z.-Y. Sun[a], S. R. Dowd[a], C. Felix[b], J. S. Hyde[b], and C. Ho[a])) [a] Dept. of Biol. Sci., Carnegie Mellon Univ., Pittsburgh, PA 15213; [b] Biophys. Res. Inst., Medical College of Wisc., Milwaukee, WI 53226.

D-Lactate dehydrogenase (D-LDH) of *E. coli*, MW 65,000, is a membrane-associated flavoprotein that oxidizes D-lactate to pyruvate while the cofactor FAD is being reduced. The semiquinone (one-electron reduced) form of D-LDH has been observed and characterized by optical and EPR spectroscopies, as a first step toward understanding the electron transfer mechanism of D-LDH. During the reaction of the fully reduced enzyme with nitroxide spin-labels, a D-LDH semiquinone is observed transiently; when the reaction proceeds in the presence of the substrate, D-lactate, this semiquinone form of D-LDH is stabilized. The optical and EPR spectra of the D-L D H semiquinone are similar to those of an anionic semiquinone FAD. Further studies, including titrations using the substrate or dithionite, and photoreduction experiments, suggest that the D-LDH semiquinone is not thermodynamically stable, but may be accumulated kinetically during the enzyme turnovers. Results of EPR experiments also suggest that divalent ions, such as Zn^{++}, may help stabilize the semiquinone form of D-LDH. [This work is supported by NIH grants GM-26874 and RR-01008.]

Th-Pos445

ENZYMIC TRANSDUCTION OF FLUCTUATING ELECTRIC SIGNALS. ((T.D. Xie[1], Y.-D. Chen[2,3], P. Marszalek[1] and T.Y. Tsong[1,3])) [1]Dept of Biochem, U of Minnesota, [2]NIDDKD, NIH, and [3]Dept of Biochem, Hong Kong U of Sci & Technol, Clear Water Bay, Kowloon, Hong Kong. (Spon. by H.M. Chen).

Membrane enzymes have the ability to transduce a signal or energy from a periodic potential such as an electric, acoustic, osmotic, or chemical potential. A previous study (Biophys. J. 67:1247 (1994)) showed that this energy coupling also applies to random telegraph fluctuating electric fields (RTF) (consisting of alternating square electric pulses of constant amplitude but of random lifetime) . To mimic more closely the catalytic action of an electric energy-transducing enzyme in a cell membrane, and to develop a general theory of electroconformational coupling (ECC), we have investigated further the effects of the combined lifetime/amplitude fluctuations on the efficiency of the energy coupling. Square electric pulses were produced by a Wavetek Model 166, 50 MHz Pulse/Function Generator which was controlled by a PC. The PC drove the pulse generator to give a train of electric pulses with lifetime fluctuating according to the RTF and amplitude fluctuating according to the Gaussian distribution function. It is shown that for an RTF signal with a given mean lifetime, the efficiency of energy coupling for the Na,K-ATPase of human erythrocytes (as monitored by the ouabain-sensitive Rb^+ pumping) depended on the standard deviation (SD) of the Gaussian function. For a field at the optimal mean frequency, the efficiency was higher for smaller SD, and lower for larger SD. For fields which digressed from the optimal frequency, the dependence of efficiency on SD was non-monotonic. Theoretical analyses were performed using the Monte Carlo method and the stochastic differential equation method. Calculations of the efficiency of energy coupling produced the main features of the experimental data. These results reaffirm the biological relevance of the ECC model. However, there was some discrepancy between experiment and theory for data obtained with RTFs which departed from the optimal frequency. Further study would be required (Correspondence to T.Y.T., Hong Kong).

Th-Pos446

CONTROL OF SINUSOIDAL (AC) MEMBRANE POTENTIAL (Ψ_{AC}) IN GIANT BARNACLE MUSCLE FIBERS UP TO 100 kHZ. ((C.M. Philips & L.W. Horn)). Dept. Physiol., Temple University School of Medicine, Philadelphia, PA. 19140

Transporter kinetic rate coefficients can be assayed by measuring stationary state transporter current amplitude or tracer flux as a function of the frequency (f) of an applied AC field (Horn, *BIOPHYS.J. 64*:281). The normal mode f's of this response function can span 4 or more decades. Series resistance (R_s) and a large membrane capacitance (C_m) usually prevent effective control of Ψ_{AC} at f > 1 kHz because the membrane impedance approaches zero. We have developed a feedback controller, which uses the usual glass pipette electrodes for the DC voltage plus a separate AC voltage measured with a wire electrode; a boost circuit to anticipate the R_sC_m filter; and a method for estimating equivalent circuit parameters of the cell (R_s, C_m and membrane resistance R_m) which employs a digital lock-in amplifier to measure the phase (ϕ) of the membrane current to at least 0.05° accuracy. The measured ϕ and circuit parameters can be used at any f to estimate Ψ_{AC}. Circuit parameters can also be estimated at any f in order to adjust for apparent f-dependence. We tested our system using standard R_mC_m circuits with R_s for a broad range of circuit parameters. The controller can maintain Ψ_{AC}'s up to 30 mV (rms) between DC and 100 kHz. The AC voltage applied between cytoplasm and ground changes 100-fold over this f-band, while the AC current changes 10^4-fold. Ψ_{AC} can be estimated and controlled by our technique to ± 2% accuracy up to 75 kHz and to ± 5% between 75 and 100 kHz. Since the transporter f-response for "small" amplitude voltages is proportional to Ψ_{AC}^2, it is possible to measure transporter f-responses at constant Ψ_{AC} with good accuracy up to 100 kHz. Reliable estimation of system time constants as small as 1.6 μsec is feasible. [Supported by the Eppley Foundation for Research].

Th-Pos447

RECONSTITUTION OF A VANADATE-SENSITIVE, PS-STIMULATED Mg^{2+}-ATPASE FROM HUMAN ERYTHROCYTE MEMBRANES. ((M. L. Zimmerman, and D. L. Daleke)) Department of Chemistry, Indiana University, Bloomington, IN 47405.

We have purified a vanadate-sensitive Mg^{2+}-ATPase from human erythrocytes that may be identical to the erythrocyte aminophospholipid flippase, an inwardly-directed, PS- and PE-specific transporter. Using detergent-phospholipid-protein mixed micelles we have shown previously that this ATPase is uniquely activated by PS (*Biochemistry* 32 (1993) 12257-12263). The enzyme is inactive in the absence of added phospholipid or in the presence of zwitterionic (PC, SM) or neutral lipids. Negatively charged lipids (PA, PI, PG) and PE partially activate the enzyme (20 - 80% of PS). In the present work, we reconstitute the enzyme into model membranes and re-examine the ability of lipids to activate the ATPase. Detergent-solubilized protein was mixed with phospholipids and the detergent was removed using hydrophobic beads (SM-2 Bio-Beads). Transmission electron microscopy of the reconstituted proteoliposomes indicates that the vesicles have an average diameter of 50 nm. The size and integrity of the vesicles was confirmed by including NBD-PC in the detergent-phospholipid-protein mixture prior to reconstitution and measuring the susceptibility of the fluorophore to externally added dithionite. Although up to 50% of the protein was lost during reconstitution, full activity of the remaining protein was recovered upon addition of PS and detergent. The ATPase was inactive when reconstituted in the presence of PC alone, consistent with our results in mixed micelles. Using PC as a carrier lipid, the enzyme was maximally activated when reconstituted in the presence of 20 mol% PS. PE, another flippase substrate, partially activated the enzyme (44% of PS V_{max}). However, in contrast to our results using mixed micelles, PI (up to 20 mol%) was unable to activate the enzyme in the absence of PS or PE. These data indicate that the reconstituted ATPase, unlike the enzyme in detergent micelles, shows a specificity for its lipid activator that is identical to the lipid specificity of the aminophospholipid flippase.

Th-Pos448

DIRECT MEASUREMENT OF THE pK OF "LYSINE A" AT THE STILBENEDISULFONATE BINDING SITE ON BAND 3.

((L.M. Schopfer and J.M. Salhany)) VA & Univ. of Nebraska Med. Centers, Omaha, NE 68198-5290.

Stilbenedisulfonates are potent inhibitors of band 3 anion exchange which bind to the protein with a 1:1 monomer stoichiometry. After formation of a reversible complex, those stilbenedisulfonates with isothiocyano moieties, such as DIDS (4,4'-diisothiocyanato-2,2'-stilbenedisulfonate), react with a lysine residue known as "lysine A," even at physiological pH, where epsilon amino groups are less reactive. This lysine (thought to be lysine 539), is proposed to be unusually reactive due to an atypically low pK. We have tested this hypothesis directly, by measuring the kinetics of covalent adduct formation after reversible binding of DIDS, using a fluorescence assay for DIDS covalent adduct formation published earlier (Schopher, L.M. & Salhany, J.M., (1992) Biochemistry 31: 12610-12617). Covalent adduct formation followed exponential kinetics under all conditions studied. The reaction rate was directly dependent on hydroxide ion concentration from pH 6.3 to 9.0. From pH 9 to 10 the measured rate became dependent on band 3 concentration indicating that the non-covalent affinity of DIDS for band 3 had become weaker. Analysis of the band 3 dependence of the measured rate gave the limiting rates and DIDS dissociation constants (Kd) in this pH range. A plot of the limiting rate vs pH increased continuously from pH 6.3 to 10, showing no tendency to plateau. A plot of pK_d versus pH was linear with a slope of 1. The line extrapolated to a K_d at physiological pH of 6.3 nanomolar, which agrees with the estimated literature value. We conclude that "lysine A" does not have an abnormally low pK, contrary to previous indications to that effect. We suggest that the high reactivity of "lysine A" at physiological pH can be explained on the basis of steric considerations alone.

Th-Pos449

Expression and function of a cysteine-less mutant form of human AE1. R.T. Timmer, P.A. Smith, and R.B. Gunn, Dept. of Physiology, Emory University School of Medicine, Atlanta, GA 30322-3110

AE1 (or Band3) is the major intrinsic membrane protein of red blood cells and is responsible for Cl^--HCO_3^- exchange. The structure and topology of this protein has been the focus of many studies that have used native amino acids as sites for site-specific chemical modification or for protease cleavage. Nearly all of the topologically informative native sites occur within the first six predicted transmembrane segments (TM) of the protein, whereas the predicted hydropathy of the protein suggests 10 to 14 TMs. Thus, the topology of one-half of the transmembrane domain of the protein remains ambiguous. In order to determine the remaining topology of AE1 we have constructed a cysteine-less mutant form of the protein in which the five native cysteines of the human protein have been changed to alanines (designated AE1(Cys0)). The current report discusses the expression and function of this cysteine-less mutant. The studies described below utilize *in vitro* transcribed AE1 cRNA prepared under conditions that yield 100-200 copies of capped cRNA (80-90% capped) per template molecule. We have expressed the native protein by injection of *Xenopus* oocytes with AE1 cRNA and we find that Cl^- flux is elevated at least four-fold compared to control injected oocytes (80 pmol/oocyte-min compared to 20 pmol/oocyte-min). In addition, the AE1-mediated flux is reversibly inhibited by 1 mM DNDS. The utility of co-injection of secreted alkaline phosphatase (SEAP) as a marker for oocyte expression viability will also be discussed. The 5' and 3' untranslated regions (UTR) of the human AE1 cDNA contain several elements predicted to be refractory to expression (e.g. stem-loop structures in the 5' UTR). Therefore, we have constructed chimeric AE1 cDNAs containing the AE1 coding region fused to heterologous 5' and 3' UTRs, e.g. the UTRs from rabbit ß-globin and a plant viral RNA (STNV) that is translated efficiently. We find that the expression of AE1 is signficantly enhanced by use of heterologous 5' and 3' UTRs (up to 10 fold). The coding region for the mutant form of the protein (AE1(Cys0)) has been fused to the same heterologous UTRs for expression in *Xenoups* oocytes. The expression and activity of AE1(Cys0) in *Xenopus* oocytes is compared to the native protein. Finally, the synthesis, glycosylation, and protease sensitivity of AE1(Cys0) in cell-free translation systems (rabbit reticulocyte and wheat germ extract) is compared to the wild-type protein. This research supported in part by NIH grant R37HL28674 to R.B. Gunn and NIH NRSA Postdoctoral Fellowship F32HL08989 to R.T. Timmer.

Th-Pos450

EFFECT OF CHLORIDE ON THE INITIAL STEP IN STILBENEDISULFONATE BINDING TO BAND 3.

((J.M. Salhany, R.L.Sloan, K.A.Cordes & L.M. Schopfer)) VA and Univ. of Nebraska Med. Centers, Omaha, NE 68198-5290.

The molecular basis for chloride and stilbenedisulfonate interaction on band 3 was investigated by measuring the kinetics of DBDS (4,4'-dibenzamido-2,2'-stilbenedisulfonate) binding to unsealed human erythrocyte ghosts and to the isolated transporter using stopped-flow fluorescence. Our results show biphasic DBDS binding kinetics. We characterized the DBDS concentration dependence of the apparent rate constants for both phases of the reaction for the first time. We then tested the effect of addition of chloride on individual rate constants. In unsealed ghosts, the fast phase apparent rate constant showed a second-order dependence on DBDS concentration, while the slow phase apparent rate constant showed saturation kinetics. These results are consistent with a classical two step binding mechanism:

$$\text{DBDS} + (\text{Band 3}) \underset{k_{-1}}{\overset{k_1}{\longleftrightarrow}} (\text{DBDS-Band 3}) \underset{k_{-2}}{\overset{k_2}{\longleftrightarrow}} (\text{DBDS-band 3})^*$$

with $k_1 = 1.2 \times 10^6\ M^{-1}\,sec^{-1}$; $k_{-1} = 2.7\ sec^{-1}$; $k_2 = 2.3\ sec^{-1}$ and $k_{-2} = 0.05\ sec^{-1}$ in the absence of chloride at physiological ionic strength. The isolated transporter also showed a biphasic time course for DBDS binding, but it had a significantly faster overall reaction velocity. This difference in reactivity was attributable to a 10-fold larger value for k_1 and a 6-fold larger value for k_{-2} when the reactions were studied in the absence of chloride. Furthermore, in contrast to band 3 in unsealed ghosts, the isolated transporter showed an apparent zero-order dependence on DBDS concentration for the slow phase of the reaction due to a 5-fold reduction in K_1 (= k_{-1}/k_1). This comparison suggests that solubilization and isolation of the transporter produces a conformational change at the intramonomeric stilbenedisulfonate site. Addition of chloride caused an acceleration in the overall binding reaction. Quantitative analysis of the reaction in unsealed ghosts revealed that chloride accelerated the reaction by increasing k_{-2} without altering k_1, k_{-1} or k_2 significantly. Chloride also had no significant effect on k_1 or k_{-1} for isolated band 3, but it did increase the apparent slow phase rate constant about 15-fold. Thus, chloride does not block or slow the initial binding of stilbenedisulfonates to band 3. Rather it increases the rate of a conformational isomerization step which occurs subsequent to inhibitor binding. We conclude that band 3 binds chloride and stilbenedisulfonates to form a ternary complex, with allosteric interactions between the substrate and inhibitor binding sites.

Th-Pos451

EVIDENCE FOR TWO DISTINCT Mg^{2+} EFFLUX MECHANISMS IN LIVER PLASMA MEMBRANE ((A. ROMANI, C. LUCA, B. GRIMBERG and A. SCARPA)) Dept. Physiol. & Biophys., CWRU, Cleveland, OH, 44106-4970, USA

The adrenergic stimulation of cardiac or liver cells prompts a large Mg^{2+} extrusion across their plasma membrane. Preliminary experimental evidence suggests the presence of a Na^+/Mg^{2+} exchanger inhibited by amiloride, and a Mg^{2+} influx inhibited by Ca^{2+}-channel blockers. We investigated the hepatocyte Mg^{2+} efflux pathways using purified plasma membranes isolated from rat livers, and loaded with 20 mM Mg^{2+}, in the absence or in the presence of 5 mM ATP. The vesicles were incubated in a medium devoided of permeant ions (200 mM Sucrose, 50 mM TRIS, pH 7.4) and Mg^{2+} efflux was measured by atomic absorbance spectrophotometry, after addition of increasing concentrations of different ions and rapid sedimentation of plasma membranes. The vesicles loaded only with Mg^{2+} extruded a sizeable amount of Mg^{2+} when NaCl, but not $CaCl_2$ or KCl, was added to the incubation medium. The extrusion by NaCl could not be accounted for by changes in osmolarity, since no Mg^{2+} efflux was stimulated by the addition of equiosmolar concentrations of Na-isothionate or choline chloride, and was almost abolished in the presence of amiloride. By contrast, the vesicles loaded with 20 mM Mg^{2+} plus 5 mM ATP extruded less Mg^{2+} upon addition of extravesicular NaCl, but released a larger amount of Mg^{2+} upon addition of increasing concentrations of Ca^{2+}. Under these experimental conditions, the co-addition of Ca^{2+} and Na^+ had an additive effect on Mg^{2+} efflux. Moreover, the Ca^{2+}-mediated Mg^{2+} efflux could also be induced by other divalent cations (Mn^{2+}, Ba^{2+}, Sr^{2+}, Co^{2+} and, to a lesser extent, Cd^{2+}), was inhibited by amiloride, but was not affected by the Ca^{2+}-channel blockers verapamil or nifedipine. A similar extrusion pattern was also observed when the vesicles were loaded with 20 mM Mg^{2+} plus 5 mM GTP or ADP, but not ATPγS. These data are the first evidence in purified liver plasma membranes for the operation of two distinct Mg^{2+} extrusion mechanisms. The first mechanism is a Na^+-dependent pathway, tentatively identified as a Na^+/Mg^{2+} exchanger, whereas the second mechanism is a Na^+-independent, ATP requiring, extrusion pathway which may exchange cellular Mg^{2+} for Ca^{2+} or other external divalent cations. Supported by N.I.H. HL 18708.

RECEPTORS AND KINASES

Th-Pos452

FUNCTIONAL INFERENCES FROM STRUCTURAL MODELS OF THE RAT δ, κ AND μ OPIOID RECEPTORS

Daniel Strahs and Harel Weinstein. Dept. of Physiology and Biophysics, Mt. Sinai School of Medicine, CUNY, New York 10029-6574

We have developed 3-D structural models of the recently-cloned opioid receptors (δ, κ and μ), members of the G-protein-coupled receptor (GPCR) superfamily. Using techniques of homology modeling, we have constructed models of the transmembrane helix (TMH) bundles. Initial predictions of the structural elements are based on the consensus indicated by average properties (e.g. hydrophobicity, conservation, and variability) and structural periodicities of these properties extrapolated from a multiple sequence alignment of opioid, somatostatin, angiotensin and related receptors *[Ballesteros and Weinstein, (1994) Meth. Neurosci., 25:366-428]*. The receptor models were constructed using the assumptions 1) that the helix bundle topology adopts a rhodopsin-like structure; 2) that the bundle structure is uniquely determined by helix-helix interactions, not by the connecting loops; and 3) that closely-related GPCRs are structurally homologous. The modeling indicates that several residues predicted in the interior of the helix bundle may contribute to the binding site of the ligands; these residues include M1.36(72), N3.35(150), F5.57(243), and N4.49(191) (the numbering scheme indicates both the relative and invariant positions of the mutation - *[Ballesteros and Weinstein, loc. cit.]*). Two single-site mutants of the μ receptor which have been investigated experimentally *[Surratt et al. (1994) J. Biol. Chem. 269, 20548-53]*, D3.32(147)A (predicted to be in the bundle interior) and H6.52(297)A (predicted to lie on the interface between TMHs 5 and 6) have also been modeled with MD simulations in order to evaluate the effects of the mutations upon bundle topology and binding site characteristics. (Supported by NIH Grants T32-DA07135 [D.S.] and DA-00060 [H.W.])

Th-Pos453

IDENTIFICATION OF THE TNFα RECEPTOR IN RAT CARDIAC MYOCYTES AND THE INHIBITORY EFFECTS OF TNFα ON L-TYPE Ca^{2+} CURRENTS

((K. Krown, K. Yasui, M. Brooker, A. Guintivano, R. Sabbadini, C. Nguyen and P. Palade)) Dept. of Biology San Diego State Univ., San Diego CA 92182. Dept. of Physiology and Biophysics Univ. of Texas Med. Branch, Galveston TX 77550.

The cytokine, tumor necrosis factor alpha (TNFα) mediates a diverse array of biological effects by its interaction with either p60 (type I) or p80 (type II) receptors. However, the mechanisms responsible for its cardiotoxic effects are poorly understood in part because the receptor(s) which mediate TNFα actions in the heart have not been characterized. We have addressed this problem by identifying TNFα receptors in rat cardiac cells using immunological, biochemical, molecular and physiological techniques. The type I receptor was demonstrated in cardiac membranes by Western blot analysis using monoclonal antibodies. The receptor is functionally competent as evidenced by ^{125}I-TNFα ligand binding experiments which included competition by unlabelled murine TNFα. Successful RT-PCR using a rat cardiac cDNA library resulted in a fragment which codes for the rat type I receptor and is consistent with expression of the receptor in cardiac cells. Further evidence for the existence of functional TNFα receptors was demonstrated physiologically by the significant TNFα-induced inhibition of L-type channel Ca^{2+} currents recorded from whole cell patch-clamped myocytes. These results are the first to confirm the existence of TNFα receptors in the heart cells and suggest that negative inotropic effects of TNFα on the heart may involve TNFα receptors and a decrease in the L-channel conductance. Supported by the AHA and the MDA.

Th-Pos454

ACTIVATION OF HUMAN CLASS II METABOTROPIC GLUTAMATE RECEPTORS CAN BE COUPLED TO CHANGES IN $[Ca^{2+}]_i$ THROUGH COEXPRESSION WITH THE RAT CYCLIC NUCLEOTIDE-GATED OLFACTORY CHANNEL. ((S.D. Hess, F.-F. Lin, S. Rao, L. Daggett, R. Kuhn, G. Velicelebi and E.C. Johnson)) SIBIA, Inc., 505 Coast Blvd. S., La Jolla, CA 92037 and CIBA-Geigy, Basel, Switzerland.

To facilitate rapid detection of adenylate cyclase inhibition resulting from activation of class II metabotropic receptors, we coupled activation of hmGluR2 or hmGluR3 to changes in $[Ca^{2+}]_i$ that could be measured with fluorescent dye-based assays. To this end, we transiently coexpressed hmGluR2 and the rat cyclic nucleotide-gated olfactory channel (rCNG; Dhallan et al., Nature 347:184) in HEK293 cells. In cells transfected with rCNG, application of 100 μM forskolin and 1 mM IBMX elicited a rise in $[cAMP]_i$ as measured by RIA to 578 ± 149 pmols per 600K cells (mean, S.D., $n=4$), which corresponds to approximately 50 μM cAMP. Digital video imaging of fura-2 loaded cells showed, in response to forskolin/IBMX, a sustained increase in $[Ca^{2+}]_i$ in 46 ± 28% of the cells ($n=3$). Markedly fewer cells responded to lower forskolin concentrations (10 or 50 μM). In cells transfected with both the rCNG and hmGluR2, 1 mM glutamate inhibited the forskolin-stimulated increase in $[cAMP]_i$ by up to 45%. Addition of 1 mM glutamate 2 min prior to forskolin/IBMX inhibited the $[Ca^{2+}]_i$ increase detected in the population average by reducing both the percentage of cells that exceeded the criterion response (from 44 to 14%, $n=2$) and by decreasing their response amplitudes. There was no significant effect of glutamate on the latency or time-to-peak of the $[Ca^{2+}]_i$ response. Glutamate also inhibited the population $[Ca^{2+}]_i$ increase in cells transfected with rCNG and hmGluR3 by lowering the percentage of cells that responded from 60 to 10% ($n=2$) and the amplitude of responding cells. These results demonstrate a novel method to rapidly detect modulation of $[cAMP]_i$ following activation of mGluR2 or mGluR3.

Th-Pos455

THE IP_3 GATED Ca^{++} CHANNEL; EFFECT OF THE PROTEIN THIOL REAGENT THIMEROSAL ON CHANNEL CONDUCTIVITY ((E. Thrower, H. Duclohier, E.J.A. Lea, G. Molle, A.P. Dawson,)), School of Biological Sciences, University of East Anglia, Norwich, NR4 7TJ, UK; URA 500 CNRS, Université de Rouen, Blvd. M. de Broglie, 76821 Mont-Saint-Aignan, France.

Rat cerebellum inositol 1,4,5-trisphosphate receptor has been solubilised and purified to apparent homogeneity using a two step purification procedure, the major step involving heparin affinity chromatography. The purified receptor has been reconstituted into planar lipid bilayer membranes by the 'dip-tip' method resulting in low noise current records. Single channel events were recorded after addition of 10μM IP_3 and 50μM ATP to the cis (cytoplasmic) side. The single channel current step was approximately 3 pA at zero p.d. and the single channel slope conductance was approximately 60pS, with 53mM Ba^{++} on the trans (luminal) side as the current carrier. In the presence of 100 μM thimerosal, a protein thiol reagent, the single channel conductance was generally 60pS, although a higher channel conductance of 80pS was observed as well. On the basis of all points histograms which can be used to determine the percentage time of the recording the channel spends in a particular state, the IP_3 receptor was found to be in the closed state for 60% of recording time, at the 60pS conductance level for 35% recording time, and at the 80pS level for 5% recording time. It can be concluded that thimerosal causes the IP_3 receptor to open to the control level (i.e. 60pS) but either enhances the effect of IP_3 or affects the channel directly by causing it to switch to a higher sub-conductance level (80pS) for a shorter duration.

Th-Pos456

PROTEIN - AND NOT CARBOHYDRATE - IS THE DETERMINANT FOR THE BINDING OF AEROLYSIN TO ITS GLYCOPROTEIN RECEPTOR. ((H.U. Wilmsen, W. Aschauer, H.J. Gruber, H. Schindler and J.T. Buckley*)) Inst. of Biophysics, University of Linz, Austria and *Dept. for Biochemistry and Microbiology, University of Victoria, Victoria B.C., Canada

Rat erythrocytes contain a 47 kDa glycoprotein that promotes membrane insertion and channel formation by the bacterial toxin aerolysin when it is reconstituted into planar lipid bilayer membranes. Treatment of the partially purified receptor with neuraminidase increased aerolysin binding and the rate of channel formation, as well as its sensivity to trypsin, suggesting that the toxin binds to a trypsin-sensitive site that is partially masked by sialic acid residues.
Complete masking was achieved by treating the receptor with wheat germ agglutinin. These results, as well as observations that receptor activity is not affected by periodate treatment, or by the presence of a range of simple and complex sugars, lead to the conclusion that at least part of the binding determinant is in the receptor's polypeptide chain, rather than in the carbohydrate portion of the molecule.

Th-Pos457

STRUCTURAL STUDIES OF LEUKOCYTE INTEGRINS BY CRYO-ELECTRON MICROSCOPY ((D. Cabral-Lilly, T.A. Springer*, M.S. Diamond* and G.G. Shipley)) Department of Biophysics, Boston University School of Medicine, Boston, MA and *Center for Blood Research, Harvard Medical School, Boston, MA

The leukocyte integrins, LFA-1, Mac-1 and p150,95, are transmembrane receptors of homeopoietic cells that play a key role in cell adhesion. The receptor complex is an $\alpha\beta$ heterodimer where both the α and β subunits are thought to contain a large extracellular domain, a single transmembrane region and a small cytoplasmic region. Cryo-electron microscopy and single particle image analysis were used to study the structure of membrane-bound Mac-1 preserved in vitreous ice. The majority of Mac-1 was reconstituted into unilamellar vesicles in the right-side-out orientation with the large extracellular domain clearly visible at the vesicle edge. Several views of the integrin were observed, most probably corresponding to different rotational orientations of the Mac-1 as viewed in projection. The molecules are mushroom shaped with a stalk extending from the membrane and an asymmetric globular head at the end. In all views the stalk is ~40 Å long. The globular region appears asymmetric in shape. The height of this region is ~70 Å, and the diameter ranges from 75 Å to 150 Å. Density of the head could be seen extending on one or both sides of the stalk, or mostly coincident with the stalk depending on the view observed. Correspondence analysis was used to classify the particles according to the density distribution of the globular region.

Th-Pos458

HETEROLGOUS MEMBRANE PROTEIN EXPRESSION IN ARCHAEBACTERIA. ((G.J. Turner, R. Reusch, L.J. Miercke, M. Betlach, and R.M. Stroud)) Dept. Biochemistry and Biophysics, UCSF, San Francisco, CA 94143.

Endogenous expression levels for most G-protein coupled receptor proteins has hampered their biochemical and biophysical characterization. The endogenous over-expression system for Bacteriorhodopsin was exploited to create a halobacterial expression system capable of producing heterologous membrane proteins. Prototype cloning vectors (designated pENDS), useful for linking sequences of the *bacterio-opsin* gene (*bop*) to coding sequences of heterologous genes, have been constructed. These vectors: i) generate fusions with various portions of the Bop protein coding region in effort to stabilize transcription and/or translation products, or ii) introduce coding sequences which "tag" gene products for the purposes of identification and/or purification, and iii) generate DNA fragments with cloning sites appropriate for transfer of heterologous genes into *H.salinarium* expression vectors (designated pHex). *bop* gene fusions and heterologous constructions being tested for expression include: i) C-terminal tagged Bop (heamagluttinin and 6-His), ii) human muscarinic receptor, iii) human serotonin type 5HT1c, and iv) yeast α mating factor receptor Ste2. pHex vectors containing *bop* gene constructions and heterologous gene coding sequences were introduced into appropriate *H.salinarium* strains. Cultures have been grown under conditions known to induce high level expression of Bop. Southern analysis indicated stably maintained plasmid copies of all introduced genes. Northern analysis indicated that sequence alterations introduced into the *bop* gene and associated regulatory regions did not alter the stability or abundance of *bop* message. Northern analysis revealed full length mRNA in all heterologous gene constructions. On characterizing the Bop constructions a novel membrane associated proteinase was identified which may be useful for separation of chimeric sequences.

Th-Pos459

TERBIUM AS A MODULATOR OF CISPLATIN ACCUMULATION IN HUMAN BREAST CANCER CELLS ((K.M. Mack, *P.A. Andrews and R.G. Canada)) Department of Physiology & Biophysics, Howard Univ. Coll. Medicine, Washington, D.C. 20059 and *Department of Pharmacology, Georgetown Univ.,Rockville, MD 20850

Cisplatin (DDP) is an effective anticancer drug. Recently, we found that terbium (Tb^{3+}) can enhance the accumulation of DDP in DDP-sensitive and DDP-resistant MCF-7 (estrogen dependent) and MDA (estrogen independent) human breast tumor cells. Tb^{3+} at 100 uM increased the accumulation of DDP in the parent MCF-7 cell line, 2.0-fold resistant MCF-7/A8 and the 4.3-fold resistant MCF-7/CH cells by 72, 75, and 129%, respectively, as assessed by atomic absorption spectrophotometry. In addition, Tb^{3+} also increased the accumulation of DDP in the parent MDA cell line, 5.7-fold resistant MDA/A13 and 10-fold resistant MDA/CH cells by 56, 72, and 51%, respectively. We believe that the enhanced cellular accumulation of DDP is facilitated by the receptor binding of Tb^{3+}. Time-resolved luminescence was used to obtain equilibrium binding constants for the Tb^{3+} binding sites. The binding affinity of Tb^{3+} was the same for each cell type. The I_{max} for the Tb^{3+}/cell complex correlated with the degree of enhancement of DDP accumulation. Our findings suggest that the combination of Tb^{3+} and DDP may enhance the cytotoxicity of DDP in both DDP-sensitive and DDP-resistant breast cancer cells.

Th-Pos460

MODEL OF A COMPLEX OF THYROTROPIN RELEASING HORMONE WITH ITS RECEPTOR ((L. J. Laakkonen[1], F. Guarnieri[1], J. H. Perlman[2], M. C. Gershengorn[2], R. Osman[1])) [1]Physiology & Biophysics, Mount Sinai School of Medicine, New York, NY 10029, [2]Division of Molecular Medicine, Cornell Univ. Med. College, New York, NY 10021 (spon. by W. A. Brodsky)

Templates for the transmembrane domain of bacteriorhodopsin (brd) and rhodopsin (rhd) structures have been built based on Baldwin's analysis of G-protein coupled receptor (GPCR) sequences. The templates provide guidelines for positioning, tilting and orienting the helices in seven transmembrane bundles. The existing brd structure has served both for scaling the templates and for relative vertical positioning of helices in the bundle. A construction of brd based on the template agrees well with the known structure. A model of rhd constructed on its template satisfies the known interaction, which was not used in the construction, between Lys296 in helix 7 and Glu113 in helix 3. Thus, the template can serve as a general guide for constructing molecular models of GPCRs. A model of the thyrotropin releasing hormone (TRH) receptor was built on the rhd template. The model agrees well with our mutational data and shows an intricate network of H-bonding in the proposed ligand binding pocket. The network has to be partially disrupted to allow the ligand to interact with residues in helices 3, 6 and 7 known to directly bind TRH. Based on the known interactions, the TRH was docked inside the receptor and mixed mode Stochastic Dynamics/Monte Carlo simulations were conducted to explore the available conformational states of the complex. The analysis of the complex shows that Tyr106 and Asn110 in helix 3 interact with the $pGlu^1$ residue of TRH, Tyr282 in helix 6 interacts with His^2 of TRH, and Arg306 in helix 7 interacts with the Pro^3NH_2 of the ligand. *Supported by NIH grant DK 43036.*

Th-Pos461

A STRUCTURAL AND FUNCTIONAL ROLE FOR THE CONSERVED NP/DP MOTIF IN HELIX 7 OF GPCR INFERRED FROM A 3D MODEL OF THE GNRH RECEPTOR. ((Karel Konvicka, Juan A. Ballesteros, Harel Weinstein)) Department of Physiology and Biophysics, Mount Sinai School of Medicine, New York, NY 10029.

In collaborative studies involving experimental probing of structure-function relations in the receptor for gonadotropin releasing hormone (GnRH) (Zhou et al., Mol. Pharmacol. 45, 165:170, 1994) we explore the mechanism of ligand binding and receptor activation using computational modeling. The key role of helix 7 suggested by the effects of mutations on ligand binding and activation focused attention on the NP (or DP as in the GnRH receptor) motif of amino acids which is conserved in most G-protein coupled receptors (GPCR). A search of structural databases revealed that the combination of the proline kink with the hydrogen bonding properties of N (or D) produces a characteristic break of the helix, and a flexible hinge which accommodates a large rearrangement in the orientation of the helix face ("Pro-kink face shift": Ballesteros & Weinstein, Biophys. J., 62:101, 1992). These special structural properties of the NP (or DP) motif are essential in determining two key characteristics of our receptor model: One is the proximity of D(319) in helix 7 to N(87) in helix 2 (Zhou et al., loc. cit.) which is achieved consistent with Oprian's findings in rhodopsin (Rao et al., Nature 367, 639:641, 1994). The other is a proposed mechanism for receptor activation due to ligand binding. The activation involves an isomerisation of the DPxxY motif in helix 7 that interacts with a cluster of conserved aromatic residues in helices 5 and 6. The conserved nature of the structural elements involved in this mechanism suggests that it may be general for all GPCR in which they appear. *Sponsored by NIH grants DK-46943 and DA-00060.*

Th-Pos462

MODELING TRANSMEMBRANE HELIX CONTACTS IN GPCR. ((Juan A. Ballesteros and Harel Weinstein)) Dept. of Physiology & Biophysics, Mount Sinai School of Medicine, New York, NY10029. (Spon. by Mark Glucksman)

A key issue in modeling the structure of G-protein coupled receptors (GPCR) is the prediction of helix-helix (Hx-Hx) packing interactions (Ballesteros and Weinstein, Meth. Neurosci. 25:366,1994). Three approaches to predict such contacts are illustrated with a model of the transmembrane portion of the 5-HT2C GPCR. 1) Helical patches of interior facing residues can predict the tilt of the Hxs: Residues within each helix were predicted individually to face the lipid, or the interior of the Hx-bundle. When analyzed on helical net representations, interior-facing residues defined continuous patches on each Hx surface. The tilt of each Hx in the bundle can be predicted from the tilting of these patches, and agrees with the Hx tilt reported for rhodopsin. These patches can be paired among Hxs to provide a prediction of specific Hx-Hx interfaces, assuming an anticlockwise and sequential Hx packing. 2) Positions in the sequence alignment of GPCRs that exhibit coordinated substitution patterns during evolution indicate spatial proximity: When coordinated sites form continuous patches, consistent with α-helical periodicity, they define Hx-Hx interfaces. Residue-to-residue interhelical contacts inferred from this criterion define relative heigths among the seven Hxs. This approach was validated experimentally for a predicted Hx2-Hx7 interaction (Zhou et al., Mol. Pharmacol.45:165,1994). 3) A resulting 3D-model of the 5-HT2C receptor is consistent with steric constraints derived from data on double revertant mutants and covalent attachment of ligands. This agreement is achieved by paying attention to the special Pro-kink conformation in Hx7 produced by H-bonding within the conserved NPxxY motif. *Supported by NIH: DA-06620, DA-09083 and DA-00060, and by Fulbright/MEC (Spain) (to JAB).*

Th-Pos463

PEPTIDES DERIVED FROM MOUSE FcγRII THAT ALTER IgG-FcγRII INTERACTIONS ((Edie C. Bowles, Bruce W. Erickson and Nancy L. Thompson)) Department of Chemistry, University of North Carolina, Chapel Hill, NC, 27599-3290

Fc receptors, which are transmembrane proteins found on the surfaces of immune cells, aid in the removal of foreign pathogens by binding to antibody-coated targets via the antibodies' Fc regions. Using the pin technique, 170 overlapping dodecapeptides were synthesized to cover the extracellular region of mouse FcγRII. These peptides were screened for antibody binding activity using multivalent mouse IgG immune complexes. Two peptides with ability to bind the immune complexes were identified: U058, RCHSWRNKLLNR, 109-121; and U059, CKGSLGRTLHQSK, 150-163. These two peptides were synthesized, oxidized to yield dimeric forms (U058d and U059d) or alkylated to give monomeric forms (U058m and U059m). Of the four peptides, only U058d altered the binding of immune complexes to immobilized FcγRII. This peptide enhanced binding at low concentrations and abolished binding at higher concentrations. Evidence for the direct interaction of U058d with IgG was provided by the observation that this peptide is retained on an IgG affinity column. Finally, the ability of the four peptides to alter the binding of fluorescently-labelled, monomeric IgG to mouse FcγRII in substrate-supported planar membranes was examined using total internal reflection fluorescence microscopy. These measurements showed that U058d enhances the binding of monomeric IgG and FcγRII. This work was supported by NIH grant GM-37145 (NLT) and by a Department of Education Fellowship (ECB).

Th-Pos464

AGGREGATION OF THE HIGH AFFINITY IgE RECEPTOR AND ENHANCED ACTIVITY OF p53/p56*lyn* PROTEIN TYROSINE KINASE ((T. Yamashita, S.-Y. Mao and H. Metzger)) NIAMS, NIH, Bethesda, MD 20892 (Spon. by S.-J. Kim)

Aggregation of the receptor with high affinity for IgE ($Fc_εRI$) on the surface of mast cells and basophils stimulates phosphorylation of protein tyrosines, a process in which p53/p56*lyn* kinase has been implicated. We measured the association between $Fc_εRI$ and the kinase, using chemical crosslinking to stabilize their interaction. In the RBL rat mast cell line, 3-4% and at most 20% of $Fc_εRI$ appear to be associated with the kinase prior to aggregation, even though there is an excess of total cellular *lyn* kinase. Aggregating the $Fc_εRI$ causes three to four times more of the kinase to associate with receptors, a process requiring a prior phosphorylation step. In an *in vitro* assay, the *lyn* associated with the aggregated receptors becomes disproportionally more phosphorylated than would be predicted from the amount of *lyn* associated with the receptors. These and other data are consistent with a model in which aggregation of the receptor leads to its transphosphorylation by constitutively associated *lyn* kinase. We propose that additional molecules of this kinase are thereby recruited, and that this markedly enhances transphosphorylation of tyrosine on the receptor and associated proteins, thereby initiating a cascade of further biochemical changes. This model is also consistent with data on receptors such as the clonotypic receptors on B and T lymphocytes, that share structural and functional features with $Fc_εRI$.

Th-Pos465

THE ROLE OF PROTEIN KINASE C AND THE CYTOSKELETON IN THE SIGNAL TRANSDUCTION OF EXTRACELLULAR ATP IN CILIATED CELLS: MONITORING BY CHANGES IN MEMBRANE FLUIDITY. ((E. Alfahel, A.H. Parola and Z. Priel)) Department of Chemistry, Ben-Gurion University of the Negev, P.O.Box 653, Beer-Sheva, 84105, Israel.

The cilia are projections of the cell surface and are covered with membrane which is continuous with the cell surface membrane. Mucus transporting cilia of a freshly excised frog palate were labeled by non-penetrating lipophilic membrane probe 1-(4-trimethylammonium phenyl)-6-phenyl-1,3,5-hexatriene, p-toluenesulfonate (TMA-DPH). The addition of extracellular ATP affected membrane fluidity. We studied the role of protien kinase C (PKC) and the cytoskeleton in the signal transduction of extracellular ATP by measuring fluorescence polarization (P) in the membrane. The following results were obtained: 1) Extracellular ATP (5-50 μM) has lowered P (maximum lowering 20% at 10 μM). 2) Cytochalasin B (18 μM), colchicine (18 μM), well known cytoskeleton reagents, reduced the ATP effect observed above. 3) Addition of both cytoskeleton reagents, each at 18 μM, abolished the ATP effect observed above. 4) Phorbol ester, 12-o-tetradecanoyl-phorbol-13-acetate (TPA), an activator of PKC, caused a drop in P (maximum 10% at 80 nM). 5) Addition of inactive-TPA (80 nM) did not induce any change in P. 6) Addition of both cytoskeleton reagents, each at 18 μM, abolished the TPA effect observed above. We conclude that PKC is involved in the signal transduction cascade induced by extracellular ATP and that there is a tight conection between PKC and the cytoskeleton.

Th-Pos466

CHARACTERIZATION OF PROTEIN KINASE C α, β AND γ ISOENZYMES. ((B.G. Allen and M.P. Walsh)) Dept. of Medical Biochemistry, University of Calgary, Alberta, Canada T2N 4N1.

Protein kinase C (PKC) is a ubiquitous and multifunctional protein serine/threonine kinase with at least twelve different isoforms. The α, β and γ isoenzymes have been described as Ca^{2+}, phospholipid and diacylglycerol dependent. The aim of this study was to characterize the regulatory properties of these isoenzymes using different substrates. PKC α, β and γ isoenzymes were purified from rat brain by EGTA extraction of the particulate fraction prepared in the presence of Ca^{2+}, anion-exchange, hydrophobic and hydroxylapatite column chromatographies. The regulatory properties of the separated isoenzymes were compared using four different substrates: histone III-S and peptides based on the pseudosubstrate domains of PKCϵ and ζ, and the phosphorylation site-containing region of myelin basic protein ($MBP_{4\text{-}14}$). Dramatic differences in the requirements for Ca^{2+}, phospholipid or diacylglycerol were observed depending on both the isoenzyme and substrate. We also observed that, unless precautions were taken to prevent oxidation, PKCα was partially converted to a form which eluted from a hydroxylapatite column after PKCα and exhibited altered regulatory properties. We conclude that regulation of PKC varies not only with the isoenzyme but also with the substrate. Furthermore, regulatory properties can be affected by oxidative modification.

Th-Pos467

IDENTIFICATION OF PKCζ-RELATED mRNAs AND MOLECULAR CLONING OF A PKCζ PSEUDOGENE TRANSCRIPT, ΨPKCζ. ((J.E. Andrea)) Dept. of Medical Biochemistry, University of Calgary, Alberta, Canada T2N 4N1.

Protein kinase C (PKC) consists of a family of at least 12 phospholipid-dependent isoenzymes. Molecular cloning has been crucial in the identification and characterization of several of these isoenzymes. Amino acid sequence comparisons revealed 4 constant (C) and 5 variable (V) domains. Functional roles have been assigned to the constant domains, including autoinhibition (C1), lipid and phorbol ester binding (C1), Ca^{2+} binding (C2) and catalysis (C3 and C4). I have conducted Northern blot analysis of rat brain mRNA using oligonucleotide probes derived from published sequences of PKCζ. A probe complementary to the V5 domain hybridized to mRNAs of 2.5 and 4.7 kb, similar to previous reports in the literature. When probed with a C1 domain-derived oligonucleotide, the same 2.5 and 4.7 kb mRNAs were detected, as well as an additional 1.75 kb message. Most surprisingly, a probe complementary to the V1 domain hybridized only to a low abundance 3.1 kb mRNA. I have cloned a PKCζ-related pseudogene cDNA, ΨPKCζ, and verified its authenticity by RNase protection and RT-PCR. The cDNA sequence of ΨPKCζ is identical to that of PKCζ except for the V1 domain. In conclusion, the 3.1 kb mRNA encodes PKCζ while the 2.5 and 4.7 kb mRNAs are transcribed from the ΨPKCζ pseudogene.

Th-Pos468

THREE DIMENSIONAL DISTRIBUTION OF PROTEIN KINASE C ISOFORMS IN GASTRIC MYOCYTES. ((D. J. Schmidt and F.S. Fay)) Univ. of Mass., Prog. in Molecular Medicine, Biomedical Imaging Group, Worcester, Ma. 01605. (Spon. by J.G. Dobson Jr.)

Activation of protein kinase C (PKC) modulates key aspects of smooth muscle contractile function such as Ca^{2+} regulation. Growing evidence supports a major role for subcellular compartmentation of proteins in ion regulation; for example, pumps and exchangers for calcium and sodium ions have been colocalized to caveolae in smooth muscles. In addition, since cells express multiple isoforms of PKC also found associated with discrete subcellular structures, localization of specific PKCs is required to assess putative roles in contraction-related processes. Therefore, high resolution 3D subcellular localization of PKC(s) was performed in freshly-dispersed toad gastric myocytes using digital imaging fluorescence microscopy with image de-blurring via constrained iterative mathematical deconvolution. Probes included a pan-PKC monoclonal antibody (mAb) selective for activated kinase, the fluorescent bis-indolylmaleimide PKC inhibitors RIM-1 and FIM-1, and isoform-specific mAbs to α–, β–, and δ–PKCs. Indirect immunofluorescence staining of fixed quiescent myocytes with m1.9, an mAb shown to selectively bind to *active* PKCs in these cells (Moore et al, Biophys.J., 64 (2P2), pA32, 1993), confirmed that report's localization of active PKC in resting cells to near-membrane areas. In contrast, RIM-1 and FIM-1 PKC inhibitors stained discrete sites throughout fixed resting myocytes. Cell-permeant FIM-1 diacetate staining revealed similiar structures in quiescent living cells. Incubation with excess of the parent inhibitor and/or Mg-ATP blocked discrete labelling. Since isoform-specific mAbs also found PKCs throughout the cell, PKCs are localized throughout resting myocytes. Staining patterns for all three mAbs included structures reminiscent of α–actinin/ dense body staining. Anti-β–PKC mAb gave more prominent near-membrane staining, implicating it as the active PKC detected in quiescent cells. Ongoing studies seek to identify PKC isoforms and structures associated with active PKC in both resting and stimulated gastric myocytes. (Support by HL 47530 and HL 14523).

Th-Pos469 ***(Presented at W-PM-D8)***

DIRECT ACTIVATION OF PROTEIN KINASE C BY 1α,25-DIHYDROXYVITAMIN D_3. ((S.J. Slater, M.B. Kelly, F.J. Taddeo, J.D. Larkin, M.D. Yeager, J.A. McLane, C. Ho and C.D. Stubbs)) Dept. of Pathology and Cell Biology Thomas Jefferson University, 1020 Locust Street, Philadelphia PA 19107

Evidence is presented that protein kinase C (PKC) is directly activated by the key metabolite of vitamin D_3, 1α,25-dihydroxyvitamin D_3 (1.25-D_3), at physiological concentrations (EC_{50} 16 ± 1 nM). The effect could be attributed to a direct interaction with a site the enzyme since the assay system used contained only purified PKC, substrate, necessary co-factors, and lipid vesicles. In common with diacylglycerol (DAG), the presence of 1,25-D_3 markedly reduced the concentration of calcium required for maximal activation of a calcium dependent isoform preparation (PKC-I). Activation of PKC-I by 1,25-D_3 in combination with DAG, or *4*β*-12*-O-tetradecanoylphorbol-*13*-acetate (TPA), was greater than that achievable by either activator individually, each being at a saturating concentration, a result also found with purified PKC-α, and -γ isoforms. This indicates that 1,25-D_3 activation involves interaction with a site distinct from the TPA or DAG binding sites, within a single PKC isozyme molecule. Activation of PKC-ϵ by 1,25-D_3 alone, or in the presence of TPA or DAG was reduced compared to PKC-I, suggesting that the C2-domain, which is absent in PKC-ϵ, may mediate in the mechanism of activation by 1.25-D_3. When phosphatidylethanolamine was present in the lipid, basal activity, and TPA or DAG stimulated activities were increased. By contrast, 1,25-D_3 stimulated activity was decreased, a result suggesting that 1,25-D_3 activated PKC may have a distinct conformation, and dissimilar interaction with the membrane lipid bilayer. The results lead us to suggest that PKC is a "membrane bound receptor" for 1,25-D_3 and as such is central in the control of signal transduction pathways regulating the non-genomic cellular responses to the hormone.

Th-Pos470

REGULATION OF PROTEIN KINASE C BY PHORBOL ESTERS AND SUBSTRATES. ((Marian Mosior and Alexandra C. Newton)) Dept. Chemistry, Indiana University, Bloomington, IN 47405-4001

Examination of the direct binding of phorbol esters to protein kinase C βII has allowed us to address the mechanism of interaction of this class of activators with conventional protein kinase Cs. Binding measurements reveal that the major role of phorbol esters is to increase the affinity of protein kinase C for membranes by several orders of magnitude. The relative increase depends linearly on the mole fraction of phorbol esters in membranes, with the potency illustrated by the finding that 1 mol% 12-myristate 13-acetate phorbol (PMA) increases protein kinase C's membrane association 40,000-fold. For comparison, diacylglycerol (DG), which also activates protein kinase C by increasing the enzyme's membrane affinity, is 250-fold less effective than PMA in altering protein kinase C's membrane affinity. The remarkably high-affinity interaction with phorbol esters allowed us to measure the direct binding of protein kinase C to PMA in neutral membranes and thus to evaluate the effect of Ca^{2+} on the phorbol ester interaction (in the absence of Ca^{2+} effects on the enzyme's interaction with acidic lipids). Changing Ca^{2+} concentrations over 5-orders of magnitude had little effect on the direct interaction of protein kinase C with PMA immobilized in phosphatidylcholine (PC) membranes. The maximal phosphorylation rate of the enzyme was identical in the presence of either DG or PMA. However, the concentration of either of these activators, as well as mol% phosphatidylserine (PS) required for half-maximal phosphorylation rate depended on a substrate. Changes in the rate and pattern of specific proteolysis of protein kinase C induced by PMA, PS and substrates allowed us to propose a new model of activation of protein kinase C by PS, PMA or DG, and substrates.

Th-Pos471

ACTIVATION OF PROTEIN PHOSPHATASE INHIBITOR-1 BY PROTEASE DIGESTED PROTEIN KINASE C (PKM). ((T. Tokui, I. Yada, S. Ando* and M. Ikebe#)) Department of Thoracic and Cardiovascular Surgery, Mie University, School of Medicine, Edobashi, Mie 514, Japan, #Department of Physiology and Biophysics, Case Western Reserve University, Cleveland, OH 44106 and *Biophysics Unit and Experimental Radiology, Aichi Cancer Center Research Institute, Chikusa-ku, Nagoya 464, Japan.

Protein phosphatase inhibitor-1 (PPI-1) is a small heat- and acid-stable protein, which specifically inhibits protein phosphatase 1 activity and therefore, it may be involved in the regulation of the level of protein phosphorylation in cells. It has been known that PPI-1 is activated only when it is phosphorylated at Thr-35 by cAMP-dependent protein kinase. We now report that PPI-1 can be phosphorylated by both protein kinase C and PKM. The major phosphorylation sites catalyzed by PKC and PKM were identified as both serine and threonine residues, however, the extent of phosphorylation by PKM was much greater than that by PKC. While PKC-induced phosphorylation failed to activate PPI-1 activity, PKM could activate the inhibitor activity. The results suggest that PKM can phosphorylate Thr-35 of the inhibitor while PKC cannot. The results also support the notion that PKM has broader substrate specificity than PKC. The identification of the phosphorylation sites (whether or not the sites are identical to those by cAMP-dependent protein kinase) is progressing. (Supported by NIH and AHA).

Th-Pos472

THE EFFECT OF cGMP ON THE SOLUTION STRUCTURE OF TYPE Iα cGMP-DEPENDENT PROTEIN KINASE (PKG). ((R. D. Mitchell, G. A. Olah, J. Corbin, S. H. Francis, D. A. Walsh, and J. Trewhella)) Dept. of Biological Chemistry, University of California, Davis, CA 95616; Los Alamos National Laboratory, Los Alamos, NM 87545; and Dept. of Mol. Physiology and Biophysics, Vanderbilt University, Nashville, TN 37232-0615

PKG and PKA contain highly homologous catalytic and regulatory domains, however, in PKG these reside within the same polypeptide chain. We have obtained information on the solution structure of PKG using Fourier transform infra-red spectroscopy (FTIR) to determine the secondary structure content and small angle x-ray scattering (SAXS) to determine the overall conformation. Second derivative and Fourier self-deconvolution analysis of the FTIR spectra have allowed for assignment of the individual components of secondary structure. There appears to be little, if any, secondary structural change in PKG upon binding of cGMP. However, the overall conformation as determined by SAXS changes dramatically. Guinier and pair distance distribution function (P(r)) analysis of the SAXS data has determined that the unactivated enzyme is characterized by a radius of gyration (R_g) of 41.8 ± 0.7 Å, a radius of gyration of cross section (R_c) of 20.8 ± 0.4 Å, and a maximum linear dimension (d_{max}) of 133 Å. Activation of PKG by the addition of cGMP causes a conformational change that is characterized by an 18% increase in R_g, a 40% decrease in R_c, and a 27% increase in d_{max}. The shape of the P(r) function also indicates a significant redistribution of interatomic vectors within the volume of the particle upon cGMP binding. These data show that a large conformational change occurs upon cGMP-dependent activation of PKG, likely reflecting the movement of the regulatory domain to allow access of protein substrates to the catalytic site.

Th-Pos473

PROBING THE ACTIVE SITE OF PHOSPHORIBULOKINASE WITH SPIN-LABELLED ATP ANALOGUES. ((H.A. Koteiche, C. Narasimhan^{+}, J.A. Runquist^{+}, J.S. Hyde and H.M. Miziorko^{+})) Biophysics Research Institute and $^{+}$Dept. of Biochemistry, Medical College of Wisconsin, Milwaukee, WI 53226.

Phosphoribulokinase (PRK) is an octameric enzyme of the Calvin cycle that phosphorylates ribulose-5-phosphate (Ru5P). Spin-labelled analogues, containing a proxyl spin label (SL) coupled to the phosphoryl chain of adenine nucleotides, were synthesized to probe the active site of PRK from *Rhodobacter sphaeroides*, expressed in E. coli. The progress of the syntheses was followed by ^{31}P NMR spectroscopy. The products, ATP-SL and ADP-SL, were characterized by NMR, ESR and UV spectroscopy. ESR spectra of nitroxides can be used to assess the degree of binding of the probes to proteins. ATP-SL and ADP-SL show different binding characteristics to PRK. The Scatchard plot of ATP-SL exhibits a linearity suggestive of independent binding to 2 sites per monomer. In the binary E· ATP-SL complex, the binding is very tight (K_D=7μM). The Scatchard plot of ADP-SL however indicates weaker cooperative binding with a stoichiometry of 1 site per monomer. Kinetic data show that ATP-SL and ADP-SL are competitive inhibitors with respect to ATP. ESR data indicate that bound ATP-SL can be displaced by each of the enzyme substrates. Titration with the allosteric effector NADH shows a concentration dependent, saturable release of the bound ATP-SL probe. Work is in progress to characterize the effect of the Ru5P, ATP and NADH on ADP-SL binding. These probes are being used to evaluate the structural integrity of PRK catalytic mutants.

Th-Pos474

Preliminary NMR Studies of Diacylglycerol Kinase, a 13 kDa Integral Membrane Enzyme. ((Prakash Badola, Todd Ridky, and Charles R. Sanders)) Dept. of Physiology and Biophysics, Case Western Reserve University, Cleveland, Ohio 44106. (Spon. by Thomas Gerken).

Microbial diacylglycerol kinase (DAGK) is remarkable for its small size, its lack of homology to any other kinase (including the mammalian DAGK), in the fact that it is about 80% membrane-embedded, and in the topological complexity of the reaction it catalyzes (DAG and PA: membranous; MgATP and MgADP: water soluble). We describe the membrane topology of this enzyme (Smith et. al., *J. Bacter.* 176, 5459-5465, 1994) and our development of a non-radioisotopic assay of its activity in mixed micelles. NMR studies in the presence of only catalytic quantities of DAGK indicate that the DAGK-reaction equilibrium constant is surprisingly close to unity, that dibutyrylglycerol is the shortest chained symmetric DAG which can serve as a substrate, and that ATPase activity cannot be detected for DAGK. This poster also describes attempts to assess the NMR spectroscopic properties of this enzyme under three general sets of conditions: (i) solubilized in organic solvents, (ii) solubilized in micelles, (iii) solubilized in a bilayered system. These studies represent a small first step towards a more detailed NMR study of the structure of this membrane enzyme. *This work was supported by NIH (GM 47485) and was made possible by a gift from James Bowie (UCLA) of a DAGK-overproducing strain of E. coli and accompanying purification methods.*

Th-Pos475

DIFFERENTIAL ACTION OF FLUORESCENT TYR-KINASE INHIBITORS K252A AND K252B IS RELATED TO MEMBRANE SOLUBILITY NOT PERMEABILITY ((David E. Wolf, C.A. McKinnon, K. Ratliff, M.-C. Daou, and A.H. Ross)) Worcester Foundation for Experimental Biology, Shrewsbury, MA. 01545 (Spon. by E.J. Luna)

The K252 compounds are potent inhibitors of tyr-kinases. It has been proposed that the differential activity of the two forms of this inhibitor, K252a and K252b, result from the higher membrane permeability of the K252a form. Using the natural fluorescence of these compounds we have shown that both of these forms preferentially partition into hydrophobic environments, with the K252a form being the more hydrophobic. Using quantitative low light level video fluorescence microscopy we have found that both forms rapidly cross the cell plasma membrane but that the K252a form preferentially partitions into the endomembranes. Thus the selective activity of these compounds appears to correlate not with membrane permeability but with membrane solubility.

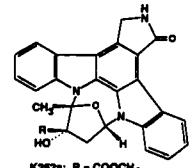

K252a: R = $COOCH_3$
K252b: R = COOH

Th-Pos476

REVERSIBLE BINDING KINETICS OF G-PROTEIN SUBUNITS AT PLANAR PHOSPHOLIPID MEMBRANES. ((Elizabeth A. Downs, Richard R. Neubig, and Daniel Axelrod)) Biophysics Research Division, Dept. of Pharmacology, and Dept. of Physics, University of Michigan, Ann Arbor, MI 48109

In some models of G-protein function, the α subunit dissociates from the plasma membrane while βγ is usually thought to be confined to the membrane. To begin to investigate the interactions of G protein subunits with a lipid surface, we measured the kinetics of binding of fluorescent-labeled purified G-protein subunits to lipids by means of total internal reflection/fluorescence recovery after photobleaching (TIR/FRAP). Phospholipid planar bilayers were prepared on glass coverslips with brain phosphatidylserine:egg phosphatidylcholine (PS/PC ratio1:3). In the presence of 0.2-0.4% cholate, eosin-labeled βγ subunit associates with the lipids and about 65-75% of the association appears to be reversible on a time scale of several tens of seconds. Surface diffusion of the βγ subunit does not appear to contribute to the fluorescence recovery kinetics. Differences between α and βγ and the role of detergent in these phenomena will be discussed. Supported by NSF MCB 9405928 (to D.A.) and NIH GM39561 (to R.N.)

Th-Pos477

A MUTAGENESIS STUDY OF PUTATIVE G-PROTEIN BINDING SITES ON THE C-TERMINUS OF GIRK1. ((K.M. Hurley, A Kuznetsov, G. Lipkind, L. H. Philipson and D.J. Nelson)) Depts. of Neurology, Medicine, and Pharmacology & Physiology Science, The University of Chicago, Chicago, IL 60637

In an effort to identify potential G protein binding sites on GIRK1, we used a structural algorithm designed to identify areas of secondary structure likely to form coiled coils, and found four such structures on the C terminus of GIRK1. We have focused our attention on CCα, the longest and most highly amphipathic helix of the four. Deletion mutations by restriction digest have shown that eliminating large portions of the C terminus from residue 403 but retaining CCα, preserves GIRK current. However, restriction digest which eliminates CCα at residue 272 produces a non functional channel. Further mutational analysis on epitope tagged channels has shown that specific excision of CCα despite retaining the integrity of the remainder of the C terminus also produces a null mutant. Finally, single amino acid substitutions by site directed mutagenesis of residues with large polar side chains for smaller hydrophobic ones which are likely to interfere either sterically with βγ associating with CCα or which disrupt the charge separation of the amphipathic helix do not produce functional channels. Western blots of membrane preparations from oocytes expressing these mutant channels demonstrate that appropriately sized proteins are being synthesized and targeted to the membrane fraction of the cell. Supported by NIH PO1 DK 44840

Th-Pos478

NERVE GROWTH FACTOR RECEPTOR DYNAMICS AND SUBUNIT ASSOCIATION STUDIED BY FLUORESCENCE RECOVERY AFTER PHOTOBLEACHING, COPATCHING, AND SITE DIRECTED MUTAGENESIS ((D.E. Wolf, C.A. McKinnon, M.C. Daou, P.J. Condon, M.B. Lachyankar, and A.H. Ross)) Worcester Foundation for Experimental Biology, Shrewsbury, MA 01545 ((D.R. Kaplan and R.M. Stephens)) NCI Frederick Cancer Research and Development Center, Gaithersburg, MD 21701

It has been proposed that the functional high affinity nerve growth factor receptor is a heterodimer of two proteins gp75 and gp140^{trk}. We have obtained direct evidence of the existence of this complex by a combined approach of FRAP, copatching fluorescence confocal microscopy, and site directed mutagenesis. When gp75 is expressed alone in either mammalian PC12 cells or using a baculovirus in insect Sf9 cells it is highly mobile as determined by FRAP. Coexpression with gp140^{trk} causes a reduction in the mobile fraction. Gp140^{trk} immobilization of gp75 is not observed if the cytoplasmic domain of gp75 is removed or if a point mutation of gp140^{trk}, which lacks a functional tyr-kinase domain, is expressed. Direct evidence of the gp75-gp140^{trk} complex was obtained by copatching studies. It was found that patching of gp75 by crosslinking antibodies resulted in copatching of gp140^{trk}. These studies lead to a refined model of the high affinity nerve growth factor receptor and elucidation of the specific domains of the two subunits involved in complexing, immobilization, and function.

Th-Pos479

cAMP BINDING TO MITOCHONDRIAL ADENINE NUCLEOTIDE TRANSLOCASE IN VIVO AND AFTER PURIFICATION ((C. Marfella, A. Romani and A. Scarpa)) Dept. Physiol. & Biophys., CWRU, Cleveland, OH, 44106-4970, USA [Spon. C. Moravec].

cAMP induces a sizable Mg^{2+} efflux from isolated heart or liver mitochondria, which is inhibited by atractyloside, a specific inhibitor of Adenine Nucleotide Translocase (AdNT). The nature of the interaction of cAMP to AdNT was investigated. Phosphorylation of AdNT was not observed and binding studies performed onto the purified protein showed a saturation kinetic of 80 nM. cAMP agarose affinity chromatography of purified AdNT was performed and 10% of the total AdNT applied was specifically eluted only by cAMP. The same experiment was performed using the whole mitochondrial protein either in absence or presence of detergent. Flow through and AdNT eluted from the column by cAMP were run onto SDS-PAGE. The 32 kDa monomeric AdNT (in the flow through lane) and the 64 kDa dimeric AdNT (in the cAMP eluted lane) were identified through western blot analysis. Mitochondrial proteins cross-linked with 8-azido-cAMP showed that cAMP specific elution from the cAMP affinity column was decreased but not abolished. Also under these conditions, SDS-PAGE and western blot analysis recognized cAMP bound AdNT as a dimer. Supported by N.I.H. HL 18708.

Th-Pos480

STIMULATION OF FAST AND SLOW GATING OF SINGLE CARDIAC L-TYPE CALCIUM CHANNELS BY CANTHARIDIN, A PHOSPHATASE INHIBITOR. ((S. Herzig and J. Neumann*)) Departments of Pharmacology, Universities of Kiel and Hamburg*, 24105 Kiel, FRG

Cantharidin exerts a positive inotropic effect in guinea-pig papillary muscles (e.g., at 3 and 10 μM, by 176% and 183%, n = 11). In vitro, it inhibits cardiac protein phosphatase subtypes with half-inhibitory concentrations of 2.70 μM (type 1 phosphatase, n = 5) and 0.13 μM (type 2A phosphatase, n = 6), respectively. The two known functional sequelae of cAMP-dependent phosphorylation of cardiac L-type calcium channels, i.e. enhanced availability (slow gating) and increased high open-probability (mode 2), may be selectively controlled by these two different protein phosphatase subtypes. Therefore, we studied the effects of cantharidin (15-19 μM) on the gating behavior of single L-type calcium channels. Long-lasting (> 1000 sweeps, 150 ms-steps from -100 to +20 mV, 600 ms-intervals, n = 5) cell-attached recordings (70 mM Ba^{2+}) were obtained in guinea-pig cardiomyocytes. Cantharidin moderately (by $\approx$ 20%) enhanced ensemble average current and channel availability. Fast, modal gating was analysed according to Yue et al. (1990, PNAS 87: 753-7). The fraction of active sweeps containing mode 2-activity was enhanced slightly, but significantly from 1.2% to 2.9%. Slow (availability) gating was investigated in single-channel patches, using discrete-time Markov analysis (Herzig et al., 1993, BJ 65: 1599-1612). Cantharidin slowed the rate constant representing dephosphorylation. In summary, cantharidin stimulates cardiac calcium channels in a manner qualitatively similar to other phosphatase inhibitors, like okadaic acid. Its effects are in accordance with its rather low potency to inhibit protein phosphatases, and with little selectivity for type 2A-, compaed with type 1-phosphatase.

Th-Pos481

METHACHOLINE-INDUCED CURRENTS AND $[CA^{++}]_i$ IN FRESHLY DISSOCIATED AIRWAY SMOOTH MUSCLE CELLS ((B.K. Fleischmann and M.I. Kotlikoff)) Department of Animal Biology, University of Pennsylvania, Philadelphia, Pa, 19104. (Spon. by B.M. Salzberg)

In order to examine calcium-permeant membrane conductances activated by muscarinic agonists in smooth muscle, single equine tracheal myocytes were voltage clamped using the nystatin patch-clamp technique, and cytosolic free calcium concentration $[Ca^{++}]_i$ simultaneously measured by fura-2 microspectrofluorimetry. Cells were loaded with the cell permeant form of the calcium sensitive dye fura-2 (fura 2-AM, 2μM for 10 minutes) and voltage clamped using the nystatin perforated patch clamp technique. Intracellular solutions contained cesium to block outward currents, and all experiments were performed at 35°C. Methacholine (Mch, 50 μM) was applied to voltage-clamped myocytes by a puffer pipette (20-50 seconds) and reliable and repetitively evocable current and $[Ca^{++}]_i$ responses were recorded. Both the current and calcium responses to Mch were biphasic. A large inward current (often greater than 1 nA with 130 mM Cl^- in the pipette) inactivated rapidly and was followed by a sustained current of low amplitude that relaxed only after agonist application. The large, inactivating current was identified as a calcium-activated chloride current on the basis of the shift of the reversal potential of the evoked current in low chloride solutions, and its activation by caffeine. The sustained component consisted of a noisy conductance that was independent of the Cl^- gradient, but dependent on the monovalent cation gradient and was not activated by calcium release. The biphasic $[Ca^{++}]_i$ response also consisted of a large transient followed by a sustained rise in $[Ca^{++}]_i$. The sustained elevation of $[Ca^{++}]_i$ was only observed under conditions that evoked the sustained current. Thus muscarinic agonists activate a a non-selective cationic conductance that is calcium permeant and may play an important role as a long lasting influx pathway for calcium. (Supported NIH HL-45239)

Th-Pos482

THE DUAL ROLES OF INTRACELLULAR Ca(II) ON Ca(II) OSCILLATIONS IN HeLa CELLS. ((D.-M. Zhu, E. Tekle, C.Y. Huang, and P.B. Chock)) Laboratory of Biochemistry, NHLBI, NIH, Bethesda, MD 20892.

The cytosolic Ca(II) has been implicated to provide both positive and negative controls of intracellular Ca(II) release in studies using vesicles and permeabilized hepatocytes. We report here that intracellular Ca(II) elevated to a suitable level by electroporation is sufficient to initiate Ca(II) oscillations in the absence of an agonist in HeLa cells. In Ca(II)-free buffer, electroporation did not alter ongoing Ca(II) oscillations or initiate oscillations in resting cells. However, with 50-100 μM Ca(II) in the buffer, electroporation either caused an increase in the frequency of ongoing Ca(II) oscillations or induced Ca(II) oscillations in resting cells without an agonist. This observation was not altered by the addition of ryanodine, suggesting that the ryanodine-sensitive pools were not involved. When the external Ca(II) level in the buffer was increased to $\geq$200 μM, electroporation produced a prolonged Ca(II) peak, which failed to initiate Ca(II) oscillations in nonstimulated cells, but irreversibly abolished ongoing oscillations induced by histamine. Quantitation of IP_3 revealed that intracellular IP_3 level was increased from ~1 to ~3 μM, 12 sec after electroporation with a buffer containing 50 μM Ca(II). Taken together, the data suggest that phospholipase C can be activated by elevated intracellular Ca(II) in the absence of an agonist to generate IP_3 and thereby induces Ca(II) oscillations. The mechanistic implications of these observations will be discussed.

Th-Pos483

α1-ADRENERGIC MODULATION OF K CHANNELS IN OOCYTE MODEL SYSTEM. ((J.-A. Yao, H. Zhang, J. Tseng-Crank*, G.-N. Tseng)) Dept Pharmacology, Columbia U., New York, NY 10032, * Molecular Genetics, Glaxo, Research Triangle Park, NC 27709.

We studied the effects of α1-adrenergic stimulation on the slow delayed rectifier K channel by coexpressing a human minK clone (hIsK) and a human α1B-adrenergic receptor clone (α1B) in Xenopus oocytes. 100 uM phenylephrine (PE) had no effects on uninjected oocytes. In oocytes expressing α1B alone, PE induced a membrane current that was sensitive to external Cl removal or prazosin (PRA, 10 uM) pretreatment, consistent with the notion that α1B is coupled to phospholipase C in oocytes and α1B stimulation leads to IP_3 production, Ca_i release and activation of an endogenous Cl channel (I_{Cl}). PE had no effect on hIsK expressed alone in oocytes. In oocytes coexpressing hIsk and α1B (bathed in a Cl-free solution), PE increased hIsK current amplitude in 67% of the cells (n=18) by 20-160% (average 70%). This effect could be prevented by PRA pretreatment. Unlike the time course of PE-induced I_{Cl}, the effects of PE on hIsk occurred with a prominent delay (1-2 min) and reversed extremely slowly after washout of PE. Also unlike I_{Cl} which could be induced by PE repetitively, second exposure to PE induced much smaller (<10%) or no increase in hIsK. These observations suggest that hIsk enhancement following α1B stimulation may not be simply due to Ca_i release, but may involve some Ca_i-dependent enzymatic process. Staurosporine 0.1 uM pretreatment did not prevent PE-induced hIsK increase, suggesting that PKC is not essential for this phenomenon. Our data suggest that oocytes are a useful model for studying signal transduction in α1-adrenergic receptor modulation of ion channels. We are currently testing and comparing the effects of stimulating α1B and α1C on hIsK and other K channel clones.

Th-Pos484

FUNCTIONAL COUPLING OF $ß_2$-ADRENOCEPTOR TO BOTH G_s AND A PERTUSSIS TOXIN-SENSITIVE G PROTEIN IN CARDIAC MYOCYTES ((R-P. Xiao, X-W. Ji, and E.G. Lakatta)) GRC, NIA, NIH, Baltimore, MD 21224

Recently we demonstrated that the effects of $ß_2$-adrenoceptor ($ß_2$AR) stimulation on cardiac excitation-contraction coupling are dissociated from the $ß_2$AR stimulated increase in cAMP, suggesting that $ß_2$ARs might couple to multiple G proteins. Here we report that in pertussis toxin (PTX) treated rat ventricular myocytes (incubation with PTX (0.75 μg/ml) at 37°C > 3 h) the maximal effects of the $ß_2$AR agonist, zinterol (ZINT, 10^{-5}M) on L-type Ca^{2+} current (I_{Ca}, step from V_h -40 to 0 mV), cytosolic Ca^{2+} (Ca_i) transient (Indo-1 fluorescence) and contraction (CONT, photodiode array) in cells (stimulated at 0.5 Hz at 25°C) are potentiated by 2.5-, 1.7- and 2.0-fold, respectively (each $P<0.001$). Fig. shows that the dose-response curve of ZINT to increase CONT amplitude (% of control, non-Indo loaded cells) was shifted to left by a order of magnitude following PTX treatment. These results demonstrate that the G_i-coupled $ß_2$AR also activates a PTX-sensitive G protein. As neither the control I_{Ca}, Ca_i transient or CONT, nor the effects of $ß_1$AR agonist, NE, (10^{-9}M to 10^{-5}M) on these parameters were significantly altered by PTX treatment, the potentiating effect of PTX is confined to $ß_2$AR stimulation. The activation of functionally opposite G proteins by $ß_2$AR stimulation may provide a mechanism to protect the heart from Ca^{2+} overload during ßAR stimulation. The non-cAMP mechanism via which $ß_2$AR augments I_{Ca}, Ca_i and CONT, however, remains unknown.

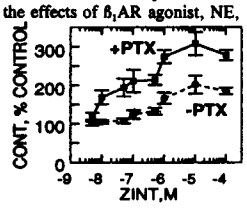

Th-Pos485

THE EFFECT OF β_2 ADRENERGIC RECEPTOR STIMULATION ON L-TYPE I_{Ca} OF ADULT AND NEWBORN RABBIT HEART ((C.B.Lu and R.Kumar and R.W.Joyner)) Todd Franklin cardiac Laboratory, Children's Research Center, Department of Pediatrics, School of Medicine, Emory University, Atlanta, GA 320030

We have found that both β_1 and β_2 adrenoceptors (ARs) coexist in ventricles of newborn (NB) and adult rabbit (AD) hearts by autoradiographic binding studies. The present study aims to determine whether β_2 AR play an important role in the physiological regulation on cardiac I_{Ca} in single ventricle cells of both NB and AD rabbit using whole cell voltage clamp techniques. Our results shown that 1) non-selective β AR agonist ISO (0.1 uM) has a 70 % and a 120% increase on I_{Ca} for NB and AD ventricular cells respectively. 2) Highly selective $ß_1$ receptor antagonist CGP (0.5 uM) did not affect the amplitude of I_{Ca} for either NB or AD rabbit ventricular cells. However, CGP can reverse ISO's effect on I_{Ca} of both NB and AD. Pretrement with CGP completely abolished the effect of ISO on I_{Ca}, however CGP did not interfere with a Forskolin (adenylate cyclase activator) induced increase on I_{Ca} in both NB and AD cells. 3) The selective β_2 AR agonist Zinterol (1-10 uM) did not have any effect on I_{Ca} of either NB or AD cardiac cells. Higher doses of Zinterol (up to 30 uM) only has weak effect on I_{Ca} of NB cardiac cell (less than 10%). These results suggest that although β_2 AR exists in NB and AD ventricular cells, its physiological regulation on cardiac cell I_{Ca} in NB or AD rabbit heart is not as important as β_1 AR.

Th-Pos486

ILOPROST RELAXES GUINEA-PIG AORTA, BUT NOT THROUGH ACTIVATION OF ATP-SENSITIVE K^+ CHANNELS.
((M. BOLACH, S. HALL & L.H. CLAPP)) Cardiovascular Research, UMDS, St. Thomas's Hospital, London SE1 7EH, U.K.

Prostacyclin and its stable analogue, iloprost, hyperpolarize and relax vascular smooth muscle. Recent evidence suggests these agents dilate coronary blood vessels by activation of K_{ATP} channels. The aim of this study was to assess the role of these or other K^+ channels in relaxations to iloprost in strips of guinea-pig aorta. Iloprost (0.05-1μM) relaxed tissues precontracted with 25 mM K^+ in the presence and absence of endothelium. Maximum relaxation occurred at 1 μM (54 ± 7%; mean ± sem, n=6) which was significantly ($p<0.001$) reduced (11±3%, n=8) when K^+ was raised to 60 mM. Similarly, iloprost (0.05-1μM) inhibited contractions to phenylephrine (6 μM), with 0.6 μM relaxing strips by 50 ± 5% (n=9) and taking ~16 min to recover by 50%. In the presence of glibenclamide (10 μM), a K_{ATP} channel blocker, relaxations and recovery time were potentiated at all concentrations, increasing to 79 ± 7% ($p<0.01$; n=7) and 25 min, respectively, at 0.6 μM iloprost. The increase in recovery time, but not the potentiation was mimicked by the cyclo-oxygenase inhibitor, indomethacin (10 μM). Furthermore, the effects of iloprost were significantly inhibited by tetraethylammonium chloride (TEA; 2 mM), which reduced the relaxation of 25 mM K^+ contractions at 0.1 μM iloprost from 53 ± 5% (n=6) to 23 ± 5% (n=6, $p<0.002$). TEA (2mM) could also inhibit relaxation to isoprenaline (1 μM), but not levcromakalim (10 μM). These results suggest that iloprost (possibly *via* cAMP) produces relaxation of guinea-pig aorta largely by opening K^+ channels, and that Ca-activated K^+ channels rather than K_{ATP} channels are involved in vasodilation. Furthermore, it would appear that iloprost releases a constricting factor, the effect of which can be blocked by glibenclamide.

Supported by the Wellcome Trust. LHC is a wellcome Trust Fellow.

Th-Pos487

ALLOMETRIC DESCRIPTION OF RENAL WEIGHT AFTER CISPLATIN THERAPY IN RATS. R.P. Spencer, Yu. Natochin.* University of Connecticut Health Center, Farmington, CT 06030, and The Sechenov Institute of Evolutionary Physiology and Biochemistry, Russian Academy of Sciences, St. Petersburg, Russia.

Cisplatin (CP) has been used in therapy of malignant tumors. When CP is given intraperitoneally to male rats, a gain in kidney weight & loss of body weight occurs. Kidney weights of 8 control rats (148-219 g) and 9 given 5 mg/kg of CP were analyzed by an allometric equation, in log form: log K = p.log B + log C, where kidney weight (K) is given by body weight (B) and a constant, over 5 days.

Controls: log K = 0.87 log B - 1.63 corr. coeff. = 0.87
CP rats: log K = 0.97 log B - 2.00 corr. coeff. = 0.85

There thus appeared to be an ordered relationship between kidney and body weights over this time period. We also analyzed body weight at day 5 (W) as a function of that at day 1 (w).

Controls: W = 1.15 w - 1.80 corr. coeff. = 0.99
CP rats: W = 0.88 w + 7.94 corr. coeff. = 0.96

Increase in renal weights in CP rats may be due to edema & altered functional ability. Body weight loss is attributed to CP damage to intestinal epithelium and decreased food intake. However, renal and body weight changes appeared to be closely related. It is uncertain if this tight coupling is pertinent when other chemotherapeutic agents are used.